The Design, Synthesis and Characterization of Polynuclear Materials for Applications in Catalysis

Banothile Charity Events Makhubela

University of Cape Town,

South Africa

February 2012

The Design, Synthesis and Characterization of Polynuclear Materials for Applications in Catalysis

By

Banothile Charity Events Makhubela

A thesis submitted in fulfilment of the requirements for the degree of

Doctor of Philosophy

Department of Chemistry

University of Cape Town,

South Africa

Supervisor : Dr Gregory S. Smith

Co-supervisor : Dr Anwar Jardine

February 2012

Declaration

I declare that **The Design, Synthesis and Characterization of Polynuclear Materials for Applications in Catalysis** is my own work and to the best of my knowledge has never been reported or submitted for any degree or examination in any university. All sources of information used herein are cited, acknowledged and completely referenced at the end of each chapter.

_____ _____

Banothile C.E. Makhubela Date

Acknowledgements

I wish express my heartfelt gratitude and appreciation to the following individuals, without whose contribution this thesis would not be possible:

The Sovereign God, for the opportunity and grace to carry out this work.

My supervisor Dr Gregory S. Smith and co-supervisor Dr Anwar Jardine for their guidance, patience, encouragement, support and invaluable training throughout this project.

Mr Pete Roberts and Mr Noel Hendricks for recording of NMR spectra. Mr Piero Benincasa for elemental analyses and EI-MS. Dr Hong Su for the single crystal X-ray structure determinations, Dr Crystel Tinguely for ICP-MS analyses, Mr Mohammed Jaffer who helped with TEM studies and Prof Michael Claeyes for his assistance with lab space and allowing me to use their GC after the unfortunate fire in our research labs.

My colleagues in the UCT organometallic research group for their support, encouragement and helpful discussions.

The National Research Foundation-Deutscher Akademischer Austausch Dienst (NRF-DAAD), Canon Collins Trust, and the DST-NRF Center of Excellence in Catalysis (c*change) for funding.

Dr Emma B. Hager for proof-reading this thesis. The late Prof John R. Moss and Dr Akella Sivaramakrishna for mentoring me during my early days of research.

I wish to dedicate this thesis to my family [Mndawe J. Makhubela and Ntombikayise A. Makhubela (*parents*); Sharon, Bhekizwe, Muzi and Bakhona (*siblings*); and Gertrude Ngubane (*late aunt*)] and friends, thank you all for the unconditional love and support throughout my life.

Abstract

The synthesis and characterization of new chitosan- and 6-deoxy-6-amino chitosan-supported ligands is discussed. This was achieved *via* the reaction of either 2-pyridinecarboxaldehyde or 2-(diphenylphosphino)benzaldehyde with the accessible amino groups of chitosan to afford chitosan-supported Schiff base ligands (**2.1**-**2.4**) bearing iminopyridyl and iminophosphine functionalities on the surface. Complexation reactions with $[PdCl_2(COD)]$ and $[RhCl(CO)_2]_2$ gave the corresponding chitosan-supported complexes (**2.5**-**2.8**) and (**2.13**-**2.14**). These metal-containing materials and their precursors were isolated as air and moisture stable solids which proved insoluble in common organic solvents and have been characterized analytically and spectroscopically using: ultraviolet-visible (UV-vis), Fourier transform infrared, solid state ^{13}C NMR and solid state ^{31}P NMR spectroscopy, elemental analysis, thermogravimetric analysis (TGA), transmission electron microscopy (TEM), powder X-ray diffraction (P-XRD) as well as inductively coupled plasma mass spectrometry (ICP-MS).

Mononuclear Pd^{II} and Rh^{I} complexes were prepared by complexation of 1,3,4,6-tetra-*O*-acetyl-β-D-glucosimino and cyclohexylimino ligands (**2.9**-**2.10**) and (**2.15**-**2.16**) with $[PdCl_2(COD)]$ and $[RhCl(CO)_2]_2$ to yield new model complexes (**2.11**-**2.12**) and (**2.17**-**2.18**). The complexes have been characterized using spectroscopic and analytical techniques including ^{1}H NMR, ^{31}P NMR, UV-vis and FT-IR spectroscopy, elemental analysis and mass. spectrometry. The structure of Rh^{I} complex (**2.17**) was unambiguously determined using X-ray crystallography. The application of the chitosan-supported Pd^{II} complexes (**2.5**-**2.8**) and their mononuclear analogues (**2.11**-**2.12**) as catalyst precursors in Suzuki-Miyaura and Heck cross-coupling reactions is reported. The catalyst precursors all displayed catalytic activity in this regard and a discussion of their activity, selectivity, stability and recyclability is presented. The Rh^{I} catalyst precursors (**2.13**-**2.14**) and (**2.17**-**2.18**) are effective in the hydroformylation of 1-octene.

Abstract

The synthesis and characterization of low generation pyridylimine Pd^{II} and Rh^{I} metallodendrimers is described. Schiff base condensation of tris-2-(aminoethyl)amine with 2-pyridinecarboxaldehyde afforded dendrimer (**4.2**) with pyridylimine functionalities on the periphery. Complexation reactions with $[PdCl_2(COD)]$, $[RhCl(CO)_2]_2$ and $[RhCl(COD)]_2$ yielded the corresponding metal-containing dendrimers with $-PdCl_2$, -RhCl(CO) and -Rh(COD) moieties on the periphery. The metallodendrimers and their precursor were poorly soluble and highly thermally stable and have been characterized using ^{1}H NMR, ^{13}C NMR, ^{31}P NMR and FT-IR spectroscopy, elemental analysis as well as mass spectrometry.

Pyridylimine Pd^{II} and Rh^{I} complexes (**4.3**-**4.5**) were obtained by the reaction of 4-(2-pyridylimine) benzyl alcohol ligand (**4.1**) with the appropriate metal precursor. These new complexes were fully characterized using ^{1}H NMR, ^{13}C NMR and FT-IR spectroscopy, elemental analysis as well as mass spectrometry. The molecular structure of complex (**4.3**) was determined by single crystal X-ray diffraction.

The evaluation of catalyst precursors (**4.4**-**4.5**) and (**4.7**-**4.8**) in the hydroformylation of 1-octene is presented. These systems proved highly active and selective for this reaction. Aldehydes were favoured at moderate to high temperatures (95 °C and 75 °C) and pressure (30 bars), while more *iso*-octenes were formed at low temperature (55 °C) and pressures (5 and 10 bars).

Abbreviations

Å	= angstrom
Ar	= aromatic or aryl
AcOH	= acetic acid
acac	= acetyl acetonate
Bu	= butyl
COD	= 1,5-cyclooctadiene
ca	= approximately
DMSO	= dimethylsulfoxide
DCM	= dichloromethane
DMF	= dimethylformamide
Et_2O	= diethyl ether
EtOAc	= ethyl acetate
EtOH	= ethanol
Et_3N	= triethylamine
MeOH	= methanol
Me	= methyl
pyr	= pyridyl
Ph	= phenyl
Pr	= propyl
TMS	= tetramethylsilane
THF	= tetrahydrofuran
NMR	= nuclear magnetic resonance
Hz	= Hertz

Abbreviations

MHz	= megahertz
ppm	= parts per million
δ	= chemical shift
s	= singlet (*NMR*) and strong (*FT-IR*)
d	= doublet
m	= multiplet
br m	= broad multiplet
sept.	= septet
J	= Coupling constant
room temp.	= room temperature
°C	= degrees Celsius
FT-IR	= Fourier Transform Infrared
cm^{-1}	= wavenumbers
m	= medium
vs	= very strong
w	= weak
br	= broad
EI-MS	= electron impact mass spectrometry
ESI-MS	= electrospray ionization mass spectrometry
ICP-MS	= Inductively Coupled Plasma- Mass spectrometry
m/z	= mass to charge ratio
vide ante	= see earlier
vide infra	= see later

Abbreviations

$[M]^+$	= molecular ion
UV-vis	= ultraviolet-visible spectroscopy
nm	= nanometer
P-XRD	= powder X-ray diffraction
TGA	= thermogravimetric analysis
2θ°	= 2 theta degrees
TEM	= transmission electron microscopy
GC	= gas chromatography
decomp.	= decomposes
equiv.	= equivalent
DS	= degree of substitution
°	= degrees
Eq.	= equation
g	= gram
nd	= not determined
tlc	= thin layer chromatography
TOF	= turnover frequency
ee	= enantiomeric excess
PS	= polystyrene
DVB	= divinylbenzene
PEG	= polyethylene glycol
PE	= polyethylene
M_w	= molecular weight

Publications

Journal articles:

- Banothile C.E. Makhubela, Anwar Jardine, Gregory S. Smith
  Rh(I) complexes supported on a biopolymer as recyclable and selective hydroformylation catalysts.
  Green Chemistry, (**2012**), 14, 338-347.

- Banothile C.E. Makhubela, Anwar Jardine, Gregory S. Smith
  Pd nanosized particles supported on chitosan and 6-deoxy-6-amino chitosan as recyclable catalysts for Suzuki–Miyaura and Heck cross-coupling reactions.
  Applied Catalysis : A Genenal, (**2011**), 393, 231-24.

Patents filed:

- Banothile C.E. Makhubela, Anwar M. Jardine, Gregory S. Smith, *A Polymer Support*, Provisional Patent number: 2009, ZA PPA 2009/06358

Conference contributions:

- **Biopolymer-supported Rh complexes as recyclable hydroformylation catalysts,** *Catalysis Society of South Africa Conference (CATSA), Muldersdrift, Misty Hills, Gauteng, 13-16 Nov.* ***2011***.
  Banothile C.E. Makhubela, G.S. Smith, and A.M. Jardine (Oral).

- **Biopolymer-supported transition metal catalysts: A Contribution to Green Chemistry**
  3nd Annual Academy of Science of South Africa (ASSAf)- DST-NRF Young Scientist' Conference, Sept 26-28, ***2011.***
  Banothile C.E. Makhubela, G.S. Smith, and A.M. Jardine (Oral).

- **Biopolymer-supported transition metal catalysts**
  3rd UCT Chemistry Dept. Equity Development Programme (EDP) Seminars, Jun 17, ***2011.***
  Banothile C.E. Makhubela, G.S. Smith, and A.M. Jardine (Oral).

- **Pd and Rh functionalized chitosan as recyclable biopolymer-supported catalysts.**
  40th South African Chemical Institute (SACI) National Convention and Federation of

- *African Chemical Societies (FACS) meeting: A prelude event to the International Year of Chemistry, Johannesburg, Jan. 16-21,* ***2011***.
  Banothile C.E. Makhubela, G.S. Smith, and A.M. Jardine (Oral).

- **Heterogenization of Rh complexes on chitosan-Schiff base supports for hydroformylation**
  Catalysis Society of South Africa Conference (CATSA), Bloemfontein, Free State University, 7-10 Nov. ***2010***.
  Banothile C.E. Makhubela, G.S. Smith, and A.M. Jardine (Poster).

- **Chitosan-supported Pd(II) Schiff base complexes for Suzuki- Miyaura and Heck cross-coupling reactions**.
  24th International Conference on Organometallic Chemistry (ICOMC), Taipei Int. Convention Center, Taiwan, Jul. 18-23 ***2010***.
  Banothile C.E. Makhubela, G.S. Smith, and A.M. Jardine (Poster, Best Poster Award).

- **Heck and Suzuki cross-coupling catalyst based on imino-pyridyl and iminophosphine Pd complexes immobilized on a biopolymer**.
  South African Chemical Institute (SACI) Inorganic Chemistry Conference, Bloemfontein, ***2009***.
  Banothile C.E. Makhubela, G.S. Smith, and A.M. Jardine (Poster).

- **Recyclable Heck and Suzuki cross-coupling catalyst based on imino-pyridyl and iminophosphine PdII complexes immobilized on a biopolymer.**
  Catalysis Society of South Africa Conference (CATSA), Goudini Spa, Western Cape, ***2009***.
  Banothile C.E. Makhubela, G.S. Smith, and A.M. Jardine (Poster).

Table of Contents

Chapter 1

Historic Overview of Catalysis and Literature Review of Immobilized Homogeneous Catalysts

1.1 Catalysis

Catalysis is an extremely useful process that is used to facilitate a variety of chemical transformations in nature, industry as well as research and development. The term catalysis was coined by Baron J.J. Berzelius in 1835 to describe the property of substances that facilitate an increased rate of chemical reactions without being consumed by them.

Almost 90 % of all commercially produced chemical products involve catalysts at some stage in the process of their manufacturing. [1] In 2005, catalytic processes generated about US$ 900 billion in product worldwide. [2] Inevitably, catalysis plays a significant role in improving standards of living in societies through the many catalytic processes leading to pharmaceuticals, foods, consumer goods and agrochemicals, to name but a few. Notable industrial application areas of catalysis are highlighted in **Table 1.1**.

Table 1.1. Highlight of industrial applications of catalysis. [3]

Area	Process	Example
Energy Processing	-Petroleum refining. -Fuel cell technology. -Biofuels processes.	-Catalytic cracking, alkylation. -Anodic and cathodic reactions in fuel cells. -Inorganic- and bio-catalysts in biofuels production.
Bulk Chemicals	-Large scale chemicals production.	-Production of HNO_3 and H_2SO_4 (oxidation). -Production of NH_3 and MeOH (hydrogenation).
Fine Chemicals	-Production of Active Pharmaceutical Ingredients (APIs), their intermediates and excipients.	-Catalytic Heck reaction in preparing an inter-mediate for synthesis of Rilpilvirine (HIV infection treatment drug).[4] -Synthetic polymers such as polyethyleneglycol (PEG) as binders in tablets.
Food Processing and Biology	-Production of margarine. - Natural processes. -Agrochemicals production.	-Catalytic hydrogenation of fats. -Enzymes as catalysts in metabolism and catabolism. -Pesticide, herbicide and fertilizer production for improving crop yields.

Table 1.1. Highlight of industrial applications of catalysis continued. [3]		
Area	**Process**	**Example**
The Environment	-Environmental steward-ship.	-Hazardous materials treatment. -Effluent water treatment. -Reduction of emissions from gasoline/diesel engines (catalytic convertors).

Some of the early discoveries in transition metal catalysis involved platinum in i) Humphrey Davy and Johann Wolfgang Döbereiher's research on *platinum catalyzed lighter technology* (in the 1820s), ii) *the contact process* (Peregine Phillips, 1831), iii) *electrocatalysis* (William Robert Grove, 1830s) and iv) Wilhelm Ostwald's *Ostwald process* (in the 1880s). Since then, research in catalysis has grown to be a major field in applied sciences involving many areas, notably in material science, water resource management, chemical engineering and organometallic chemistry.[5]

1.2 Homogeneous Catalysis

Many organometallic compounds fall under the category of homogeneous catalysts, which function in the same phase as the reactants or substrate. [6,7] Pioneering works in the field of homogeneous catalysis were carried out by i) Otto Roelen, who discovered catalytic *hydroformylation* (the "oxo synthesis") of alkenes to aldehydes and alcohols using $[HCo(CO)_4]$ (in the 1930s), [6a-b,7a] ii) Karl Ziegler and Giulio Natta who developed Ziegler-Natta *polymerization* catalysts based on titanium for manufacturing of various polymeric materials, [6c-d] iii) Geoffrey Wilkinson who described *hydrogenation* of alkenes to alkanes using $[RhCl(PPh_3)_3]$ (in the 1960s). [6e,7b]

It is upon such foundations that homogenous catalysts have developed into major contributors to the chemical industry, being employed in such processes as the commercial production of i) *acetic acid* by carbonylation of methanol (by Monsanto, catalyzed by $[RhI_2(CO)_2]^-$), ii) *adiponitrile* (by Dupont, catalyzed by Ni) and iii) *butanal* (by OXEA, former Ruhr Chemie-Rhone Poulenc Process, catalyzed by Rh/TPPTS) (TPPTS = trisodium tris(*m*-sulfophenyl)phosphine) . [8,9]

Homogeneous catalysis possesses the advantage of more efficient utilization of catalyst through such means as higher activity and selectivity as well as milder reaction conditions in order to conserve chemicals and energy. These attributes are desirable from the industrial process perspective. [6a,9] However, these catalytic systems suffer from problems associated with separation and recovery of the active catalysts from the reaction media and catalyst destruction at high temperature and pressure. [6a,10]

1.3 Heterogeneous Catalysis

Heterogeneous catalysts are distinguished from homogeneous catalysts by the different phases present during the reaction - usually the heterogeneous catalyst is in the solid phase. [6a] Typically, the catalytically active component(s) (metal particles) are dispersed on a support. Various materials ranging from metal oxides (silica, alumina and other metal oxides) mesoporous materials (MCM-41, SBA-15) and various kinds of carbon can be employed as solid supports. [11]

The main advantage of using a heterogeneous system is the relative ease of catalyst separation from the product which aids continuous chemical processes in industry. Moreover, dispersion of the active sites (metal particles) on the support increases the surface area available for catalytic activity. It also enhances catalyst stability when high temperature and pressure reaction conditions are used by utilizing the important mechanical and morphological properties of the support. [12] However, heterogeneous catalysts suffer from drawbacks such as irreproducibility, poor selectivity and metal leaching into the products – the latter phenomenon being particularly undesirable when using expensive transition metals and in the pharmaceutical industry where residual metal at the Active Pharmaceutical Ingredient (API) level has to be less than 10 ppm. [4] **Table 1.2** highlights the advantages and disadvantages of homogeneous and heterogeneous catalysis. By harnessing the advantages of both these systems, challenges associated with catalyst separation, metal leaching, catalyst stability and selectivity have in many instances been overcome- by immobilizing the homogeneous catalyst on a solid support.

Table 1.2. Comparison of homogeneous versus heterogeneous catalysts. [6,10-12]

Homogeneous	Heterogeneous
-Catalysts: Metal complex -Better defined single active sites, as a result: • Selectivity for desired product can be tuned. • Mechanisms of reactions are better understood. -Operate under milder reaction conditions.	-Catalyst: metal or metal oxide on a support. -Multiple active sites are not well-defined, as a result: • Selectivity for desired product is usually poor. • Catalysts and reactions are often irreproducible. -Requires high temperatures and pressures.
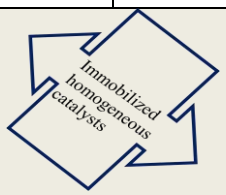	
-Often decomposes at high temperatures and pressures leading to activity loss. -Separation from reaction mixture is a challenge and costly. -Special reactions: hydroformylation of alkenes, methanol carbonylation and asymmetric synthesis etc.	-Stable to high temperatures and pressures. -Easily separated from the reaction mixture. -Special reactions: Harber process, exhaust emission catalytic convertors.

1.4 Immobilized homogeneous catalysts

Interest in the development of environmentally benign syntheses and industrially competitive catalysts has led to immobilization of homogeneous systems (transition metal/organometallic complexes) on soluble and insoluble supports. The idea is to anchor the homogeneous catalyst to a support, thus combining the advantages of homogeneous and heterogeneous catalysis. [9] Supports can be materials such as synthetic polymers (polystyrene, polyacrylates etc.), inorganic oxides (functionalized silica or alumina), dendritic scaffolds or biopolymers (cellulose, chitosan, wool etc).[9,13-14] The supported homogeneous catalysts often retain their activity and selectivity, can be readily separated from the product(s) and operate under mild conditions identical to their homogeneous counterpart. Furthermore, recycling the catalyst by means of simple filtration is made possible leading to lower energy costs and greener technologies. For these reasons, there have been extensive investigations into synthesizing, characterizing and examining various polymer-supported catalysts. [13-14]

This chapter reviews some of the, organic polymer-, inorganic hybrid polymer-organometallic polymer- and biopolymer-supported homogeneous catalysts that have emerged from this research field. Focus is placed on their use in the more common industrial and organic synthetic processes, such as, polymerization, oligomerization, metathesis, hydroformylation, carbonylation, hydrosilylation, carbon-carbon cross-coupling, oxidation, Diels-Alder, hydrogenation, N-Arylation, as well as Michael and Huisgen additions. Thus, other catalytic transformations, including, aldol condensation, halogenation, hydroboration, allylic substitution, to name but a few, are excluded for reason that would render this review far too elaborate. Detailed information on these can be found in the literature. [13] Discussion aspects around the supported catalysts' activity and selectivity, stability (in comparison to their homogeneous counterparts where applicable), recyclability, extent of metal leaching, reaction conditions and/or media and preparation (in some examples) are highlighted.

1.5 Synthetic organic polymer-immobilized homogeneous catalysts.

From a synthetic polymer point of view, polystyrene (PS) is the most popular support due to its cost effectiveness, mechanical robustness and chemical inertness. [9,13i] PS may be cross linked with divinylbenzene (DVB) giving rise to Merrifield's resin which was first employed in synthetic procedures in the 1960s. [15] However, other organic polymers such as polyethylene glycol (PEG), polyethylene (PE), polyacrylic acid (PA) amongst others are well documented in literature. [16]

1.5.1 Phosphinated organic polymer supports.

Phosphines are the most widely used ligands in homogeneous catalysis systems, due to their remarkable stabilizing capabilities through a combination of electronic and inductive effects in comparison to other ligands. In light of this, phosphine functionalized supports were originally produced in the 1970s to provide extra stability and support for homogeneous catalysts. Triphenylphosphine polystyrene (PS-PPh_3, **1.1**) and diphenylphosphinomethyl polystyrene (PS-PPh_2, 1.**2**) have been the most commonly employed in this regard (**Fig. 1.1**).[17] Polymers (**1.1** and **1.2**) can be readily obtained commercially and coordinate to many metals (e.g. Ru, Rh. Ni, Pd, Pt). [13g]

(**1.1**) (**1.2**)

Fig. 1.1. The two most popular phosphine-functionalized polymer supports.

Metathesis

Since its discovery, olefin metathesis has experienced dramatic developments allowing for the synthesis of both well-defined functional polymers, block-co-polymers and complex organic molecules of commodity, optical and pharmaceutical relevance. Access to these has been made possible through various metathesis-based reactions such as ring-opening metathesis polymerization (ROMP), acyclic diene metathesis (ADMET), ring-opening cross metathesis and ring-closing metathesis. In 2005, Y. Chauvin, R. H. Grubbs and R. R. Schrock were awarded the Nobel Prize in Chemistry for the development of the metathesis method.

The first well-defined supported Grubbs-type metathesis catalysts (**1.3** and **1.4**), using phosphine derived polystyrene-co-divinylbenzene (PS-DVB), were reported in 1995 (**Fig. 1.2**). These supported catalysts displayed low activity in metathesis of *cis*-2-pentene and ring-opening metathesis polymerization (ROMP) of norborn-2-ene. Selectivity was also said to depend on reaction time. [18]

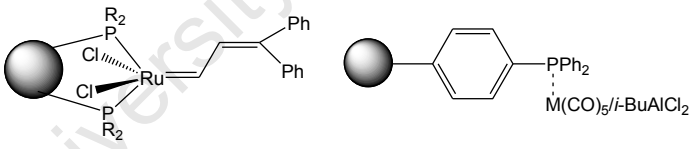

(**1.3**), R = Ph
(**1.4**), R = Cy

(**1.5**), M = Mo
(**1.6**), M = W

Fig. 1.2. Phosphinated polymer-supported metathesis catalysts.

Using polymer (**1.1**), molybdenum and tungsten supported catalysts (**1.5** and **1.6**) were prepared and found to be active for the metathesis of *trans*-3-heptene with good separation and recyclability (**Fig. 1.2**). [19]

Carbon-carbon cross-coupling reactions: Suzuki-Miyaura, Heck and Sonogashira

Since their discovery in the 1970s, palladium-catalyzed carbon-carbon cross-coupling reactions have played an important role in organic synthesis, particularly as a means to accessing molecules or intermediates of biological relevance. The Heck, Stille, Suzuki-

Miyaura, Negishi and Sonogashira reactions facilitate the formation of carbon-carbon bonds between not only sp^2 carbons as was originally, but also between combinations of sp, sp^2 and sp^3 carbon atoms. The impact of these transformations and importance has recently been recognized through the awarding of the 2010 Nobel Prize in Chemistry to R.F. Heck, E. Negishi and A. Suzuki. [20]

Rather surprisingly, the first example of a polymer-assisted Suzuki reaction was reported only in the late 90s, where PS-Pd^0 catalyst (**1.7**) was used for coupling a number of organoboranes with alkenyl bromides, iodobenzene and aryl triflates (**Fig. 1.3**). Yields comparable to those obtained with the homogeneous catalyst [$Pd(PPh_3)_4$] were reported and the catalyst could be used up to ten times. [20h]

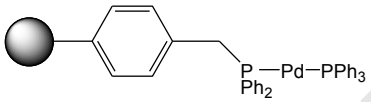

(**1.7**)

Fig. 1.3. Phosphinated polymer-supported Suzuki-Miyaura cross-coupling catalyst.

In 2005, Luo *et al.* described a carboxylate-bridged palladacycle-supported catalyst (**1.9**). This palladacycle was attached by metallation of phosphine containing polymer (**1.8**) (**Eq. 1.1**). Catalyst (**1.9**) was then successfully used in Heck chemistry and could be recycled four times (yields of cinnamate of up to 80%). [21]

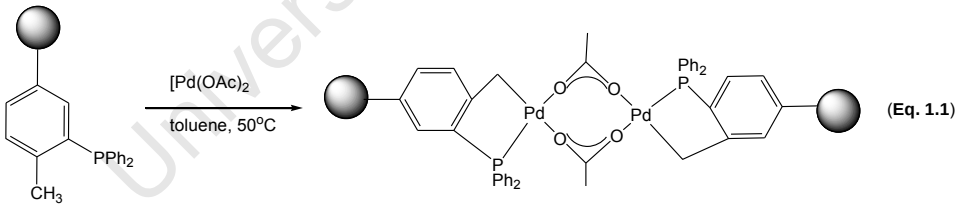

(**1.8**) (**1.9**) (**Eq. 1.1**)

Coupling of aryl chlorides with boronic acids and esters etc. is a challenge, due to the lower activity of aryl chlorides relative to the corresponding aryl iodides or bromides. However, aryl chlorides are of interest due to their low cost and availability.

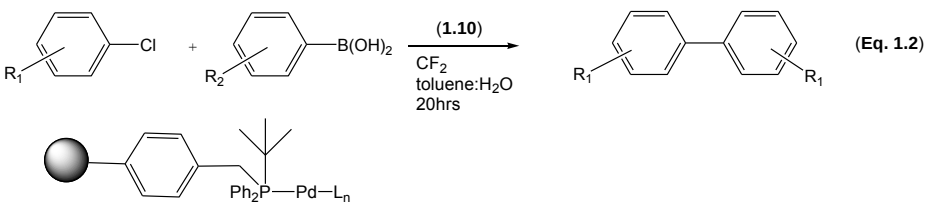

(**1.10**) (**Eq. 1.2**)

Supported complex (**1.10**) was applied in the formation of biaryl compounds from aryl chlorides using 0.4 mol% palladium (**Eq.1.2**). The catalyst could be recycled up to seven times without significant loss of efficiency. [22]

Bekherad *et al* prepared a palladium(0) diphenyphosphine ethane (dppe) complex attached to a PS support (**1.11**) (**Eq. 1.3**) and applied this in the copper-free Sonogashira coupling of terminal alkynes with aryl acid chlorides. The supported catalysts could be recycled up to 10 times after which product yields dropped. [23]

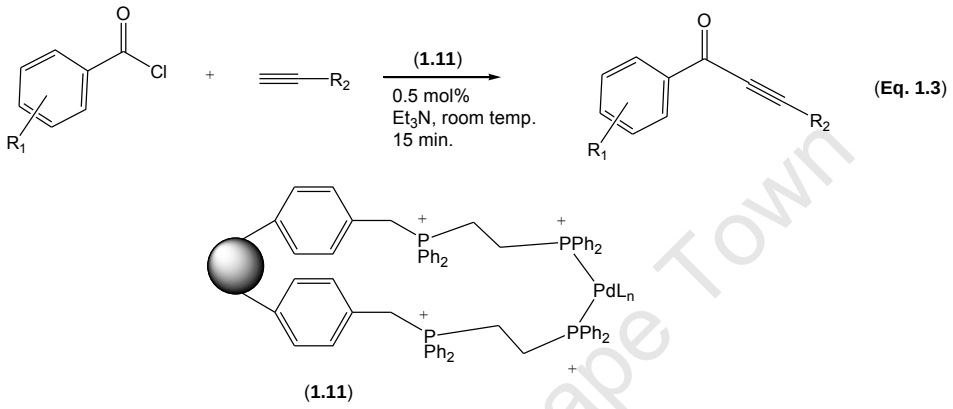

Hydroformylation

Hydroformylation has been widely used in industry for the production of aldehydes since its discovery in 1938. Over the past decades, much effort has been directed toward the synthesis of highly active and selective catalysts for the hydroformylation reaction, using different transition metals. [6b,24a] The most commonly used catalysts for this reaction are based on rhodium complexes due to its high activity and selectivity at milder conditions, therefore the current section discusses rhodium-supported catalysts only.

Fujita *et al.* have prepared a supported catalyst *in situ* from [Rh(acac)$(CO)_2$] and phosphinated polymer (**1.2**) (*vide ante,* **Fig. 1.1**). The resulting catalyst was applied in the hydroformylation of 1-hexene with syngas ($CO:H_2$, 1:1) (**Eq. 1.4**). The reaction was carried out in both supercritical CO_2 ($scCO_2$) and in organic solvents (toluene and ethyl acetate). Reactions in $scCO_2$ displayed superior reactivity and selectivity for the desired linear aldehydes over those in organic solvents. The supported catalyst was recycled and reused three times without loss of efficiency. [24b]

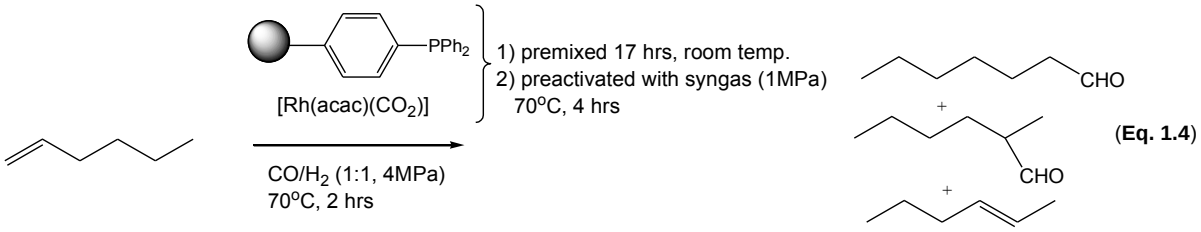

(**Eq. 1.4**)

A survey of the literature reveals that various homogeneous catalysts or catalyst precursors have been attached to phospinated polymer matrices for applications in a number of catalytic reactions and some of these are presented in **Table 1.3**.

Table 1.3. Literature examples of phosphinated polymer-supported catalysts. [25-28]

Catalyst	Catalysed reaction	Reference
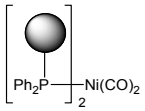	Oligomerization	25
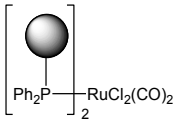	Hydrogenation	25
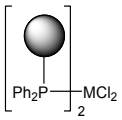	Hydrogenation	26a
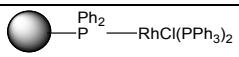	Hydrogenation	26b
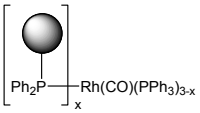	Hydroformylation	27a
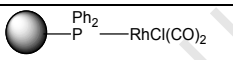	Hydroformylation	27b
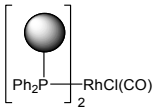	Carbonylation	27a
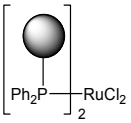	Hydrogenation	28a
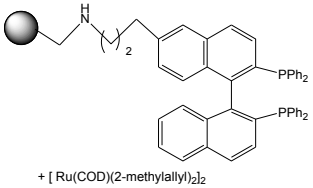	Asymmetric hydrogenation	28b

1.5.2 Non-phosphinated polymer supports.

Several types of non-phosphinated supported catalysts have been accessed through coordination of transition metals to polymer-supported versatile ligands such as oxazolines, Schiff bases and N-heterocyclic carbenes. [13c,i]

Diels-Alder

The Diels-Alder reaction has been one of the best methods for the preparation of six-membered carbocycles with control of up to four stereogenic centers in an atom-economical way. This topic has been recently reviewed by Cossy and co-workers. [13o]

Menger *et al.* described the synthesis of two copper loaded polystyrene-based catalysts and their application in the reaction of (**1.12**) with (**1.13**) (**Eq. 1.5**). The supported catalysts gave better yields than the [Cu(OAc)] catalyzed reaction. [29]

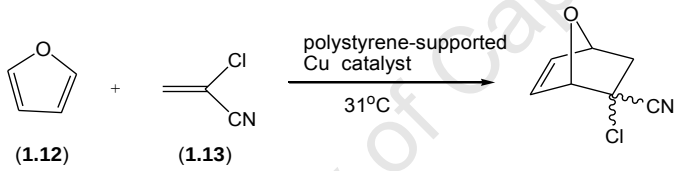

(**1.12**) (**1.13**) (**Eq. 1.5**)

Polymer-supported bis(oxazoline) copper complexes have been utilized in the Diels-Alder reaction of (*E*)-3-butenoyl-1,3- oxazolidin-2-one with cyclopentadiene. The results showed considerably lower selectivity as compared to when the mononuclear complexes were employed. [30]

Oxidation

The potential benefits of developing catalysts for selective conversion of alkanes and alkenes (readily available and fairly accessible feedstocks respectively) to more valuable oxidized products such as alcohols, aldehydes, ketones, carboxylic acids and their derivatives is of paramount importance. To this end, cross-linked polystyrene supported-Schiff base complexes of Fe^{III}, Co^{II}, Ni^{II} and Cu^{II} were shown to be highly active catalysts in the oxidation of cyclohexene and styrene using H_2O_2 as an oxidant. The reactions displayed a

first order dependence on the concentration of the substrate and the catalysts, while moderately cross-linked (10%) polymers showed enhanced catalytic activity. [31]

The polymer-supported cobalt complex (**1.14**) (**Fig. 1.4**) was used in oxidation of cyclohexane in the presence of molecular oxygen. A mixture of cyclohexanone and cyclohexanol was obtained without leaching of cobalt metal from the polymer support.[32a]

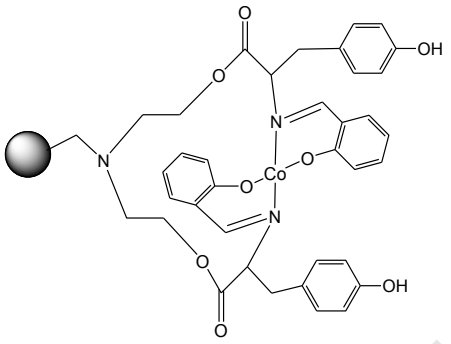

(**1.14**)

Fig. 1.4. Polymer-supported cobalt Schiff base oxidation catalyst.

More recently a thiosemicarbazone Cu^{II} complex anchored on a polystyrene support was found to be highly active for oxidation of alkenes (styrene, cyclohexene, cyclooctene, limonene and α-pinene) using H_2O_2 as an oxidant. Excellent selectivities for aldehydes (up to 93%) and ketones (up to 100%) were recorded and the catalysts could be reused five times without significant loss of activity. The supported catalyst was more active than its homogeneous counterpart. [32b]

Polymerization and Metathesis

Considerable attention has been paid to the immobilization of metallocene complexes (for polymerization of olefins) on polymer supports. Unlike the inorganic supports, the organic polymer supports do not significantly affect the properties of the final polyolefin. [13l] As such, Stark *et al.* reported that bis(cyclopentadiene) zirconium dichloride supported on cross-linked PS produced polyethylene (PE) with catalyst activities of 13 kg (PE/mol Zr h bar) for MAO/Zr = 300 and 167 kg (PE/mol Zr h bar) for MAO/Zr = 2000 at 70 °C (MAO = methyl aluminium oxide). The homogeneous counterpart catalyst [Cp_2ZrCl_2] (Cp = cyclopentadiene) showed a relatively higher activity of 507 kg (PE/mol Zr h bar) for MAO/Zr = 1000. The PE

obtained exhibited high molecular weight (M_w > 6000 00 g/mol), a relatively narrow dispersity (M_w/M_n = 2.9-3.4), was spherically shaped and in the millimetre range in size. [33]

A series of unbridged metallocene dichlorides [Cp^*CpMCl_2] (Cp^* = C_5Me_4H and M = Ti and Zr) were anchored on Merrifield resin. When used for ethylene polymerization (MAO/M = 1000) these systems exhibited a low activity of between 20 to 161 kg (PE/mol M h bar). The PE particles that formed were irregular in shape. Encouragingly, no reactor fouling indicative of metal leaching was observed. [34]

The immobilization of [$RuCl_2(PCy_3)_2$(=CHPh)] on a polyvinylpyridine based resin has been reported (**Eq. 1.6**). Turnover numbers of < 20 were observed for various ring-closing metathesis (RCM) reactions using catalyst (**1.15**) which also showed 10% activity by the fifth cycle. Ruthenium contamination of the product was much lower than when using homogeneous catalysts. [35]

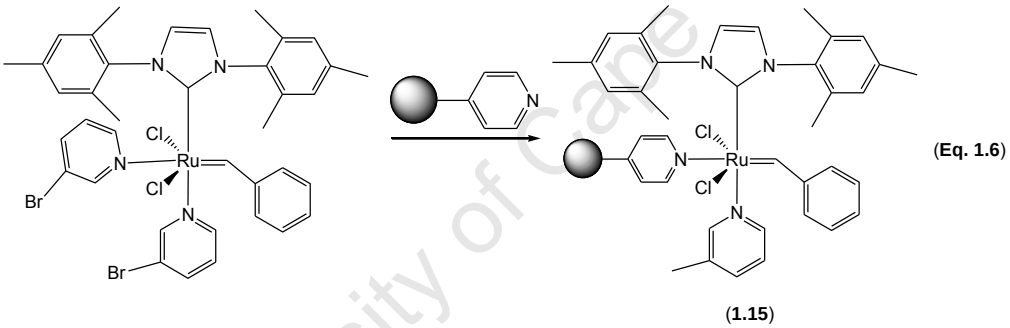

(**Eq. 1.6**)

(**1.15**)

Various supported versions of [MoO_3] based catalysts are widely used in industrial petrochemical processes. [18b,36] However, few examples of supported well-defined Schrock type catalysts are known due to the oxygen and moisture sensitivity of these molybdenum based systems. Buchmeiser and co-workers reported on the synthesis of a supported chiral Schrock catalyst (**Scheme 1.1**). The polynorbonene support displayed excellent swelling attributes, resulting in better accessibility to catalytic sites and so lower amounts of catalyst required for metathesis reactions. Molybdenum leaching was reported to be < 5%. [37]

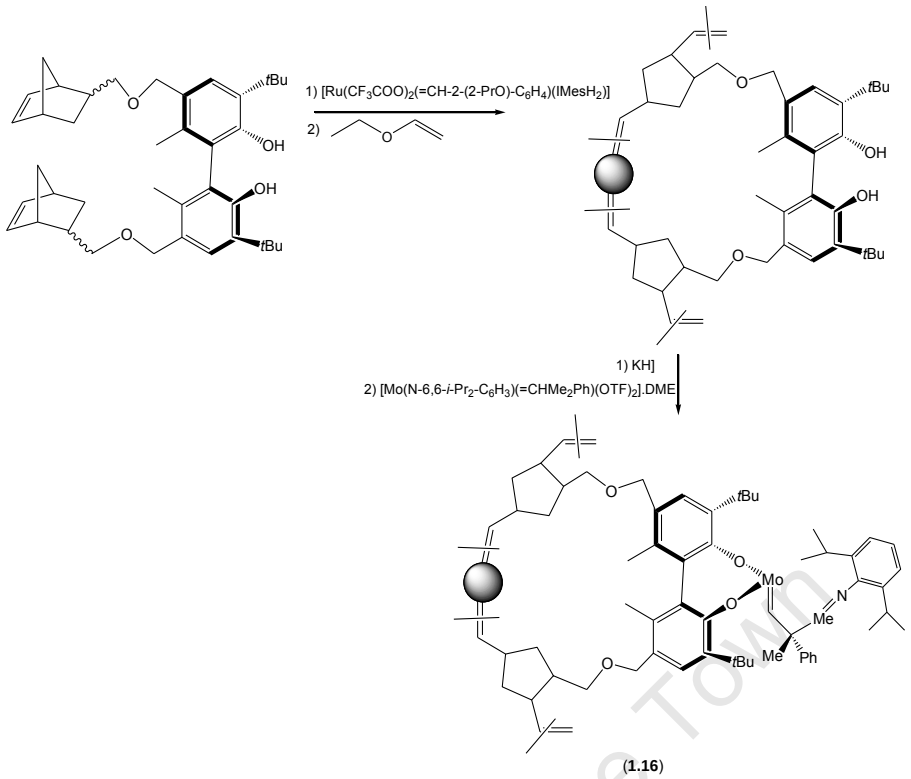

Scheme 1.1. Outline of the preparation of supported chiral Schrock catalyst (**1.16**).

Hydrogenation and hydroformylation

Paul Sabatier discovered nickel-catalyzed hydrogenation in 1897 and since then it has developed into a pivotal reaction in industry and academic research laboratories. [38a] This process is used in forming petrochemicals, pharmaceuticals (including chiral molecules) and foods - employing either H_2 gas or hydrogen transfer agents using various platinum group metals.

A series of asymmetric transfer hydrogenation rhodium catalysts supported on polyester, polyureas and polythioureas were described by Lamaire and co-workers. These supported catalysts promoted transfer hydrogenation of acetophenone in the presence of 2-propanol and potassium hydroxide at 70 °C. Substrate conversions varied from 20-100 % while enantioselectivities (ee) were in the range of 0-60%. Furthermore, recycling the catalyst was possible with no loss of activity and enantioselectivity. [38b]

Asymmetric transfer hydrogenation of acetophenone was also described using a polymer-supported N-toluenesulfonyl-1,2-diphenyl ethylenediamine (TsDPEN) ruthenium catalyst (**1.17**) (**Eq. 1.7**). It was found that the degree of cross-linking of the polymer support was of

lesser importance to activity, where even the highly cross-linked polymer supported catalyst afforded high product yield. [39]

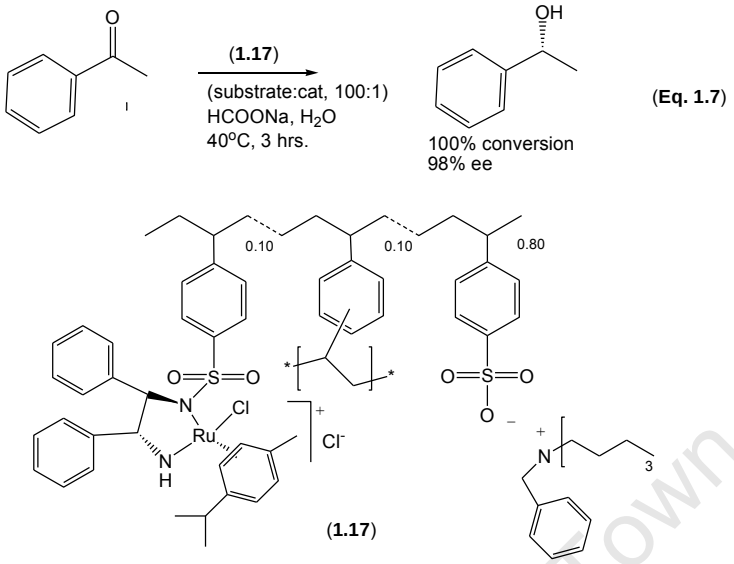

The poly(oxazoline) rhodium catalyst (**1.18**) was successfully reused four times in hydroformylation of 1-octene under aqueous biphasic conditions using a mixture of water and 1-octene (**Fig. 1.5**). The turn-over frequency (TOF) varied from 1100 to 2360 h^{-1} and rhodium leaching into the product phase was found to be 2.7% as determined by inductively coupled plasma optical emission spectroscopy (ICP-OES). [40]

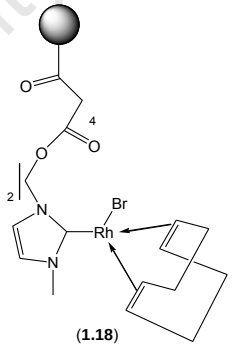

Fig 1.5. Poly(2-oxazoline)-supported rhodium hydroformylation catalyst (**1.18**).

Carbon-carbon cross-coupling

Due to the crucial role which carbon-carbon cross-coupling reactions play in organic synthesis as a means of accessing target drugs and their intermediates, much effort has been placed in developing more efficient polymer-supported palladium catalysts for this purpose. **Table 1.4** below presents a few of the systems that have emerged in the past five years.

Table 1.4. Literature examples of polymer-supported catalysts used for carbon-carbon cross-coupling reactions.

Catalyst	Support	Coupling reaction	Comments	Ref.
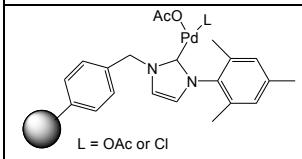	Macroporous polystyrene (PS)	Suzuki-Miyaura	Reasonable yields of coupled products obtained in aqueous dimethylformamide (DMF) at 80°C over 8-18 hrs.	41
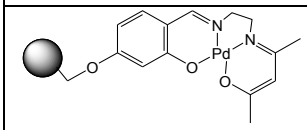	Merrifield resin	Suzuki-Miyaura	High yields of coupled products obtained in aqueous toluene at 90°C over 24 hrs. < 1ppb of Pd leached into the products.	42
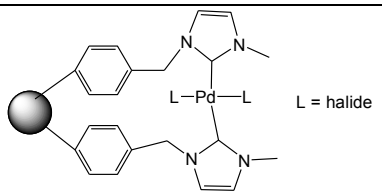	PS	Sonogashira, Suzuki-Miyaura and Heck	Yields of coupled products varied from 90-98%. Reactions were carried out using $CsCO_3$ and piperidine bases at 60 and 100°C respectively.	43
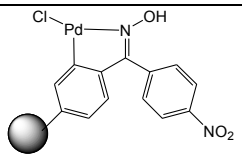	PS	Heck	87% yield of coupled product using 1 mol% of catalyst. Efficiency of the supported catalyst was in line with the homogeneous catalyst. Negligible (0.06-0.08 ppm) Pd leaching.	44
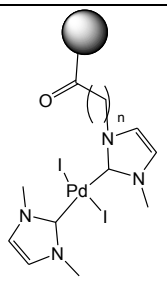	Poly(2-oxazoline)	Heck and Suzuki-Miyaura	Good catalytic activities with *ca* 93% yields after 3 hrs at 90°C using 0.67 mol% catalyst in the Heck reaction. High TOF (5200 h^{-1}) achieved with 0.1 mol% catalyst at 80°C in the Suzuki reaction.	45
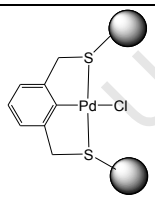	Poly(ethylene glycol)	Heck	Reactions performed in aqueous dimethylacetamide (DMA) under microwave in over 10-30 minutes using 0.01 mol% catalyst. Pd leaching was < 0.5% and catalyst/product separation effected by phase separation.	46a,b
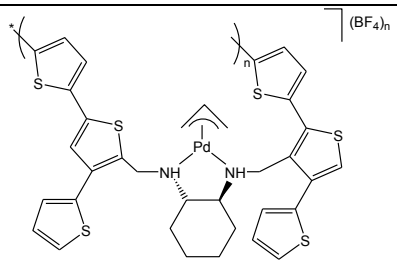	Polythiophene	Suzuki-Miyaura	Good yields of coupled products in toluene:MeOH. The supported catalyst was easily recoverd and reused six times.	46c

1.6 Inorganic hybrid polymer-immobilized homogeneous catalysts

Homogeneous catalysts have also been covalently attached to inorganic polymer based supports in efforts to overcome expensive separation and purification steps as well as catalysts costs. Typically, the inorganic surface or inorganic polymer is functionalized with a ligand site of organic or polymeric nature followed by complexation of the metal to the support as illustrated in **Scheme 1.2**. [47-52] The most commonly used inorganic supports are silicone based materials such as silica, silane, polysilane and polysiloxane. **Table 1.5** presents some of the polymerization, oxidation, Heck cross-coupling, hydrosilylation and hydrogenation supported catalysts that have been reported in this area.

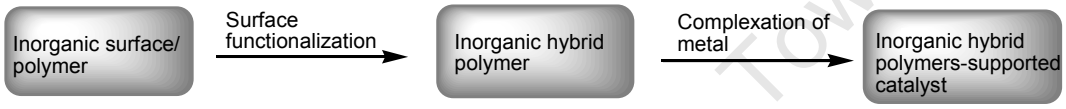

Scheme 1.2 Simplistic illustration of the preparation of inorganic hybrid polymer-supported catalysts.

Table 1.5. Literature examples of inorganic hybrid polymer-supported catalysts.

Catalyst & support	Catalyzed reaction	Comments	Ref.
Polymethylsiloxane- Zr	Polymerization (MAO co-catalyst)	Activities of 70 kg (PE/mol Zr h bar) with Al/Zr = 600 and 14 kg (PE/mol Zr h bar) with Al/Zr = 50 were displayed at 60°C	47a
Amino silica-Ti	Polymerization (borane/alkylaluminium co-catalyst)	Activities of ≈ 29 kg (PE/mol Ti h bar) with Al/Ti = 400 at 25°C over 10 minutes. The supported catalyst displayed superior activity over homogeneous analogues.	11g
Spherical polysiloxane-Mo	Epoxidation (*tert*-butyl hydroperoxide oxidant)	High activity and selectivity was displayed and supported catalyst's activity was superior to $[MoO_2(acac)_2]$.	48
Aminoethoxy silane-Mn	Asymmetric epoxidation (NaOCl oxidant)	High activities (yields: 90-99%) and enantioselectivity (ee: 69-96%) displayed at 0°C. Catalyst was recycled four times with retention of enantioselectivity. No leaching of Mn was detected by inductive coupled plasma (ICP).	11h
Linear, star & hyperbranched polysiloxane-Pd	Heck cross-coupling (methyl- &butyl-acrylate with iodobenzene)	Activity of the supported catalysts were comparable to $[PdCl_2(PhCN)_2]$. Supported catalysts were reused ten times with considerable Pd leaching evident by X-ray fluorescence analysis (XRF).	49a
Soluble polysiloxane-Pd	Heck cross-coupling (methyl acrylate with iodobenzene)	Activity of the supported catalyst was comparable to $[PdCl_2(PhCN)_2]$. Supported catalyst was reused five times with low Pd leaching as determined by atomic absorption spectrometry (AAS).	49b
Polysiloxane capsules-Pd	Heck cross-coupling (methyl acrylate with *p*-substituted iodobenzene)	The supported catalyst was active and stereoselective for *trans*-coupled products and was reused.	50
Vinyl polysiloxane-Pt & Rh	Hydrosilylation (with dimethylphenylsilane)	Both Pt and Rh supported catalysts exhibited good activity at 40°C and the activity decreased with repeated use.	51a
Arsine silica-Rh	Hydrosilylation (with triethoxysilane)	Good activities (yields: 89-92%) were displayed at 95°C. The supported catalyst was reused four times without loss of activity.	51b
Zeolite polysiloxane-Pd	Hydrogenation (with H_2)	Excellent activities (yields: 91-100%) were displayed at 40°C. The supported catalyst was reused several times without appreciable loss of activity.	52a
Cp^* polysiloxane-Rh ($Cp^* = C_5Me_4H$)	Hydrogenation (with H_2)	Supported catalysts displayed moderate activity (TOF: 1.60 mol (mol/Rh min.)) and selectivity.	52b

1.7 Organometallic polymer catalysts

A wide variety of organometallic polymers have become available since the 1990s. This has been achieved through the development of new compatible synthetic approaches. Thus, organometallic polymer research has advanced through i) preparing such material in high molecular weight, ii) elucidating their properties (including redox, optical and magnetic) and iii) applying them as functional materials. Notable applications of organometallic polymers include in sensors, memory and light emitting devices, solar cells, nanolithography, conducting materials, controlled release and catalysis. [53-56] The appeal of organometallic polymers for catalysis lies in the fact that, unlike organic- and inorganic hybrid-polymer supported catalysts, these possess inherent well-defined active sites which eliminate negative effects such as poor accessibility, random anchoring, or disturbed geometry - phenomena that often result in poor activity and selectivity in classical immobilization. Organometallic polymer-supported catalysts are also often soluble and thus operate under true homogeneous conditions and can be separated from solution by nano or ultrafiltration.

This section deals with the use of organometallic polymers containing transition metals in the main chain (**1.19**, **Fig. 1.6**) and the subdivision of hyper-branched/dendritic (**1.20**, **Fig. 1.6**) organometallic polymers in catalysis. [57-60] Organometallic polymers containing main group metals (e.g. Sn and Pb) and lanthanides (e.g. Eu) are excluded here - the reader is referred to the literature for reading in this regard. [61]

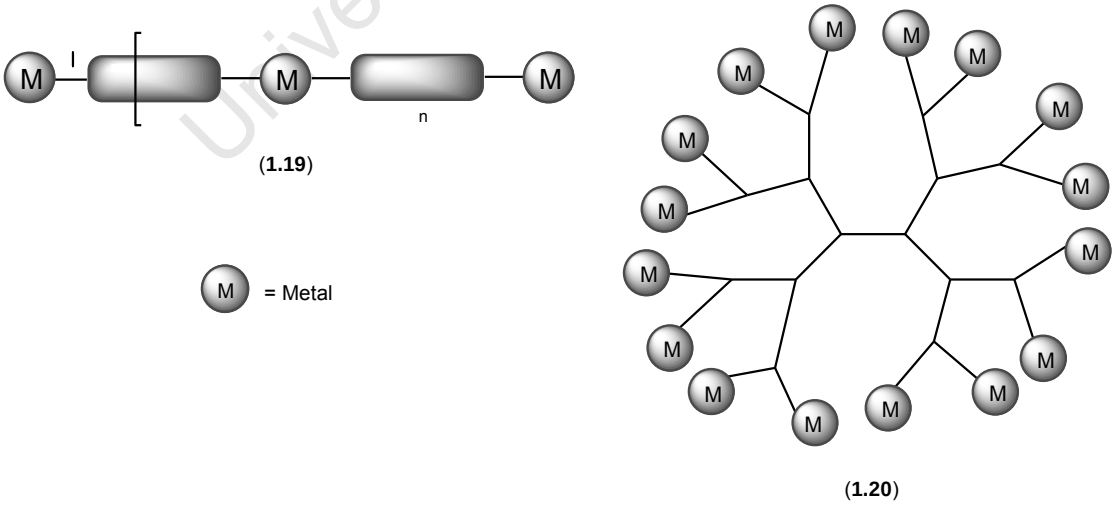

Fig. 1.6. Depiction of main chain and hyper-branched/dendritic organometallic polymers.

1.7.1 Main chain organometallic polymers in catalysis

Main group organometallic polymers can be accessed *via* two main protocols. Firstly, by polymerization of the metal-containing monomer (route (**a**), **Scheme 1.3**) which can lead to synthesis of organometallic polymers with a uniform distribution of the metal complexes and hence a higher dispersion of the metal sites - a beneficial property for catalysis. [62a] Some examples of organometallic polymer catalysts used in various catalytic reactions are listed in **Table 1.6**. Secondly, organometallic polymers can be prepared by coordination of metal salts/complexes to macromolecular or polytopic ligands (route (**b**), **Scheme 1.3**). These materials are functional metal-organic assemblies also known as coordination polymers, constructed by cross-linking of polytopic ligands with metal centres.[62a]

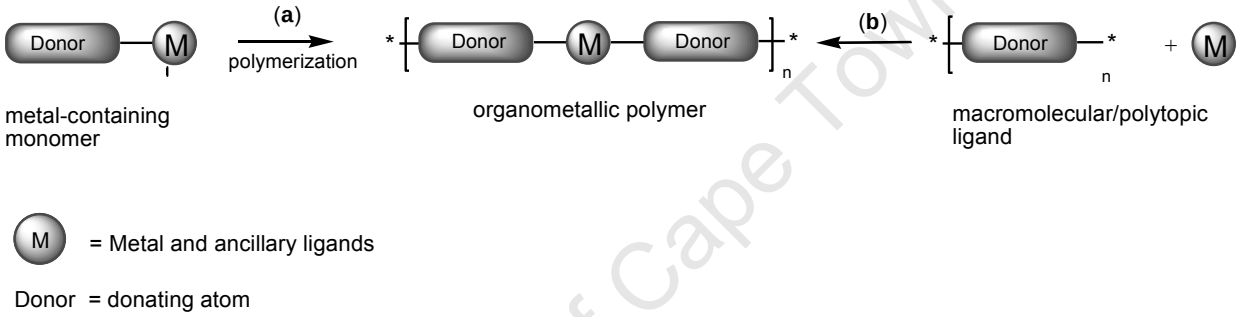

Scheme 1.3. Schematic representation of the preparation of organometallic polymers.

Table 1.6. Examples of organometallic polymers prepared *via* route (**a**) and their catalyzed reactions.

Metal-containing monomer	Co-monomer	Reaction catalysed	Comments	Ref.
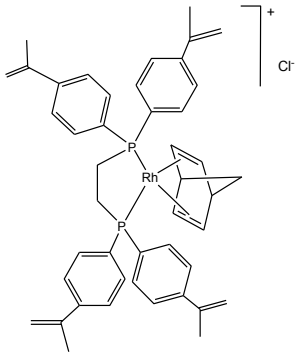	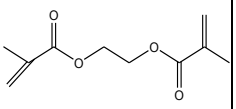	Hydrogenation	The supported catalyst was active in hydrogenation of alkenes (yields: 88-99%). The supported catalyst was less reactive than its homogeneous counterpart and reused six times with slight decrease in activity.	63
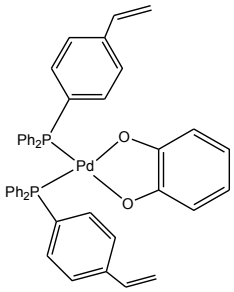	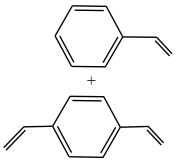	Suzuki-Miyaura & Stille cross-coupling	Suzuki-Miyaura reaction: *p*-bromoanisole and phenylboronic acid coupling gave 81% yield, while $[PdCl_2(PPh_3)_2]$ gave 55 % yield. Stille reaction: coupling of 4-nitrobromobenzene with tributylphenyltin, gave 95% yield of 4-nitrobiphenyl. The supported catalyst was reused without loss of activity.	64
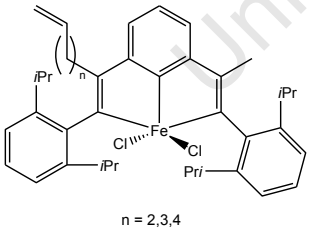 n = 2,3,4	-	Ethylene polymerization	Supported catalyst displayed lessening of fouling of the reactor walls.	65
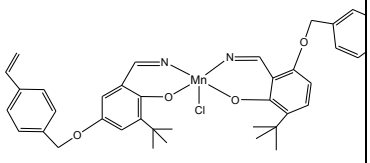	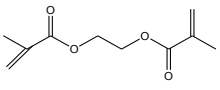	Asymmetric epoxidation	The supported catalyst was active (yield: 68%) and poorly enantioselective (ee: 30%) Low ee was counterbalanced by increased catalyst stability compared to the homogeneous catalyst.	66

Hydrogenation, Suzuki-Miyaura cross-coupling.

Rhodium coordination polymer (**1.21**) was generated through non-covalent interactions (hydrogen bonding and coordination interactions) of a chiral polyphosphine ligand with $[Rh(COD)]BF_4$ precursor. Asymmetric hydrogenation of dihydro-α-amino acid derivatives proceeded smoothly to complete conversion within 20 hrs (**Eq. 1.8**) using supported catalysts (**1.21**). The products were obtained in 91-96 % ee which was comparable to results obtained using the analogous homogeneous system. Furthermore, catalyst (**1.21**) was reused for at least ten cycles with maintained activity and ICP analyses of the product solutions did not provide evidence for metal leaching within the detection limit of the instrument. [67a]

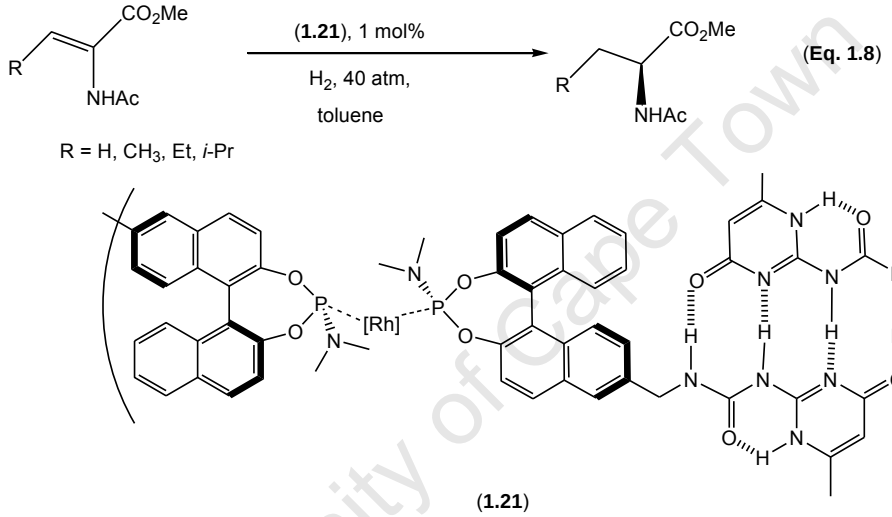

(**1.21**)

One area where organometallic polymers have potential is in electrocatalysis, where incorporation of the transition metal into a highly conductive polymer is essential. To this end, transition metal-containing polythiophene has proven effective in catalyzing the four electron reduction of dioxygen to water on an electrode. [67b]

Uozumi and co-workers reported the use of a palladium complex polymer (**1.22**) (**Fig. 1.7**) as a membrane self-assembled inside a microchannel reactor. This was then used efficiently in the Suzuki-Miyaura cross-coupling of aryl iodides with aryl boronic acids under microflow conditions. Instant and nearly quantitative formation of coupled products in the channels was observed. The authors concluded that self assembling of organometallic polymers inside a microchannel reactor might be advantageous for performing catalytic reactions compared to the conventional flask reaction system. [68]

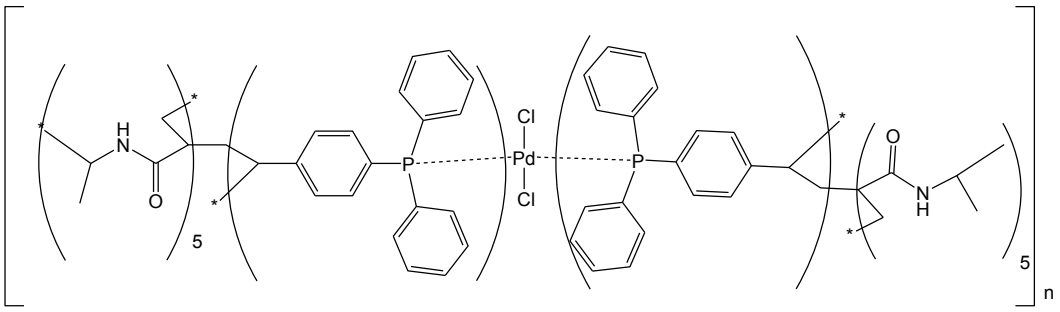

(**1.22**)

Fig. 1.7. Palladium-cross-linked polymer (**1.22**) used in Suzuki-Miyaura coupling reactions.

Oxidation and polymerization.

Mori and co-workers showed that a three-dimensional microporous organometallic polymer (**1.23**) (**Fig. 1.8**) is an effective oxidation supported catalyst. Thus, oxidation of primary or secondary alcohols proceeded with moderate activity (TOF: 0.04-0.8h^{-1}) under ambient pressure of O_2 or air at room temperature. Excellent selectivity for the corresponding aldehydes or ketones (selectivities: 95-99%) were recorded and the supported catalyst (**1.23**) was reused at least two times without loss of activity. [69]

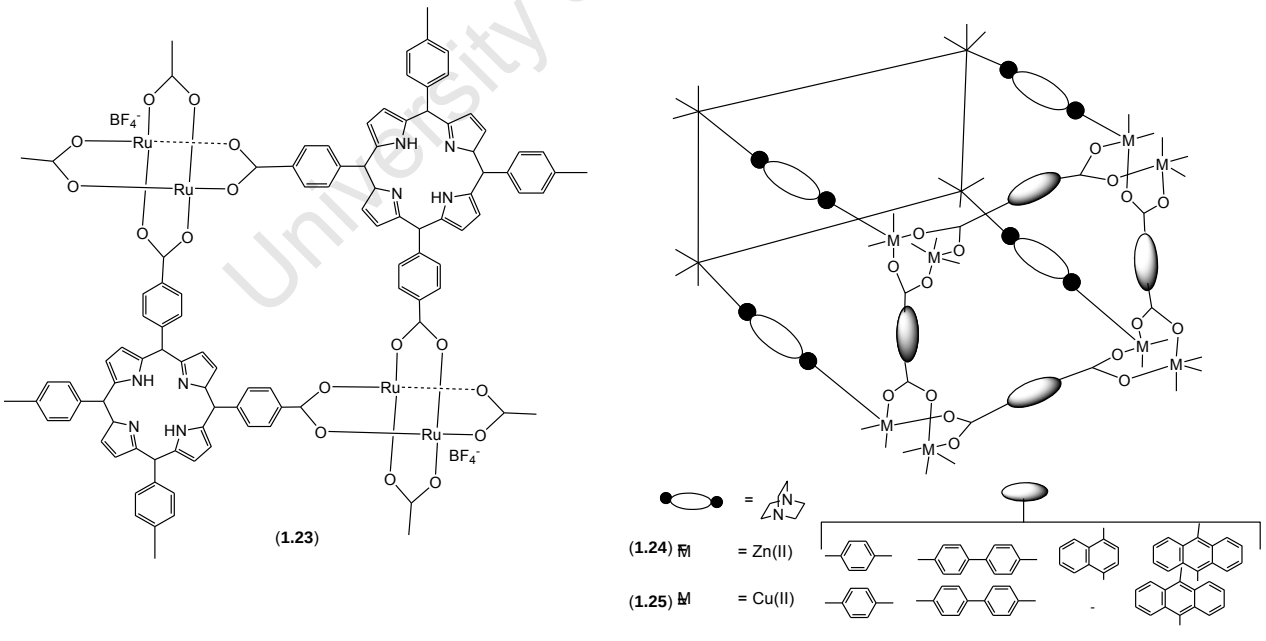

Fig. 1.8. Porous three-dimensional organometallic polymers (**1.23**-**1.25**).

The first example of radical polymerization within tunnels of porous organometallic polymers was reported in 2005 by Kitagawa and co-workers who successfully carried out styrene polymerization using supported catalysts (**1.24** and **1.25**). The resulting PS chain was encapsulated in the nanochannels and was released from the host by treatment with aqueous NaOH. Gel permeation chromatography (GPC) measurements of the resulting PS revealed similar molecular weight distributions (polydispersities, M_w/M_n: *ca* 1.6). [70]

1.7.2 Dendrimer immobilized homogeneous catalysts

Dendrimers are perfectly defined macromolecules comprising of central core emanating several generations of branches (**1.20**) (**Fig. 1.6**). This class of compounds fall within the subdivision of organometallic polymers by virtue of their hyper-branched macromolecular nature. Metal centres may be introduced into the dendrimer, either at the core, interstitial sites or periphery giving rise to metallodendrimers (which can serve as dendrimer-supported catalysts). This approach facilitates stability as well as increased concentration of active catalytic sites and thus draws from the properties of homogeneous and heterogeneous catalysis allowing for more stable catalytic structures which can be recycled by ultrafiltration. A large number of metallodendrimers and their catalytic investigations have been reported including those based on polycarbosilanes (PCS) [71], polyamidoamines (PAA) [72], polyarylethers (PAE) [73] and polypropyleneimines (PPI) [60,74]. A few examples of dendrimers used to support homogeneous catalysts follow.

Polymerization, Heck cross-coupling and hydroformylation

A carbosilane dendrimer bearing a half-sandwich titanium catalyst (**1.26**) (**Fig. 1.9**) was used in ethylene polymerization in the presence of MAO co-catalyst. The supported catalyst was moderately active giving 134 kg (PE/ mol Ti h bar). Interestingly, the aged solution of catalyst/substrate was more active affording 800 kg (PE/ mol Ti h bar) and this was attributed to formation of dendrimer aggregates with an increased size with time. PE with high molecular weight (M_w: 663,000-1,000,000 g/mol) and low polydispersities (M_w/M_n: 1.5-1.6) were obtained. [75]

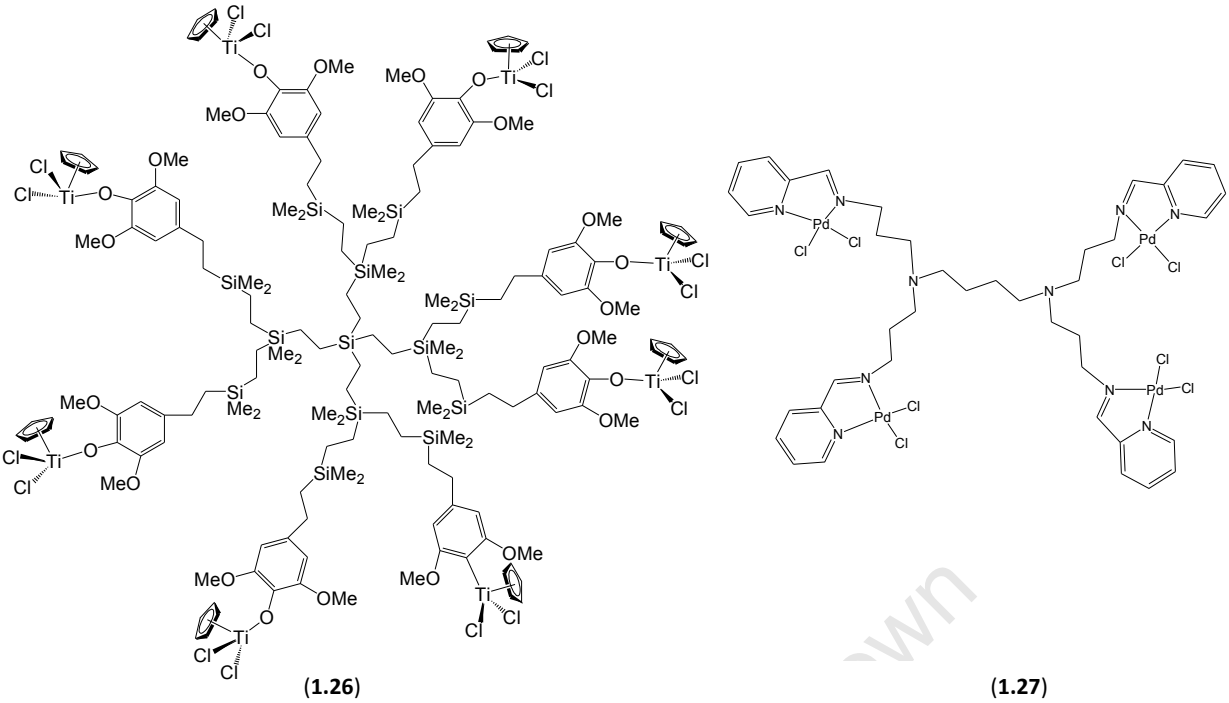

Fig. 1.9. Polycarbosilane second-generation titanodendrimer (**1.27)**.

Polypropyleneimine (PPI) has been widely used as supports for homogeneous Pd^{II}, Ni^{II} and Rh^{I} catalysts.[60,74]

PPI pyridylimine Pd^{II} supported catalyst (**1.27**) (**Fig. 1.9**) has been used for ethylene polymerization reactions in the presence of MAO co-catalyst. Activities of 39 kg (PE/ mol Pd h bar) for Al/Pd = 1000 were observed and the resulting PE exhibited a molecular weight of 1.400.000 g/mol and a polydispersity of 2.9. [60a]

The same 1st generation PPI pyridylimine Pd^{II} supported catalyst (**1.27**) was employed in Heck cross-coupling of iodobenzene with methyl acrylate and styrene at 82°C in acetonitrile. This supported catalyst displayed slightly better activity (conversion: 96% after 8 hrs) than its 2nd generation analogue (conversion: 92% after 8 hrs), while the mononuclear Pd^{II} catalyst showed comparable activity (conversion: 95% after 8 hrs). The initial slower conversion observed when using the 2nd generation metallodendrimer was attributed to a longer induction period required. The metallodendrimers proved to be stable, with no formation of any palladium black species during reactions, while the mononuclear catalysts decomposed during the reactions.

More recently 1st and 2nd generation PPI iminophosphine and pyridylimine Rh^{I} metallodendrimers have been reported as hydroformylation catalysts. These

metallodendrimer catalyst systems proved to be active in hydroformylation of 1-octene under mild conditions (75°C, 30 bars) and similar selectivity for linear aldehydes products were recorded as when the mononuclear counterpart was used. [74b]

1.8 Biopolymer-immobilized homogeneous catalysts

Recent efforts in the development of more cleaner and sustainable chemistry has led to the use of biopolymers as supports for catalysis. This is mainly because biopolymers are readily available in nature, biodegradable and non-toxic. As such, biopolymers such as starch [76], gelatine [77], alginate [78], cellulose [79], chitin and chitosan [80] have been investigated as supports for homogeneous catalysts. We now discuss chitosan-supported homogeneous catalysts.

1.8.1 Chitosan-immobilized catalysts

Chitosan is an aminopolysaccharide obtained by alkaline deacetylation of chitin (**Fig. 1.10**). Chitin is one of the most abundant polysaccharides in nature, being present in the cuticles of insects, the cell walls of fungi and the exoskeletons of crustaceans.

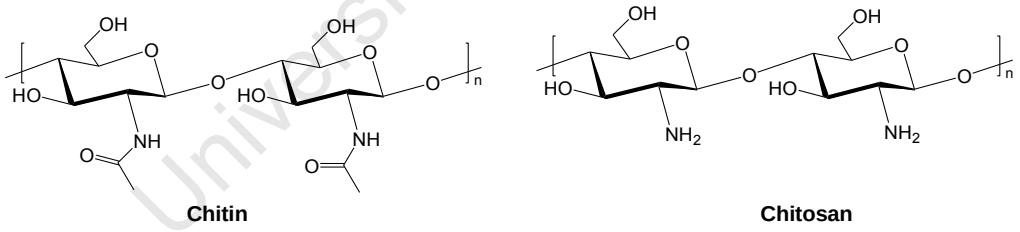

Fig. 1.10. Idealized structures of chitin and chitosan. (Chitosan is rarely 100% deacetylated, it is therefore more accurately described as a copolymer intermediate between chitin and chitosan.).

Apart from being employed as a support for catalysis, chitosan has seen applications as water treatment and metal recovery agents [81], in sensors and detectors [82,83], in food treatment [84] and in drug delivery [85] to name but a few. Indeed a growing number of papers have been published since the 80s in the area of chitosan supported catalysts. [14]

The presence of hydroxyl and amino groups (the amino groups being most important) on the chitosan allow for metal incorporation by i) chelation at near neutral pH (group (**a**) **Fig. 1.11**) ii) electrostatic attraction on protonated amine groups in acidic solutions (group (**b**) **Fig. 1.11**) or iii) chitosan metal reduction and/or co-precipitation (group (**c**) **Fig. 1.11**). A number of catalysts have been prepared by mixed metal chelation-reduction-precipitation. [14,86] Conditioning of the chitosan is essential to enhance the diffusion properties of the material which ultimately affects the diffusion of reaction substrates and products during catalysis. Thus, chitosan has been conditioned to beads, flakes, fibres and hallow fibres, membranes as well as supported on inorganic surfaces. A great deal of work on the aforementioned type of chitosan-supported catalysts has been published and discussed in recent reviews. [14,86]

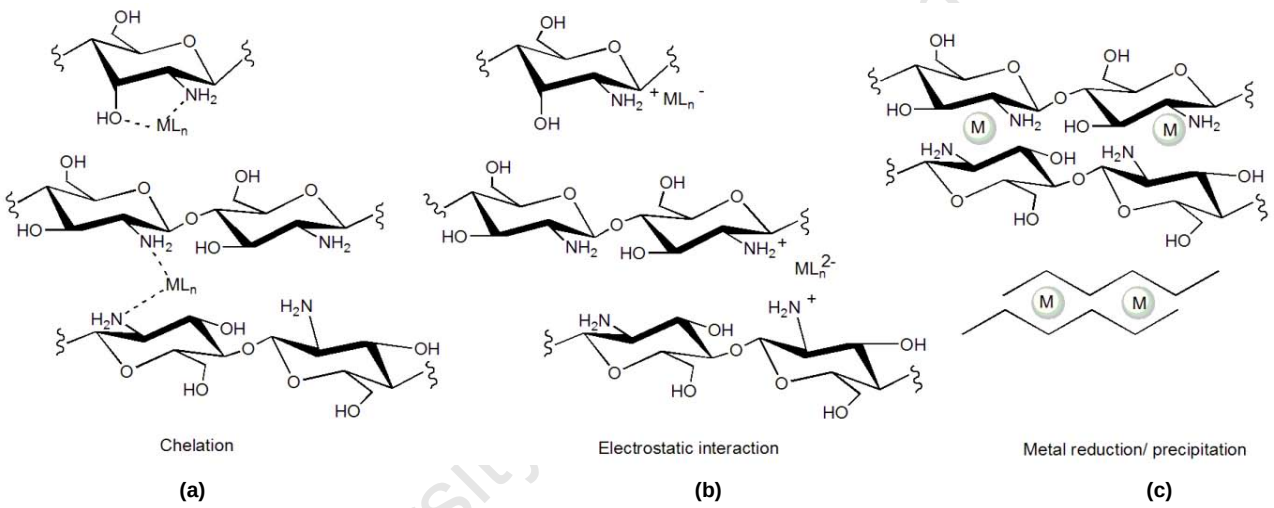

Fig. 1.11. Incorporation methods of metals onto chitosan.

Another approached to accessing chitosan-supported catalysts which has been less investigated, is coordination of metals to ligand-functionalized chitosan. This method has the advantage of i) increased catalyst stability not only by exploiting the biopolymer's mechanical properties but through strong coordination (complex formation) - which also often leads to high reduction or even total inhibition of metal leaching. Additionally, these systems open the door to better characterized and well-defined biopolymer supported catalysts (characterization can be assisted by model complexes). [87a] This in turn can lead to fine-tuning the supported catalyst to obtain desired products. The current section briefly discusses preparation and characterization aspects of ligand-functionalized chitosan-supported homogeneous catalyst and their application in various catalytic transformations.

Schiff base formation

Probably the mildest and most straightforward route to functionalizing primary amine containing materials is the reaction with an aldehyde to form the corresponding imine. This has been used for attachment of several groups, particularly aromatic aldehydes to chitosan.[87-98] In general the preparation protocol of chitosan-Schiff base supported homogeneous catalyst involves reaction of the chitosan with the corresponding aldehyde in catalytic amounts of acetic acid under reflux conditions for 10-20 hrs. Once the chitosan-Schiff base ligand is obtained it is then treated with the relevant metal precursor (e.g. Mn, Ni, Pd, Cu, Co) either at room temperature or at reflux over extended periods (1-5 days) prior to preconditioning by washing to remove loose/uncoordinated metal.

Characterization of these materials often involves the use of techniques such as i) thermal gravimetric analysis (TGA) and Differential scanning calorimetry (DSC) to determine the catalyst stability and verify content; ii) Fourier Transform infrared (FT-IR) and solid state ^{13}C NMR spectroscopy as well as powder X-ray diffraction (P-XRD) and elemental analysis to confirm modification/functionalization of the chitosan; iii) X-ray photoelectron (XPS) and atomic absorption spectroscopy as well as inductively coupled plasma (ICP) to quantify and confirm binding of the metal at ligand sites and iv) scanning electron and transmission electron microscopy to observe morphology and surface properties. [87-98]

Carbon-carbon cross-coupling reactions: Suzuki-Miyaura, Heck and Sonogashira

A chitosan iminopyridyl Pd catalyst (**1.28**) was prepared and successfully used in the Suzuki-Miyaura and Heck cross-coupling reactions (**Scheme 1.4**). For the Suzuki-Miyaura reactions the best yield (87%) was obtained at 143 °C after 6 hours. Good to excellent yields were obtained for a range of aromatic substrates. In the Heck reaction catalyst (**1.28**) gave 82% of butyl cinnamate in 42 hours at 100 °C in xylene solvent. The catalyst was reused at least five times with consistent activity for both reactions and no Pd leaching tests were recorded in the study. [88]

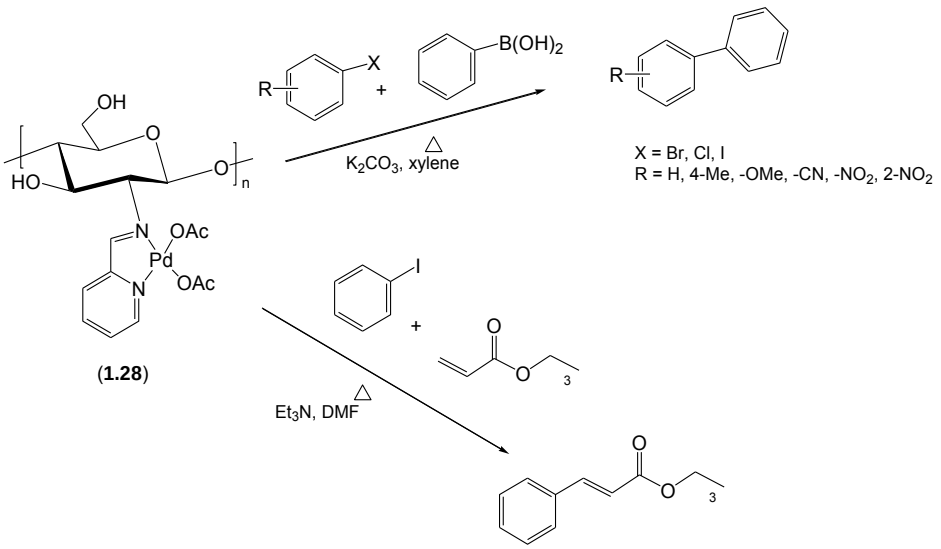

Scheme 1.4. Catalytic Heck and Suzuki-Miyaura reactions carried out using chitosan-iminopyridyl Pd catalyst (**1.28**).

In 2005, Cui and co-workers reported that 1.0 mol% of a chitosan-salicylaldimine Pd catalyst was effective in the Heck cross-coupling of acrylic acid with iodobenzene at 100 °C (yields: 97%) over 3 hours in DMF solvent. Coupling of substituted iodobenzene with styrene and methyl acrylate also afforded coupled products in good yields ranging between 94-98%. The catalyst was reused several times. Furthermore, this catalyst proved to be more efficient than a similar Pd catalyst prepared by chelation of Pd to the amino groups of chitosan. [89]

Another chitosan-salicylaldimine catalyst was reported for the Heck reaction by Xu *et al.* This catalyst proved to be highly active (yields: 80-99%) and selective (for the *trans* coupled product exclusively) in cross-coupling of substituted and unsubstituted aryliodide, with various olefins at temperatures ranging between 70-140 °C (**Eq. 1.9**). Additonally, the catalyst was recovered and reused several times. [90]

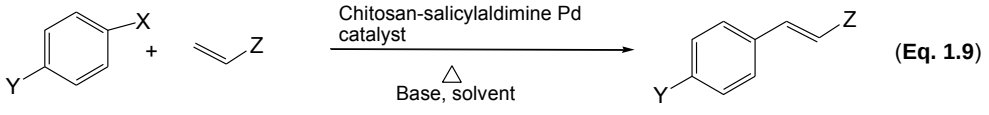

X = Br or I
Y = H,CO_2H, OMe
Z = CO_2H, $CONH_2$, CO_2Bu^n, CO_2Me, CO_2Et, Ph

Recently a chitosan-Schiff base Pd/Co catalyst (**1.29**) (**Fig. 1.12**) was reported for Heck cross coupling of acrylamide with phenyl halide. The best yield (*ca.* 86%) was afforded when a Pd:Co ratio of 3:1 was loaded onto the chitosan-Schiff base ligand. Thus, optimal conditions were established when 1:1.8 molar ratio of PhI:acrylamide, 18 mmol of Et_3N base and 0.125g

of catalyst (**1.29**) were employed in DMF solvent at 110 °C over 1 hour. Under these conditions *ca* 94% of coupled products were obtained and catalyst (**1.29**) was reused ten times without significant loss of activity. [91]

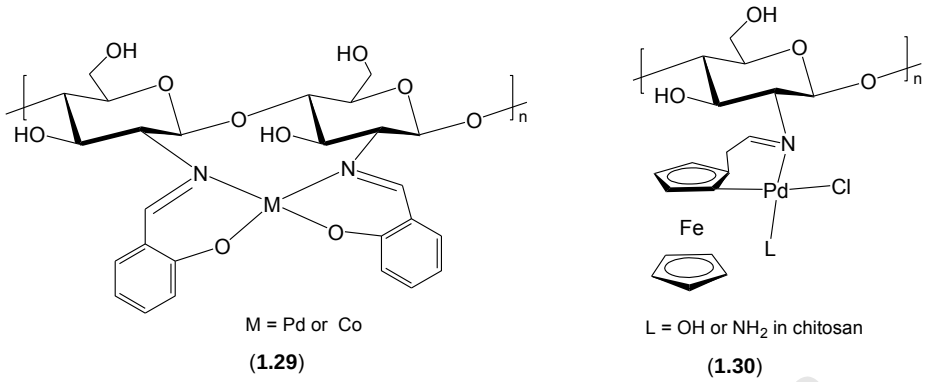

Fig. 1.12. Chitosan salicylaldimine Pd/Co catalysts (**1.29**) and chitosan-ferrocenylimine palladacycle (**1.30**).

A chitosan-ferrocenylimine palladacycle (**1.30**) (**Fig. 1.12**) was successfully used in the Heck cross-coupling of substituted and unsubstituted iodobenzene with arylamide. Optimal conditions were established when the molar ratio of PhI:acrylamide:Et_3N was 1:1.1:2.0 and using 2.3 x 10^{-2} g of catalyst (**1.30**) in DMF at 100°C over 40 minutes. Under these conditions 98% of cinnamamide was afforded and catalyst (**1.30**) was reused up to four times with consistent yields. [92] It follows therefore from these examples that having an additional metal incorporated into the catalyst assists in stabilizing active Pd sites and promotes catalysis.

Leonhardt *et al.* reported on the preparation and catalytic activity of chitosan-salicylaldimine and –pyridylimine Pd catalysts for Suzuki-Miyaura, Heck and Sonogashira cross-coupling reactions under thermal and microwave heating. Reactions were carried out effectively in organic solvents under thermal heating (Suzuki-Miyaura, yields: up to 95%) and in water under microwave heating (Suzuki-Miyaura, yields: > 99%); Heck, yields: up to 90%) and (Sonogashira, yields: up to 70%). Studies also revealed that catalysts prepared by co-precipitation afforded inferior yields. [93]

Oxidation and oxidative carbonylation

Coordination of manganese and nickel to a modified chitosan-Schiff base has been reported. These catalysts were found to catalyze oxidation of hydrocarbons such as *n*-propylbenzene, isopropylbenzene and ethylbenzene using molecular oxygen under mild conditions (1 atm, 30-40 °C) (**Scheme 1.5**). [94]

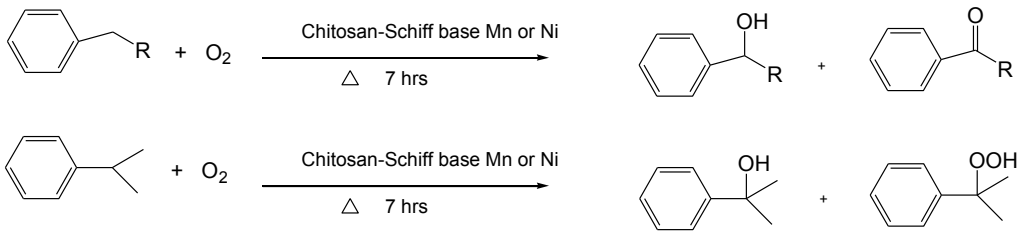

Scheme 1.5. Outline of *n*-propyl-, isopropyl- and ethyl-benzene oxidation using modified chitosan-Schiff base catalysts.

Modified chitosan-Schiff base copper complex (**1.31**) (**Fig. 1.13**) was used in the oxidation of cyclohexene using molecular oxygen (1 atm) at 27 °C over 7 hours. Catalyst (**1.31**) was active in forming 2-cyclohexen-ol (5%), 2-cyclohexen-one (16%) and cyclohexene hydroperoxide (49%) from cyclohexene as determined by GC-MS and GC-IR. [95]

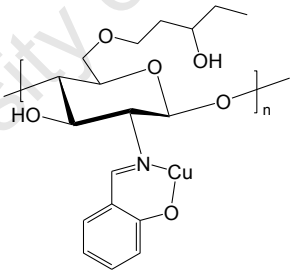

(**1.31**)

Fig. 1.13. Proposed structure of modified chitosan-Schiff base Cu catalyst (**1.31**).

Chitosan-Schiff base Co^{II} and Pd^{II} complexes have been reported in aerobic oxidation of cyclohexane to cyclohexanol, cyclohexanone and other minor unidentified by-products. For both catalysts the conversion increased with increase in oxygen pressure from 0.8-1.6 MPa. Moreover, high temperature favoured the formation of cyclohexanone. The catalysts were recovered and reused four times during which time conversion of cyclohexane dropped from *ca* 10% to 7% however, selectivity changed only slightly. [96]

Xia and co-workers reported that a chitosan-Schiff base Co^{II} catalyst was active in oxidative carbonylation of 2-aminoalkan-1-ols to oxazolidin-2-ones (**Eq. 1.10**). Optimum conditions were established when NaI promoter was used at 120 °C in 1,4-dioxane solvent over 25 hours. Under these conditions, 98% of product (**2b**) was afforded. No catalyst recovery and reuse was reported. [97]

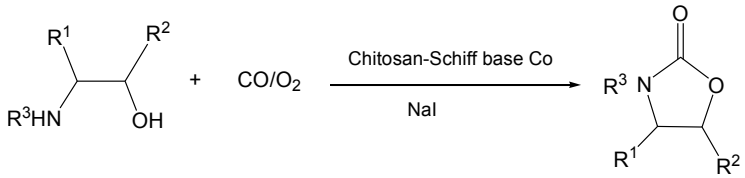

(**Eq. 1.10**)

(**1a**)	=	H H H	(**2a**)
(**1b**)	=	H Me H	(**2b**)
(**1c**)	=	Me H H	(**2c**)
(**1d**)	=	Et H H	(**2d**)
(**1e**)	=	*i*Pr H H	(**2e**)
(**1f**)	=	Me_2 H H	(**2f**)
(**1g**)	=	H H CH_2CH_2OH	(**2g**)

Cyclopropanation of olefins and [3+2] Huisgen cycloaddition

Chitosan-Schiff base copper catalyst (**1.32**) has been applied in cyclopropanation of styrene with ethyldiazoacetate (**Eq. 1.11**). Although good activities were possible (yields: up to 93%) enantioselectivity was generally very low indicating that the chiral nature of the chitosan backbone does not induce selectivity. The best results were seen with styrene:ethyldiazoacetate ratio of 17:1 and the catalyst was recovered and reused after the reactions. [98]

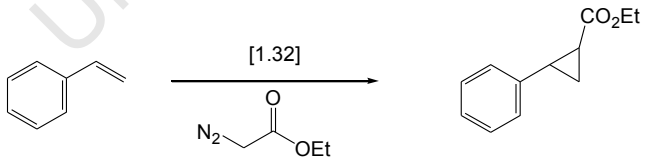

(**Eq. 1.11**)

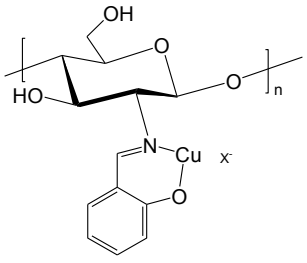

(**1.32**)

Quignard and co-workers reported a series of chitosan-Schiff base Cu^{I} catalysts for azide-alkyne Huisgen [3+2] cycloaddition ("click") reactions (**Eq. 1.12**) The best results were obtained for all the catalysts when DMSO solvent was employed. However good yields were also afforded when using the green chemistry compatible solvent EtOH (yield > 95%). The chitosan-supported catalysts were more stable in reactions carried out in air than the corresponding homogeneous catalysts. The best performing supported catalyst displayed consistent activity in the cycloaddition of phenylacetylene with benzyl azide for four cycles and no copper metal was detected by ICP from the products of each cycle. [99]

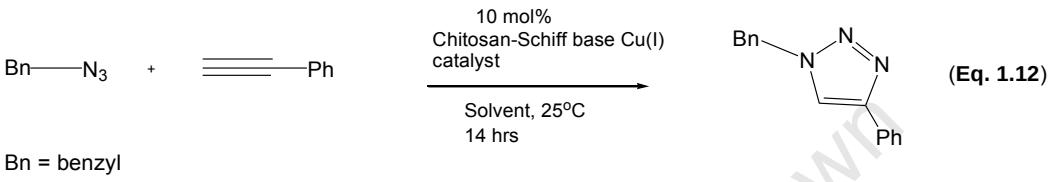

(**Eq. 1.12**)

1.9 Concluding remarks

In efforts to overcome the challenges faced by homogeneous and heterogeneous catalysis such as separation of the catalyst/product solution, catalyst stability, activity and selectivity as well as metal leaching, researchers have immobilized homogeneous catalysts on soluble and insoluble polymer supports. Other methods such as the use of ionic liquid and supercritical fluids have also been investigated, though not discussed in the current review.

Supports that have been used include organic-, inorganic hybrid-, organometallic- and bio-polymers. Organic and inorganic hybrid polymers require initial preparation and prefabrication which can lead to expensive lengthy preparation protocols, thus introducing negative effects such as reduced catalytic activity and/or selectivity, poor accessibility to the active sites, random anchoring or disturbed geometry of the active sites on the support.

Organometallic polymers have the advantage of evenly dispersed and more accessible active sites that are well-defined. This approach often results in higher activity and selectivity owing to greater similarity to homogeneous catalysis, however metal leaching still remains a problem.

The use of biopolymers is appealing because they are i) widely and readily available in nature and can be thus seen as sustainable supports, ii) they are biodegradable and non-toxic and therefore environmentally friendly. The introduction of coordinating ligands can be carried

out mildly and straightforward, thus leading to more well-defined stable catalyst systems which display negligible or no metal leaching.

Based on this knowledge, we set out to prepare and characterize biopolymer-supported transition metal complexes and organometallic polymers (metallodendrimers) for applications in catalytic carbon-carbon cross-coupling and hydroformylation reactions.

1.10 Scope and Objectives of the Thesis

There are marked developments in the use of organometallic compounds for the purpose of catalysis. These compounds are increasingly being employed as new more robust catalyst precursors by immobilization on polymers. The objectives of the research described in this thesis were to prepare and characterize biopolymer-supported transition metal complexes and organometallic polymers (metallodendrimers) and investigate their potential utility in catalysis.

Biopolymer-supported transition metal complexes: This project dealt with the preparation of chitosan- and modified chitosan-supported transition metal complexes *via* surface structural modification of chitosan. Characterization of these materials was effected using an array of spectroscopic and analytical techniques. The applicability of these supported complexes as Suzuki-Miyaura and Heck cross-coupling as well as hydroformylation catalyst precursors was then studied.

Organometallic hyperbranched polymers: Several metallodendrimers have been reported in the literature. Our approach centred on functionalisation of the periphery of low generation or intermediate sized tris(2-aminoethyl)amine dendrimer. The aim of this work was to introduce terminal pyridylimine ligands on the periphery of the dendrimer, in order to subsequently complex transition metals at these sites. The resulting metallodendrimers were fully characterized and their efficacy as hydroformylation catalyst precursors was studied.

1.11 Organization of the Thesis

This thesis is divided into two sections, **Section I**, which encompasses **chapter 2** and **3** deals with the preparation and characterization of chitosan- and modified chitosan-supported transition metal complexes using Schiff base condensation chemistry and their applications in catalysis respectively. **Section II** comprises **chapters 4** and **5** and details the synthesis and characterization of organometallic polymers (metallodendrimers) and their applications in catalysis respectively.

Chapter 1 provides an overall background and describes the scope of the thesis. In this chapter, the approaches to immobilizing transition metal complexes on various polymer supports (such as organic-, inorganic hybrid-, dendritic- (hyber-branched) and bio-polymers) and their effectiveness in various catalytic reactions is described.

Chapter 2 details the preparation and characterization of new chitosan- and modified chitosan-supported Pd^{II} and Rh^{I} complexes. The preparation and characterization of mononuclear analogues of these compounds are also discussed. These compounds were prepared by Schiff base condensation of 2-pyridinecarboxaldehyde and 2-(diphenylphosphino)benzaldehyde with the amino groups of the chitosan, 1,3,4,6-tetra-*O*-acetyl-β-D-glucosamine or cyclohexyl amine.

Chapter 3 records the application of the chitosan and modified chitosan-supported Pd^{II} complexes as precursors in the Suzuki-Miyaura and Heck cross-coupling reactions. Studies on hydroformylation using chitosan-supported Rh^{I} complexes are reported. The catalyst precursors' activity, selectivity, recyclability, stability and versatility are discussed together with comparisons to their mononuclear analogues.

Chapter 4 describes the synthesis and characterization of four new pyridylimine metallodendrimers and some pyridylimine mononuclear complexes. This was achieved by Schiff base condensation of 2-pyridinecarboxaldehyde with tris(2-aminoethyl)amine to form a pyridylimine dendrimer. The tris-2-(2-pyridylimine ethyl)amine dendrimer was further reacted with $[PdCl_2(COD)]$, $[RhCl(CO)_2]_2$ and $[RhCl(COD)_2]$ to afford Pd^{II} and Rh^{I} metallodendrimers.

In **Chapter 5**, catalytic hydroformylation reactions, using the Rh^{I} pyridylimine based systems (metallodendrimers) discussed in **Chapter 4** are described. Their activity and selectivity in comparison to the mononuclear pyridyl imine complexes is presented.

Chapter 6 gives overall concluding remarks to this research.

1.12 References

1. (a) Market Report: World Catalyst Market, Acmite Market Intelligence(**2008**) *accessed 06th Oct. 2010*. (b) Recognizing the Best In Innovation: Breakthrough catalysts, R&D Magazine, Sept. (**2005**) pp 20, *accessed 26th Feb. 2011*.
2. US Climate Change Technology Programme- Technology Options for the Near and Long Term, Aug. (**2005**), *accessed 01st Mar. 2011*.
3. (a) Types of Catalysis, Chemguide, *accessed 21st Feb. 2011.* (b) http://en.wikipedia.org/wiki/catalysis, *accessed 21st Feb 2011.* (c) IUPAC, Compendium of Chemical Technology, 2nd Ed, (The "Gold Book"), (**1997**) - online corrected version, (**2006**). (d) Twelve Principles of Green Chemistry, United States Environmental Protection Agency, *accessed 21st Feb. 2011*.
4. (a) D. Schils, F. Stappers, G. Solberghe, R. Van Heck, M. Coppens, D. Van der Donck, T. Callewaert, F. Meeussen, E. De Bie, K. Eersels E. Schouteden, *Org Proc. Res. and Dev.,* (**2008**), 12, 530.
5. (a) http://www.ravensdown.co.nz/Resources/Education/History.htm, *accessed 08th Mar 2011*. (b) A Historical Overview. Mendeleev and the Periodic Table, *accessed 08th Mar 2011.* (c) P.M.D. Collins, The Pivotal Role of Platinum in the Discovery of Catalysis, *accessed 10th Mar. 2011.* (d) Ostwald Wilhelm, Improvements in the Manufacture of Nitric Acid and Nitrogen Oxides, No 698, 09th Jan (**1902**)-accepted 20th Mar(**1902**). (e) The First Comprehensive Biography on Fritz Harber: D. Stolzenberg, Fritz Harber, VCH, Weinheim (**1994**). (f) J. Meurig Thomas, Angew. Chem. Int. Ed. Engl., (**1994**), *33*, 913.
6. (a) D.T. Cole-Hamilton, R.P Tooze, Catalyst Seperation Recovery and Recycling 1-8, *Springer Printed in the Netherlands*, (**2006**), chapter 1. (b) O. Roelen, *US Patent 2327066* (**1943**). (c) A.F. Hill, Organotransition Metal Chemistry, *Wiley-Interscience: New York,* (**2002**), pp 136-140. (d) M. Bochmann, Organometallics 1, Complexes with Transition Metal-Carbon σ bonds, *Oxford University Press, New York*, (**1994**), pp 69-76. (e) J. A. Osborn, F.H. Jardine, J.F. Young, G. Wilkinson, *J. Chem. Soc. A*, (**1966**), 32, 1711.
7. (a) B. Cornils, W.A. Herrmann, M. Rasch, "Otto Roelen Pioneer in Industrial Homogeneous Catalysis, *Angew Chem. Int. Ed*., (**1994**), 33, 2144. (b) M.L.H. Green, W.P. Griffith- Sir Geoffrey Wilkinson, 14th July 1921- 26th Sept. 1996, *Biographical Memoirs of Fellows of the Royal Society*, (**2000**), 46, 595.
8. (a) J.F. Roth, J.H. Creddock, A. Hershman, F.R. Paulik, *Chem Tech.,* (**1971**), 1, 600. (b) M.W. Farlow, *US Patent 2518608*, (**1947**).

9. C.P. Tsonis, *J Chem. Edu.,* (**1984**), 61, 479 and references therin.
10. C. Elschenboich, *Organometallics 3rd Ed., Wiley-VCH: Weinheim* (**2006**), p786-790.
11. (a) K. Köhler, Lecture Series, Modern Methods in Heterogeneous Catalysis Research, Fritz Harber Institute, *10th Nov.* (**2006**), *accessed 28th Feb. 2011*. (b) S.R. Seydmonir S. Abdo, R.F. How, *J. Phys. Chem.,* (**1982**), 86, 1233. (c) C. Moreno-Castilla, M A. Ferr-Garcia, J. Rivera-Utrilla, J.P. Joly, *Energy and Fuels,* (**1994**), 8, 1233. (d) D. Cauzzi, M. Costa, L. Gonsalvi, M.A. Pellinhelli, G. Preieri, A. Tiripicchio, R. Zanoni, *J. Organomet Chem.,* (**1997**), 541*,* 377. (d) K. Ebitani, Y. Fujie, K. Kaneda, *Languir,* (**1999**), 15*,* 3557. (e) N. Ikengaga, T. Tsuruda, K. Senma, T. Yamaguchi, Y. Sakurai, T. Suzuki, *Ind. Eng. Chem. Res.,* (**2000**), 39, 1228. (f) M. Jezequel, V. Du faud, M.J. Ruiz-Garcia, F. Carrillo-Hermosilla, U. Neugebauer, G.P. Niccolai, F. Lefebvre, F. Bayard, J. Corker, S. Fiddy, J. Evans, J-P. Broyer, J. Malinge, J-M. Basset, *J. Am. Chem. Soc.,* (**2001**), 123, 3520. (g) J. Wrzyszcz, M. Zawadzki, A.M. Trzeciak, J.J. Ziółkowski, *J. Mol. Catal. A: Chemical,* (**2002**)*,* 189*,* 203. (h) M.C. Iliuta, I. Iliuta, B.P.A. Grandjean, F. Larachi, *Ind. Eng. Chem. Res.,* (**2003**), 42*,* 3203. (i) M.W. Mckittrick, C.W. Jones, *J. Am. Chem. Soc.,* (**2004**), 126, 3052. (j) R.I. Kureshy, I. Ahmad, N.H. Khan, S.H.R. Abdi, K. Pathak, R.V. Jasra, *Tetrahedron: Asymmetry*, (**2005**), 16, 3562. (k) P. Li, S. Kawi, *J. Catal.,* (**2008**), 257*,* 23. (l) D. Barkhuizen, I. Mabaso, E. Viljoen, C. Welker, M. Claeys, E. van Steen, J.C.Q, Fletcher, *Pure Appl. Chem.,* (**2006**), 78, 1759. (m) R.I. Kureshy, I. Ahmad, K. Pathak, N.H. Khan, S.H.R. Abdi, R.V., Jasra, *Catal. Commun*., (**2009**), 10*,* 572. (n) N. Navascuès, M. Escuin, Y. Rodas, S. Irusta, R.Mallada. J. Sanatamaria*, Ind. Eng. Chem. Res.,* (**2010**), 49, 6941.
12. R.L. Augustine, Heterogeneous Catalysis for Synthetic Chemists, *Marcel Dekker Inc. New York,* (**1996**), pp 149-312.
13. (a) D.C. Bailey, S.H. Langer, *Chem. Rev.,* (**1981**), 81, 109. (b) C. Saluzzo, M. Lemaire, *Adv. Synth Catal.,* (**2002**), 344, 915. (c) C. Jöhnsson, K. Hallman, H. Andersson, G. Stemme, M. Malkoch, E. Malmström, A. Hult, C. Moberg, *Bioorg. Med. Chem. Lett.,* (**2002**), 12, 1857. (d) Y. Chavin, D. Commereuc, F. Dawans, *Prog. Polym. Sci.,* (**1977**), 5, 95. . (e) N.E. Leadbeater, M. Marco, *Chem. Rev.,* (**2002**), 102, 3217. (f) Y. Uozumi, *Top Current Chem.,* (**2004**), 242, 77. (g) M. Guino, K.KM. Hii, *Chem. Soc. Rev.,* (**2007**), *36*, 608. (h) J. Lu, P.H. Toy, *Chem. Rev.,* (**2009**), 109, 815. (i) K.C. Gupta, A.K. Sutar, C-C. Lin, *Coord. Chem. Rev.,* (**2009**), 253, 1926. (j) D.E. Bergbreiter, J. Tian, C. Hongfa, *Chem. Rev.,* (**2009**), 109, 530. (k) N. Kann, *Molecules,* (**2010**), 15, 6306. (l) B. Heurtefeu, C. Bouilhac, E. Cloutet, D. Taton, A. Deffieux, H. Cramail, *Prog. Polym. Sci.,* (**2011**), 36,

89. (m) L.A. van de Kuil, D.M. Grove, J. W. Zwikker, L.W. Jenneskens, W. Drenth, I.G. Van Koten, *Chem. Mater.,* (**1994**), 6, 1675. (n) A.C. Albèniz, N. Carrera, *Eur. J. Inorg. Chem.,* (**2011**), 15, 2347. (o) S. Reymond, J. Cossy, *Chem. Rev*., (**2008**), 108, 5359. (p) J.A. Labinger, *J. Mol. Catal. A: Chem.,* (**2004**), 220, 27.

14. (a) E. Guibal, V. Thierry, B.F. Peirano, *Ion Exchange and Solvent Extraction* (**2007**), 18, 151. (b) E. Guibal, *Prog. Polym. Sci.,* (**2005**), 30, 71. (c) D.J. Macquarrie, J.J.E. Hardy, *Ind. Eng. Chem. Res.*, (**2005**), 44, 8499. (d) B.J. Arena, *US Patent 4, 274,980* (**1981**).
15. (a) M. Mutter, H. Hagenmaier, E. Bayer, *Angew. Chem. Int. Ed.,* (**1971**), 10, 811-. (b) E. Bayer, M. Mutter, *Nature*, (**1972**), 237, 512.
16. (a) D.E. Bergbreiter, *Med. Res. Rev.,* (**1999**), 19, 439. (b) D.E. Bergbreiter, *Catal. Today,* (**1998**), 42, 389.
17. M.J. Farrall, J.M.J Frechèt, *J. Org. Chem.,* (**1976**), 41, 3877.
18. S.T. Nguyen, R.H. Grubbs, *J. Organomet. Chem.,* (**1995**), 497, 195.
19. (a) S. Warwel, P. Buschmeyer, *Angew Chem. Int. Ed.,* (**1978**), 17, 131. (b) M.R. Buchmeiser, *Chem. Rev.,* (**2009**), 109, 303.
20. (a) R.F. Heck, Org.React., (1982), 27, 345. (b) J.K. Stille, *Angew. Chem. Int. Ed. Engl.,* (1986), 25, 508. (c) N. Miyaura, A. Suzuki, Chem. Rev., (1995), 95, 2457. (d) E-I. Negishi, Acc. Chem. Res., (1982), 15, 340. (e) K. Sonogashira, *Comprehensive Organic Synthesis*, Eds.: B.M. Trost, I. Fleming, Pergamon Press, Oxford, **(1991)**, 3, pp. 521. (f) A. Rudolph, M. Lautens, Angew. Chem, Int. Ed., (2009), 48, 2656. (g) Nobel Foundation: http://nobelprize.org/nobel_prizes/chemistry/laureates/2010/press.html. *accessed 2nd March 2011*. (h) S.B. Jang, *Tetrahedron Lett.,* **(1997**), 38, 1793.
21. F-T. Luo, C. Xue, S-L. Ko, Y-D. Shao, C-J. Wu, Y-M. Kuo, *Tetrahedron,* (**2005**), 61, 6040.
22. S. Schweizer, J.M. Becht, C. Le Drian, *Tetrahedron* (**2010**), 66, 765.
23. (a) M. Bakherad, A. Keivanloo, B. Bahramian, M.A. Rajaie, *Tetrahedron Lett.,* (**2010**), 51, 33. (b) M. Bakherad, A. Keivanloo, B. Bahramian, S. Mihanparast, *Tetrahedron Lett.,* (**2009**), 50, 6418.
24. (a) P. Eibracht, L. Barfacker, C. Buss, C. Hollmann, B.E. Kistsos-Rzychon, C.L. Kranemann, T. Rische, R. Roggenbuck, A. Schmidt, *Chem. Rev.,* (**1999**), 99, 3329 and references therein; (b) S.I. Fujita, S. Akihara, S. Fujisawa, M. Arai, *J. Mol. Catal. A: Chem.,* (**2007**), 268, 244.
25. C.U. Pittman Jr, L.R. Smith, *J. Am. Chem. Soc.,* (**1975**), 97, 1742.

26. (a) E. Bayer, V. Schurig, *Angew. Chem. Int. Ed.,* (**1975**), 14, 493. (b) E. Ȧrstad, A.G.M. Barnett, L. Teddeschi, *Tetrahedron Lett.,* (**2003**), 44, 27, 2703.
27. (a) J.M. Tibitt, B.C. Gate, J.R. Katzer, *J. Catal.,* (**1975**), 38, 505. (b) Y. Uozumi, M. Nakazono, *Adv. Synth. Catal.,* (**2002**), 344, 274.
28. (a) C. Saluzzo, T. Lamouille, D. Hèrault, M. Lemaire, *Bioorg. Med. Chem. Lett.,* (**2002**), 12, 1841. (b) D.J. Bayston, J.L. Fraser, M.R. Aston, A.D. Baxter, M.E.C. Polywka, E. Moses, *J. Org. Chem.,* (**1998**), 63, 3137.
29. (a) F.M. Menger, T. Tsuno, *J. Am Chem. Soc.,* (**1989**), 111, 4903. (b) E. Vieira, P. Vogel, *Helv. Chim. Acta,* (**1982**), 65, 1700.
30. J.M. Fraile, J.I. Garcia, M.A. Harmer, C.I. Herrerias, J.A. Mayoral, *J. Mol. Catal. A: Chem.,* (**2001**), 165, 211.
31. K.S. Chettiar, K. Sreekumar, *Polym. Int.*, (**1999**), 48, 455.
32. (a) S. Kulkarni, M. Alurkar, A. Kumar, *Appl. Catal. A: Gen.,* (**1996**), 142, 243. (b) M. Islam, D. Hossain, P. Mondal, K. Tuhina, A.S. Roy, S. Mondal, M. Mobarak, *Transition Met Chem.,* (**2011**), 36, 223
33. M. Stork, M. Koch, M. Klapper, K. Müllen, H. Gregorius, U. Rief, *Macromol. Rapid Commun.,* (**1999**), 20, 210.
34. A.S. Shearer, Y.R. de Miguel, E.A. Minnich, D. Pochan, C. Jenny, *Inorg. Chem. Commun.,* (**2007**), 10, 262.
35. (a) K. Mennecke, K. Grela, U. Kunz, A. Kirschning, *Synlett.,* (**2005**), 2948. (b) A. Kirshning, K. Harmrolfs, K. Mennecke, J. Messinger, U. Schon, K. Grela, *Tetrahedron Lett.,* (**2008**), 49, 3019.
36. E.M. Zahidi, H. Oudghiri-Hassani, P.H. McBreen, *Nature,* (**2001**), 409, 1023.
37. R.M. Kröll, N. Schuler, S. Lubbad, M.R. Buchmeiser, (**2003**), 2742.
38. (a) E.K. Rideal, "Presidential address: Concepts in catalysis. The contributions of Paul Sabatier and of Max Bodenstein". *J. Chem. Soc., (Resumed)*, (**1951**), 1640. (b) P. Sabatier (150th anniversary of his birthday). *Russian Journal of Applied Chemistry* (**2004**), 77, 1909. (c) F. Touchard, P. Gamez, F. Fache, M. Lamaire, *Tetrahedron Lett.,* (**1997**), 38, 2275.
39. N. Haraguch, K. Tsuru, Y. Arakawa, S. Istuno, *Adv. Synth. Catal.,* (**2008**), 350, 2295.
40. (a) M.T. Zarka, M. Bortenschlager, K. Wurst, O. Nguyken, R. Weberskirch, *Organometallics,* (**2004**), 23, 481.

41. (a) D.H. Lee, J.H. Kim, B.H. Jun, H. Kang, J. Park, Y.S. Lee, *Org. Lett.,* (**2008**), 10, 1609. (b) X.M. Zeng, T.X. Zhang, Y.C. Qin, Z.J. Wei, M.M. Luo, *Dalton Trans.,* (**2009**), 8341.
42. N.T.S. Phan, P. Styring, *Green Chem.,* (**2008**), 10, 1055.
43. (a) J.H. Kim, D.H. Lee, B.H. Jun, Y.S. Lee, *Tetrahedron Lett.,* (**2007**), 48, 7079. (b) Y.C. Qin, W. Wei, M.M. Luo, *Synlett.,* (**2007**), 2410.
44. (a) E. Alacid, C. Najera, *Eur. J. Org. Chem.,* (**2008**), 3102. (b) E. Alacid, C. Najera, *ARKIVOC,* (**2008**), 50.
45. (a) D. Schonfelder, K. Fischer, M. Schmidt, O. Nguyken, R. Weberskirch, *Macromol.,* (**2005**), 38, 254. (b) D. Schonfelder, O. Nguyken, R. Weberskirch, *J. Organomet. Chem.,* (**2005**), 690, 4648.
46. (a) D.E. Bergbreiter, P.L. Osburn, J.D. Frels, *Adv. Synth. Catal.,* (**2005**), 347, 172. (b) D.E. Bergbreiter, S. Furyk, *Green Chem.,* (**2005**), 6, 280. (c) M. Bandini, A. Pietrangelo, R. Sinisi, A. Umani-Ronchi, M.O. Wolf*, Eur. J. Org. Chem.,* (**2009**), 348, 2110.
47. a) H.G. Alt, P. Schertl, A. Köppl, *J. Organomet. Chem.,* (**1998**), 568, 263. (b) J-M. Basset, F. Lefebvre, C. Santini, *Coord. Chem. Rev.,* (**1998**), 1703.
48. K.I. Alder, D.C. Sherrington, *Chem. Commun.,* (**1998**), 131.
49. (a) M. Cypryk, P. Pospiech, K. Strzelec, K. Wasikowska, J.W. Sobczak, *J. Mol. Catal. A Chem.,* (**2010**), 319, 30. (b) M. Cypryk, P. Pospiech, K. Strzelec, J.W. Sabczak, *Phosphorus, Sulfur and Silicon*, (**2009**), 184, 1586.
50. H. Wang, X. Zheng, P. Chen, X. Zheng, *J. Mater. Chem.,* (**2006**), 16, 4701.
51. (a) Z.M. Michalska, Ł. Rogalski, K. Rózga-Wijas, J. Chojnowski, W. Fortuniak, M. Scibiorek, *J. Mol. Catal. A: Chem.,* (**2004**), 208, 187. (b) G. Liu, M. Cai, *J. Mol. A: Chem.,* (**2006**), 258, 257.
52. (a) Z-X. Liu, K. Jiang, M-Y. Huang, Y-Y. Jiang, *Polym. Adv. Technol.,* (**1999**), 10, 112. (b) J. Čermák, M. Kvičalová, V. Blechta, *Appl. Organometal. Chem.,* (**2000**), 14, 164.
53. (a) G.R. Whittell, I. Manners, *Adv, Mater*., (**2007**), 19, 3439. (b) J-C. Eloi, L. Chabanne, G.R. Whittell, I. Manners, *Materials Today*, (**2008**), 11, 28.
54. X. Wang, R. McHale, *Macromol. Rapid Commun.,* (**2010**), 31, 331.
55. (a) K.J.T. Noonan, D.P. Gates, *Annu. Rep. Prog. Chem. Sect. A,* (**2008**), 104, 394. (b) E. Rivard, *Annu. Rep. Prog. Chem. Sect. A,* (**2010**), 106, 391. (c) E. Rivard, *Annu. Rep. Prog. Chem. Sect. A,* (**2011**), 107, 319.
56. K.A. Williams, A.J. Boydtan, C.W. Bielawski, *Chem. Soc. Rev*., (**2007**), 36, 729.
57. C. Diaz, M.L. Valenzuela, *Macromol.,* (**2006**), 16, 123.

58. N. Hagihara, K. Sonogashira, S. Takahashi, *Adv. Polym. Sci.,* (**1981**), 141.
59. (a) D.A. Fouche, B.Z. Tang, I. Manners, *J. Am. Chem. Soc.,* (**1992**), 114, 6246. (b) W.Y. Chan, A.J. Lough, I. Manners, *Organometallics,* (**2007**), 26, 1217.
60. (a) G. Smith, R. Chen, S. Mapolie, *J. Organomet. Chem.,* (**2003**), 673, 111. (b) R. Malgas, S.F. Mapolie, S.O Ojwach, G.S. Smith, J. Darkwa*, Catal. Commun.,* (**2008**), 9, 1612.
61. V. Dragutan, I. Dragutan, H. Fischer, I. *Inorg. Organomet. Polym.,* (**2008**), 18, 18.
62. (a) P. Mastrorilli, C.F. Nobile, *Coord. Chem. Rev.,* (**2004**), 377. (b) Z. Wang, G. Chen, K. Ding, *Chem. Rev.,* (**2009**), 109, 322.
63. (a) R.A. Taylor, B.P. Santora, M.R. Gagnè, *Org. Lett.,* (**2000**), 2, 1781. (b) S.L. Vison, M.R. Gagnè, *Chem. Commun.*, (**2001**), 1130.
64. A.N. Cammidge, N.J. Baines, R.K. Bellingham, *Chem. Commun.,* (**2001**), 2588.
65. F.A.R. Kaul, G.T. Puchta, H. Schneider, F Bielert, D. Mihalios, W.A. Herrmann, *Organometallics,* (**2002**), 21, 74.
66. (a) B.B. De, B.B. Lohray, S. Sivaram, P.K. Dahl, *Tetrahedron: Asymmetry,* (**1995**), 6, 2105. (b) B.B. De, B.B. Lohray, S. Sivaram, P.K. Dahl, *J. Polym. Sci. A: Polym. Chem.,* (**1997**), 35, 1809.
67. (a) L. Shi, X. Wang, C.A. Sandoval, M. Li, Q. Qi, Z. Li, K. Ding, *Angew. Chem. Int. Ed.,* (**2006**), 45, 4108. (b) R.P. Kingsborough, T.M. Swager, *Chem. Mater.,* (**2000**), 12, 872.
68. Y. Uozumi, Y.M.A. Yamada, T. Beppu, N. Fukuyama, M. Ueno, T. Kitamori, *J. Am. Chem. Soc.,* (**2006**), 128, 15994.
69. C.N. Kato, M. Ono, T. Hino, T. Ohmura, W. Mori, *Catal. Commun.,* (**2006**), 7, 673.
70. (a) T. Uemura, K. Kitagawa, S. Horike, T. Kawamura, S. Kitagawa, M. Mizuno, K. Endo, *Chem. Commun.,* (**2005**), 5968. (b) T. Uemura, Y. Ono, K. Kitagawa, S. Kitagawa, *Macromol.,* (**2008**), 41, 87.
71. D. De Groot, P.G. Emmerink, C. Coucke, J.N.H. Reek, P.C.J. Kamer, P.W.N.M. van Leeuwen, *Inorg. Chem. Commun.,* (**2000**), 3, 711.
72. S.C. Bourque, H. Alper, L.E. Manzer, P. Arya, *J. Am. Chem. Soc.,* (**2000**), 122, 956.
73. T. Fujihara, Y. Obora, M. Tokunaga, H. Sato, Y. Tsuji, *Chem. Commun.,* (**2005**), 4526.
74. (a) G.S. Smith, S.F. Mapolie, *J. Mol. Cat. A: Chem.,* (**2004**), (b) N.C. Antonels, J.R. Moss, G.S. Smith, *J. Organomet. Chem.,* (**2011**), 696, 2003.
75. S. Arèvalo, E. de Jesus, F.J. de la Mata, J.C. Flores, R. Gomez, M.M. Rodrigo, S. Vigo, *J. Organomet. Chem.,* (**2005**), 690, 4620.

76. K. Huang, L. Xue, Y-C. Hu, M-Y. Huang, Y-Y. Jiang, *React. Funct. Polym*., (**2002**), 50, 199.

77. X. Zhang, Y. Gang, B. Han, M-Y. Ying, M-Y, Ying, M-Y. Huang, Y-Y. Jiang, *Polym. Adv. Technol.,* (**2001**), 12, 642.

78. W-L. Wei, H-Y. Zhu, C-L. Zhao, M-Y. Huang, Y-Y. Jiang, *React. Funct. Polym.,* (**2004**), 59, 33.

79. (a) K. Huang, J. Hu, M-Y. Huang, Y-Y. Jiang, *Polym. Adv. Technol.,* (**2001**), 12, 711. (b) H-W. Liu, F. Xin, L-M. Wu, M-Y. Huang, Y-Y. Jiang, *Polym. Adv. Technol.,* (**2002**), 13, 210.

80. (a) E. Chiessi, B. Pispisa, *J. Mol Catal.,* (**1994**), 87, 177. (b) F. Quignard, A. Choplin, A. Domanrd, *Langmuir,* (**2000**), 16, 1906. (c) E. Sin, S-S. Yi, Y-S Lee, *J. Mol. Catal. A: Chem.,* (**2010**), 315, 99. F. Peirano, T. Vincent, F. Quignard, M. Robitzer, E. Guibal, *J. Membr. Sci.,* (**2009**), 30.

81. (a) E. Guibal, T. Vincent, S. Spinelli, *Separation Sci. Technol.,* (**2005**), 40, 633. (b) A. Butewicz, K.C. Gavilan, A.V. Pestov, Y. Yatluk, A.W. Trochimczuk, E. Guibal*, J. Appl. Polym. Sci.,* (**2010**), 116, 3318. (c) L.A.S. Sopena, M. Ruiz, A.V. Pestov, A.M. Sastre, Y. Yatluk, E. Guibal, *Cellulose*, (**2011**), 18, 309. (d) D. Thakre, S. Jagtap, N. Sakhare, N. Labhsetwar, S. Meshram, S. Rayalu, *Chem. Engineering J.,* (**2010**), 158, 315.

82. (a) Y-C. Tsai, S-Y. Chen, C-A. Lee, *Sensors and Actuators B* (**2008**), 135, 96. (b) J. Li. RE. Yuan, Y. Chai, X. Che, W. Li, X. Zhang, *Microchim Acta,* (**2011**), 172, 163.

83. A. Tiwari, D. Terada, P.K. Sharma, V. Parashar, C. Yoshikawa, A.C. Pandey, H. Kobayashi, *Anal. Methods,* (**2011**), 3, 217.

84. J. Linden, R. Stoner, K. Knuston, C. Gardner-Hughes, *Org. Dis. Control Elicitors, Agro Food Industry Hi-Te,* (**2000**), pp 12-15.

85. (a) A. Bayat, A.M.M. Sadeghi, M.R. Avadi, M. Amini, M. Rafiee-Tehrani, A. Shafiee, R. Majlesi, H.E. Junginger, *J. Bioactive and Compatible Polym.,* (**2006**), 21, 433. (b) R-M. Wang, N-P. He, P-F. Song, Y-F. He, L. Ding, Z-Q. Lei, *Polym. Adv. Technol.,* (**2009**), 20, 959.

86. (a) Y. Sun, Y. Guo, Q. Lu, X. Meng, W. Xiaohua, Y. Guo, Y. Wang, X. Liu, *Catal. Lett.,* (**2005**), 100, 213. (b) D-Q. Zhou, M. He, Y-H. Zhang, M-Y. Huang, Y-Y. Jiang, *Polym Adv. Technol.,* (**2003**), 14, 287. (c) K. Martina, S.E.S. Leonhardt, B. Ondruschka, M. Carini, A. Binello, G. Cravotto, *J. Mol. Catal. A: Chemical* (**2011**), 334, 60. (d) A. Di Giuseppe, M. Crucianelli, M. Passacantando, S. Nisi, R. Saladino*, J. Catal.* (**2010**), 276, 412-422. (e) L-F. Xiao, F-W. Li, C-G. Xia, *Appl. Catal. A: Chem.,* (**2011**), 334, 60. (f)

F.P. Blondet, T. Vincent, E. Guibal, *Int. J. Biological, Macromol.,* (**2008**), 43, 69. (g) A.E. Kadib, K. Molvinger, C. Guiman, F. Quignard, D. Brunel *Chem. Mater.,* (**2008**), 20, 2198. (h) V. Caló, A. Nacci, A. Monopoli, A. Fornaro, L. Sabbatini, N. Cioffi, N. Ditaranto, *Organometallics,* (**2004**), 23, 5154. (i) R.B. da Silva, A.F.L. Neto, L.S.S. dos Santos, J.R. de Oliviera Lima, M.A. Chaves, J.R. dos Santos Jr, G.M. de Lima, E.M. de Moura, C.V.R. de Moura, *Bioresource Technol.,* (**2008**), 99, 6793. (j) J. Ru, Z. Huayue, L. Xiaodang, X. Ling, *Chem. Engineering J.,* (**2009**), 152, 537. (k) T.S. Rezende, G.R.S. Anderade, L.S. Baretto, N.B. Costa Jr, L.F. Gimenez, L.E. Almeida, *Materials Lett.,* (**2010**), 882. (l) J. Lasri, T.C.O. Mac Leod, A.J.L. Pombeiro, *Appl. Catal. A: General,* (**2011**), 397, 94. (m) A.V. Kucherov, N.V. Kramareva, E.D. Fiashina, A.E. Koklin, L.M. Kustov*, J. Mol. Catal. A: Chem.,* (**2003**), 198, 377. (n) . Huang, C-C. Cai, J. Luo, H. Zhou, Y.A. Guo, S-Y. Liu, Can. J. Chem., (**2008**), 86, 199. (o) E.V. Slivinskii, N.V. Kolesnichenko, *Russ. Chem. Bull. Int. Ed*., (**2004**), 53, 2449. (p) H-M. Guan, X-S. Cheng, *Polym Adv. Technol.,* (**2004**), 15, 89. (q) N.V. Kolesnichenko, A.E. Batov, N.A. Markova, E.V. Slivinsky, *Russ. Chem. Bull. Int. Ed*., (**2002**), 51, 259.

87. (a) A. Burkhardt, H. Görls, W. Plass*, Carb. Res.,* (**2008**), 343, 1266. (b) J.E. dos Santos, E.R. Dockal, E.T.G. Cavalheiro, *Carb. Res.,* (**2005**), 60, 277. (c) Guinesi, E.T. Cavaheiro, *Carb. Polym.,* (**2006**), 65, 557. (d) K. Kurita, S. Mori, Y. Nishiyama, M. Harata, *Polym. Bulletin*, (**2002**), 48, 159. (e) C. Demetgül, S. Serin, *Carb. Polym*., (**2008**), 72, 506.
88. J.J.E. Hardy, S. Hubert, D.J. Macquarrie, A.J. Wilson, *Green Chem.,* (**2004**), 6, 53.
89. Y. Cui, L. Zhang, Y. Li, *Polym. Adv. Technol.,* (**2005**), 16, 633.
90. X. Xu, P. Lui, S-H. Li, P. Zhang, X-Y. Wang, *React. Kinet. Catal. Lett.,* (**2006**), 88, 217.
91. L-X. Wang, Z-W. Wang, G-S. Wang, X-D. Lin, J-G. Ren, *Polym. Adv. Technol.,* (**2010**), 21, 244.
92. Y. Yang, G. Li, Z. Song, X. Yang, P. Lui, *Lett. Org. Chem.,* (**2010**), 7, 533.
93. S.E.S. Leonhardt, A. Stolle, B. Ondruschka, G. Cravotto, C. De Leo, K.D. Jandt, T.F. Keller, *Applied Catal. A: General,* (**2010**), 30.
94. Y. Chang, Y. Wang, Z. Su, *J. Appl. Polym Sci.,* (**2002**), 83, 2188.
95. Chang, Y. Wang, F. Zha, R. Wang, *Polym. Adv. Technol.*, (**2004**), 15, 284.
96. J. Tong, Z. Li, C. Xia, *J. Mol. Catal. A: Chem.,* (**2005**), 197.
97. J. Lui, W. Sun, S. Zheng, C. Xia, *Hel. Chim. Acta.,* (**2007**), 90, 1593.
98. (a) W. Sun, C-G. Xia, H-W. Wang, *New J Chem.,* (**2002**), 26, 755. (b) H. Wang, W. Sun, C. Xia, *J. Mol Catal.,* (**2003**), 206, 199.

99. M. Chtchigrovsky, A. Primo, P. Gonzalez, K. Molvinger, M. Robitzer, F. Quignard, F. Taran, *Angew. Chem. Int. Ed.,* (**2009**), 48, 5916.

Chapter 2

Chitosan-Supported Pd^{II} and Rh^{I} Complexes and their Precursors: *Synthesis and Characterization*

2.1 Introduction

The previous chapter detailed some of the immobilized catalysts/catalyst precursors that have emanated from efforts to overcome the problems related to homogeneous and heterogeneous catalysis. [1-3] For example, supporting transition metal catalysts on insoluble polymer supports can improve their stability without compromising the activity and selectivity of the homogeneous catalyst. Supported catalysts also allow simplified recovery and reuse of the catalyst as well as physical separation of the active metal site, thus minimizing catalyst self-destruction. [3a-b]

Due to the inherent advantages of heterogenizing homogeneous catalysts through immobilization on solid supports, a great deal of effort has been devoted to these developments.[1-3] However, the majority of these reported catalysts are based on synthetic organic polymer supports (polystyrene, poly(ethylene) glycol etc.) and inorganic supports (silica, alumina or other metal oxides) including commercial catalysts such as $[(PPh_3)_4Pd]$~crosslinked polystyrene-bound and Pd^0 on alumina. [2a-c] Recent efforts in the development of cleaner and sustainable chemistry have led to the use of biopolymers as catalyst supports. Biopolymers are readily available in creation and can be used as suitable supports for many reagents and catalysts, offering the advantages of being renewable, biodegradable and non-toxic. As such, biopolymers such as cellulose, gelatine and starch have been investigated as catalyst supports. [3]

Chitosan is produced by deacetylation of the abundant biopolymer chitin, a key constituent of the exoskeletons of crustaceans and the cell walls of algae (**Fig. 2.1**). [1,3,4] It has been shown to exhibit interesting biopesticidal, antifungal and anticancer properties and has been used successfully in food and water treatment. [3a,4a-e]

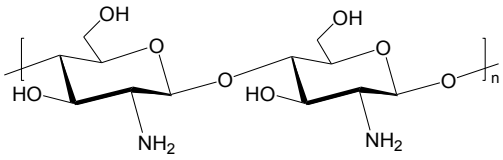

Chitosan

Fig. 2.1. Idealized structures of chitosan.

Chitosan can be readily transformed into films or fibres and has found applications as adsorbents for metals, in medicine and in drug delivery. [1,3,4] Its chirality, insolubility (in many organic solvents) and capability of being cast into films and fibres from dilute acid makes chitosan an excellent candidate as a support for catalysts. In this respect, several catalytic systems using chitosan as a support are known. [3,5] Functionalization of chitosan to provide coordination sites has been carried out and this has provided catalysts for oxidation, cyclopropanation of olefins, Suzuki and Heck cross coupling reactions. [3,4,6] This chapter discusses the synthesis and characterization of chitosan- and 6-deoxy-6-amino chitosan-supported Schiff base Pd^{II} complexes and mononuclear Pd^{II} analogues as well as chitosan-supported Schiff base Rh^{I} complexes and their mononuclear Rh^{I} analogues. The next chapter will report on the application of these supported and mononuclear complexes in catalysis.

2.2 Synthesis and characterization of chitosan-immobilized Schiff base ligands and corresponding Pd^{II} complexes

*2.2.1 Chitosan- and 6-deoxy-6-amino chitosan-supported Schiff base ligands (**2.1-2.4**) and corresponding Pd^{II} complexes (**2.5-2.8**)*

Chitosan-supported ligands (**2.1**-**2.4**) were prepared *via* Schiff base condensation of the amino groups on the chitosan backbone with either 2-pyridinecarboxaldehyde or 2-(diphenylphosphino)benzaldehyde in refluxing methanol over 10 hours (**Scheme 2.1** and **2.2**). Subsequent stirring of these supported ligands (**2.1**-**2.4**) with $[PdCl_2(COD)]$ precursor complex in acetone over 48 hours (**Scheme 2.1** and **2.2**) resulted in several chitosan-supported Pd^{II} complexes (**2.5**-**2.8**). The chitosan-supported ligands and complexes (**2.1**-**2.8**) were obtained in good to moderate yields. The yellow to dark yellow chitosan-supported complexes are air -and moisture-stable and can be stored on bench-top for up to 12 months without decomposition. These materials were characterized using elemental analysis, inductively coupled plasma mass spectrometry (ICP-MS), ultraviolet visible spectroscopy

(UV-vis), Fourier transform infrared spectroscopy (FT-IR), thermogravimetric analysis (TGA), powder X-ray diffraction (PXRD) and transmission electron microscopy (TEM). In addition, solid state ^{31}P NMR was conducted to confirm coordination of Pd to the chitosan-supported iminophosphine based ligand (**2**.**2**).

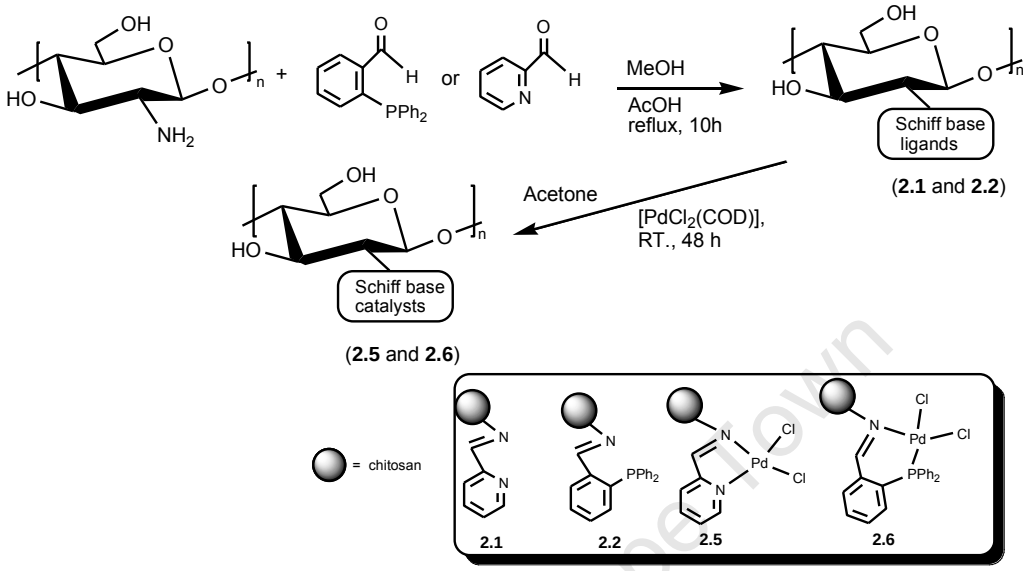

Scheme 2.1 Outline for the preparation of chitosan-supported Schiff base ligands (**2.1** and **2.2**) and chitosan-supported complexes (**2.5** and **2.6**).

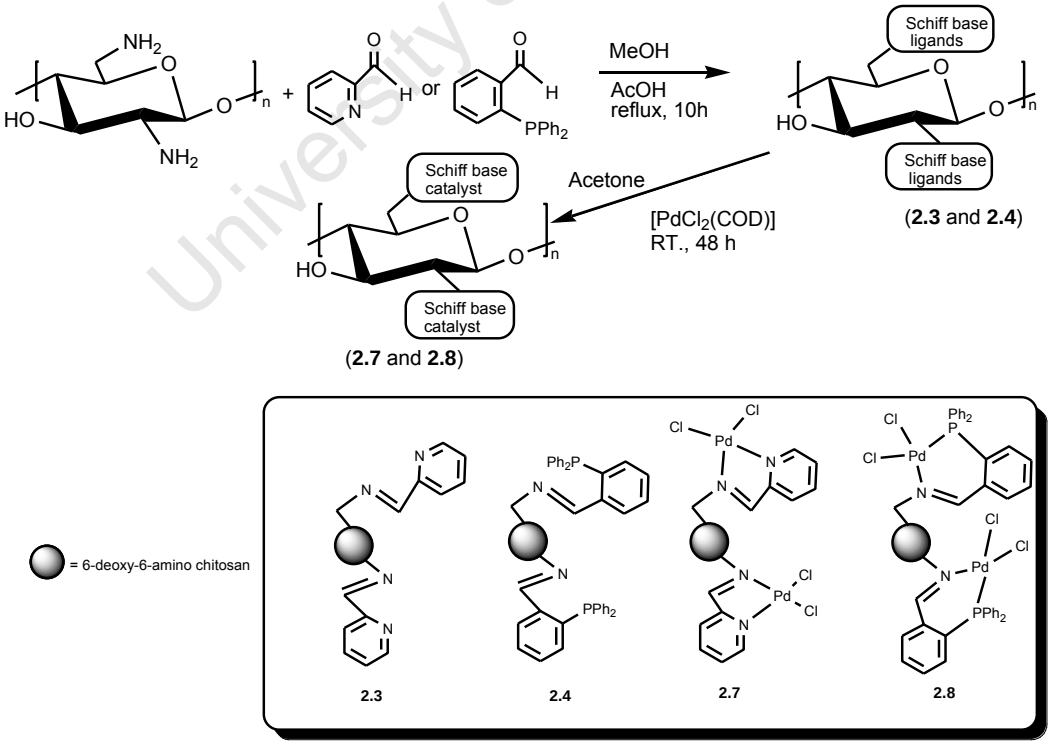

Scheme 2.2 Outline for the preparation of chitosan-supported Schiff base ligands (**2.3** and **2.4**) and chitosan-supported complexes (**2.7** and **2.8**).

Comparison of the elemental analyses results of the supported Schiff base ligands (**2.1**-**2.4**) with the corresponding supported complexes (**2.5**-**2.8**) evidenced partial complexation of the Pd, through decreases in the percentage of CHN content in the materials (**Table 2.1** and **2.2**). Approximately 20% of the nitrogen atoms in the low molecular weight chitosan used in these experiments were acetylated. Therefore, 2.10 $mmolg^{-1}$ are present as free NH_2 units. [1b] Of these supported ligands, 7% (**2.1**) and 6% (**2.2**), have been functionalized with Schiff base groups. This corresponds to 0.150 $mmolg^{-1}$ (**2.1**) and 0.120 $mmolg^{-1}$ (**2.2**), final loading of the ligand sites (**Table 2.1**).

The free NH_2 functionalities in 6-deoxy-6-amino chitosan amounts to 2.99 $mmolg^{-1}$. Of these 7% (**2.3**) and 6% (**2.4**) were functionalized with 2-pyridylimine and 2(diphenylphosphino)imine groups respectively. Loading of the imine ligands in (**2.3**) and (**2.4**) was higher than that of (**2.1**) and (**2.2**); this was expected due to the presence of more NH_2 sites in 6-deoxy-6-amino chitosan (**Table 2.1**). From the analyses, it can be seen that not all NH_2 sites have reacted to form imines, suggesting that many are inaccessible given that chitosan is a weakly swelling polymer at pH 3-4.5 in methanol - since 15 % of the polymer is still acetylated.

Table 2.1. Microanalyses, yields and degree of substitution (DS) of chitosan-Schiff base ligands.

Compound	**Elemental analysis EA** (%)				**Loading** (DS) ($mmolg^{-1}$)		**Yield** (%)[d]
	C	H	N	C/N	EA	UV[a]	
Chitosan	40.92	6.02	7.85	5.21	2.10[b]	-	-
6-deoxy-6-amino chitosan	44.35	7.04	8.14	5.45	2.99[c]	-	-
2.1	46.47	5.89	10.39	4.47	0.15	0.13	84
2.2	44.63	5.92	6.44	6.93	0.12	0.12	69
2.3	48.12	5.89	9.10	5.28	0.20	0.18	60
2.4	47.96	6.50	7.28	6.58	0.18	0.14	65

[a] Absorbance is dependent on conc., solvent and pH. [7b] [b] Free NH_2 (accessible and inaccessible) determined using literature [1b]. [c] loading of NH_2 in 6-deoxy-6-amino chitosan previously determined by a fluorescamine assay [7a]. [d] Yield by mass.

In addition to elemental analysis data, the loading of ligand sites was also determined using UV spectroscopy. Measurement of the absorbance of increasing amounts (0.5 -11.0 x 10^{-6} M, in methanol) of the aldehydes (2-pyridinecarboxaldehyde and 2(diphenylphosphino)benzaldehyde) which gave linear (R = 0.995) calibration curves. Thus,

the absorbances of the supported imines, once cleaved with dilute HCl were measured and used to determine the imine loading (**Table 2.1**). [7b]

The degree of substitution (DS) was calculated from the elemental analyses data using equation 2.1. [8a] This equation slightly overestimates the values obtained by UV analysis, potentially due to the residual water molecules in the biopolymer (**Table 2.1**).

$$DS = \Delta_{C/N}/\{M_{C/N}(1\text{-}DA)], \qquad \textbf{(Eq. 2.1)}$$

where $\Delta_{C/N}$ is the C/N percentage ratio differences of these elements in the derivatives and in the original starting material (chitosan or 6-deoxy-6-amino chitosan), $M_{C/N}$ is the ratio of C to N molar mass and DA is the degree of acetylation of the starting material. [8a]

Metal loading was determined using ICP-MS, and the results showed Pd loadings of 0.044 (**2.5**), 0.054 (**2.6**), 0.121 (**2.7**) and 0.123 $mmolg^{-1}$ (**2.8**) (**Table 2.2**). Thus for the supported Pd complexes approximately 27% (**2.5**), 45% (**2.6**), 60% (**2.7**) and 62% (**2.8**) of the ligands are occupied by metal. Generally, the Pd loading levels are comparable to similar chitosan-Pd species reported in literature. [1a-c]

UV-vis studies were conducted on complexes (**2.11**) and (**2.12**) (*vide infra* **Scheme 2.3**), in order to confirm molecular Pd^{II} loading onto supported complexes (**2.5**) and (**2.6**). Similar to mononuclear complexes (**2.11**) and (**2.12**) (absorbance peaks at 360 nm and 330 nm respectively), supported complexes (**2.5**) and (**2.6**) displayed absorbance peaks at 358 nm and 332 nm respectively (**Fig 2.2** (**a-d**)). The presence of similar, though weak peaks for supported complexes (**2.5**) and (**2.6**), suggests that a low loading of Pd complexes on the chitosan structure has been attained. [1a]

Table 2.2 Microanalyses, yields and Pd content of chitosan-Schiff base complexes.

Chitosan-catalyst	**Metal**	**Elemental analysis EA** (%)				**Pd loading** ($mmolg^{-1}$)	**Yield** (%)[b]
		C	H	N	C/N	ICP value [a]	
2.5	Pd	38.82	4.87	6.11	6.21	0.044	96
2.6	Pd	39.32	4.16	4.26	9.23	0.054	88
2.7	Pd	43.88	5.70	7.42	5.91	0.121	91
2.8	Pd	42.08	6.16	4.14	10.16	0.123	67

[a] Determined using ICP-MS. [b]Yield by mass.

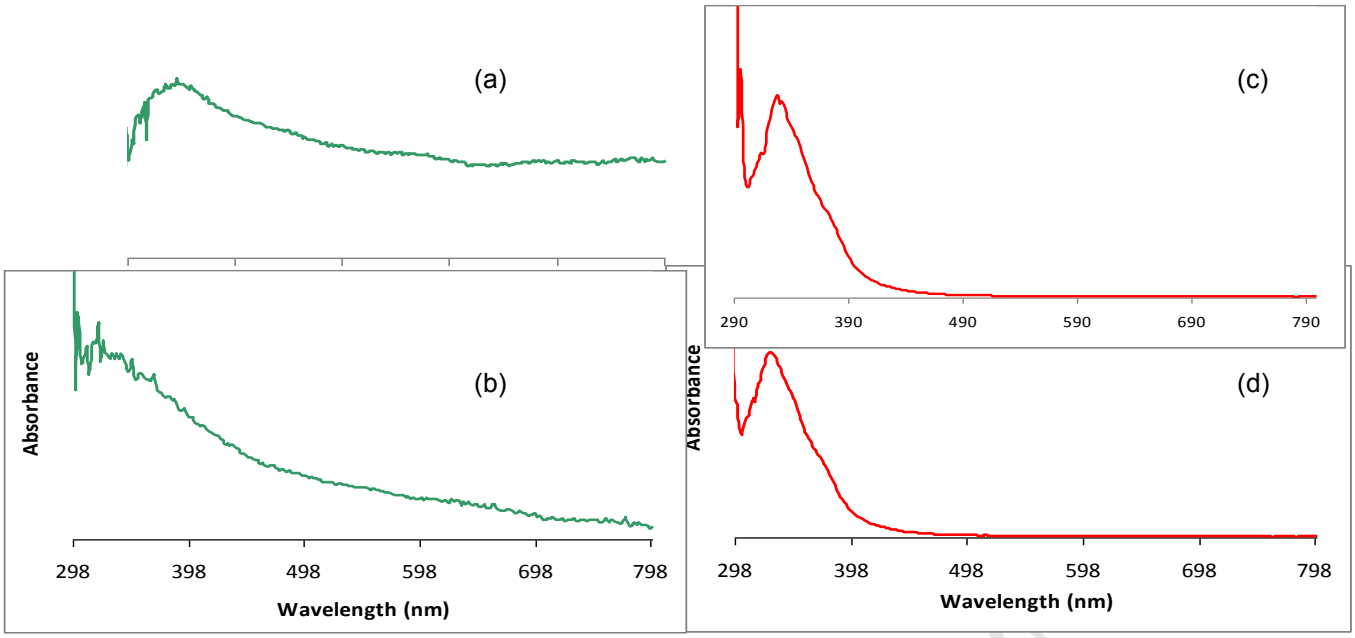

Fig. 2.2. UV-vis spectra (recorded as glycerol mulls) showing absorbance peaks of chitosan-supported complexes: **2.5** (a) and **2.6** (b) and complexes **2.11** (c) and **2.12** (d). Absorbance in arbitrary units (AU).

The IR spectral data for the chitosan-Schiff base derivatives (**2.1**-**2.4**) showed characteristic imine (C=N) stretching vibrations in the range of 1631-1648 cm^{-1}. There were also new bands in the range of 1559-1590 and 695-817 cm^{-1} which were not present in the starting materials (chitosan or 6-deoxy-6-amino chitosan). They were attributed to the (C=C) stretching vibrations and (C-H) bending vibrations in the aromatic ring of the Schiff-base ligands respectively.

Upon complexation of the chitosan-Schiff bases with Pd, subtle shifts in the imine stretching vibrations were observed. This is possibly due to low degree of incorporation of the Pd. Also, overlapping of the imine bands coordinated to Pd with those that are uncoordinated may occur since most of the imine sites were left unaltered during complexation.

The chitosan-based complexes and their corresponding chitosan-Schiff base ligands proved to be insoluble in most common solvents including THF, EtOH, MeOH, acetone and water, but showed slight swelling in DMSO.

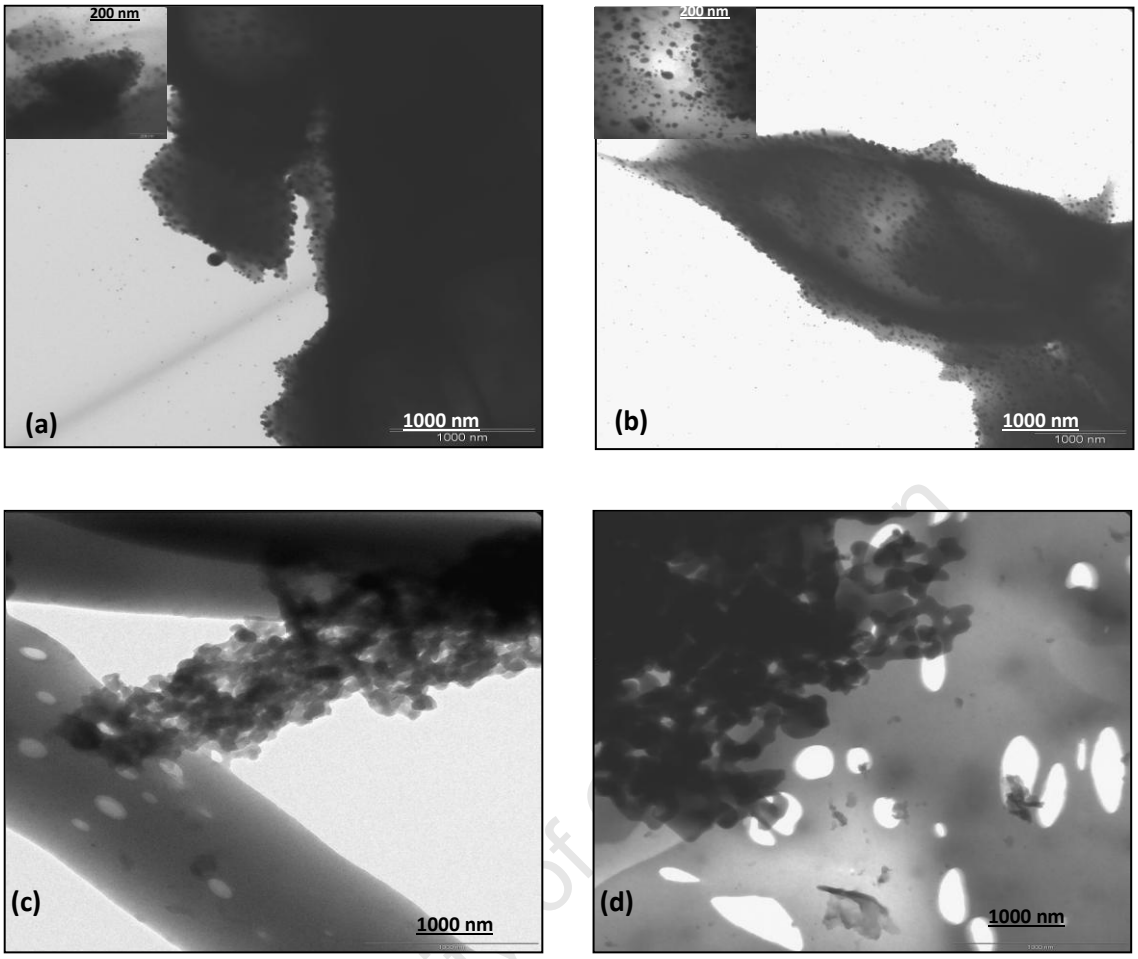

Fig. 2.3. TEM images of chitosan-supported complexes **2.5** (a), **2.6 (**b), **2.7** (c) and **2.8 (**d).

TEM images of supported complexes (**2.5**) and (**2.6**) taken at 1000 nm showed that these materials formed evenly dispersed nano-sized Pd particles across the biopolymer (**Figs. 2.3** (**a** and **b**)). The majority of these particles lie in the 15-20 nm range. Supported complexes (**2.7**) and (**2.8**) formed nano-sized Pd particles of average size 80-120 nm (**Figs.2.3** (**c** and **d**)). The existence of Pd particles visible through TEM imaging may imply intermolecular interactions between angstrom size molecular Pd^{II} sites on the biopolymer resulting in nanosized particles. Willocq *et al.* have also seen Pd and Ru particles of size range 2-6 nm on phosphine functionalized active carbon, in which surface coordination of Pd and Ru organometallic complexes was achieved through the phosphines on the active carbon. [9a-b]

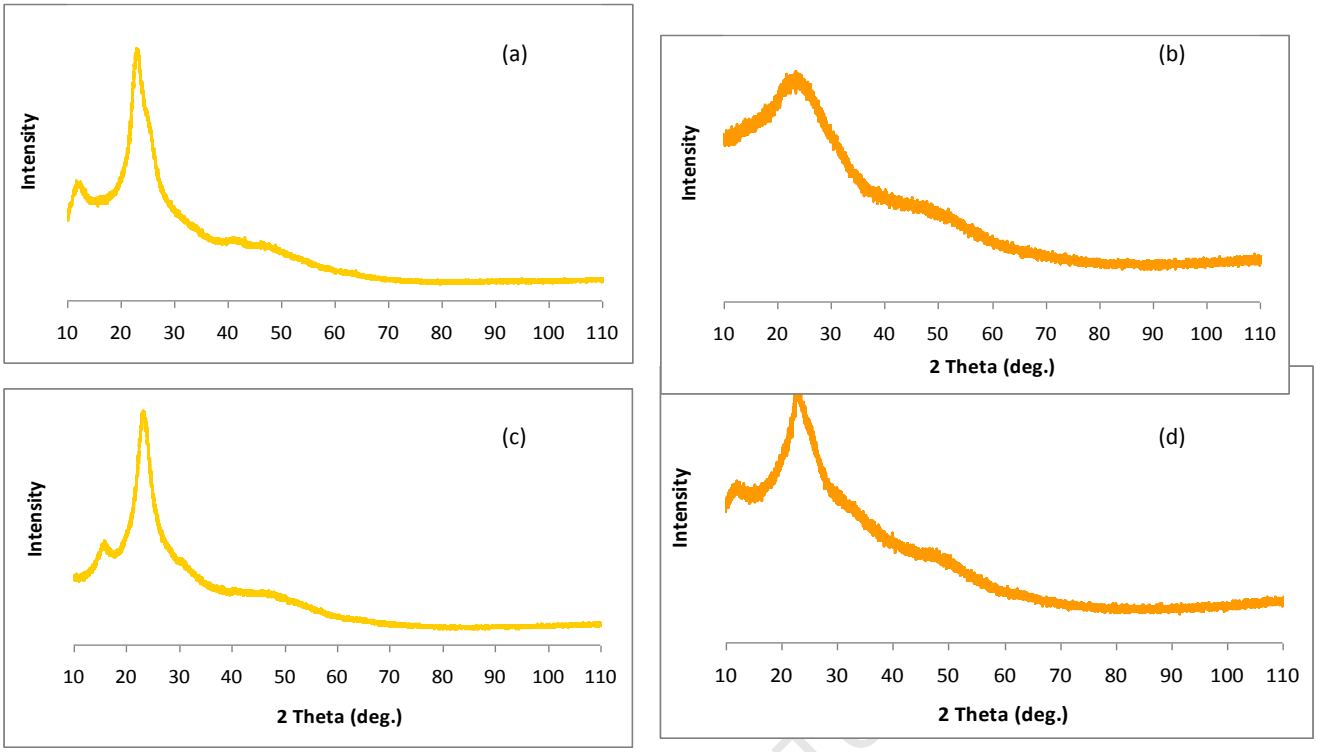

Fig. 2.4. Powder X-ray diffraction diagrams of chitosan-supported complexes (**2.5-2.8**) (a-d) Intensity in AU.

Characteristic Pd^0 peaks (2θ = 40˚, 45˚, 68˚ and 80˚) were not observed in the diffractograms of supported complexes (**2.5-2.8**), implying that Pd exists in an amorphous state on the chitosan structure (**Figs. 2.4** (**a-d**)). [1f] It was interesting to see that the crystallinity of chitosan was of fairly good quality showing well resolved specific peaks at 2θ = 15˚ and 25˚.[3e-f, 6e] As expected the 6-deoxy-6-amino chitosan has lower crystallinity, due to the reaction steps involved in introducing the second amino group (**Figs. 4** (**b** and **d**)).

The supported-Pd complexes (**2.5-2.8)** were analyzed thermally by thermal gravimetric analysis (TGA) in air (**Figs. 2.5** (**a-b**)). The TGA graphs of the supported complexes showed that these materials are stable up to 240 ˚C, following which a significant weight loss due to degradation of the biopolymer is observed. Thus the chitosan-Pd complexes would be capable of withstanding high reaction temperatures up to slightly below 240 ˚C. The 3.5-5.0% weight loss of the materials before the degradation is attributed to the desorption of water.[6c-d] Similar thermal analysis results were observed for the other two supported complexes (**2.7** and **2.8**) (see Appendix: **section a, Fig. a**).

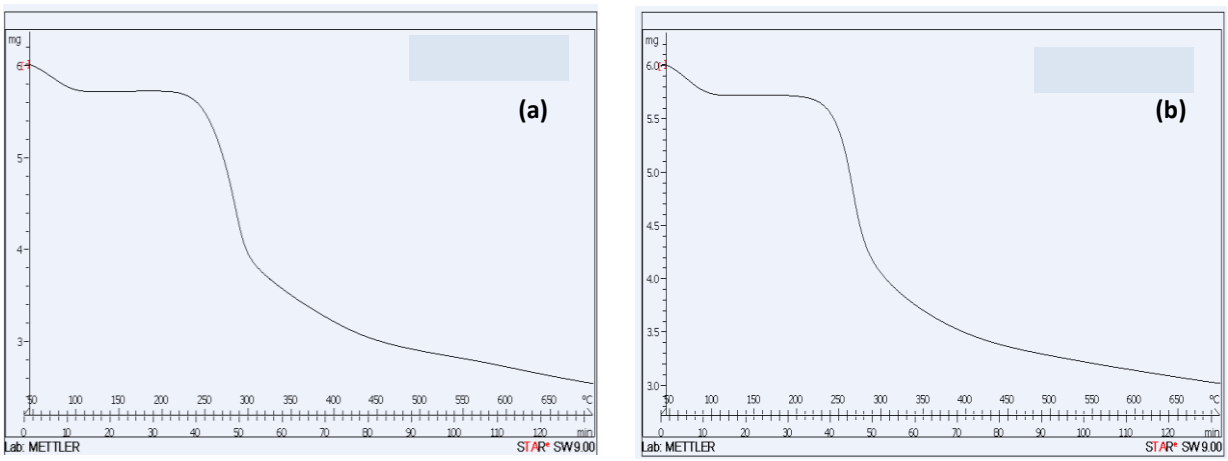

Fig. 2. 5. TGA plots of chitosan-supported complexes (a) **2.5**, (b) **2.6**.

Solid state ^{31}P NMR of the precursor chitosan-iminophosphine ligand (**2.2**) showed a signal at δ -18.5 ppm (**Fig 2.6a**) This further indicated that the ligand was successfully anchored to the chitosan support as this shift corresponded with the chemical shift obtained for the soluble ligand seen at δ -13.0 ppm. A peak due to phosphine oxide was also present at δ 35.0 ppm. [10a] The complex [$PdCl_2$(COD)] was reacted with the chitosan-iminophosphine and the solid ^{31}P NMR spectrum of the resulting chitosan-supported complex (**2.6**) showed a decrease in intensity of the peak at δ -18.5 ppm, and the appearance of a peak at *ca* δ 20.0 ppm assigned to phosphine coordinated to Pd^{II} complex (**Fig 2.6b**). This effect was previously observed in phosphine-Rh complexes attached to a peptide synthesis resin. [10b] These solid state ^{13}P NMR experiments indicated that there are changes on the chitosan structure on forming the chitosan-supported Schiff base ligand (**2.2**) and subsequent complex formation. To this effect, we have reason to believe molecular Pd^{II} complexes do exist on the chitosan and 6-deoxy-6-amino chitosan supports, and it would thus be fair to assume the same for the chitosan-supported Pd materials (**2.5** and **2.7**).

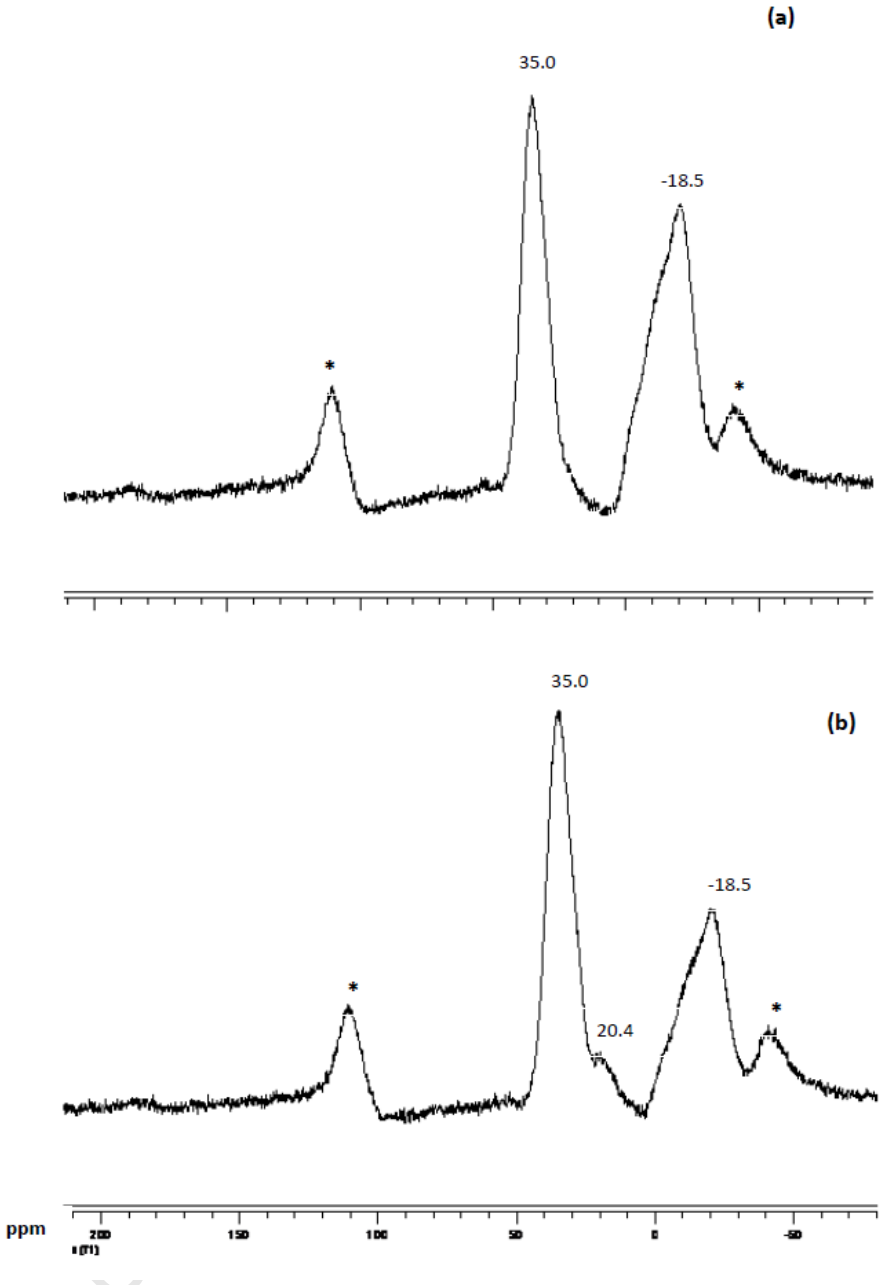

Fig. 2.6. Solid state ^{31}P NMR spectra of (a) chitosan-iminophosphine ligand (**2.2**) and (b), chitosan-supported Pd complex (**2.6**). ^{31}P one-pulse experiments were performed on 100 mg of each sample using a Bruker AMX 400 spectrometer at a ^{31}P frequency of 15 kHz at room temperature. Chemical shifts were referenced to Na_2HPO_4 at δ = 0 ppm. Signals arising from side bands are marked with an asterisk (*).

2.3 Synthesis and characterization of Pd^{II} mononuclear complexes

*2.3.1 1,3,4,6-tetra-O-acetyl-β-D-glucosyl-iminopyridyl and –iminophosphine Pd^{II} complexes (**2.11** and **2.12**)*

As model compounds for the heterogenized complexes (**2.5** and **2.6**), mononuclear Pd^{II} complexes (**2.11** and **2.12**) were also prepared *via* the Schiff-base condensation reaction of 1,3,4,6-tetra-*O*- acetyl-β-D-glucosamine hydrochloride to form 1,3,4,6-tetra-*O*-acetyl-β-D-glucos-2- pyridylimine (**2.9**) and 1,3,4,6-tetra-*O*-acetyl-β-D-glucos-2(diphenylphosphino)imine (**2.10**) which were subsequently reacted with $[PdCl_2(COD)]$ (**Scheme 2.3**). [10c] All compounds (**2.9-2.12**) were characterized using elemental analysis, ^1H and ^{31}P NMR spectroscopy, UV-vis spectroscopy (*vide ante,* **Fig. 2.1**), FT-IR spectroscopy and mass spectrometry.

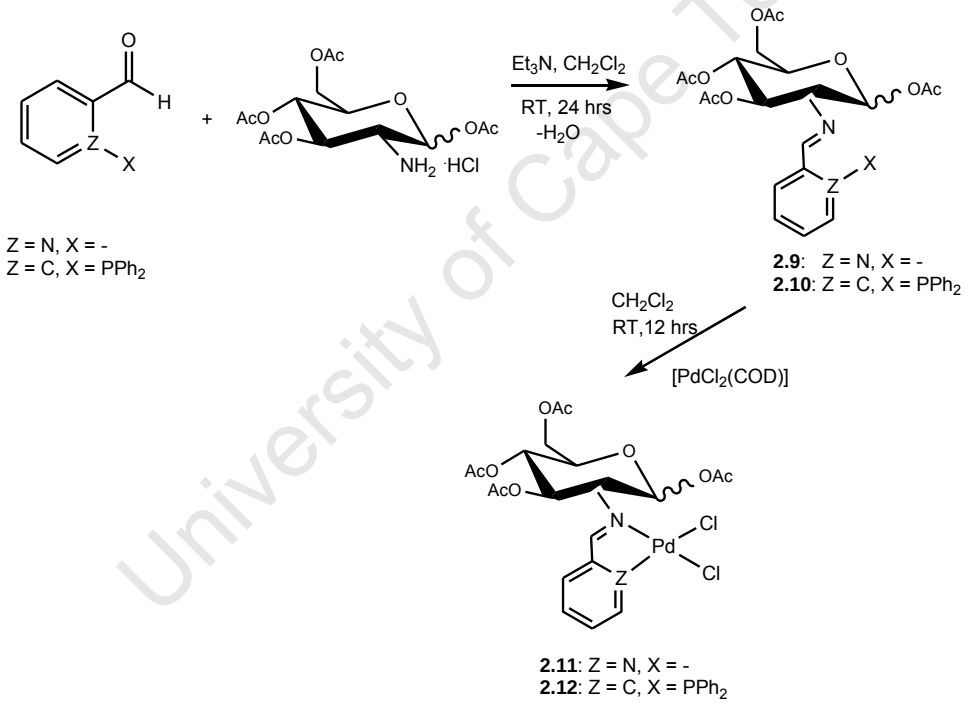

Scheme 2.3. Outline for the preparation of Schiff base ligands (**2.9** and **2.10**) and mononuclear Pd^{II} complexes (**2.11** and **2.12**).

The Schiff base ligands (**2.9** and **2.10**) were isolated as white and yellow solids respectively in good yields (78-90 %). They were soluble in most common organic solvents such as dichloromethane, chloroform, methanol and tetrahydrofuran.

Elemental analyses data were in agreement with the proposed formulations. The ^{1}H NMR spectra of ligands (**2.9** and **2.10**) displayed signals for the protons on the glucose ring in the range of δ 3.03-6.00 ppm and 4 singlets for the acetyl protons in the region of δ 2.03-2.21 ppm. The Schiff base condensation reaction was confirmed by the appearance of peaks in the range of δ 8.61-8.63 ppm assigned to the imine protons in ligands (**2.9** and **2.10**). The ^{31}P NMR spectrum of ligand (**2.10**) displayed a singlet at δ -13.01 ppm for **-**PPh_2.

The IR spectra of ligands (**2.9** and **2.10**) all displayed broad absorption bands at ≈ 1750 cm^{-1} assigned to the (C=O) vibrations. Common strong absorption bands were observed in the region of 1650 and 1697 cm^{-1} ($\nu(C=N)_{imine}$) in ligands (**2.9** and **2.10**) respectively. Additionally, ligand (**2.9**) showed a medium absorption band at 1593 cm^{-1} which was assigned to the pyridyl imine vibration. EI-mass spectrometry further confirmed the integrity of ligands (**2.9** and **2.10**) by displaying base peaks at *m/z* 394.10 (100%) and 577.14 (100%) for the $[M\text{-}OAc]^{+}$ ions respectively.

$[PdCl_2(COD)]$ was reacted with ligands (**2.9** and **2.10**) by stirring at room temperature in dichloromethane to afford complexes (**2.11** and **2.12**) (**Scheme 2.3**). These new complexes (**2.11** and **2.12**) were obtained as orange and yellow solids in good yields (90 and 92 %) respectively.

Elemental analyses and mass spectral data were consistent with the proposed structures for complexes (**2.11** and **2.12**). The ESI-mass spectral data for these complexes displayed $[M\text{-}OAc]^{+}$ *m/z* = 587.0 (96%) (**2.11**) and $[M\text{-}2H]^{+}$ (**2.12**) m/z = 794.1 (50%) as the highest molecular weight fragment.

^{1}H NMR spectra of complexes (**2.11** and **2.12**) showed imine protons in the region of δ 7.97-8.40 ppm. The observed upfield shifts relative to the free ligands evidenced coordination of the imine nitrogen to the palladium centre. This could be attributed to back-bonding from palladium to the imine bond and/or due to conformational changes experienced by the ligand in order to facilitate coordination of the imine nitrogen to the palladium centre. [10d]

The ^{31}P NMR spectrum of complex (**2.12**) displayed the expected downfield shift to δ 35.99 ppm from δ -13.01 ppm in the ligand (**2.10**) due to coordination of the phosphine moiety to palladium.

IR spectra of complexes (**2.11** and **2.12**) displayed shifts in the imine absorption bands from higher (**2.9** 1650 cm^{-1} and **2.10** 1697 cm^{-1}) to lower wavenumbers (**2.11** 1624 cm^{-1} and **2.12** 1676 cm^{-1}) due to palladium coordination. This decrease in stretching frequency is due to sigma donation of electrons from the imine nitrogen to the palladium centre, thus resulting in a slight loss in the double bond character of the imine bond.

2.4 Synthesis and characterization of chitosan-immobilized Rh^I complexes

*2.4.1 Chitosan-supported iminopyridyl and iminophospine Rh^I complexes (**2.13-2.14**)*

Chitosan-supported Rh complexes (**2.13** and **2.14**) were readily prepared by treatment of chitosan-Schiff base ligands (**2.1** and **2.2**) with $[RhCl(CO)_2]_2$. Thus, a mixture of the corresponding chitosan-Schiff base ligand (loading value: 0.12 $mmolg^{-1}$ (**2.1**) and 0.13 $mmolg^{-1}$ (**2.2**)) and an excess amount of $[RhCl(CO)_2]_2$ was stirred in dry acetone at room temperature (**Scheme 2.4**). The chitosan-supported Rh^I complexes (**2.13** and **2.14**) were obtained in good yields as stable light-orange and –purple solids respectively. They have been characterized by microanalysis, FT-IR, UV-vis, solid state ^{31}P and ^{13}C NMR spectroscopy, ICP-MS, P-XRD and TEM. Using these methods the proposed structure of the chitosan Schiff base ligands (**2.1** and **2.2**) and chitosan-supported complexes (**2.13** and **2.14**) have been verified to be as depicted in **Scheme 2.4** with the consideration of random anchoring.

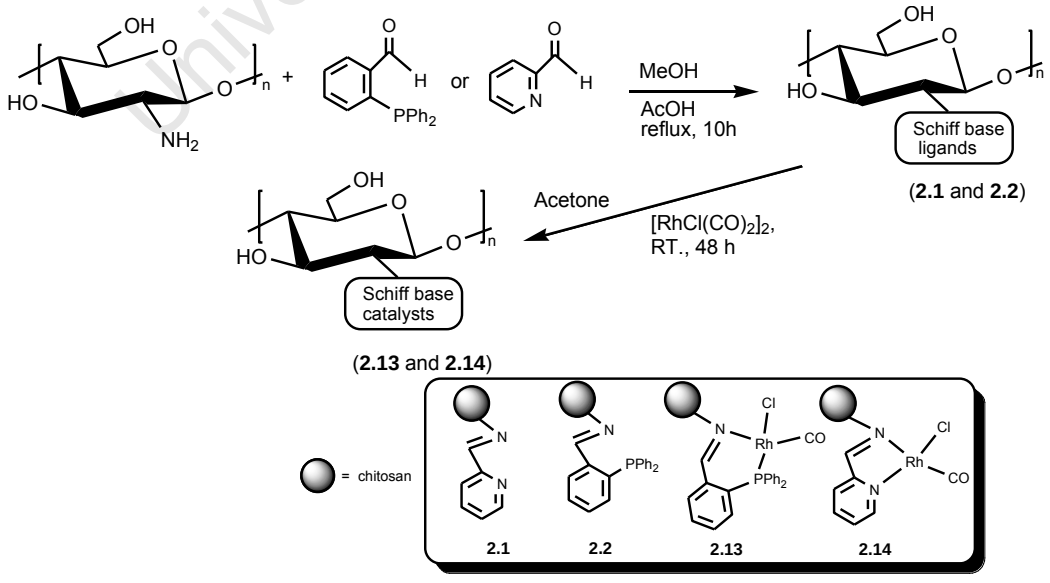

Scheme 2.4. Outline for the preparation of supported Schiff base ligands (**2.1** and **2.2**) and chitosan-supported complexes (**2.13** and **2.14**).

The partial complexation of Rh to the supported Schiff base ligands was supported by microanalysis data, which indicated changes in the percentage of C, H and N when moving from the supported ligands (**2.2** and **2.2**) to the supported complexes (**2.13** and **2.14**) (**Table 2.3**). ICP-MS results confirmed Rh loading values amounting to 0.145 mmolg^{-1} (**2.13**) and 0.092 mmolg^{-1} (**2.14**). These are slightly higher than those reported for analogous chitosan-supported Pd complexes, possibly implying that the biopolymer has a stronger affinity for Rh.

Table 2.3 Microanalyses, loadings and yields of compounds (**2.1-2.2** and **2.13-2.14**).

Compound	**Elemental analyses** (%)				**Ligand/Rh loading** (mmol g^{-1})	**Yield** (%)[d]
	C	**H**	**N**	**C/N**		
Chitosan	40.92	6.02	7.85	5.21	2.10[a]	-
2.2	44.63	5.92	6.44	6.93	0.12[b]	69
2.1	46.47	5.89	10.39	4.47	0.13[b]	84
2.13	39.42	4.12	4.35	9.06	0.145[c]	94
2.14	38.47	4.91	5.77	6.16	0.092[c]	90

[a] Free NH_2 (accessible and inaccessible) determined by microanalysis [8a]. [b] Determined using UV, absorbance is dependent on conc, solvent and pH [8b].[c] Determined using ICP-MS. [d] Yield by mass.

IR absorption bands at 1640 cm^{-1} (**2.13**) and 1650 cm^{-1} (**2.14**) (1591 cm^{-1} pyridyl imine) were observed for the imine (C=N) vibrations together with terminal carbonyl (Rh-*C*≡*O*) bands at 1998 cm^{-1} (**2.13**) and 2003 cm^{-1} (**2.14**). The existence of one carbonyl band suggests that one isomer is preferred for the supported molecular Rh complexes (see Appendix: **section b Fig. b**).

UV-vis studies conducted on supported complexes (**2.13** and **2.14**) as glycerol mulls revealed absorbance peaks at 319 nm and 348 nm for (**2.13** and **2.14**) respectively, these are in a similar range to those of their homogenous analogues 322 nm (**2.17**) and 342 nm (**2.18**) (see Appendix: **section c Fig. c**). These similar though weak peaks observed in UV-vis indicate the presence of molecular Rh complexes on the chitosan.

TEM is widely used for the elucidation of morphology, particle size and shape as well as distribution and has proven very useful in this application. [11-14] The particle sizes of supported complexes (**2.13** and **2.14**) were observed from TEM images to be spherically shaped nano-sized particles with sizes in the ranges of 3-7 nm (**2.13**) and 4-8 nm (**2.14**) (**Fig. 2.7**). They are uniformly dispersed across the biopolymer support and mostly equidistant.

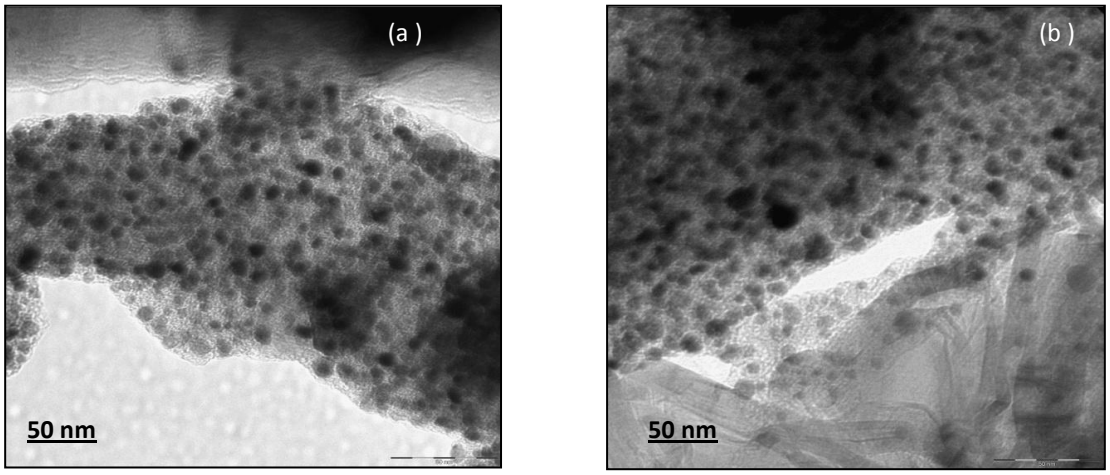

Fig. 2.7. TEM images of chitosan-supported Rh^{I} complexes (a) **2.13** and (b) **2.14.**

The crystallinity of the supported complexes was examined by powder X-ray diffraction (**Fig. 2.8**). No Rh peaks were observed in the diffractograms of supported complexes (**2.13** and **2.14**), meaning that the Rh particles are not composed of single crystallites. However, specific chitosan peaks (2θ = 15° and 25°) were evident on the diffractograms of both materials. This indicated high crystallinity of the chitosan support and suggests that the basic structure of the chitosan is not hindered during preparation of the supported complexes.

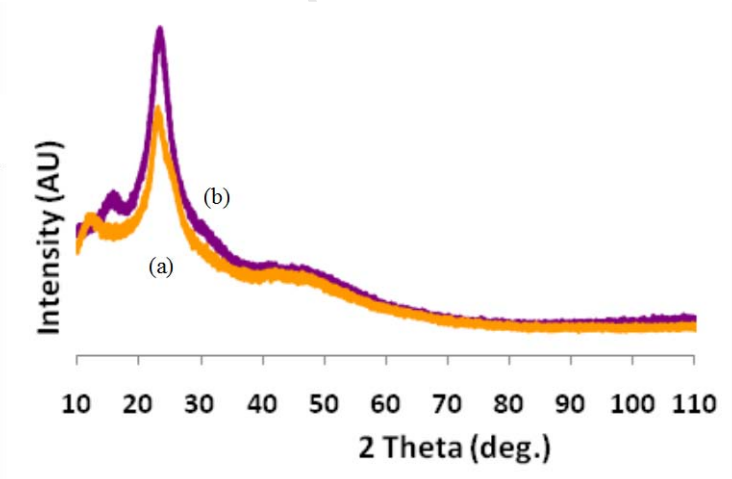

Fig. 2.8. Powder X-ray diffraction diagrams of chitosan-supported Rh^{I} complexes (a) **2.13** and (b) **2.14**.

Solid state ^{31}P NMR of the precursor chitosan-iminophosphine ligand (**2.2**) showed a signal at δ -18.5 ppm (**Fig 2.9a**). This further indicates that the ligand has been successfully anchored to the chitosan support as this shift corresponds with the chemical shift obtained for

the soluble ligand (**2.15**) (**Scheme 2.4**) seen at δ -13.0 ppm. A peak due to phosphine oxide was also present at δ 35.0 ppm.[10a] The complex $[RhCl(CO)_2]_2$ was reacted with the chitosan-iminophosphine and the solid state ^{31}P NMR spectrum of the resulting supported complex (**2.13**) showed a decrease in intensity of the peak at δ -18.5 ppm, and the appearance of a peak at δ 56.6 ppm assigned to the Rh complex (**Fig 2.9b**). This effect was previously observed in similar $[RhCl(PPh_3)_3]$ immobilized on phosphinated MCM-41. [10a-b] These NMR experiments indicated that there are changes of the chitosan structure on forming the chitosan-supported Schiff base ligand (**2.2**) and subsequent complex formation. To this effect, we have reason to believe molecular Rh^I complexes do exist on the chitosan support, and it would thus be fair to assume the same for the chitosan-supported iminopyridyl complex (**2.14**).

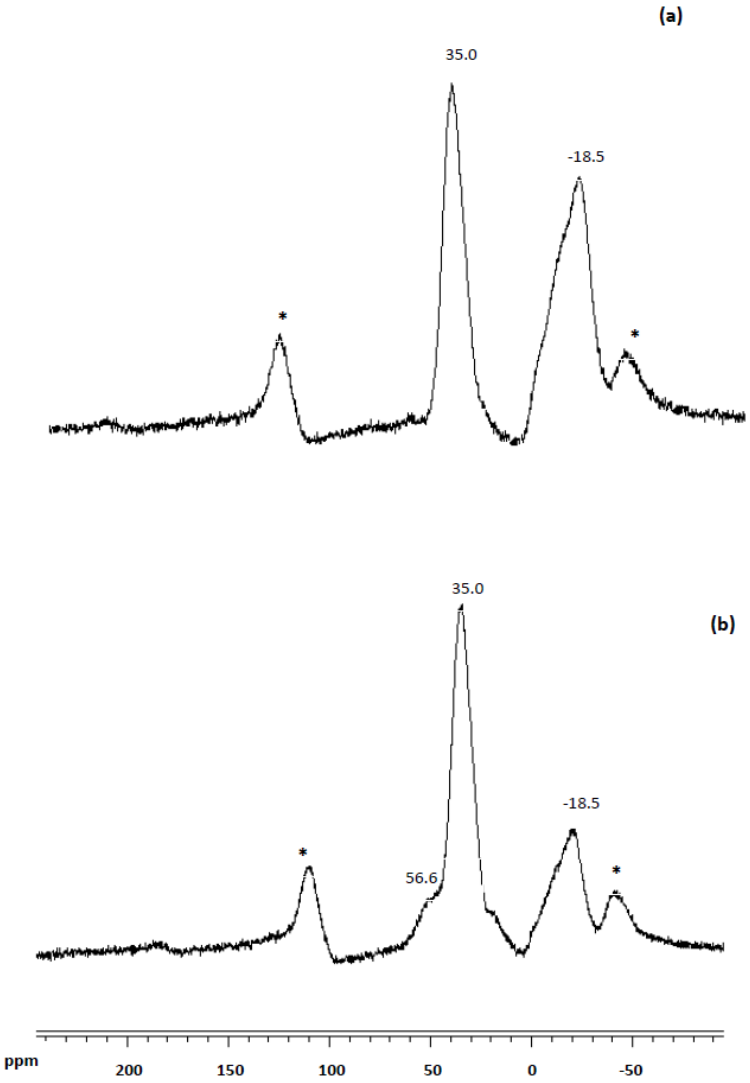

Fig. 2.9. Solid state ^{31}P NMR spectra of (a) chitosan-iminophosphine ligand (**2.2**) and (b), Chitosan-supported Rh complex (**2.13**). ^{31}P one-pulse experiments were performed on a Bruker AMX 400 spectrometer at a ^{31}P frequency of 15 kHz at room temperature. Chemical shifts were referenced to Na_2HPO_4 at δ = 0 ppm. Signals arising from side bands are marked with an asterisk (*).

The solid state ^{13}C NMR spectrum of the chitosan-supported iminophosphine ligand (**2.2**) evidenced successful anchoring of the iminophosphine ligand by the signal due to the imine carbon at δ = 174.0 ppm as well as a signal for the aromatic carbons at δ = 131.0 ppm (**Fig. 2.10** (a)). There is a slight drop in intensity of C_2 and C_4 carbons upon complexation of the Rh (**Fig. 2.10** (b)). This phenomenon strongly suggests possible spatial interactions of the coordinated complex with C_2 and C_4 of the chitosan backbone. Thus, further evidence of subtle structural modification of the chitosan can be seen on proceeding from chitosan-supported iminophosphine ligand (**2.2**) to chitosan-supported Rh complex (**2.13**).

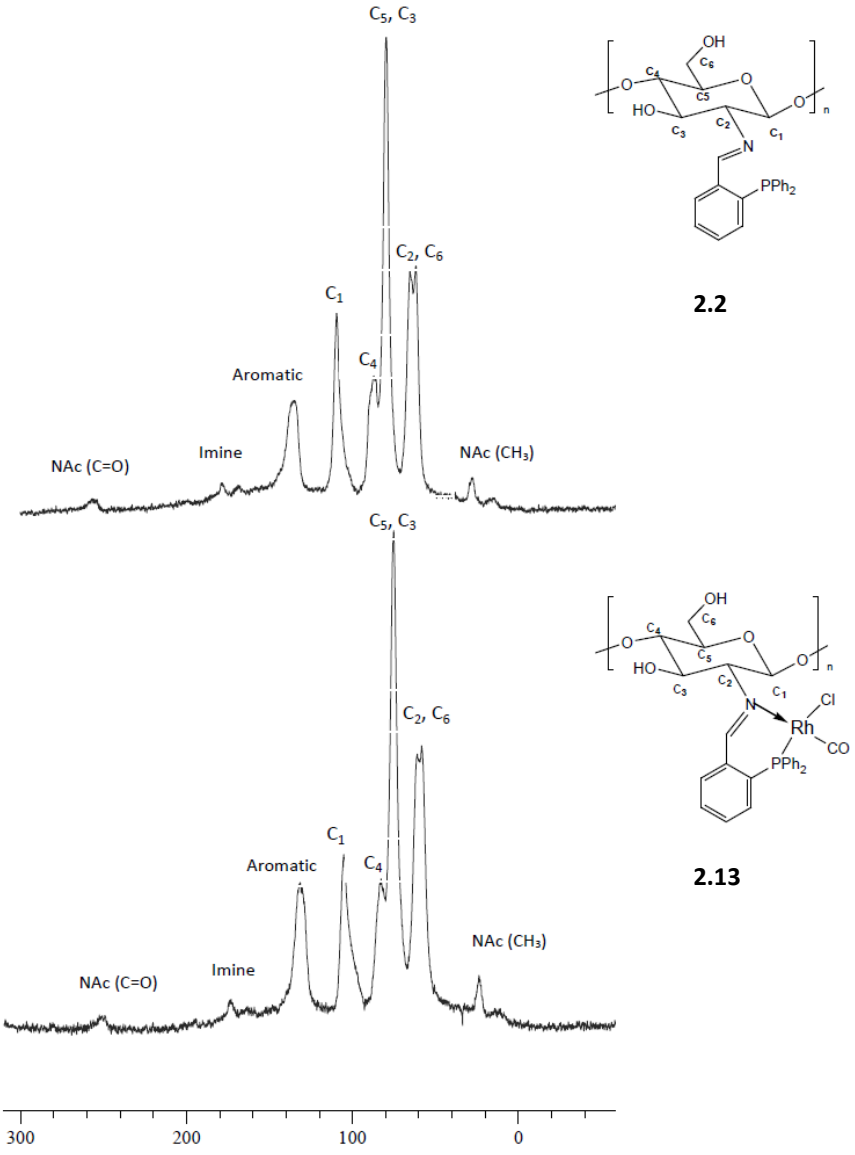

Fig. 2.10. Solid state ^{13}C NMR spectra of (a) chitosan-iminophosphine ligand (**2.2**) and (b), Chitosan-supported Rh complex (**2.13**). ^{13}C one-pulse experiments were performed on a Bruker AMX 400 spectrometer at a ^{13}C frequency of 121 kHz at room temperature. Chemical shifts were referenced to TMS at δ = 0 ppm.

2.5 Synthesis and characterization of Rh^I mononuclear complexes

*2.5.1 Cyclohexyl-iminopyridyl and - iminophosphine Rh^I complexes (**2.17-2.18**)*

The mononuclear analogues of chitosan-supported Rh^I complexes (**2.13** and **2.14**) were prepared by reaction of cyclohexyl-2-(diphenylphosphino)imine and cyclohexyl-2-iminopyridyl ligands (**2.15** and **2.16**) with $[RhCl(CO_2)]_2$ in dichloromethane (**Scheme 2.5**). The products were isolated in good yields (84% and 89%) as air- and moisture-stable bright orange and purple crystalline solids, respectively. Complex **2.17** decomposed without melting at 220 °C while **2.18** displayed a melting range of 182-185 ℃. These new complexes (**2.17** and **2.18**) have been characterized by microanalysis, FT-IR, ^1H and ^{31}P NMR spectroscopy, single X-ray diffraction and mass spectrometry.

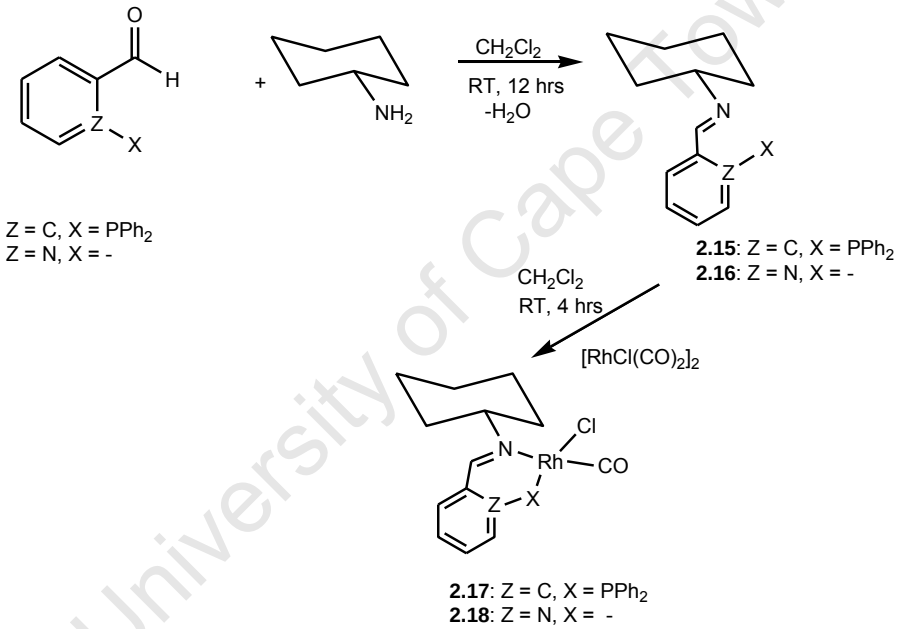

Scheme 2.5. Outline for the preparation of Schiff base ligands (**2.15** and **2.16**) and Rh^I complexes (**2.17** and **2.18**).

Microanalysis data for complexes (**2.17** and **2.18**) were in agreement with the calculated percentage C, H and N. Strong absorption bands, assignable to the imine C=N functionality were observed at 1625 cm^{-1} (**2.17**) and 1626 cm^{-1}(**2.18**) (pyridyl imine at 1609 cm^{-1} in complex (**2.18**)). Evidence for the coordination of the Rh metal center was observed through a shift from 1628 cm^{-1} in the cyclohexyl-2-(diphenylphosphino)imine ligand (**2.15**) to 1625 cm^{-1} in complex (**2.17**). Similarly a shift from 1646 cm^{-1} in the cyclohexyl-2-pyridyimine

ligand (**2.16**) to 1626 cm^{-1} in complex (**2.18**) was observed. Single very strong carbonyl (C≡O) bands at 1993 cm^{-1} and 1995 cm^{-1} suggested one preferred isomer in complexes (**2.17** and **2.18**) respectively . Based on the molecular structure of complex (**2.17**) (*vide infra* **Fig. 2.11**) this isomer is one bearing the terminal carbonyl group *trans* to the imine nitrogen.

NMR spectroscopy supported coordination of the cyclohexyl-2-(diphenylphosphino)imine ligand (**2.15**) in a chelating manner to form a Rh^{I} complex. This was seen in the shifting of two resonance signals in the ^{1}H NMR spectra. The signal due to the methine proton displayed an upfield shift from δ 8.73 ppm in (**2.15**) to δ 8.27 ppm in the Rh complex (**2.17**). Furthermore the protons on the carbon adjacent to the imine nitrogen showed a downfield shift from δ 3.03 ppm to δ 4.53 ppm. ^{31}P NMR evidenced coordination of phosphorus to Rh when the singlet observed in the cyclohexyl-2-(diphenylphosphino)imine ligand (**2.15**) (δ -13.45 ppm), shifted further downfield (δ 48.20 ppm) and appeared as a doublet with coupling constant 165 Hz in the spectrum of complex (**2.17**). This is consistent with Rh-P coupling. [15] For complex (**2.18**), a shifting of the methine proton resonance from δ 8.51 ppm in (**2.16**) to δ 8.35 ppm in (**2.18**) was seen as well as a downfield shift of the protons on the carbon adjacent to the imine nitrogen from δ 3.41 ppm to δ 4.53 ppm.

ESI-mass spectrometry further confirmed the integrity of the complexes (**2.17** and **2.18**) by displaying base peaks at *m/z* 502.1 (99%) and 318.92 (98%) for $[M\text{-}Cl]^{+}$ ions.

Single crystals of complex (**2.17**) were obtained by slow evaporation from dichloromethane : *n*-hexane. [16,17a] An ORTEP drawing of complex (**2.17**) with the corresponding labelling scheme is shown in **Fig. 2.11** together with selected bond lengths and angles. The molecular structure shows a 4-coordinate square-planar geometry around the Rh center, with the terminal carbonyl group *trans* to the imine functionality. The geometric parameters around the Rh atom are comparable with those found in similar complexes [RhCl(PyP)(CO)] (PyP = 1-(2-diphenylphosphino)ethylparazole)[17b] and [RhCl(P-N)(CO)] (P-N = 2-(diphenylphosphino)propylimine. [15] The angle P(1)-Rh(1)-Cl(1) (171.327(1)°) deviates from the expected 180°, indicating some distortion imposed by the 6-membered chelate ring about the Rh atom. This effect is also seen to cause deviation of the angle N(1)-Rh(1)-P(1) (84.91(4)°) from 90°.

Table 4.4 Selected bond distances and angles for rhodium (**2.17**).	
Bond distances (Å)	**Bond angles (°)**
Rh(1)-N(1) 2.1318(1)	N(1)-Rh(1)-P(1) 84.91(4)
Rh(1)-P(1) 2.2016(4)	N(1)-Rh(1)-Cl(1) 91.62(4)
Rh(1)-Cl(1) 2.4028(4)	C(1)-Rh(1)-Cl(1) 87.95(5)
Rh(1)-C(1) 1.8261(1)	C(1)-Rh(1)-P(1) 95.68(5)
N(1)-C(2) 1.2823(2)	P(1)-Rh(1)-Cl(1) 171.327(1)
N(1)-C(21) 1.4927(2)	C(1)-Rh(1)-N(1) 178.71(6)

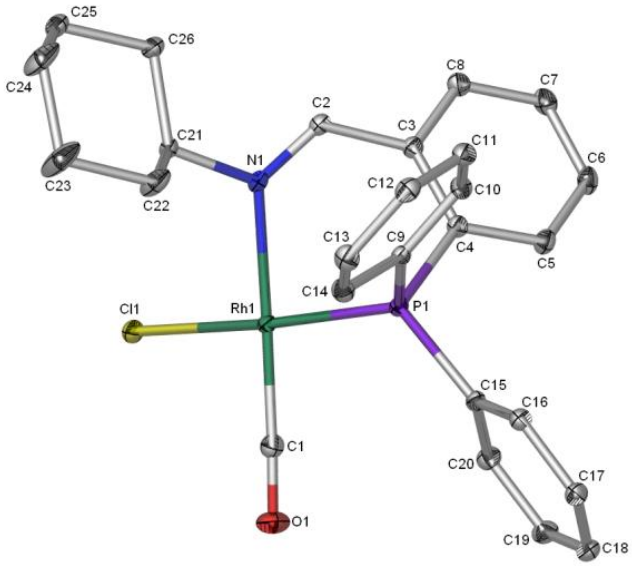

Fig. 2.11. Molecular structure of the mononuclear Rh^{I} iminophosphine complex (**2.17**) showing ellipsoids at the 50% probability level with hydrogen atoms omitted for clarity.

2.6 Summary and Conclusions

In summary, several new chitosan- and 6-deoxy-6-amino chitosan-supported Pd^{II} and Rh^{I} complexes and their precursors have been successfully prepared in a stable form. These materials were characterized using a variety of complementary techniques including elemental analysis, UV-vis, FT-IR, ICP-MS, PXRD, TEM, TGA as well as ^{31}P and ^{13}C solid state NMR. Stable mononuclear model Pd^{II} and Rh^{I} complexes of the chitosan-supported complexes were also prepared and characterized using ^{1}H and ^{31}P NMR, UV-vis and FT-IR spectroscopy, mass spectrometry, elemental analysis and single crystal X-ray crystallography. These chitosan-supported complexes and their mononuclear analogues have been

investigated as catalyst precursors in Suzuki-Miyaura and Heck cross-coupling reactions (Pd) as well as hydroformylation (Rh). These catalytic testing results are reported in chapter 3.

2.7 Experimental

Low molecular weight chitosan (Cat. No. 44,886-9, deacetylation 75-85% average molecular weight of < 6000 units), 1,5-cyclooctadiene (COD), 2-pyridinecarboxaldehyde and 2(diphenylphosphino)benzaldehyde were purchased from Sigma-Aldrich and used as received. 6-deoxy-6-amino chitosan [7a] and 1,3,4,6-tetra-*O*-acetyl-β-D-glucosamine hydrochloride [18] were prepared according to reported procedures. All solvents were obtained commercially and distilled under N_2 prior to use. Methanol, ethanol dichloromethane and acetone were dried over calcium hydride. $PdCl_2$ and $RhCl_3.3H_2O$ were obtained from Johnson Matthey. $[PdCl_2(COD)]$ [7c] and $[RhCl(CO)_2]_2$[19] were prepared according to literature procedures.

UV-vis spectra were obtained at ambient temperature using a Varian Cary 50 Conc. UV-vis spectrophotometer with samples prepared as glycerol mulls. Powder X-ray diffraction (PXRD) data was collected on a Bruker D8 Advanced diffractometer (Co-Kα-radiation, λ = 1.78897 Å). IR spectra were recorded as KBr disks on a Perkin-Elmer Spectrum One FT-IR spectrophotometer. Elemental analyses were conducted with a Thermo Flash 1112 Series CHNS-O Analyzer. Ionisation (ESI) mass spectrometry was carried out on a Waters API Quattro Micro triple quadrupole mass spectrometer in the positive-ion mode. Electron Impact mass spectrometry was conducted on an Agilent 6890 N mass spectrometer. Inductively coupled plasma-mass spectrometry was obtained using a Perkin-Elmer Elan600 quadrupole ICP-MS with a Cetax LSX-200 UV laser module. TEM imaging was done on a JEOL 1200EXII CRYO TEM. ^1H and ^{31}P NMR spectra were recorded on a Varian XR400 MHz spectrometer using tetramethylsilane (TMS) as the internal standard (for ^1H) and H_3PO_4 as the external standard (for ^{31}P). Solid state ^{31}P and ^{13}C NMR one-pulse experiments were conducted on a Bruker AMX 400 spectrometer at a ^{31}P frequency of 15 kHz and ^{13}C frequency of 121 kHz at room temperature. Chemical shifts were referenced to either Na_2HPO_4 or TMS at δ = 0 ppm. Single crystal X-ray intensity data were collected on a Nonius Kappa-CCD diffractometer using graphites monochromated MoKα radiation. The temperature was controlled by an Oxford Cryostream cooling system (Oxford Cryostat). The strategy for data collections was evaluated using the Bruker Nonius "Collect" program. Data

were scaled and reduced using DENZO-SMN software. Absorption corrections were made empirically utilizing the SADABS program. The structure was solved by direct methods and refined using full matrix least-squares with the program SHELXL-97 refining F^2. Packing diagrams were produced using the program PovRay and graphic interface X-seed. All non-H atoms were refined anisotropically.

*2.7.1 General procedure for the synthesis of 6-deoxy-6-amino chitosan- and chitosan-Schiff base ligands (**2.1-2.4**).*

Chitosan and the corresponding aldehydes (30 mmol) were refluxed in methanol (30 ml) and acetic acid (3 ml) for 10 hours. After completion of the reaction, the chitosan-Schiff base ligands were collected by filtration and washed thoroughly with distilled water, ethanol then acetone (50 ml each) respectively. The product was then dried under vacuum at 60 °C for 8 hours.

6-deoxy-6-amino chitosan-Schiff base ligands (**2.3**) and (**2.4**) were prepared by a similar procedure as above.

*Preparation of chitosan-2-pyridylimine (**2.1**).*

Compound (**2.1**) was prepared using chitosan (1.90 g) and 2-pyridinecarboxaldehyde (2.87 ml, 30.08 mmol). The product was obtained as a light brown solid. Yield by mass, (1.60 g, 84%). **FT-IR** (KBr): 3422 ν(OH), 2881 ν(C-H), 1649, ν(C=N), 1590 ν(pyridyl C=N), 1569 ν(C=C), 1153-1070 ν(pyranose) and 776 cm^{-1} ν(aromatic C-H). Elemental analysis (%), Found: C, 54.79; H, 6.02; N, 10.39.

*Preparation of chitosan-2(diphenylphosphino)imine (**2.2**).*

Compound (**2.2**) was prepared using chitosan (0.500 g) and 2-(diphenylphosphino)benzaldehyde (0.160 g, 0.56 mmol). The product was obtained as a light brown solid. Yield by mass, (0.725 g, 69%). **FT-IR** (KBr): 3429 ν(OH), 2917 ν(C-H), 1642, ν(C=N), 1577 ν(aromatic C=C), 1158-1024 ν(pyranose) and 665 cm^{-1} ν(aromatic C-H). Elemental analysis (%), Found: C, 44.63; H, 6.92; N, 7.03.

*Preparation of 6-deoxy-6-amino chitosan-2-pyridylimine (**2.3**).*

Compound (**2.3**) was prepared using 6-deoxy-6-amino chitosan (0.400 g) and 2-pyridinecarboxaldehyde (1.20 ml, 12.53 mmol). The product was obtained as a brown solid. Yield by mass (0.241 g, 60%). **FT-IR** (KBr): 3434 ν(OH), 2919 ν(C-H), 1648 ν(C=N), 1591 ν(pyridyl C=N), 1569 ν(aromatic C=C), 1154-1069 ν(pyranose) and 777 cm^{-1} ν(aromatic C-H). Elemental analysis (%), Found: C, 50.08; H, 5.89; N, 9.10.

*Preparation of 6-deoxy-6-amino 2(diphenylphosphino)imine (**2.4**).*

Compound (**2.4**) was prepared using 6-deoxy-6-amino chitosan (0.500 g) and 2-(diphenylphosphino) benzaldehyde (0.142 g, 0.490 mmol). The product was obtained as an orange solid. Yield by mass, (0.324 g, 65%). **FT-IR** (KBr): 3436 ν(OH), 2913 ν(C-H), 1639 ν(C=N), 1154-1023 ν(pyranose) and 697 cm^{-1} ν(aromatic C-H). Elemental analysis (%), Found: C, 45.66; H, 6.22; N, 7.28.

*2.7.2 General procedure for the synthesis of 6-deoxy-6-amino chitosan- and chitosan-Schiff base Pd^{II} complexes (**2.5-2.8**).*

The 6-deoxy-6-amino chitosan- and chitosan-Schiff base ligands were stirred with [$PdCl_2$(COD)], in acetone at room temperature over 48 hours. After the reaction, the supported Schiff base catalysts were collected by filtration (suction), "conditioned" by refluxing in ethanol for 10 hours in order to remove unreacted Pd, washed with distilled water, ethanol then acetone (50 ml each) respectively then dried under vacuum at 60 °C for 8 hours.

*Preparation of chitosan-2-pyridylimine-Pd complex (**2.5**)*

Compound (**2.5**) was prepared using chitosan-Schiff base (**2.1**) (0.500 g, 0.025 mmol) and [$PdCl_2$(COD)] (0.021 g, 0.075 mmol). The product was obtained as a yellow solid. Yield by mass, (0.482 g, 96%). **FT-IR** (KBr): 3418 ν(OH), 2881 ν(C-H), 1651 ν(C=N), 1591 ν(pyridyl

C=N), 1569 ν(aromatic C=C), 1152-1068 ν(pyranose) and 776 cm^{-1} ν(aromatic C-H). Elemental analysis (%), Found: C, 48.82; H, 5.92; N, 9.05. **ICP-MS** (Pd, $mmolg^{-1}$): 0.044.

*Preparation of chitosan-2(diphenylphosphino)imine-Pd complex (**2.6**)*

Compound (**2.6**) was prepared using chitosan-Schiff base (**2.2**) (0.350 g, 0.035 mmol) and [$PdCl_2$(COD)] (0.030 g, 0.105 mmol). The product was obtained as a pale yellow solid. Yield by mass, (0.310 g, 88%). **FT-IR** (KBr): 3429 ν(OH), 2920 ν(C-H), 1639 ν(C=N), 1576 ν(aromatic C=C), 1154-1023 ν(pyranose) and 669 cm^{-1} ν(aromatic C-H). Elemental analysis (%), Found: C, 44.54; H, 5.65; N, 5.10. **ICP-MS** (Pd): 0.054 $mmolg^{-1}$.

*Preparation of 6-deoxy-6-amino chitosan-2-pyridylimine-Pd complex (**2.7**)*

Compound (**2.7**) was prepared using 6-deoxy-6-amino chitosan-Schiff base (**2.3**) (0.200 g, 0.02 mmol) and [$PdCl_2$(COD)] (0.017 g, 0.06 mmol). The product was obtained as a dark yellow solid. Yield by mass, (0.218 g, 91%). **FT-IR** (KBr): 3419 ν(OH), 2918 ν(C-H), 1639 ν(C=N), 1595 ν(pyridyl C=N), 1566 ν(aromatic C=C), 1152-1066 ν(pyranose) and 775cm^{-1} ν(aromatic C-H). Elemental analysis (%), Found: C, 44.08; H, 5.70; N, 7.42. **ICP-MS** (Pd): 0.121 $mmolg^{-1}$.

*Preparation of 6-deoxy-6-amino chitosan-2(diphenylphosphino)imine-Pd complex (**2.8**)*

Compound (**2.8**) was prepared using 6-deoxy-6-amino chitosan-Schiff base (**2.4**) (0.350 g, 0.035 mmol) and [$PdCl_2$(COD)] (0.150 g, 0.052 mmol). The product was obtained as a dark orange solid. Yield by mass, (0.100 g, 67%). **FT-IR** (KBr): 3428 ν(OH), 2920 ν(C-H), 1638 ν(C=N), 1576 ν(aromatic C=C), 1152-1021 ν(pyranose) and 667 cm^{-1} ν(aromatic C-H). Elemental analysis, Found: C, 42.08; H, 6.50; N, 4.12. **ICP-MS** (Pd): 0.123 $mmolg^{-1}$.

*Preparation of 1,3,4,6-tetra-O-acetyl-β-D-glucosyl-2-pyridylimine (**2.9**) and its Pd^{II} complex (**2.11**)*

1,3,4,6-tetra-*O*-acetyl-β-D-glucosamine hydrochloride (0.500 g, 1.440 mmol) was treated with Et_3N (0.218 g, 2.160 mmol) in dry CH_2Cl_2 (30 ml) for 15 min. 2-pyridinecarboxaldehyde (0.154 g, 1.440 mmol) was then added to the solution and the contents were stirred for 24 hours at room temperature. Anhydrous magnesium sulphate was transferred to the stirred solution and the mixture was filtered; the solvent was removed by rotary evaporation to give a white solid of the 1,3,4,6-tetra-*O*-acetyl-β-D-glucosyl-2-pyridylimine ligand (**2.9)**. Yield, (0.243 g, 90%). Mp.: 49-52 ˚C. **FT-IR** (KBr): 2960 (s) ν(C-H), 1754 (vs) ν(C=O), 1650 (s) ν(C=N), 1593 (m) ν(pyridyl C=N), 1569 (m) ν(aromatic C=C), 1220-1206 (vs) ν(pyranose) and 779 cm^{-1} (s) ν(aromatic C-H). **^{1}H NMR** (400 MHz, DMSO-d_6, 25°C): δ (ppm) = 8.66 (d, 1H, J = 4.8 Hz, Ar_{pyr}), 8.63 (s, 1H, imine), 8.00 (m, 1H, **Ar**$_{pyr}$), 7.76 (m, 1H, **Ar**$_{pyr}$), 7.36 (m, 1H, **Ar**$_{pyr}$), 6.00 (d, 1H, $J_{H,H}$ = 9.5 Hz, C-**H**$_{pyranose}$), 5.48 (t, 1H, $J_{H,H}$ = 9.7 Hz, C-**H**$_{pyranose}$) , 5.18 (t, 1H, $J_{H,H}$ = 8.37 Hz, C-**H**$_{pyranose}$), 4.16 (dd, 2H, $J_{H,H}$ = 1.9, 12.4 Hz, C**H**$_2$), 4.00 (m, 1H, C-**H**$_{pyranose}$ 4), 3.60 (dd, 1H, $J_{H,H}$ = 9.5 Hz, C-**H**$_{pyranose}$), 1.98-2.21 (4s, 12H, **OAc**). Elemental analysis calculated for $C_{21}H_{28}N_2O_9$ (%): C, 55.75; H, 6.24, N, 6.19, Found: C, 55.43; H, 6.18; N, 6.27. **EI-MS**: m/z 394.10, $[M\text{-}OAc]^+$, 100%.

$[PdCl_2(COD)]$ (0.131 g, 0.459 mmol) was added to the 1,3,4,6-tetra-*O*-acetyl-β-D-glucosyl-2-pyridylimine ligand (0.200 g, 0.459 mmol) in dry CH_2Cl_2 (25 ml) and the reaction mixture was stirred at room temperature. After 12 hours, the solvent was removed by rotary evaporation to afford an orange solid which was washed with *n*-hexane (3 x 25 ml) and dried under vacuum for 2 hours. Compound (**2.11**); Yield, (0.180 g, 90%). Mp.: decomp. without melting at 248 ˚C. **FT-IR** (KBr): 2957 (s) ν(C-H), 1754 (vs) ν(C=O), 1624 (s) ν(C=N), 1588 (m) ν(pyridyl C=N), 1569 (m) ν(aromatic C=C), 1224-1214 (vs) ν(pyranose)and 770 cm^{-1} (s) ν(aromatic C-H). **^{1}H NMR** (400 MHz, DMSO-d_6, 25°C): δ (ppm) = 9.03 (d, 1H, J = 5.3 Hz, **Ar**$_{pyr}$), 8.40 (s, 1H, imine), 8.36 (m, 1H, **Ar**$_{pyr}$) , 8.17 (m, 1H, **Ar**$_{pyr}$), 7.91 (m, 1H, **Ar**$_{pyr}$), 6.44 (d, 1H, $J_{H,H}$ = 8.37 Hz, C-**H**$_{pyranose}$), 5.44 (m, 1H, C-**H**$_{pyranose}$), 5.21 (t, 1H, $J_{H,H}$ = 9.1 Hz, C-**H**$_{pyranose}$), 4.24 (dd, 2H, $J_{H,H}$ = 4.1, 12.6 Hz, C**H**$_2$), 4.12 (m, 1H, C-**H**$_{pyranose}$), 3.99 (m, 1H, C-**H**$_{pyranose}$), 1.92-2.29 (4s, 12H, **OAc**). Elemental analysis calculated for $C_{20}H_{24}Cl_2N_2O_9Pd$ (%): C, 39,14; H, 3.94, N, 4.56, Found: C, 39.33; H, 3.10; N, 4.77. **ESI-MS**: m/z 587.0, $[M\text{-}OAc]^+$, 96%.

*Preparation of 1,3,4,6-tetra-O-acetyl-β-D-glucosyl-2(diphenylphosphino)imine (**2.10**) and its Pd^{II} complex (**2.12**)*

The protected sugar 1,3,4,6-tetra-*O*-acetyl-β-D-glucosamine hydrochloride (0.280 g, 0.806 mmol) was treated with Et_3N (0.122 g, 1.209 mmol) in dry CH_2Cl_2 (25 ml) for 15 min. 2-(diphenylphosphino)benzaldehyde (0.233 g, 0.806 mmol) was then added to the solution and the contents were stirred for 24 hours at room temperature. Anhydrous magnesium sulphate was transferred to the stirred solution and the mixture was filtered, the solvent was removed by rotary evaporation to give a yellow solid of the 1,3,4,6-tetra-*O*-acetyl-β-D-glucosyl-2(diphenylphosphino)imine ligand (**2.10**) which was dried under vacuum for 2 hours. Yield, (0.218 g, 78%). Mp.: 109-111 ˚C. **FT-IR** (KBr): 2977 (s) ν(C-H), 1755 (vs) ν(C=O), 1697 (s) ν(C=N), 1674 (s) ν(aromatic C=C), 1254-1228 (vs) ν(pyranose) and 700 cm^{-1} (s) ν(aromatic C-H). **^{1}H NMR** (400 MHz, DMSO-d_6, 25°C): δ (ppm) = 8.61 (s, 1H, imine), 6.98-7.52 (br m, 14H, **Ar**), 5.46 (d, 1H, $J_{H,H}$ = 8.5 Hz, C-**H**$_{pyranose}$), 5.03 (m, 1H, C-**H**$_{pyranose}$), 4.11 (m, 1H, C-**H**$_{pyranose}$), 4.08 (d, 2H, $J_{H,H}$ = 2.0 Hz, C**H**$_2$), 3.82 (m, 1H, C-**H**$_{pyranose}$), 3.03 (m, 1H, C-**H**$_{pyranose}$), 2.03-2.17 (4s, 12H, **OAc**). **^{31}P{^{1}H} NMR** (121 MHz, DMSO-d_6, 25°C): δ (ppm) = -13.01, (s). Elemental analysis calculated for $C_{34}H_{38}NO_9P$ (%): C, 64.24; H, 6.03, N, 2.20. Found: C, 64.11; H, 6.22; N, 2.89 **EI-MS**: m/z 577.14, $[M\text{-}OAc]^+$, 99%.

$[PdCl_2(COD)]$ (0.184 g, 0.646 mmol) was added to the 1,3,4,6-tetra-*O*-acetyl-β-D-glucosyl-2(diphenylphosphino)imine ligand (0.400 g, 0.646 mmol) in dry CH_2Cl_2 (30 ml) and this was stirred at room temperature. After 12 hours, the solvent was removed by rotary evaporation to afford a yellow solid (of compound (**2.12**)) which was washed with *n*-hexane (3 x 25 ml) and dried under vacuum for 2 hours. Yield, (0.401 g, 92%). Mp.: 146-147 ˚C. **FT-IR** (KBr): 2946 (s) ν(C-H), 1747 (vs) ν(C=O), 1676 (s) ν(C=N), 1573 (m) ν(aromatic C=C), 1242-1211 (vs) ν(pyranose) and 693 cm^{-1} (s) ν(aromatic C-H). **^{1}H NMR** (400 MHz, DMSO-d_6, 25°C): δ (ppm) = 7.97 (s, 1H, imine), 7.36-7.52 (br m, 14H, **Ar**), 5.93 (d, 1H, $J_{1,2}$ = 8.20 Hz, C-**H**$_{pyranose}$), 5.39 (m, 1H, C-**H**$_{pyranose}$), 5.21 (t, 1H, $J_{H,H}$ = 9.7 Hz, C-**H**$_{pyranose}$), 4.17 (dd, 2H, $J_{H,H}$ = 4.1, 12.0 Hz, C**H**$_2$), 4.00 (m, 1H, C-**H**$_{pyranose}$), 3.54 (m, 1H, C-**H**$_{pyranose}$), 1.92-2.05 (4s, 12H, **OAc**). **^{31}P{^{1}H} NMR** (121 MHz, DMSO-d_6, 25°C): δ (ppm) = 35.99, (s). Elemental analysis calculated for $C_{33}H_{34}Cl_2NO_9PPd$ (%): C, 49,74; H, 4.30; N, 1.76. Found: C, 49.18; H, 4.58; N, 1.77. **EI-MS**: m/z 794.1, $[M\text{-}2H]^+$, 50%.

*2.7.3 General procedure for the synthesis of chitosan-Schiff base Rh^I complexes (**2.13-2.14**).*

The appropriate chitosan-Schiff base ligand was stirred with $[RhCl(CO)_2]_2$, in acetone at room temperature over 48 hours. After the reaction, the supported Schiff base complexes were collected by filtration (suction), "conditioned" by refluxing in ethanol for 10 hours in order to remove unreacted Rh, washed with distilled water, ethanol and acetone (50 ml each), and then dried under vacuum at 60 °C for 8 hours.

*Preparation of chitosan-2-(diphenylphosphino)imine-Rh complex (**2.13**).*

Compound (**2.13**) was prepared using chitosan-2-(diphenylphosphino)imine (**2.2**) (0.350 g, 0.035 mmol) and $[RhCl(CO_2)]_2$ (0.040 g, 0.105 mmol) The product was obtained as a light orange solid and then dried under vacuum at 60 °C for 8 hours. Yield, (0.299 g, 85%). **FT-IR** (KBr) : 3434 (s) ν(O-H), (m) 2913 ν(C-H), 2003 (s) ν(C≡O), 1640 (s) ν(C=N), 1575 (m) ν(aromatic C=C), (br, s) 1154-1071 ν(pyranose) and (s) 895 cm^{-1} ν(aromatic C-H). Elemental Analysis (%): Found C, 40.47; H, 4.62; N, 4.35. **ICP-MS** (Rh): 0.145 $mmolg^{-1}$.

*Preparation of chitosan-2-pyridylimine-Rh complex (**2.14**).*

Compound (**2.14**) was prepared using chitosan-2-pyridylimine (**2.1**) (0.500 g, 0.025 mmol) and $[RhCl(CO_2)]_2$ (0.029 g, 0.075 mmol). The product was obtained as a purple solid and then dried under vacuum at 60 °C for 8 hours. Yield, (0.488 g, 94%). **FT-IR** (KBr): 3435 (s) ν(O-H), (m) 2917 ν(C-H), 1998 (s) ν(C≡O), 1650 (s) ν(C=N), 1591 (m) ν(pyr. C=N), 1570 (m) ν(aromatic C=C), (br, s) 1152-1070 ν(pyranose) and (s) 776 cm^{-1} ν(aromatic C-H). Elemental Analysis (%): Found C, 46.47; H, 5.91; N, 5.77. **ICP-MS** (Rh): 0.092 $mmolg^{-1}$.

*2.7.4 Synthesis of cyclohexylimine ligands (**2.15-2.16**).*

*Preparation of cyclohexyl-2-(diphenylphosphino)imine ligand (**2.15**).*

Cyclohexyl amine (0.211 g, 2.13 mmol) in CH_2Cl_2 (25 ml) was treated with 2-(diphenylphosphino) benzaldehyde (0.493 g, 1.70 mmol) over 12 hours at room temperature.

After 12 hours anhydrous magnesium sulphate was transferred to the stirred solution and the mixture was filtered, the solvent was removed by rotary evaporation to give a light yellow solid of compound (**2.15**), which was dried under vacuum for 2 hours. Yield, (0.630 g, 92%). mp.: 98-99 ˚C. **FT-IR** (KBr): 2923 (s) ν(C-H), 1628 (s) ν(C=N), 1584 (m) ν(aromatic C=C) and 695 cm^{-1} (s) ν(aromatic C-H). **^{1}H NMR** (400 MHz; DMSO-d_6, 25°C) δ (ppm) = 8.73 (1H, d, imine, $^{4}J_{PH}$ = 4.4 Hz), 7.86 (1H, m, **Ar**), 7.21-7.66 (12H, br m, **Ar**), 6.77 (1H, m, **Ar**), 3.03 (1H, t, **H**CN=), 0.99-1.78 (10H, br m, C**H$_2$**). **^{31}P{^{1}H} NMR** (121 MHz; DMSO-d_6, 25°C) -13.01 (s). Elemental analysis calculated for $C_{25}H_{26}NP$ (%): C, 80,84; H, 7.06, N, 3.77, Found C, 79.33; H, 7.06; N, 2.13. **EI-MS**: m/z 370.7, $[M-H]^+$, 100%).

*Preparation of cyclohexyl-2-pyridylimine ligand (**2.16**).*

Cyclohexyl amine (2.00 g, 20.17 mmol) in CH_2Cl_2 (35 ml) was treated with 2-pyridinecarboxaldehyde (1.72 g, 16.08 mmol) over 12 hours at room temperature. After this time anhydrous magnesium sulphate was transferred to the stirred solution and the mixture was filtered, the solvent was removed by rotary evaporation to give viscous yellow oil of compound (**6a**), which was dried under vacuum for 2 hours. Yield, (2.2 g, 73%). **FT-IR** (KBr): 2910 (s) ν(C-H), 1646 (s) ν(C=N), 1609 (m) ν(pyr. C=N), 1566 (m) ν(aromatic C=C) and 744 cm^{-1} (s) ν(aromatic C-H.). **^{1}H NMR** (400 MHz; DMSO-d_6, 25°C) δ (ppm) = 8.58 (1H, m, **Ar**), 8.51 (1H, s, imine), 7.90 (1H, t, $^{3}J_{HH}$ = 7.7 Hz **Ar**), 7.70 (1H, m, **Ar**), 7.48 (1H, m, **Ar**), 3.41 (1H, m, **H**C=N), 1.02-1.88 (br m, 10H, C**H$_2$**). Elemental analysis calculated for $C_{12}H_{16}N_2$ (%): C, 76.55; H, 8.57, N, 14.88, Found C, 76.24; H, 8.22, N, 14.07. **EI-MS**: m/z 187.02, $[M-H]^+$, 99%.

*2.7.5 Synthesis of cyclohexylimine Rh^{I} complexes (**2.17-2.18**).*

*Preparation of cyclohexyl-2-(diphenylphosphino)imine Rh^{I} complex (**2.17**).*

$[RhCl(CO_2)]_2$ (0.078 g, 0.202 mmol) in CH_2Cl_2 (20 ml) was added to a solution of cyclohexyl-2(diphenylphosphino)imine ligand (**2.15**) (0.150 g, 0.404 mmol) in CH_2Cl_2 (15 ml) and this was stirred at room temperature. After 4 hours, the solvent was removed by rotary evaporation to afford a bright orange solid which was purified by column chromatography as follows: A solution of the crude product in CH_2Cl_2 (10 ml) was passed

through a silica packed column and eluted with ethyl acetate. The product associated with the bright orange band was collected, the solvent removed by rotary evaporation and the bright orange crystalline solid product (**2.17**) was isolated and dried under vacuum for 3 hours. Single crystals of complex (**2.17**) were obtained by slow evaporation from CH_2Cl_2:*n*-hexane (1:1) Yield, (0.178 g, 82%). mp., decomposes without melting at the onset of 220 ˚C. **FT-IR** (KBr): 2930 (s) ν(C-H), 1993 (vs) ν(C≡O), 1625 (s) ν(C=N), 1563 (m) ν(aromatic C=C) and 696 cm^{-1} (s) ν(aromatic C-H). **^{1}H NMR** (400 MHz; DMSO-d_6, 25°C) δ (ppm) = 8.27 (1H, s imine), 7.87 (1H, m, **Ar**), 7.36-7.71 (12H, br m, **Ar**), 6.83 (1H, m, **Ar**), 4.53 (1H, t, 1H, **H**CN=), 0.98-1.97 (10H, br m, C**H$_2$**). **^{31}P{^{1}H} NMR** (121 MHz; DMSO-d_6, 25°C) δ (ppm) = 48.20 (d, $^1J_{RhP}$ = 165 Hz). Elemental analysis calculated for $C_{26}H_{26}Cl_2NOPRh$ (%) C, 58,06; H, 4.87, N, 2.60, Found C, 58.69; H, 4.94; N, 2.39,. **EI-MS**: m/z 502.1, $[M\text{-}Cl]^+$, 99% .

*Preparation of cyclohexyl-2-pyridylimine Rh^I complex (**2.18**)*

$[RhCl(CO_2)]_2$ (0.200 g, 0.516 mmol) in CH_2Cl_2 (15 ml) was added to a solution of cyclohexyl-2-pyridylimine ligand (**2.16**) (0.186 g, 1.030 mmol) in CH_2Cl_2 (20 ml) and this was stirred at room temperature. After 4 hours, the solvent was removed by rotary evaporation to afford a purple solid of complex (**2.18**) which was dried under vacuum for 3 hours. Yield, (0.250 g, 89%). **mp**.: 182-185 ˚C. FT-IR (KBr): 2935 (s) ν(C-H), 1626 (s) ν(C=N), 1597 (m) ν(pyr. C=N), 1566 (m) ν(aromatic C=C) and 778 cm^{-1} (s) ν(aromatic C-H). **^{1}H NMR** (400 MHz; DMSO-d_6, 25°C): δ (ppm) = 8.89 (1H, m, **Ar**), 8.35 (1H, s, imine), 8.25 (1H, t, ^3J = 7.6 Hz **Ar**), 8.00 (1H, m, **Ar**), 7.68 (1H, m, **Ar**), 4.01 (1H, m, **H**C=N), 0.99-1.86 (10H, br m, 10H, C**H$_2$**). Elemental analysis calculated for $C_{13}H_{16}ClN_2ORh$ C, 44.03; H, 4.55, N, 7.90, Found C, 44.61; H, 4.25; N, 7.17., **ESI-MS**: m/z 318.92, $[M\text{-}Cl]^+$, 98%.

2.8 References

1. (a) G. Haung, C-C. Cai, J. Luo, H. Zhou, Y.-A. Guo, S.-Y. Liu, *Can. J. Chem.,(***2008**), 86, 199; (b) J.J.E. Hardy, S. Hubert, D.J. Macquarrie, A.J. Wilson, *Green Chem.*, (**2004**), 6, 53-56; (c) F. Quignard, A. Chaplin, A. Domard, *Langmui*r, (**2000**), 16, 9106.
2. (a) L. Yin, J. Liebscher, *J. Chem. Rev*., (**2007**), 107, 133; (b) N.T.S. Phan, M. Van Der Sluys, C.W. Jones, *Adv. Synth. Catal.*, (**2006**), 242, 77; (c) Palladium Catalysts, http://www.sigmaaldrich.com/chemistry/drug-discovery/product-highlights/palladium-catalysts.html, (**2010**), *accessed 13th March 2010*.
3. (a) E. Guibal, *Prog. Polym. Sci.,* (**2005**), 30, 71 and references therein; (b) D.J. Macquarrie, J.J.E. Hargy, *Ind. Eng. Chem. Res.,* (**2005**), 44, 8499 and references therein; (c) E. Sin, S-S. Yi, Y-S. Lee, *J. Mol. Catal. A: Chem.,* (**2010**), 315, 99; (d) H-M. Guan, X-S. Cheng, *Polym. Adv. Technol.*, (**2004**), 15, 89; (e) F. Peirano, T. Vincent, F. Quignard, M. Robitzer, E. Guibal, *J. Membrane Science*, (**2009**), 329, 30; (f) S-S. Yi, D-H. Lee, E. Sin, Y-S. Lee, *Tetrahedron Letters*, (**2007**), 48, 6771; (g) C. Lou, Y. Zhang, Y. Wang, *J. Mol. Catal. A: Chemical,* (**2005**), 229, 7. (h) V. Calò, A. Nacci, A. Monopoli, A. Fornaro, L. Sabbatini, N. Cioffi, N. Ditaranto, *Organometallics*, (**2004**), 23, 5154.
4. (a) Z. Guo, R. Xing, S. Liu, Z. Zhang, X. Ji, L. Wang, P. Li, *Carb. Res.*, (**2007**), 342, 1329; (b) R-M. Wang, N-P. He, P-F. Song, Y-F. He, L. Ding, Z-Q. Lei, *Polym. Adv. Technol.*, (**2009**), 20, 959; (c) R-M. Wang, N-P. Pe, P-F. Song, Y-F. He, L. Ding, Z. Lei, *Pure Appl. Chem.*, (**2009**), 81, 2397; (d) J. Linden, R. Stoner, K. Knustson, C. Gardner-Hughes, *Org. Disease Control Elicitors, Agro Food Industry Hi-Te,* (**2000**), p12-15; (e) S.F. Ausar, N. Passalacqua, L.F. Castagna, I.D. Bianco, D.M. Beltramo, *Int. Dairy Journal,* (**2002**), 12, 899.
5. (a) M. Adlim, M.A. Bakar, K.Y. Liew, J. Ismail, *J. Mol. Catal. A: Chem*., (**2004**), 212, 141; (c) J. Zhao, B. Xie, G. Wang, S. Song, Y. Sun, Reack. Kinet. *Catal. Lett.,* (**2009**), 96, 101; (d) K.R. Reddy, N.S. Kumar, P.S. Reddy, B. Sreedhar, M.L. Kantam, *J. Mol. Catal. A: Chem.*, (**2006**), 252, 12.
6. (a) W. Sun, C.-G. Xia, H.-W Wang, *New J. Chem.,* (**2002**), 26, 755; (b) Y. Cui, L. Zhang, Y. Li, *Polym. Adv. Technol.,* (**2005**), 16, 633; (c) C. Peniche-Covas, W. Argüelles-Monal, J. San Roman, *Polym. Dergrad. Stab.*, (**1993**), 39, 21; (d) J. Estiela do Santos, E.R. Dockal, É.T.G. Cavalheiro, *J. Therm. Anal. Cal.*, (**2005**), 79, 243; (e) L-X. Wang, Z-W. Wang, G-S. Wang, X-D. Lin, J-G. Ren, *Polym. Adv. Technol.*, (**2010**), 21, 244; (f) S.E.S. Leonhardt, A. Stolle, B. Ondruschka, G. Cravotto, C. De Leo, K.D. Jandt, T. F. Keller,

Applied Catal. A: General, (**2010**), 379, 30; (g) J. Tong, Z. Li, C. Xia, *J. Mol. Catal. A: Chem.*, (**2005**), 231, 197; (h) C. Demetgül, S. Serin, *Carb. Res.,* (**2008**), 72, 506; (i) X. Xu, P. Liu, S-H, Li, P. Zhang, X-Y. Wang, *React. Kinet. Catal. Lett.,* (**2006**), 88, 217; (j) S. Alesi, F. Di Maria, M. Mellucci, D.J. Macquarrie, R. Luque, G. Barbarella, *Green Chem.,* (**2008**), 10, 517.

7. (a) M. Namane, P. Njogu, A. Jardine, unpublished work; (b) K. Tømmeraas, S.P. Strand, W. Tian, L. Kenne, K.M. Vårum, *Carb. Res*., (**2001**), 336, 291; (c) H.C. Clark, L.E. Manzer, *J. Organomet. Chem.,* (**1973**), 59, 411; (d) T. Satoh, H. Kano, M. Nakatani, N. Sakairi, S. Shinkai, T. Nagasaki, *Carb Res.*, (**2006**), 341, 2406.
8. (a) Y. A. Skorik, C. A. R. Gomes, M. T. S. D. Vasconcelos, Y. G. Yatluk, *Carb. Res*., (**2003**), 338, 271; (b) K. Kurita, S. Mori, Y. Nishiyama, M. Harata, *Polym. Bulletin*, (**2002**), 48, 159.
9. (a) C. Willocq, S. Hermans, M. Devillers, *J. Phys. Chem.,* (**2008**), 112, 5533; (b) M.J. Gronnow, R. Luque, D.J. Macquarrie, J.H. Clark, *Green Chem.,* (**2005**), 7, 552.
10. (a) Z. Li, Q. Peng, Y. Yuan, *Appl. Catal. A: General*, (**2003**), 239, 79. (b) S.R. Gilbertson, X. Wang, G.S. Hoge, C.A. Klug, J. Schaefer, *Organometallic*s, (**1996**), 15, 4678. (c) A Brukhart, H. Görls, W. Plass, *Carb. Res.,* (**2008**), 343, 1266. (d) K.R. Reddy, W-W. Tsai, K. Surekha, G-H. Lee, S-M. Peng, J-T. Chen, *J. Chem. Soc. Dalton Trans.,* (**2002**), 1776
11. (a) P. Arya, N. Verugopal Rao, J. Singkhonrat, *J. Org. Chem.,* (**2000**), 65, 1881; (b) R. Van Heerbeek, P.C.J. Kamer, P.W.N.M. van Leeuwen, J.N.H Reek, *Chem. Rev*., (**2002**), 102, 3717; (c) P. Li, S. Kawi, *J. Catal*., (**2008**), 257, 23.
12. (a) G.O. Evans, C.U. Pittman, R. Mc Millan, R.T. Beach, R. Jones, *J. Organomet. Chem.*, (**1975**), 87, 189; (b) F. Shibahara, K. Nozaki, T. Matsuo, T. Hiyama, *Bioorg. Med. Chem. Lett.,* (**2002**), 12, 1825; (c) F. Shabahara, K. Nozaki, T. Hiyama, *J. Am. Chem Soc.*, (**2003**), 125, 8555; (d) D.E. Bryant, M. Kilner, *J. Mol Catal. A: Chem.*, (**2003**), 193, 83; (e) E.V. Slivinskii, N.V. Kolesnichenko, *Russ. Chem. Bull. Int. Ed*., (**2004**), 53, 2449.
13. (a) M.A. Valenzuela, G. Aguilar, P. Bosch, H. Armendariz, P. Salas, A. Montoya, *Catal. Lett.,* (**1992**), 15, 179; (b) A.M. Trzeciak, J.J. Ziołkowski, Z. Jaworska-Galas, W. Mista, J. Wrzyszcz, *J. Mol. Catal.,* (**1994**), 88, 13; (c) J. Wrzyszcz, M. Zawadzki, A.M. Trzeciak, J.J. Ziołkowski, *J. Mol. Catal. A: Chem.* (**2002**), 189, 203; (d) L. Huang, S. Kawi, *Catal. Lett.,* (**2004**), 92, 57.
14. (a) J.P.K. Reynhardt, Y. Yang, A. Sayari, H. Alper, *Chem. Mater*., (**2004**), 16, 4095; (b) X. Lan, W. Zhang, L. Yan, Y. Ding, X. Han, L. Lin, X. Bao, *J. Phys. Chem. C*, (**2009**), 113, 6589.

15. N. C. Antonels, B. Therrien, J. R. Moss, G. S. Smith, *Inorg Chem. Commun.,* (**2009**), 12, 716.
16. (a) See appendix **Section d** for summary of data collection and CIF file for the single crystal X-ray structure of complex (**2.17**).
17. (a) L. J. Farrugia*, J. Appl. Cryst.,* (**1997**), 30, 565. (b) S. Burling, L.D. Field, B.A. Messerle, K.Q. Vuong, P. Turner, *Dalton Trans.,* (**2003**), 4181.
18. (a) H. Myszka, D. Bednarczyk, M. Najder, W. Kaca, *Carb. Res.,* (**2003**), 338, 133; (b) C. T. Bailey, G. C. Linsesky, *J. Chem. Edu.,*(**1985**), 62, 896.
19. A.J. Deeming, P.J. Sharratt, *J. Organomet. Chem*., (**1975**), 99, 447.

Chapter 3

Catalytic studies using chitosan-supported precursors: *Suzuki-Miyaura, Heck and Hydroformylation reactions*

3.1 Introduction: Carbon-carbon cross-coupling

Palladium-catalyzed cross-coupling reactions of organo-halides with olefins (Heck) and organo-boronic acids (Suzuki-Miyaura) for carbon-carbon bond formation are extremely useful to the chemical industry and in research. Since their discovery they have evolved into an important technique in preparing biologically active functionalized biphenyls which are imperative intermediates or products in drug discovery, pharmaceuticals and agricultural compounds. [1-3] The impact and importance of cross-coupling reactions was recognized through the 2010 Nobel Prize in Chemistry to R.F. Heck, E. Negishi and A. Suzuki. [3]

Historically, palladium complexes such as $[Pd(OAc)_2]$ and $[Pd(PPh_3)_2Cl_2]$ have been widely used as homogeneous catalyst systems in cross coupling reactions. [1] However, these homogeneous catalytic systems suffer from problems associated with the separation and recovery of the active catalyst as well as instability at high temperatures. These drawbacks have so far precluded their industrial exploitation. [4] Also, from the perspective of process development, homogeneous catalysts require expensive phosphine ligands (to generate the active catalyst) which are often not available in bulk. Metal contamination of the products is inevitable when using homogeneous catalysts, an undesirable result especially in the pharmaceutical industry. [1,2] Therefore, there is a need to develop improved and practical strategies for recycling active catalysts for economical and environmental stewardship reasons.[4]

Most of the problems related to homogeneous catalysts can be solved by immobilizing the catalyst or catalyst precursor on polymer supports with good solvation attributes. [5-7] For example, supporting transition metal catalysts on insoluble polymer supports can improve their stability without compromise in the activity and selectivity of the homogeneous catalyst. Supported catalysts also allow simplified recovery and reuse of the catalyst as well as physical separation of the active site, thus minimizing catalyst self-destruction. [7a-b] In the previous chapter we reported on the preparation and characterization of chitosan-supported

Pd^{II} and Rh^{I} complexes and their mononuclear analogues. We now discuss the results obtained from the application of the palladium series of compounds as catalyst precursors in Suzuki-Miyaura and Heck cross-coupling reactions (Section 3.2). The rhodium supported and mononuclear complexes were tested in hydroformylation of 1-octene and results thereof follow in Section 3.4.

3.2 Carbon-carbon cross-coupling reactions

3.2.1 Suzuki-Miyaura reactions

The activities of catalyst precursors (**2.5-2.8**) (**Fig. 3.1**) were examined in the Suzuki-Miyaura reaction of aryl halides with phenylboronic acid (**Scheme 3.1**).

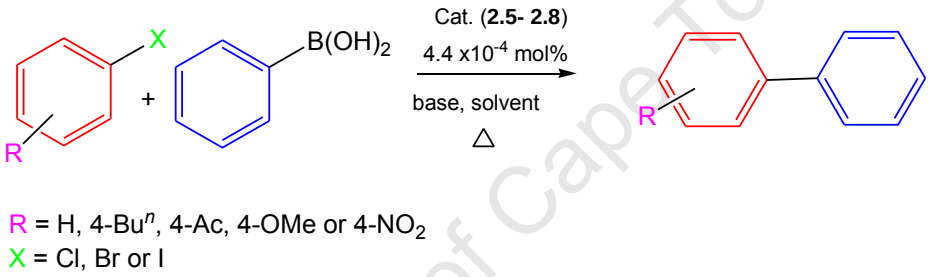

Scheme 3.1. Outline for the Suzuki-Miyaura reactions carried out using catalyst precursors (**2.5-2.8**).

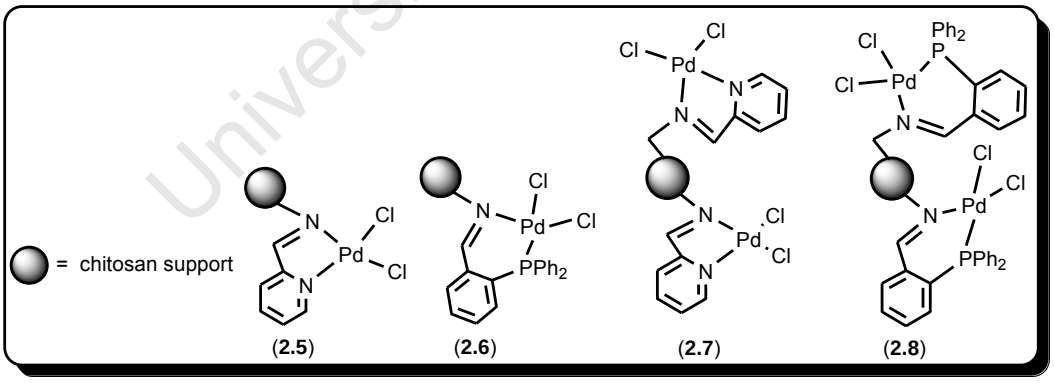

Fig. 3.1. Catalyst precursors employed in carbon-carbon cross-coupling reactions (Suzuki-Miyaura and Heck) (**2.5-2.8**).

Under conditions similar to those reported in literature (143 °C),[5b] catalyst precursors (**2.5**) and (**2.7**) gave yields of 87% and 85% respectively (**Table 3.1** , entries **5-7**), while catalyst precursor (**2.6**) afforded 65% of biphenyl. On varying the reaction temperature (143 °C, 130

˚C and 95 ˚C), it was observed that the optimal temperature for Suzuki-Miyaura cross-coupling using catalyst precursors (**2.6** and **2.8**) was 130 ˚C. Subsequently, all other reactions were performed at this temperature, resulting in good catalytic activities (4.4 x 10^{-5} mol% Pd used) as evidenced by moderate to high TONs (**Table 3.1**). Our catalyst precursors' TON values are comparably higher than those reported in literature, even where a larger mol% catalyst was used. [5b,8] Generally, the iminophosphine supported catalysts afforded better yields than their iminopyridyl counterparts and this can be attributed to the better stabilizing nature of phosphorus donor ligands compared to nitrogen. When substituted bromobenzenes were employed (**Table 3.1** entries **8-11**) a good yield of the coupled product was obtained for the substrate containing *p*-NO_2 and *p*-Bu^n substituents (TONs 904 and 879 respectively). The *p*-OMe and *p*-Ac containing substrates gave low yields and the catalyst precursor decomposed to a black species, possibly Pd^0 particles.

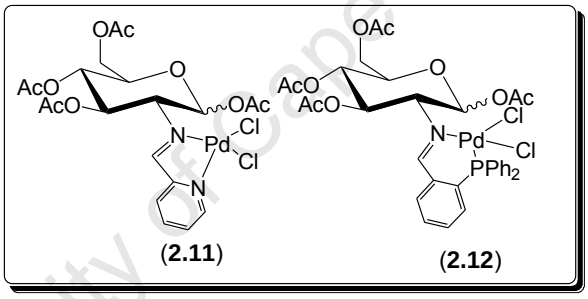

Fig. 3.2. Homogeneous catalyst precursors (**2.11** and **2.12)**.

Table 3.1. Suzuki-Miyaura cross coupling reactions d by supported Pd catalysts (**2.5-2.8**) and (**2.11-2.12**).

Entry	Catalyst [a]	R	X	Base	Conversion (%)[b]	TON [(mol $_{Prod.}$)/(mol $_{Pd}$)][c]	Selectivity (%)
1	**2.6**	H	Br	K_2CO_3	98	1144	>99
2	**2.8**	H	Br	K_2CO_3	96	1116	>99
3	**2.5**	H	Br	K_2CO_3	82	959	99
4[d]	**2.6**	H	Br	K_2CO_3	48	558	98
5[e]	**2.5**	H	Br	K_2CO_3	87	1016	99
6[e]	**2.7**	H	Br	K_2CO_3	85	1144	99
7[e]	**2.6**	H	Br	K_2CO_3	65	763	98
8	**2.6**	*p*-NO_2	Br	K_2CO_3	76	904	99
9	**2.6**	*p*-OMe	Br	K_2CO_3	26	320	97
10	**2.6**	*p*-Ac	Br	K_2CO_3	19	221	97
11	**2.6**	*p*-Bu^n	Br	K_2CO_3	75	879	98
12[f]	**2.6**	H	Br	K_2CO_3	100	1167	>99
13[f]	**2.6**	*p*-Ac	Br	K_2CO_3	99	1160	>99
14[f]	**2.7**	*p*-NO_2	Br	K_2CO_3	87	1015	>99
15	**2.11**	H	Br	K_2CO_3	84	1010	99
16	**2.12**	H	Br	K_2CO_3	100	1167	>99

[a] Reactions carried out in xylene (20 ml) over 6 h, with 5.1 mmol of arylhalide, 7.5 mmol of phenylboronic acid, 10 mmol of base and $4.47x10^{-4}$ mmol Pd catalyst precursor (loading = 0.044 (**2.5**); 0.054 (**2.6**); (**2.7**) 0.121 and (**2.8**) 0.123mmolg^{-1}) at 130 ˚C unless stated otherwise. [b] GC conversions obtained using *n*-decane as an internal standard and are based on the amount of arylhalide employed in relation to authentic standard biphenyl or substituted biphenyl. [c] Maximum TON from reaction at 4 hours. [d] Reaction carried out at 95 ˚C. [e] Reaction carried out at 143 ˚C. [f] Reaction carried out in EtOH:H_2O (1:1, 20 ml). (Error estimate: (**2.5**) = ± 0.10; (**2.6**) = ± 0.10; (**2.7**) = ± 0.11 and (**2.8**) = ± 0.10).

As shown in (**Table 3.1** entries **1-3**) and (**Table 3.2** entries **1-6**), the aryl bromides gave the best yields followed by aryl iodide while the less reactive aryl chloride gave the poorest product yield. Thus, unexpectedly the order of reactivity follows: Br > I > Cl. In addition to the bond dissociation energies, we suspect a possible halide size contribution to this unexpected result, however further extensive experiments involving the effect of halide would be necessary to confirm this. When sodium carbonate was used as the base,

conversions dropped by approximately 60% under these reaction conditions (**Table 3.2** entries **7-10**). Reactions performed in EtOH : H_2O (1:1 ratio) drastically improved product yields to as high as 100% (**Table 3.1** entries **12-14**), indicating that the chitosan-supported catalyst precursors work well in aqueous conditions. The homogeneous complexes (**2.11** and **2.12**, **Fig. 3.2**) displayed good activity (TONs 1010 and 1167 respectively) for the Suzuki reactions (entries **15-16**), but showed decomposition to a black species minutes into the reaction. This suggests that the chitosan support plays a crucial stabilizing role in the supported Schiff-base catalysts in these reactions. On the other hand, the proximate anomeric acetate may play a role in promoting reduction of the Pd^{II} to $[Pd(OAc)_2]$ in the reactions involving homogeneous catalyst precursors (**2.11** and **2.12**).

Table 3.2 Suzuki-Miyaura cross coupling reactions catalyzed by supported Pd catalysts (**2.5**-**2.8**), effect of base and aryl halide.

Entry	Catalyst [a]	R	X	Base	Conversion (%)[b]	TON [(mol $_{Prod.}$)/(mol $_{Pd}$)][c]	Selectivity (%)
1	**2.6**	H	Cl	K_2CO_3	5	56	97
2	**2.7**	H	Cl	K_2CO_3	1	12	97
3	**2.8**	H	Cl	K_2CO_3	8	88	97
4	**2.6**	H	I	K_2CO_3	34	397	97
5	**2.7**	H	I	K_2CO_3	29	342	98
6	**2.5**	H	I	K_2CO_3	71	823	99
7	**2.6**	H	Br	Na_2CO_3	21	249	98
8	**2.5**	H	Br	Na_2CO_3	32	346	99
9	**2.8**	H	Br	Na_2CO_3	26	309	99
10	**2.7**	H	Br	Na_2CO_3	34	405	99

[a] Reactions carried out in xylene (20ml) over 6 h, with 5.1 mmol of arylhalide, 7.5 mmol of phenylboronic acid, 10 mmol of base and $4.47x10^{-4}$ mmol Pd catalyst presursors (loading = 0.044 (**2.5**); 0.054 (**2.6**); (**2.7**) 0.121 and (**2.8**) 0.123mmolg^{-1}) at 130 °C unless stated otherwise. [b] GC conversions obtained using *n*-decane as an internal standard and are based on the amount of arylhalide employed in relation to authentic standard biphenyl or substituted biphenyl. [c] Maximum TON from reaction at 4 hours. (Error estimate: (**2.5**) = ± 0.10; (**2.6**) = ± 0.10; (**2.7**) = ± 0.11 and (**2.8**) = ± 0.10).

On following the conversion to biphenyl over time, it was observed that the reaction is almost complete in the first 15 minutes when using supported catalysts (**2.5**) and (**2.6**) (**Fig. 3.3**). Catalysts (**2.7**) and (**2.8**) exhibited lower activity and required longer time for near completion. The homogeneous catalyst precursors (**2.11** and **2.12**) showed similar activity to

the chitosan-supported ones, with the iminophosphine complex being slightly more active than its iminopyridyl counterpart. This phenomenon is also evident when comparing the activities of catalyst precursors (**2.5-2.8**).

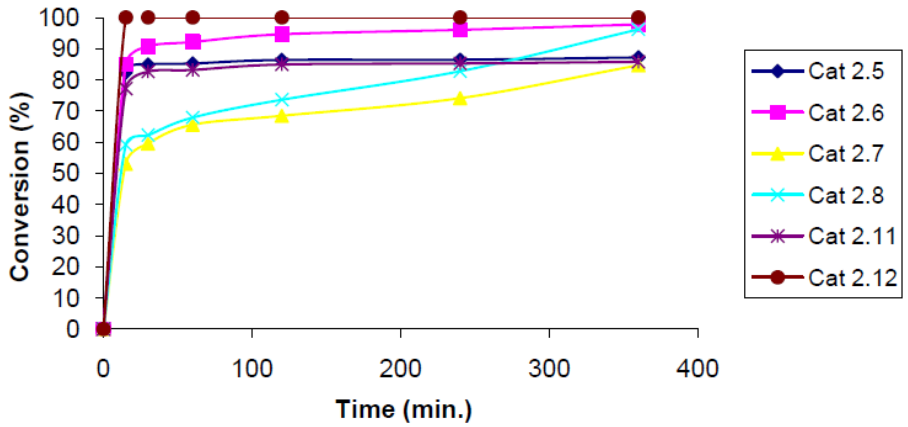

Fig. 3.3. Percentage conversions to biphenyl over time for catalyst precursors (**2.5-2.8**). Reactions carried out in xylene (20 ml) over 6 h, with 5.1 mmol of aryl halide, 7.5 mmol of phenylboronic acid, 10 mmol of base and 4.47×10^{-4} mmol Pd catalyst (loading = 0.044 (**2.5**); 0.054 (**2.6**); (**2.7**) 0.121 and (**2.4**) 0.123mmolg^{-1}) at 130 °C unless stated otherwise. (Average error estimate: (**2.5**) = ± 0.10; (**2.6**) = ± 0.11; (**2.7**) = ± 0.12; (**2.8**) = ± 0.13; (**2.11**) = ± 0.10 and (**2.12**) = ± 0.12).

3.2.2 Reusability of catalysts

Catalysts (**2.5-2.8**) were recovered by simple filtration and washed with water, ethanol then acetone and oven dried. The catalysts could be reused at least five times without significant loss of activity (**Fig. 3.4**). Loss of activity in the 6th run may be due to poisoning or fouling of the catalysts by waste inorganics and unreacted reagents therefore blocking the active Pd sites. Sintering of the nanosized Pd particles (thus decreasing the catalyst surface area) also occurs as evidenced by TEM images of catalyst precursors (**2.5** and **2.6**) after five cycles (**Fig. 3.5 a** and **b**). This is possibly induced by the fairly high temperature at which the reactions were carried out.

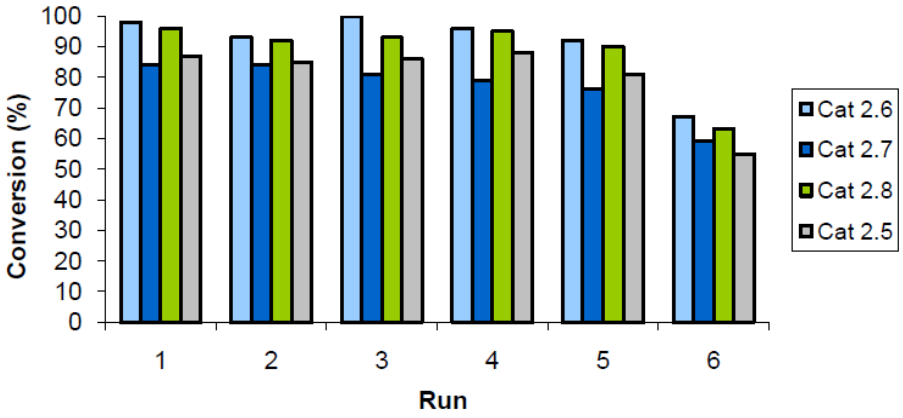

Fig. 3.4. Recycle runs of catalyst precursors (**2.5-2.8**). Reactions carried out in xylene (20 ml) over 6 h, with 5.1 mmol of aryl halide, 7.5 mmol of phenylboronic acid, 10 mmol of base and $4.47x10^{-4}$ mmol Pd catalyst (loading = 0.044 (**2.5**); 0.054 (**2.6**); (**2.7**) 0.121 and (**2.8**) $0.123mmolg^{-1}$) at 130 ˚C unless stated otherwise. (Average error estimate: (**2.5**) = ± 0.10; (**2.6**) = ± 0.11; (**2.7**) = ± 0.12; (**2.8**) = ± 0.12).

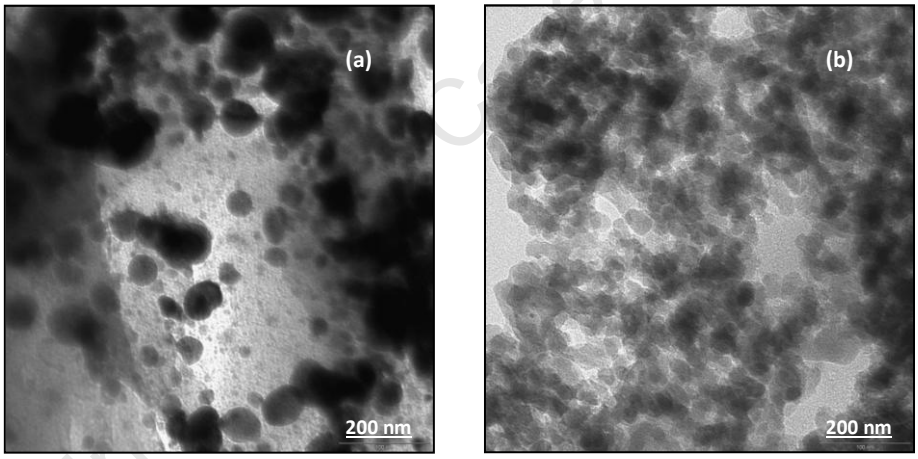

Fig. 3.5. TEM images of used supported catalysts **2.5** (a) and **2.6** (b).

3.2.3 Pd leaching tests

A hot filtration test, whereby the catalyst was filtered off 5 minutes after the reaction started followed by the filtrate taken back to the reaction temperature stopped the catalytic reaction. Thus, effectively proving the heterogeneous nature of the supported catalyst without a measurable homogeneous contribution (**Fig. 3.6).** Furthermore, no Pd was detected by ICP-MS analysis in this mixture together with samples from (entries **1**, **3** and **6**, **Table 3.1**). Coordination of Pd to the biopolymer-supported Schiff-base ligands has shown no evidence

of Pd leaching into the products. This provides evidence of chitosan acting as a good scaffold for Pd^{II} catalyst precursors. [1,2,5]

A test was performed to establish whether the reactions were catalyzed by Pd^0 or Pd^{II} species. A reaction using catalyst precursor (**2.6**) in the presence of mercury resulted in no inhibition of catalytic activity (94% yield). This result suggested predominantly heterogeneous catalysis since it is known that mercury forms an amalgam with Pd^0 species and this would have resulted in inhibition of catalytic activity.

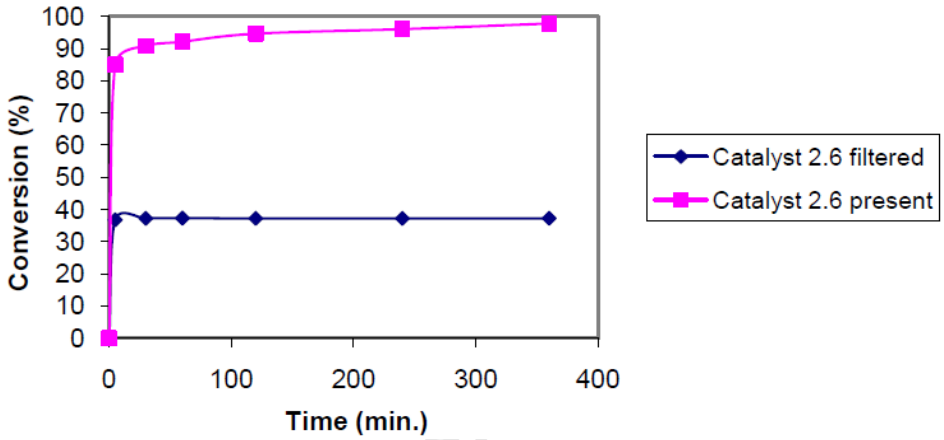

Fig. 3.6. Effect of removing Pd catalyst (**2.6**) from reaction (hot filtration test catalyst (**2.6**) removed after 5 min.). Reactions carried out in xylene (20 ml) over 6 hours, with 5.1 mmol of arylhalide, 7.5 mmol of phenylboronic acid, 10 mmol of base and 4.47×10^{-4} mmol Pd catalyst (loading = 0.054 (**2.6**) $mmolg^{-1}$) at 130 ˚C. . (Average error estimate: (**2.6**) = ± 0.11).

3.2.4 Heck reactions

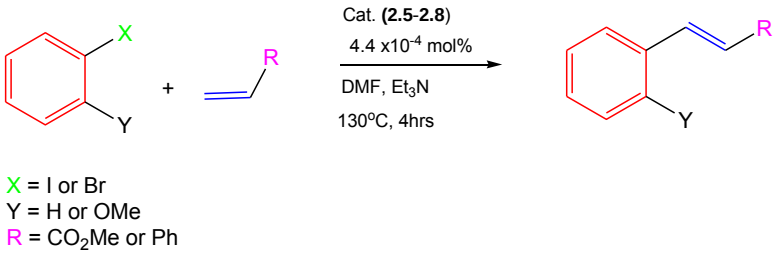

Scheme 3.2. Outline for the Heck reactions carried out using catalysts (**2.5-2.8**).

Heck reactions were also investigated under similar temperature conditions as utilized for the Suzuki-Miyaura reactions (**Scheme 3.2**). The reactions using catalyst precursors (**2.5** and **2.7**)

with iodobenzene and methyl acrylate produced 98% and 99% *trans*-methylcinnamate respectively in 4 hours at 130 ˚C (**Table 3.3** entries **1** and **3**). Coupling of styrene and iodobenzene using (**2.6** and **2.8**) was also accomplished, giving 99% and 90% of *trans*-stilbene respectively with good TONs of 1209 and 1086 (**Table 3.3** entries **2** and **4**). Thus, the aforementioned catalytic reactions lead to regiospecific formation of the *trans* isomer products; this was confirmed by GC analysis and NMR spectroscopy. With 2-methoxy iodobenzene, poor yields of the coupling products were obtained (**Table 3.3** entries **5** and **6**), which was also the case for the bromobenzene substrate (**Table 3.3** entry **7**). Furthermore, catalyst precursors (**2.5**-**2.8**) gave better yields of the coupled product when compared to a commercial polystyrene-supported catalyst for unsubstituted iodobenzene under similar reaction conditions. [6c]

Table 3.3. Heck cross coupling reactions catalyzed by supported Pd catalysts (**2.5**-**2.8**).

Entry	**Catalyst** [a]	**X**	**Y**	**R**	**Conversion** (%)[b]	**TON** [(mol $_{Product}$) /(mol $_{Catalyst}$)]
1	**2.5**	I	H	CO_2Me	98	1110
2	**2.6**	I	H	Ph	99	1150
3	**2.7**	I	H	CO_2Me	99	1209
4	**2.8**	I	H	Ph	90	1086
5	**2.8**	I	OMe	Ph	20	237
6	**2.7**	I	OMe	CO_2Me	62	757
7	**2.5**	Br	H	CO_2Me	8	93

[a] Reactions carried out in DMF (20 ml) over 4 hours, with 5.3 mmol of iodobenzene, 5.3 mmol of methyl acrylate or styrene, 10 mmol of triethylamine and $4.47x10^{-4}$ mmol Pd catalyst precursor (loading = 0.044 (**2.5**); 0.054 (**2.6**); (**2.7**) 0.121 and (**2.8**) 0.123mmolg^{-1}) at 130 ˚C unless stated otherwise. [b] GC conversions obtained using *n*-decane as an internal standard and are based on the amount of iodobenzene employed in relation to authentic standard *trans*-methyl cinnamate or *trans*-stilbene. Error estimate: (**2.5**) = ± 0.11; (**2.6**) = ± 0.10; (**2.7**) = ± 0.12 and (**2.8**) = ± 0.12).

3.3 Summary and Conclusions: Carbon-carbon cross-coupling reactions

Chitosan-supported Pd catalysts exhibited high activity towards the Suzuki-Miyaura and Heck cross-coupling reactions in xylene and aqueous ethanol solvents, with no measurable amount of Pd detected in the reaction products. The supported catalyst precursors displayed good activity at low Pd loading (4.4×10^{-4} mol %) and in aqueous media. Though the mononuclear model catalyst precursors also showed good activity for Suzuki-Miyaura cross-

coupling, they could not be recycled and reused, thus the chitosan environment plays an essential stabilizing role on the supported catalysts in the reactions. The supported catalyst precursors could be easily separated and recovered from the reaction mixture (by filtration) and reused up to five times. The combination of advantages displayed by the chitosan-supported catalyst precursors such as ease of preparation, high catalytic activity, stability, reusability, versatility (organic or aqueous solvent catalysis) and no measurable Pd leaching, prove that these catalyst precursors should be considered as viable alternatives in cross-coupling reactions on efficiency, environmental stewardship and economical grounds.

3.4 Introduction: Hydroformylation

Hydroformylation has been widely used in industry for the production of aldehydes from alkenes since its discovery in 1938. An important example is the OXEA process (former Ruhrchemie/Rhône-Poulenc) which has been producing 8.0 x 10^5 tons of C_4 and C_5 aldehydes from propene or butene annually since 1984.[9] This process employs a $Rh/P(C_6H_4SO_3Na)_3$ catalyst. Aldehydes are the starting material for making many useful secondary products such as i) alcohols (production of detergents) and ii) specialty chemicals (which are relevant to organic synthesis of fragrances and complex natural products). [9] In 1995, production capacity reached 6.6 x 10^6 tons. Over the past several decades, much effort has been directed toward the synthesis of highly active and selective catalysts for the hydroformylation reaction, using different transition metals. [9] The most commonly used catalysts for this reaction are based on Rh complexes due to its high activity and selectivity under milder conditions. It has been established that hydroformylation activity with regards to metal atom follows the trend: Rh>> Co>> Pt. [9b-d]

However, the practical application of homogeneous hydroformylation systems in industry has been limited by problems associated with separation of the catalyst/product mixture. Additionally, the process of separation by distillation is energy-intensive, time consuming and corrosive to equipment. [9b]

Consequently, several approaches have been employed in solving this problem, such as, aqueous biphasic, supported aqueous-phase, supported liquid-phase, supercritical fluids, ionic liquids and supported ionic liquid-phase catalyst systems. [9-14] Despite overcoming the separation challenge, these approaches often result in metal leaching and low regioselectivity

for the aldehyde products. Alternatively, the homogeneous catalysts have been immobilized on solid supports such as dendritic scaffolds, polymers, metal oxides, mesoporous materials and various forms of carbon. [15-18] However, these catalysts often suffer the drawbacks of reduced catalyst activity and irreproducibility.

Recently, researchers have looked to biopolymers as supports for transition metal catalysts due to their appealing abundance in nature, renewability, biodegradability and non-toxicity. [7] The use of several biopolymers like alginate, starch, gelatine, cellulose and chitosan have been reported in this regard. [7,19-21] Indeed, these efforts are leading to more cleaner and sustainable chemistry. The following section reports on the evaluation of chitosan-supported Rh^{I} complexes and their mononuclear analogues as catalyst precursors in 1-octene hydroformylation. There is an interest to develop catalyst systems to hydroformylate higher olefins (>C_6) as these are important precursors to flavourants, fragrances, acids, esters amines and alcohols,

3.5 Hydroformylation reactions

3.5.1 Hydroformylation of 1-octene

The potential of the chitosan-supported and mononuclear Rh^{I} complexes ((**2.13**-**2.14**) and (**2.17**-**2.18**), **Fig. 3.7**) to catalyze the hydroformylation reaction was evaluated using 1-octene as the substrate (**Scheme 3.3**). The conversions of 1-octene were monitored by GC and in general products formed at optimal conditions were aldehydes (branched and linear) by hydroformylation as well as some quantities of internal *iso*-octenes (*cis* and *trans* 2- and 3-octene) by isomerization. No hydrogenation products were observed.

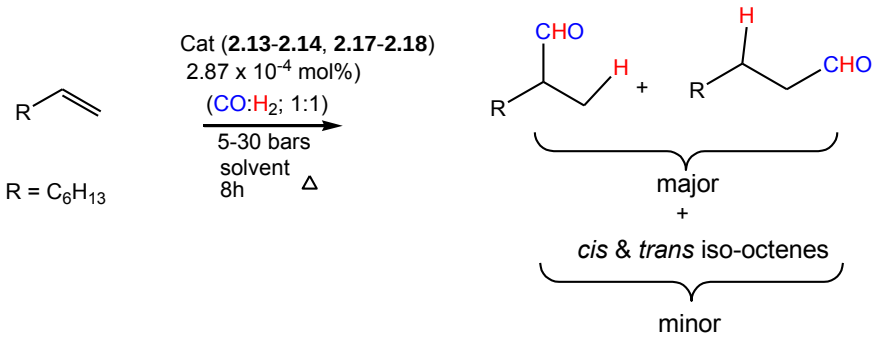

Scheme 3.3. Outline for the hydroformylation reactions carried out using catalyst precursors (**2.13**-**2.14**) and (**2.17**-**2.18**).

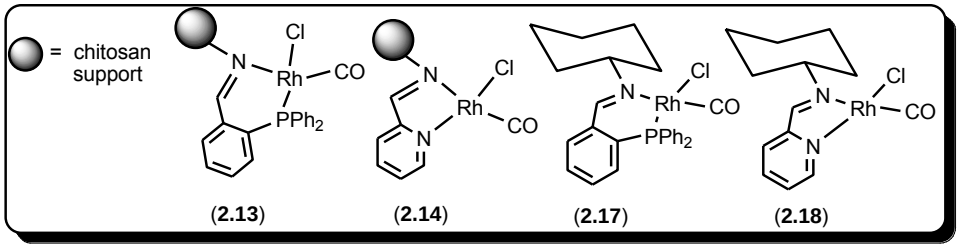

Fig. 3.7. Catalyst precursors employed in hydroformylation reactions (**2.13-2.14**) and (**2.17-2.18**).

The chitosan supported catalysts (**2.13** and **2.14**) displayed similar reaction rates (**Fig. 3.8**) and conversions after 8 hours. The mononuclear analogues also exhibited similar reaction rates and conversions with all catalysts displaying steady increase patterns. The supported catalysts (**2.13** and **2.14**) displayed low to no activity over the first 2 hours, indicative of an induction period required to ensure diffusion of the syngas into the solvent followed by accessing of the Rh sites on the chitosan. In contrast to that, the mononuclear analogues showed a higher catalytic rate over the first 4 hours. Similar differences in the rate of conversion between homogeneous catalysts supported on SBA-15 have been reported. [15c]

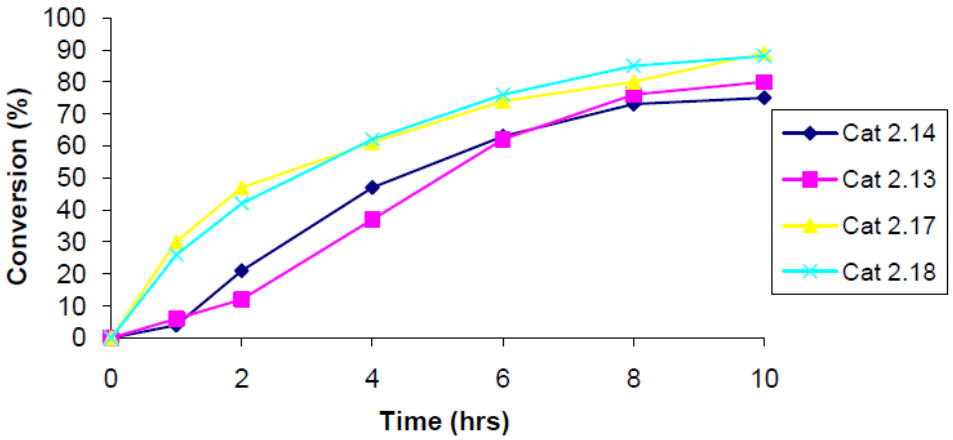

Fig. 3.8. Percentage conversion of 1-octene over 8 hours using catalyst precursors (**2.13-2.14**) and (**2.17-2.18**), data collected at 75 °C and 30 bars. (Average error estimate: (**2.13**) = ± 0.12; (**2.14**) = ± 0.11; (**2.17**) = ± 0.17 and (**2.18**) = ± 0.10).

3.5.2 Effect of pressure

At temperature = 75 °C and syngas pressure = 5 bars, hydroformylation of 1-octene gave poor conversions to predominantly *iso*-octenes (**Fig. 3.9** and **Table 3.4**, entries 1-4). Upon increasing the syngas pressure to 10 bars, higher conversions of 1-octene were afforded, though more *iso*-octenes were formed here too (**Table 3.4**, entries 5-8). Good conversions of 1-octene to the desired linear aldehyde product were therefore seen at 30 bars and 75 °C using catalysts (**2.13**-**2.14**) and (**2.17**-**2.18**) (*vide infra*, **Figs. 3.10b** and **3.11a**). The supported catalysts show swelling in aqueous ethanol solvent (1:1 ratio), however poor activity was observed due to low solubility of the long hydrocarbon chain of the 1-octene substrate in aqueous medium. Hydroformylation of shorter chain α-olefins may yield better results.[22]

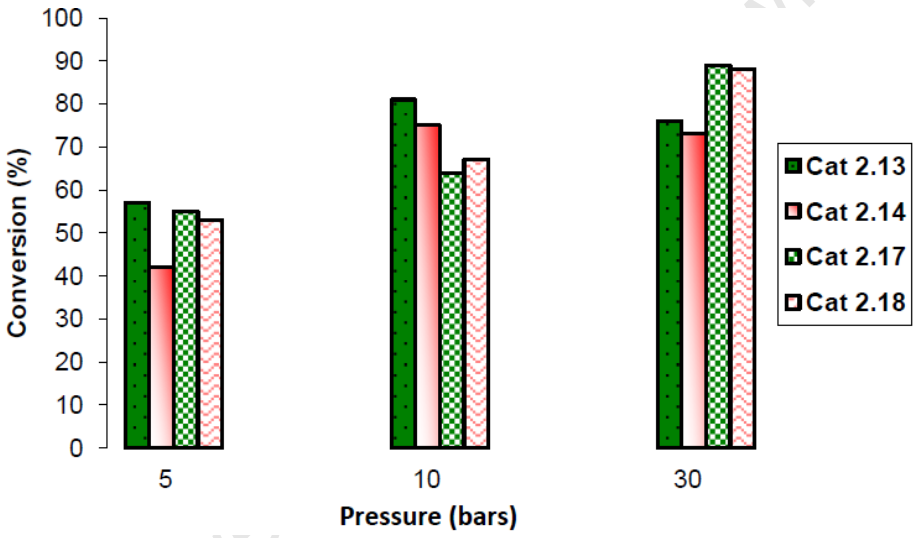

Fig. 3.9. Percentage conversion of 1-octene over 8 hours using catalyst precursors (**2.13**-**2.14**) and (**2.17**-**2.18**) at 75 °C. (Average error estimate: (**2.13**) = ± 0.11; (**2.14**) = ± 0.12; (**2.17**) = ± 0.16 and (**2.18**) = ± 0.11)

Table 3.4. Hydroformylation of 1-octene at different pressures data after 8 hours.[a]

Entry	Cat.	Syngas press. (bars)	% Conversion	% Aldehyde	% *iso*-octenes	n:iso	TOF (h^{-1})[d]
1	**2.13**	5	57	10	90	43:57[b]	26
2	**2.14**	5	42	0	100	-	0
3	**2.17**	5	55	4	96	62:38[c]	10
4	**2.18**	5	53	2	98	64:36[c]	5
5	**2.13**	10	81	28	72	45:55[b]	75
6	**2.14**	10	75	5	95	70:30[b]	13
7	**2.17**	10	64	30	70	48:52[c]	78
8	**2.18**	10	67	25	75	52:48[c]	65

[a]Reactions carried out with ($CO:H_2$) (1:1) at 75 °C in xylene (10 ml) with 6.37 mmol of 1-octene and $2.87x10^{-3}$ mmol Rh catalyst precursors (loading = 0.145 (**2.13**); 0.092 (**2.14**) $mmolg^{-1}$) (Error estimate: (**2.13**) = ± 0.10; (**2.14**) = ± 0.13; (**2.17**) = ± 0.16 and (**2.18**) = ± 0.12).GC conversions obtained using *n*-decane as an internal standard in relation to authentic standard *iso*-octenes and aldehydes. [b] Regioselectivity calculated at 2 hours. [c] Regioselectivity calculated at 4 hours.[d] TOF = (mol product/mol cat.) x h^{-1}.

3.5.3 Effect of temperature

Hydroformylation of 1-octene was carried out at various temperatures using catalyst precursors (**2.13**-**2.14**) and (**2.17**-**2.18**) (T = 55, 75 and 95 °C, syngas pressure = 30 bars) (**Figs 3.10a-c**). Reactions carried out at 55 °C saw very low conversions of 1-octene to *iso*-octenes exclusively with pyridylimine-based systems (**2.14** and **2.18**), while iminophosphine-based catalysts (**2.13** and **2.17**) formed almost equal amounts of aldehydes and *iso*-octenes. At 95 °C, high conversions of 1-octene were observed to initially *iso*-octenes (monitored by GC) which were converted to aldehydes over time (8 hours). Thus at this temperature, more branched aldehydes are formed *via* hydroformylation of *iso*-octenes (**Fig 3.11b**). The optimal temperature at which good conversion (TOF = 261-111 and TON = 2088, (**2.13**)) to desired linear aldehydes was found to be 75 °C. At this temperature iminophosphine-based systems (**2.13** and **2.17**) exhibited superior selectivity for nonanal than their pyridylimine-based counterparts, reiterating reports that bulky aryl phosphine ligands influence regioselectivity (**Fig 3.11a-b**). [9f,23] Additionally, at temperature = 75 °C and syngas pressure = 30 bars (**2.13** and **2.14**) showed almost similar chemo- and regioselectivities implying that the biopolymer backbone has no impact on selectivity during hydroformylation (*vide infra*).

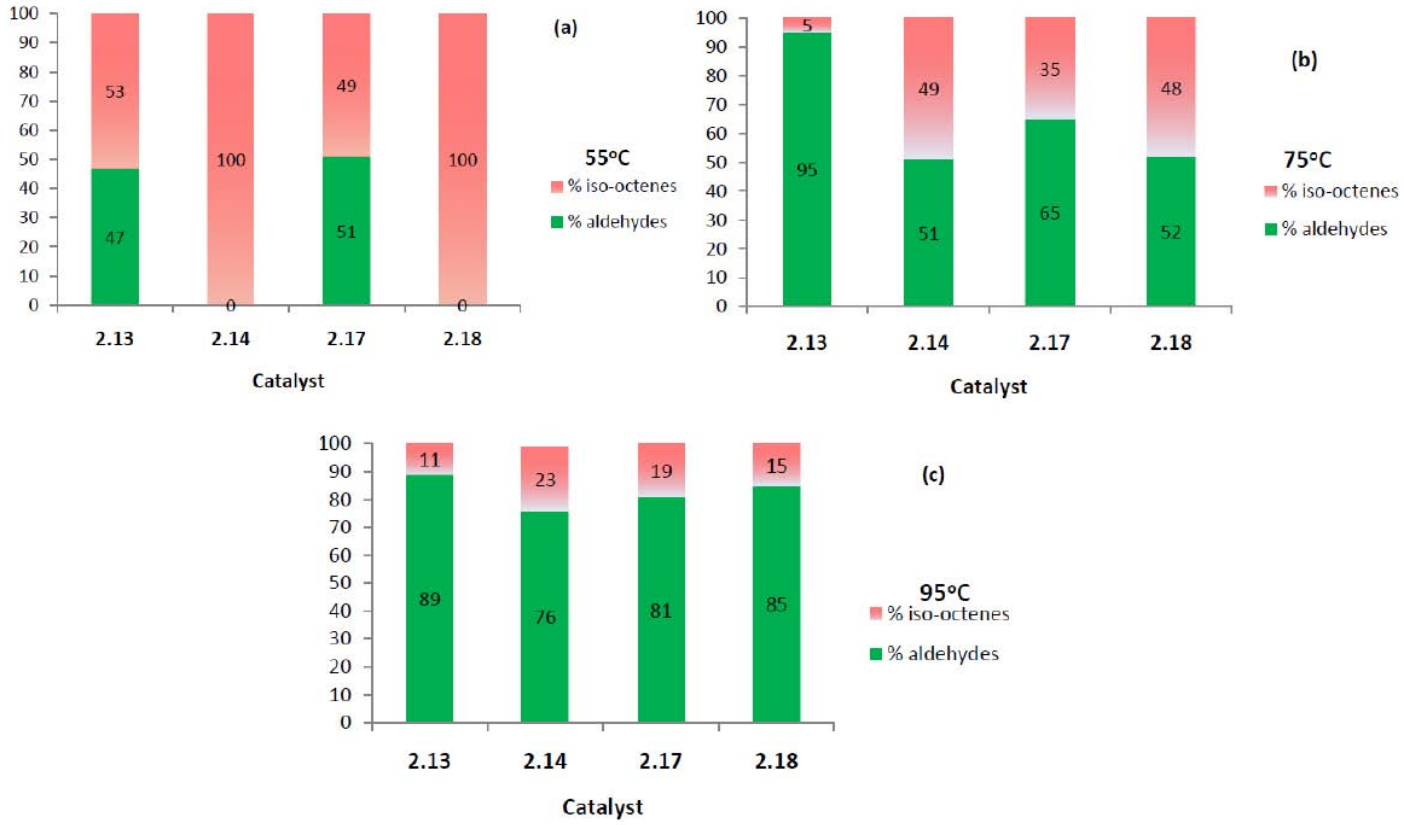

Fig. 3.10 Effect of temperature on chemoselectivity in hydroformylation of 1-octene using catalysts (**2.13-2.14**) and (**2.17-2.18**) at (a) 55 °C, (b) 75 °C and (c) 95 °C. [27c] (Average error estimate: (**2.13**) = ± 0.10; (**2.14**) = ± 0.12; (**2.17**) = ± 0.15 and (**2.18**) = ± 0.13).

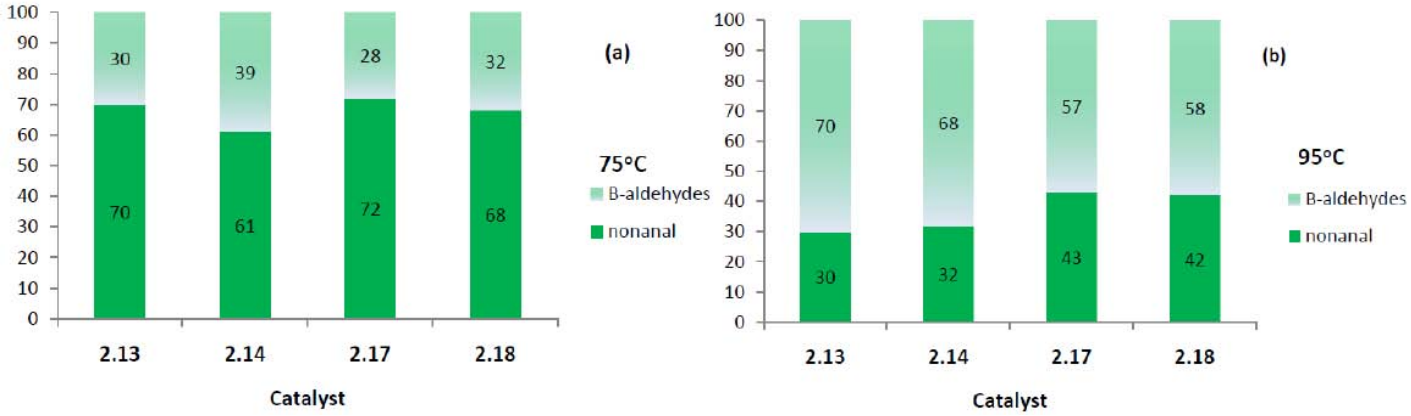

Fig. 3.11. Effect of temperature on regioselectivity in hydroformylation of 1-octene using catalysts (**2.13-2.14**) and (**2.17-2.18**) at (a) 75 °C and (b) 95 °C. [27c] (Average error estimate: (**2.13**) = ± 0.10; (**2.14**) = ± 0.11; (**2.17**) = ± 0.14 and (**2.18**) = ± 0.11).

3.5.4 Chemo- and regio-selectivities

For the established optimal conditions (T = 75 °C, syngas pressure = 30 bars), the catalyst precursors showed moderate to high (for catalyst (**2.13**)) chemoselectivity for aldehyde products (52-95%) with some amounts of *iso*-octenes (**Figs. 3.10b**). Thus, in forming aldehyde products, these reactions are in line with the green chemistry principle of atom economy. Overall, (**2.13**-**2.14**) and (**2.17**-**2.18**) favoured formation of *iso*-octenes at low temperature (55 °C) and pressures (5 and 10 bars) as has been previously reported. When compared to [$Rh(CO)_2(acac)$] under similar conditions the current catalyst precursors (**2.13**-**2.14**) and (**2.17**-**2.18**) show better regioselectivity. [24a]

In general, the catalyst precursors (**2.13**-**2.14**) and (**2.17**-**2.18**) showed regioselectivity toward linear aldehydes (nonanal) at optimal conditions, with the iminophosphine-based systems (**2.13** and **2.17**) displaying superior selectivity for nonanal (70 and 72% respectively) than iminopyridyl-based systems (**2.14** and **2.18**) (57 and 68% respectively). Formation of branched aldehydes *via* preformed *iso*-octenes was mostly favoured at syngas pressure = 10 bars, T = 75 °C and syngas pressure = 30 bars, T = 95 °C. These observations can in future be exploited in the formation of chiral aldehydes, which are highly sort after in the pharmaceutical industry.[24b-d] Furthermore, the n:iso ratio of aldehydes obtained with supported systems (**2.13** and **2.14**) was similar to when mononuclear analogues (**2.17** and **2.18**) were employed, effectively proving that the inherent chirality of the biopolymer support does not influence the catalytic behaviour around the active Rh centres. However, the support does play a crucial stabilizing role in catalyst precursor (**2.13**) allowing for this system to be recycled and reused (up to four times) while mononuclear analogues (**2.17** and **2.18**) decomposed to black species during reaction (*vide infra*). The chemo- and regioselectivity and activity displayed by the iminophosphine-based supported and mononuclear systems (**2.13** and **2.17**) compete well with related Rh supported and mononuclear systems in literature operated under higher conditions of temperature and pressure (ranging from: 80-175 °C and 50-90 bars). [25]

3.5.5 Rh leaching tests

A hot filtration test, whereby the supported systems (**2.13** and **2.14**) were filtered off 2 hours into the reaction and the filtrates taken back to reaction did not stop catalytic conversion of 1-

octene (**Fig. 3.12**). Notably, the filtrates did not show further hydroformylation of 1-octene under otherwise identical experimental conditions. Thus 0.02% (in catalysts (**2.13**)) and 0.06% (in catalysts (**2.14**)) of Rh leached into solution, as determined by ICP-MS, and this minimally catalyses isomerization. [26] This implies that chitosan-supported Rh complexes are the true active catalysts precursors for the hydroformylation reaction, while a combination of Rh complexes and colloidal particles are responsible for isomerization.

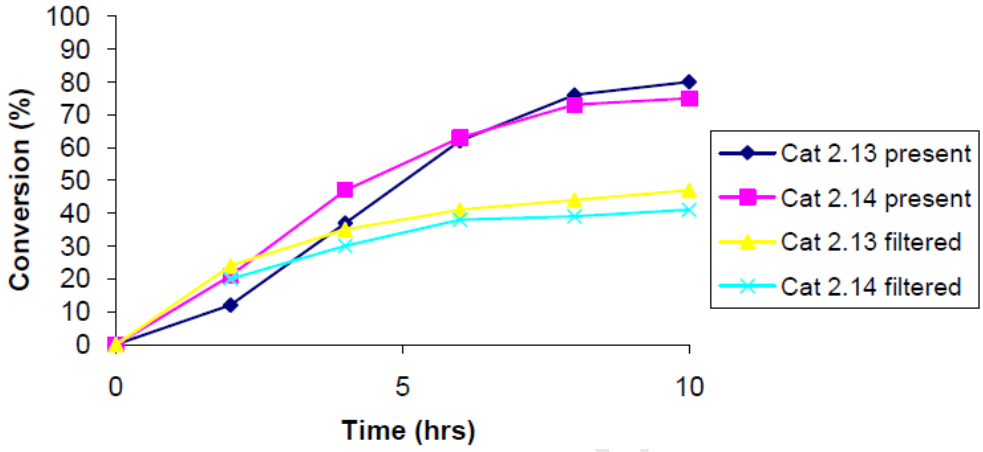

Fig. 3.12. Effect of removing supported Rh catalysts (**2.13** and **2.14**) from reaction (hot filtration test, (catalyst (**2.13** and **2.14**) removed after 2 hours). (Average error estimate: (**2.13**) = ± 0.12; (**2.14**) = ± 0.11).

3.5.6 Catalyst reusability

The supported system (**2.13**) was recycled four times with consistent conversion of 1-octene (75-79%) to mainly aldehydes. [27] Catalyst deactivation was as seen in similar Pd catalysts. [28] Notably, chemo- and regio- selectivity was maintained throughout the cycles (average n:iso = 70:30). Catalyst precursor (**2.14**) gave poor conversion (4%) on the second cycle indicative of the inferior stability of this catalyst compared to the iminophosphine-based system (**2.13**). The iminophosphine-based catalysts exhibit slightly better activity in general, this may be attributed to the bulky phosphine ligand imposing a more favourable bite angle for the substrate (1-octene) or the formation of a more stable active species based on hard and soft acid and base principles. [29]

3.6 Summary and Conclusions: Hydroformylation reactions

The chitosan-supported Rh^{I} complexes and mononuclear counterparts were active catalyst precursors in the hydroformylation of 1-octene under mild conditions with minute amounts of Rh leaching into the solution as determined by ICP-MS. Activity as well as regio- and chemo-selectivity was affected by features such as temperature and syngas pressure and under optimal conditions of 75 °C and 30 bars, good selectivity for nonanal was seen for both the supported and mononuclear catalyst precursors. Iminophosphine-based system (**2.13**) showed the best activity, chemoselectivity, regioselectivity as well as recyclability and can therefore be singled out for further development.

3.7 Experimental

Inductively coupled plasma-mass spectrometry was obtained using a Perkin-Elmer Elan600 quadrupole ICP-MS with a Cetax LSX-200 UV laser module. TEM imaging was done on a JEOL 1200EXII CRYO TEM. Catalysis products were analyzed using a Varian 3900 GC.

3.7.1 General procedure for the Suzuki-Miyaura reactions

The general procedure used for the Suzuki-Miyaura cross-coupling reactions was as follows:

A quantity equivalent to (4.47 x10^{-4} mmol) of either one of the Pd catalyst precursors (**2.5**-**2.8**) was suspended in the corresponding solvent (xylene or EtOH:H_2O, 50:50) (20 ml) and arylhalide (5.1 mmol), phenyl boronic acid (7.5 mmol), base (10 mmol) and *n*-decane (4.4 mmol) were added. The reaction mixture was then heated at the appropriate temperature and followed by GC using *n*-decane as the internal standard. The conversion was calculated relative to aryl halide, the limiting reagent of the reaction in relation to authentic standard biphenyl or substituted biphenyl.

In the case of the Pd leaching tests, 4 molar equivalents of mercury or thiolated chitosan were also added to the reaction mixture. For catalyst recycling experiments, the recovered catalysts was washed with water, ethanol and acetone (80 ml each) respectively, oven dried at 80℃ for 8 hours and reused in the subsequent run.

3.7.2 General procedure for the Heck reactions

A quantity equivalent to (0.00437 mmol, 0.00044 mol%) of any one of the Pd catalyst precursors (**2.5**-**2.8**) was suspended in DMF (20 ml) and arylhalide (5.3 mmol), methyl acrylate or styrene (5.3 mmol), triethylamine (10 mmol) and *n*-decane (4.4 mmol) were added. The reaction mixture was then heated at 130 ˚C and followed by GC using *n*-decane as the internal standard. The conversion was calculated relative to aryl halide in relation to authentic standard *trans*-methyl cinnamate or *trans*-stilbene.

3.7.3 General procedure for the hydroformylation reactions

Hydroformylation reactions were conducted in a 90 ml stainless steel autoclave. The autoclave was charged with xylene (10 ml), 1-octene (715 mg, 6.37 mmol), *n*-decane internal standard (180 mg, 1.26 mmol) and either of the Rh catalyst precursors (**2.13**, **2.14**, **2.17** or **2.18**) (2.87×10^{-3} mmol, substrate: Rh ratio = 2500:1). The autoclave was flushed three times with syngas ($CO:H_2$, 1:1 ratio) followed by pressurizing and heating to the desired syngas pressure and temperature respectively. Samples were taken every 2 hours and analyzed using gas chromatography (GC). The products were confirmed in relation to authentic *iso*-octenes and aldehydes.

3.8 References

1. R.F. Heck, *Org. React.,*(**1982**), 27, 345; b) N. Miyauara, T. Yanagi, A. Suzuki, *Synth. Commun.*,(**1981**), 11, 513.
2. (a) A. Suzuki, *J. Organomet. Chem.,* (**1999**), 576, 147; (b) A.F. Littke, C. Dai, G.C. Fu, *J. Am. Chem. Soc*., (**2000**), 122, 4020; (c) J. Albaneze-Walker, J.A. Murray, A. Soheilli, S. Ceglia, S.A. Springfield, C. Bazaral, P.G. Dormer, D.L. Hughes, *Tetrahedron*, (**2005**), 61, 6330; (d) J-S. Chen, A.N. Vasiliev, A.P. Panarello, J.G. Khinast, *Appl. Catal. A: General*, (**2007**), 325, 76.
3. (a) J.K. Stille, *Angew. Chem. Int. Ed. Engl.,* (**1986**), 25, 508. (b) N. Miyaura, A. Suzuki, *Chem. Rev.,* (**1995**), 95, 2457. (c) E-I. Negishi, *Acc. Chem. Res.,* (**1982**), 15, 340. (d) K. Sonogashira, *Comprehensive Organic Synthesis*, Eds.: B.M. Trost, I. Fleming, Pergamon Press, Oxford, **(1991**), 3, pp. 521-549. (e) A. Rudolph, M. Lautens, *Angew. Chem, Int. Ed.,* (**2009**), 48, 2656. (f) Nobel Foundation: http://nobelprize.org/nobel_prizes/chemistry/laureates/2010/press.html, *accessed 2nd March 2011*. (g) S.B. Jang, *Tetrahedron Lett.,* **(1997**), 38, 1793.
4. (a) D. Schils, F. Stappers, G. Solberghe, R. van Heck, M. Coppens, D. Van den Heuvel, P. Van der Donck, T. Callewaert, F. Meeussen, E. De Brie, K. Eersels, E. Schouteden, *Org. Proc. Res. and Dev.*, (**2008**), 12, 530; (b) P.D. Stevens, G. Li, J. Fan, M. Yen, Y. Gao, *Chem Commun.*, (**2005**) 4435.
5. (a) G. Haung, C-C. Cai, J. Luo, H. Zhou, Y.-A. Guo, S.-Y. Liu*, Can. J. Chem.*, (**2008**), 86, 199; (b) J.J.E. Hardy, S. Hubert, D.J. Macquarrie, A.J. Wilson, *Green Chem.*, (**2004**), 6, 53; (c) F. Quignard, A. Chaplin, A. Domard, *Langmuir*, (**2000**), 16, B 9106.
6. (a) L. Yin, J. Liebscher, *J. Chem. Rev,*. (**2007**), 107, 133; (b) N.T.S. Phan, M. van der Sluys, C.W. Jones, *Adv. Synth. Catal*., (**2006**), 242, 77; (c) Palladium Catalysts: http://www.sigmaaldrich.com/chemistry/drug-discovery/product-highlights/palladium-catalysts.html, (**2010**), *accessed 13th March 2010*.
7. (a) E. Guibal, *Prog. Polym. Sci.,* (**2005**), 30, 71 and references therein; (b) D.J. Macquarrie, J.J.E. Hargy, *Ind. Eng. Chem. Res.,* (**2005**), 44, 8499 and references therein; (c) E. Sin, S-S. Yi, Y-S. Lee, *J. Mol. Catal. A: Chemical,* (**2010**), 315, 99; (d) H-M. Guan, X-S. Cheng, *Polym. Adv. Technol.,* (**2004**), 15, 89; (e) F. Peirano, T. Vincent, F. Quignard, M. Robitzer, E. Guibal, *J. Membrane Science,* (**2009**), 329, 30; (f) S-S. Yi, D-H. Lee, E. Sin, Y-S. Lee, *Tetrahedron Letters*, (**2007**), 48, 6771; (g) C. Lou, Y. Zhang, Y. Wang, *J. Mol. Catal. A: Chem.,* (**2005**), 229, 7. (h) V. Calò, A. Nacci, A. Monopoli, A.

Fornaro, L. Sabbatini, N. Cioffi, N. Ditaranto, *Organometallics*, (**2004**), 23, 5154. (i) Guibal, V. Thierry, B.F. Peirano, *Ion Exchange and Solvent Extraction,* (**2007**), 18, 151; (j) S.E.S. Leonhardt, A. Stolle, B. Ondruschka, G. Cravotto, C. De Leo, K.D. Jandt, T.F. Keller, *Appl. Catal. A: Gen.,* (**2010**), 379, 30.

8. D. Olsson, O.F. Wendt, *J. Organomet. Chem*., (**2009**), 694, 3112.
9. (a) O. Roelen, *US Patent*, 2327066, (**1943**); (b) P. Eibracht, L. Barfacker, C. Buss, C. Hollmann, B.E. Kistsos-Rzychon, C.L. Kranemann, T. Rische, R. Roggenbuck, A. Schmidt, *Chem. Rev.,* (**1999**), 99, 3329 and references therein; (c) B. Cornils, W.A. Herrmann, M. Rasch M. Beller*, Angew. Chem. Int. Ed. Engl.,* (**1994**), 33, 2144; (d) B. Cornils, C.D. Frohning, C.W. Kohlpaintner*, J. Mol Catal. A,* (**1995**), 104, 17; (e) B. Cornils, W.A. Herrmann, R.W. Ecki, *J. Mol. Catal. A: Chem.,* (**1997**), (116**)**, 27; (f) D. Evans, J.A. Osborn, G. Wilkinson, *J. Chem. Soc. A*, (**1968**), 3133; (g) P.W.N.M. van Leeuwen, C. Claver, *Rh-Catalyzed hydroformylation*, Kluwer Academic, Dordrecht, 2000, pp. 6. (h) B. Cornils, W. A. Herrmann, M. Rasch, "Otto Roelen, Pioneer in Industrial Homogeneous Catalysis", *Angew. Chem. Int. Ed.,* (**1994**), 33, 2144. (i) H. Bricout, F. Hapiot, A. Ponchel, S. Tilloy, E. Monflier, *Sustainability, (***2009**), 1, 924. (j) B. Cornils, *Org. Process Res. Dev.,* (**1998**), 2, 121.
10. (a) B. Cornils, E. Wiebus, *Chemtech*., (**1995**), 25, 33; (b) B. Cornils, E.G. Kuntz*, J. Organomet. Chem.*, (**1995**), 502, 177.
11. (a) A. Riisager, K.M. Erikson, J. Hjortkjaer, R. Fehrmann, *J. Mol. Catal. A: Chem.,* (**2003**), 193, 259; (b) M.E. Davis in: B Cornils, W.A. Hermann (Eds), *Aqueous-Phase Organometallic Catalysis,* Chapter 4,7 Wiley, Weinheim, 1998, pp. 241; (c) M.E. Davis, *Chemtech.,* (**1992**), 22, 498.
12. (a) Z.K. Lopez-Castillo, R. Flores, I. Kani, J.P. Fackler Jr., A. Akgerman, *Ind. Eng. Chem. Res.*, (**2008**), 42, 3893; (b) C. Halm, M.J. Kurth, Angew. *Chem. Int. Ed. Engl*., (**1998**), 37, 510.
13. (a) J.S. Wilkes, *Green Chem.,* (**2002**), 4, 73; (b) J.L. Anthony, E.J. Maginn, J.F. Brennecke, *J. Phys. Chem*. B, (**2002**), 106, 7315; (c) J.S. Wilkes, *J. Mol. Catal. A: Chem.,* (**2004**), 214, 11.
14. (a) A. Riisager, K.M. Eriksen, P. Wasserscheid, R. Fehrmann, *Catal. Lett.,* (**2003**), 98, 149; (b) A. Riisager, R. Fehrmann, S. Flicker, R. Van Hal, M. Haumann, P. Wasserscheid, *Angew. Chem. Int. Ed.,* (**2004**), 43, 2; (c) Y. Yang, C. Deng, Y. Yuan, *J. Catal.*, (**2005**), 232, 108.

15. (a) P. Arya, N. Verugopal Rao, J. Singkhonrat, *J. Org. Chem.,* (**2000**), 65, 1881; (b) R. Van Heerbeek, P.C.J. Kamer, P.W.N.M. van Leeuwen, J.N.H Reek, *Chem. Rev*., (**2002**), 102, 3717; (c) P. Li, S. Kawi, *J. Catal*., (**2008**), 257, 23.
16. (a) G.O. Evans, C.U. Pittman, R. Mc Millan, R.T. Beach, R. Jones, *J. Organomet. Chem.*, (**1975**), 87, 189; (b) F. Shibahara, K. Nozaki, T. Matsuo, T. Hiyama, *Bioorg. Med. Chem. Lett.,* (**2002**), 12, 1825; (c) F. Shabahara, K. Nozaki, T. Hiyama, *J. Am. Chem Soc.*, (**2003**), 125, 8555; (d) D.E. Bryant, M. Kilner, *J. Mol Catal. A: Chem.*, (**2003**), 193, 83; (e) E.V. Slivinskii, N.V. Kolesnichenko, *Russ. Chem. Bull. Int. Ed*., (**2004**), 53, 2449.
17. (a) M.A. Valenzuela, G. Aguilar, P. Bosch, H. Armendariz, P. Salas, A. Montoya, *Catal. Lett.,* (**1992**), 15, 179; (b) A.M. Trzeciak, J.J. Ziołkowski, Z. Jaworska-Galas, W. Mista, J. Wrzyszcz, *J. Mol. Catal.,* (**1994**), 88, 13; (c) J. Wrzyszcz, M. Zawadzki, A.M. Trzeciak, J.J. Ziołkowski, *J. Mol. Catal. A: Chem.* (**2002**), 189, 203; (d) L. Huang, S. Kawi, *Catal. Lett., (***2004**), 92, 57.
18. (a) J.P.K. Reynhardt, Y. Yang, A. Sayari, H. Alper, *Chem. Mater*., (**2004**), 16, 4095; (b) X. Lan, W. Zhang, L. Yan, Y. Ding, X. Han, L. Lin, X. Bao, *J. Phys. Chem. C*, (**2009**), 113, 6589.
19. W-L. Wei, H-Y. Zhu, C-L. Zhao, M-Y. Huang, Y-Y. Jiang, *React. Funct. Polym.,* (**2004**), 59, 33.
20. M.J. Gronnow, R. Luque, D.J. Macquarrie, J.H. Clark, *Green Chem.,* (**2005**), 7, 552.
21. X. Zhang, Y. Geng, B. Han, M-Y. Ying, M-Y. Huang, Y.Y. Jiang, *Polym. Adv. Technol,.* (**2001**), 12, 642.
22. E.G. Kuntz, *Chemtech.*, (**1987**), 14, 570.
23. C.K. Brown, G. Wilkinson, *J. Chem. Soc. A*, (**1970**), 2753.
24. (a) N.C. Antonels, J.R. Moss, G.S. Smith, *J. Organomet. Chem.,* (**2011**), 696, 2003; (b) A.D. Worthy, C.L. Joe, T.E. Lightburn, K.L. Tan, *J. Am. Chem Soc.,* (**2010**), 132, 14757. (c) T.E. Lightburn, O.A. Paolis, K.H. Cheng, K.L. Tan, *Org. Lett.,* (**2011**), 13, 2686. (d) H. Fernández-Pèrez, P.Etayo, A. Panossian, A. Vidal-Ferran, *Chem. Rev.,* (**2011**), 111, 2119.
25. (a) W. Zhou, D. He, *Green Chem*., (**2009**), 11, 1146; (b) M.M. Taquikhan, S.B. Halligudi, S.H.R. Abdi, *J. Mol. Catal.,* (**1988**), 45, 215; (c) T. Mathivet, C. Mèliet, Y. Castanet, A. Mortreux, L. Caron, S. Tilloy, E. Monflier, *J. Mol. Catal. A: Chem.,* (**2001**), 176, 105; (d) D.U. Parmar, H.C. Bajaj, S.D. Bhatt, R.V. Jasra, *Bulletin of the Catal. Soc. Of India,* (**2003**), 2, 34-39; (e) L. Leclercq, M. Sauthier, Y. Castanet, A. Mortreux, H. Bricout, E. Monflier, *Adv. Synth. Catal*., (**2005**), 347, 55; (f) C.C. Miyagawa, J. Kupka, A. Schumpe,

J. Mol. Catal. A: Chem., (**2005**), 234, 9; (g) M. Bortenschlager, N. Schöllhorn, A. Wittmann, R. Weberskirch, *Chem. Eur. J*., (**2007**), 13, 520; (h) J.A. Bae, K-C. Song, J-K. Jeon, Y.S. Ko, Y-K. Park, J-H. Yim, *Microporous and Mesoporous Materials*, (**2009**), 123, 289; (i) J.D. Scholten, J. Dupont, *Organometallics,* (**2008**), 27, 4439; (j) S. Dastgir, K.S. Coleman, A.R. Cowley, M.L.H. Green, *Dalton Trans.,* (**2009**), 7203; (k) W. Zhou, Y. Li, D. He, *Appl. Catal. A: General*, (**2010**), 377, 114; (l) G.M. Pawar, J. Weckesser, S. Blechert, M.R. Buchmeiser, *Beilstein J. Org. Chem.,* (**2010**), 6, 1; (m) S. Dastgir, K.S. Coleman, M.L.H. Green, *Dalton Trans.,* (**2011**),40, 661; (n) R.M. Deshpande, A.A. Kelkar, A. Sharma, C. Julcour-Lebigue, H. Delmas, *Chem. Eng. Sci.,* (**2011**), 66, 1631; (o) M.T. Zarka, M. Bortenschlager, K. Wurst, O. Nuyken, R. Weberskirch, *Organometallics*, (**2004**), 23, 4817.

26. See appendix **Section e (Table a)**.
27. See appendix **Section f (Table b)**.
28. B.C.E. Makhubela, A. Jardine, G.S. Smith, *Appl. Catal. A: General*, (**2011**), 393, 231.
29. R.G. Pearson, *J. Am. Chem. Soc.,* (**1963**), 85, 3533.

Chapter 4

Pyridylimine Metallodendrimers: *Synthesis and Characterization*

4.1 Introduction

Dendrimers are polymeric compounds with highly branched structures and functionally tunable peripheral groups. They possess low polydispersities, a high degree of molecular uniformity and precisely controlled structures. Since dendrimers are built systematically, their shape is fully controllable. Dendrimers can therefore demonstrate a variety of biomedical, photophysical, tunability in size and shape as well as catalytic properties. [1] With the attachment of metals, metallodendrimers or dendrimer composites provide diverse characteristics for applications in catalysis and biomimetic catalysis, photoluminescent technology, imaging contrast agents, biomedial sensors and as therapeutic agents. [1]

Organometallic polymers of main chain and dendritic (highly branched) nature have been widely prepared for applications in catalysis (see Chapter 1, Section 1.7). [2-6] The appeal in organometallic polymers for catalysis lies in that, unlike organic- and inorganic hybrid-polymer supported catalysts, these possess inherent well-defined active sites that eliminate negative effects such as poor accessibility, random anchoring, or disturbed geometry-phenomena that often result in poor activity and selectivity in classical immobilization. Organometallic polymers are also often soluble in reaction solvents and thus operate under true homogeneous conditions and can be separated from solution by precipitation, nano- or ultra-filtration methods.

A large number of metallodendrimers and their catalytic investigations have been reported including those based on polycarbosilane (PCS) [7], polyamide [4d,8], polyarylether (PAE) [6,9] and polypropyleneimine (PPI) supports [4-5,10] to name a few. Several first- and second-generation PPI metallodendrimers bearing four and eight metal centres have been previously reported. [4-5,10]. We were interested in investigating the properties and catalytic behaviour of the intermediate sized/ low generation trinuclear analogue of these systems. This chapter discusses the synthesis and characterization of palladium- and rhodium-containing tris-2-(2-pyridylimine ethyl)amine and some mononuclear pyridylimine complexes. In order to immobilize these conplexes, we synthesized ligands (**4.1** and **4.2**). Chapter 6 will report on the application of the rhodium metallodendrimers and mononuclear complexes as catalyst precursors for hydroformylation reactions.

4.2 Synthesis and characterization of 4-(2-pyridylimine) benzyl alcohol ligand (4.1)

The new 4-(2-pyridylimine) benzyl alcohol ligand (**4.1**) was prepared by the reaction of 2-pyridinecarboxaldehyde with 4-amino benzyl alcohol at room temperature (**Eq. 4.1**).

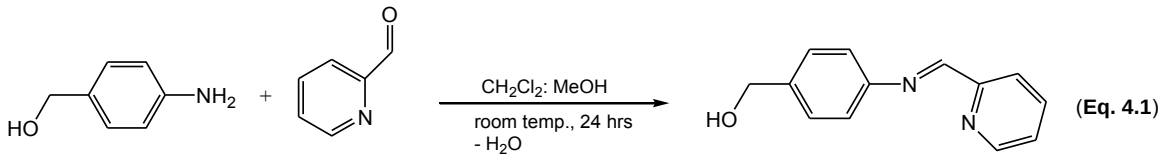

(**Eq. 4.1**)

(**4.1**)

The Schiff base ligand (**4.1**) was isolated as a light brown solid in a good yield (89 %). Ligand (**4.1**) is soluble in most common organic solvents such as dichloromethane, chloroform, methanol, diethyl ether and tetrahydrofuran. This ligand has been characterized using elemental analysis (C, H and N), FT-IR and ^{1}H NMR and ^{13}C NMR spectroscopy as well as mass spectrometry.

Elemental analyses results were in agreement with the proposed formulation and correspond well with a related 4-(4-pyridylimine) benzyl alcohol ligand that has been reported. [11a]

The ^{1}H NMR spectrum of ligand (**4.1**) displayed signals for -C**H**$_2$- and -O**H** in the range δ 4.50-5.16 ppm and aromatic resonances at δ 7.25-8.73 (**Table 4.1**). The Schiff base condensation reaction was confirmed by the appearance of a peak in the range of δ 8.69 ppm assigned to the imine proton in ligand (**4.1**).

Table 4.1 Selected spectroscopic data (^{1}H and ^{13}C NMR and IR) for ligand (**4.1**).

Ligand	**^{1}H NMR**				**^{13}C NMR**
	C**H**$_2$(ppm)	O**H** (ppm)	**H**C=N (ppm)	**Ar** (ppm)	H**C**=N (ppm)
4.1	4.50	5.16	8.69	7.25-8.73	160.63

The ^{13}C NMR spectrum for ligand (**4.1**) displayed a signal for one aliphatic carbon in the region of *ca* δ 64 ppm and aromatic carbons in the region of *ca* δ 121-154 ppm. The imine carbon was the most deshielded signal in the region of *ca* δ 160 ppm.

The FT-IR spectrum of ligand (**4.1**) displayed a broad absorption band at ≈ 3300 cm^{-1} assigned to the ν(O-H) vibrations. Two absorption bands were observed in the region of 1646 cm^{-1} ν(C=N)$_{imine}$ and 1599 cm^{-1} ν(C=N)$_{pyridyl}$ for ligand (**4.1**). EI-mass spectrometry further

confirmed the integrity of this ligand by displaying a peak at m/z 210.9 for the $[M-H]^+$ ion. In addition, the presence of benzyl alcohol (m/z 104.99) and pyridyl (m/z 78.99) fragments were consisten with the structure of ligand (**4.1**). [11b]

4.3 Synthesis and characterization of tris-2-(2-pyridylimine ethyl) amine ligand (4.2).

The tris-2-(2-pyridylimine ethyl)amine ligand (**4.2**) was prepared *via* a Schiff base condensation reaction of tris(2-aminoethyl)amine and 2-pyridinecarboxaldehyde in refluxing DCM:MeOH (30:70) over 16 hours (**Eq. 4.2**). The dendrimer was isolated as a stable light brown solid in a moderate yield of 66%. This ligand has been characterized using ^{1}H NMR, ^{13}C NMR, FT-IR spectroscopy, elemental analysis (C, H and N) and mass spectrometry.

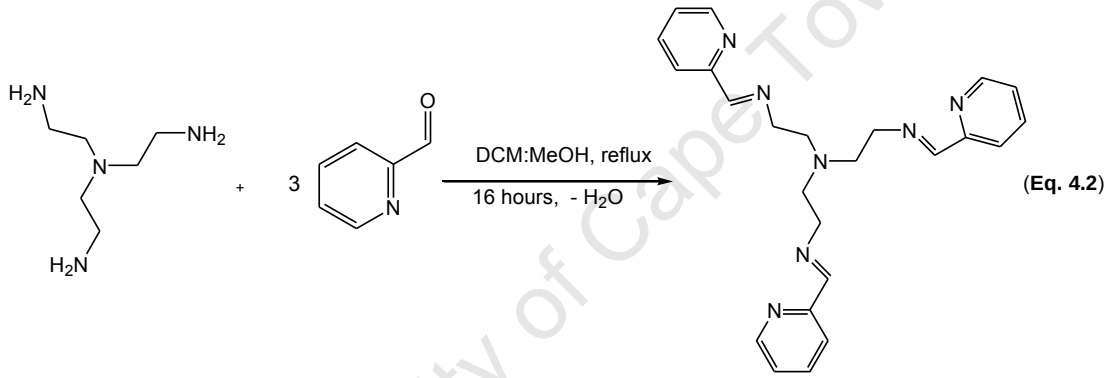

(**4.2**)

The ^{1}H NMR spectrum of ligand (**4.2**) displayed very broad overlapping signals in the aliphatic and aromatic regions. A broad signal assigned to the imine proton was seen at δ 8.42 ppm. The methylene protons of the tris(2-iminoethyl)amine core resonated in the region of δ 2.09-3.42 ppm while the aromatic and imine protons were observed at δ 8.57-7.15 ppm.

^{13}C NMR spectroscopy displayed broad but more meaningful results with the aliphatic carbons resonating at *ca* δ 54-58 ppm. The imine carbon exhibited a characteristic signal, while the aromatic carbons were seen between *ca* δ 121-153 ppm (**Table 4.2**).

Table 4.2 Selected spectroscopic data (^{13}C NMR and IR) for ligand (**4.2**).

Ligand	**^{13}C NMR**			**FT-IR**	
	CH_2(ppm)	H**C**=N (ppm)	**Ar** (ppm)	ν(C=N)$_{imine}$ (cm^{-1})	ν(C=N)$_{pyridyl}$ (cm^{-1})
4.2	54.17, 58.42	163.09	121.22-153.21	1649	1590

Characteristic FT-IR spectroscopic results were obtained for ligand (**4.2**) with absorption bands observed at 1649 cm^{-1} and 1590 cm^{-1} due to the imine and pyridyl imine moieties respectively (**Table 4.2**) (*vide infra*, **Fig. 4.3a**). This data correlates well with similar first and second generation polypropylene imine dendrimers from the literature. [4a-c,10]

EI-mass spectrometry revealed the $[M-H]^+$ (m/z = 412.78) ion, thus further supporting the formation of ligand (**4.2**). C, H and N analysis was also in agreement with the proposed structure of ligand (**4.2**).

4.4 Synthesis and characterization of 4-(imino) benzyl alcohol transition metal complexes (4.3-4.5)

*4.4.1 Synthesis and characterization of 4-(2-pyridylimine) benzyl alcohol palladium(II) complex (**4.3**).*

$[PdCl_2(COD)]$ reacted with ligand (**4.1**) by stirring at room temperature in dichloromethane to afford complex (**4.3**) (**Eq. 4.3**). This new complex (**4.3**) was obtained as a yellow solid in a good yield (73 %) and has been characterized using elemental analysis (C, H and N) FT-IR, ^{1}H NMR ^{13}C NMR spectroscopy as well as mass spectrometry .Additionally, single crystal X-ray cryatallography was used to determine the molecular structure of complex (**4.3**).

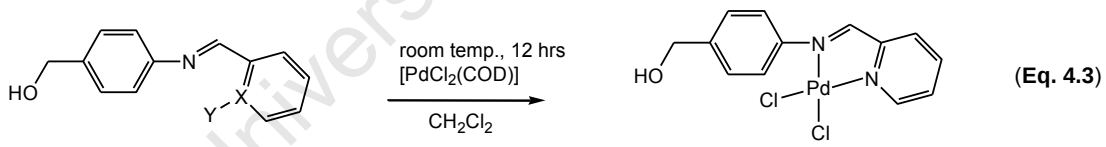

(**4.1**) (**4.3**) (**Eq. 4.3**)

Elemental analysis and mass spectral data were consistent with the proposed structure for complex (**4.3**). The mass spectral data for this complex displayed $[M-Cl]^+$ (m/z = 353.03) as the highest molecular weight ion.

The ^{1}H NMR spectrum of complex (**4.3**) displayed an imine proton in the region of δ 8.67 ppm. The observed upfield shifts relative to the free ligand evidenced coordination of the imine nitrogen to the palladium centre (**Table 4.3**). This could be attributed to back-bonding from palladium to the imine bond and/or due to conformational changes experienced by the ligand in order to facilitate coordination of the imine nitrogen to the palladium centre. [12]

Table 4.3. Selected spectroscopic (^{1}H and ^{13}C NMR as well as FT- IR) data for complex (**4.3**)[a].

Complex	^{1}H NMR	^{13}C NMR	FT-IR
	HC=N (ppm)	H**C**=N (ppm)	ν(C=N)$_{imine}$ (cm^{-1})
4.3	8.67(8.69)	172.50(160.63)	1635(1646)

[a] Ligand values in parentheses.

The ^{13}C NMR spectrum of complex (**4.3**) confirmed coordination of the imine nitrogen to palladium by a downfield shift with respect to the free ligand (**4.1**). Similar trends have been well documented. [12,13a-e]

FT-IR spectroscopy results of complex (**4.3**) displayed shifts in the imine absorption bands from higher to lower wavenumbers due to palladium coordination (**Table 4.3**). This decrease in stretching frequency is due to sigma donation of electrons from the imine nitrogen to the palladium centre, thus resulting in less double bond character of the imine bond.

The molecular structure of complex (**4.3**) was determined using single crystal X-ray diffraction (**Fig. 4.1**). [13f]

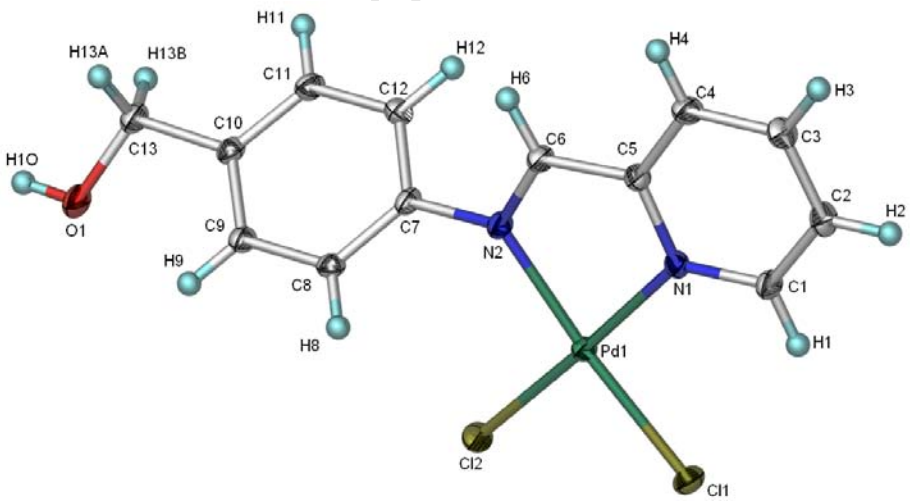

Fig. 4.1. The ORTEP structure of the molecular structure of complex (**4.3**), showing atomic labelling. Ellipsoids are at 40% probability level.

Pale yellow crystals were obtained from a concentrated solution of complex (**4.3**) in dimethylsulfoxide. Selected bond lengths and angles are given in **Table 4.4**.

Table 4.4 Selected bond distances and angles for palladium complex (**4.3**).

Bond distances (Å)		Bond angles (°)	
Pd(1)-N(1)	2.027(2)	N(1)-Pd(1)-Cl(1)	93.58(7)
Pd(1)-N(2)	2.054(2)	N(1)-Pd(1)-N(2)	80.46(1)
Pd(1)-Cl(1)	2.289(8)	N(2)-Pd(1)-Cl(2)	97.24(7)
Pd(1)-Cl(2)	2.279(8)	Cl(1)-Pd(1)-Cl(2)	88.75(2)
N(2)-C(6)	1.295(4)	N(1)-Pd(1)-Cl(2)	177.29(8)
N(1)-C(5)	1.357(4)	N(2)-Pd(1)-Cl(1)	173.88(7)

The molecular structure of complex (**4.3**) is a slightly distorted square-planar geometry around the palladium centre. Ligand (**4.1**) coordinates to the palladium with an angle of 80.46(1)° N(1)-Pd(1)-N(2). Deviation of this angle from the expected angle of 90° is attributed to the strain imposed by the five-membered chelate ring N(2)-C(6)-C(5)-N(1)-Pd(1). This reduction in the angle is compensated for by an increase in the N(2)-Pd(1)-Cl(2) angle 97.24(7)°. Similar deviations have been reported. [14] The other angles around the palladium centre (**Table 4.4**) were close to the expected 90° value. The bond lengths Pd(1)-N(1) and Pd(1)-N(2) (2.027(2) and 2.054(2) Å respectively) were in similar ranges as related diimine palladium chloride complexes (2.019 and 2.013 Å). This was also the case for Pd(1)-Cl(1) and Pd(1)-Cl(2) which has bond lengths of 2.289(8) and 2.279(8) Å respectively. Similarly, the latter bpnd lengths correlate well to related diimine palladium chloride complexes (2.277 and 2.285 Å). [14]

*4.4.2 Synthesis and characterization of 4-(2-pyridylimine) benzyl alcohol rhodium(I) complexes (**4.4-4.5**).*

In separate reactions, ligand (**4.1**) was treated with $[RhCl(CO)_2]_2$ and $[RhCl(COD)]_2$ dimers at room temperature in DCM:MeOH (1:1) to afford complexes (**4.4** and **4.5**) (**Scheme 4.1**).

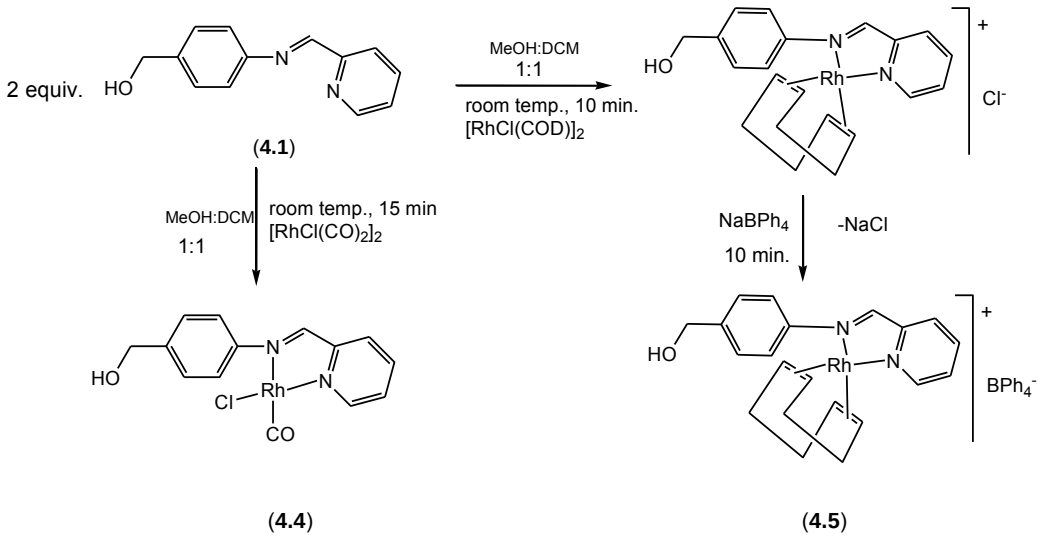

Scheme 4.1. Outline for the synthesis of rhodium complexes (**4.4** and **45**).

The products (**4.4** and **4.5**) were isolated in good to moderate yields (84 and 49 % respectively) as a stable dark orange solid (**4.4**) and a deep dark red crystalline solid (**4.5**). Complex (**4.4**) melts in the range of 178-180 °C while (**4.5**) melts at 110-113 °C. These new complexes have been by elemental analysis (C, H and N), FT-IR, ^{1}H NMR, and ^{13}C NMR spectroscopy as well as mass spectrometry.

Elemental analyses results for complexes (**4.4-4.5**) were in agreement with the calculated percentage C, H and N and ESI-mass spectra further established the integrity of the complexes through revealing base peaks at m/z = 343.8 and 441.09 for the $[M\text{-}Cl]^{+}$ and $[M\text{-}(BPh_4^{-})]^{+}$ fragments respectively (in complex (**4.5**), M = the positively charged complex without the BPh_4^{-} counter ion).

NMR spectroscopy supported coordination of rhodium to ligand (**4.1**) in a chelating manner to form the rhodium chlorocarbonyl and cyclooctadiene (COD) complexes (**4.4** and **4.5**). The ^{1}H NMR spectra of these complexes displayed an upfield shift of the imine proton signal from δ 8.69 ppm in ligand (**4.1**) to δ 8.51 ppm in complex (**4.4**) and δ 8.31 ppm in complex (**4.5**).

^{13}C NMR spectra for complexes (**4.4** and **4.5**) also displayed expected downfield shifts of imine carbon signals from *ca* δ 160 ppm in ligand (**4.2**) to *ca* δ 173 ppm in both complexes (**4.4** and **4.5**). In addition, a doublet due to the carbonyl carbon was seen at 189.47 ppm along with a Rh-C coupling of 70.28 Hz. These trends are in agreement with similar Rh^{I} complexes

that have been reported. [5,15-16] Complex (**4.5**) displayed signals at δ 29.83 and 84.63 ppm assigned to the aliphatic and alkene functionalities of the COD ligand respectively.

Evidence for the coordination of the Rh centre was further confirmed through a shift of the imine absorption band in the FT-IR spectrum of ligand (**4.1**) (1646 cm^{-1}) to 1626 cm^{-1} in complex (**4.4**) and 1617 cm^{-1} in complex (**4.5**) together with a shift in the pyridyl imine absorption band from 1599 cm^{-1} in ligand (**4.1**) to 1588 cm^{-1} in complex (**4.4**) and 1591 cm^{-1} in complex (**4.5**). These shifts are due to back-bonding from the rhodium to the imine bond, thus increasing its electron density. Additionally, a single very strong terminal carbonyl absorption band was evident at 1993 cm^{-1} suggesting one preferred isomer in complex (**4.4**).

4.5 Synthesis and characterization of tris-2-(iminoethyl) amine transition metal complexes

*4.5.1 Synthesis and characterization of tris-2-(2-pyridylimine ethyl) amine palladium dendrimer (**4.6**)*

The tris-2-(2-pyridylimine ethyl)amine ligand (**4.2**) was treated with [$PdCl_2COD$] in acetone:dichloromethane (2:1) at room temperature to produce the trinuclear low generation metallodendrimer (**4.6**) (**Eq. 4.4**). The palladium metallodendrimer was isolated as an off yellow powder in a good yield of 86% and is stable at room temperature.

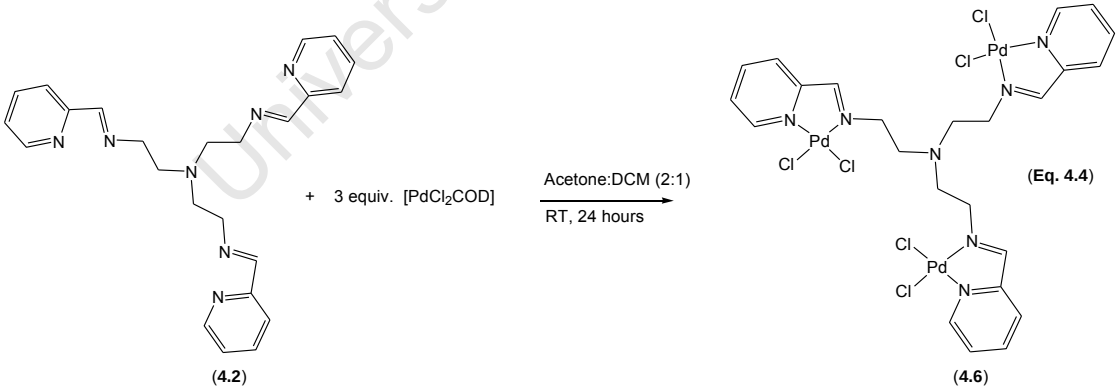

Mass spectrometry and elemental analysis gave evidence for the formation of the proposed metallodendrimer (**4.6**) by displaying a peak corresponding to the $[M\text{-}Cl]^+$ ion (m/z = 905.8) as well as satisfactory C, H and N analysis. Notably, unlike the first and second generation PPI metallodendrimers, compound (**4.6**) did not show any solvent trapping within the dendrimers arms which has been reported to affect elemental analysis. [4-5]

^{1}H NMR spectroscopy afforded a spectrum with broad overlapping multiplets in the aliphatic (δ 2.08-3.61 ppm) and aromatic (δ 7.85-8.96 ppm) regions.

More conclusive results were seen through ^{13}C NMR spectroscopy wherein the imine carbon displayed a downfield shift, thus evidencing back-bonding from palladium to the imine bond upon its coordination to ligand (**4.2**) (**Table 4.5**). Carbon signals assigned to the aromatic carbons occur as broad overlapping signals in the region of *ca* δ 125-156 ppm, while the aliphatic carbons resonate further upfield at *ca* δ 60 and 46 ppm.

Table 4.5 Selected spectroscopic data (^{13}C NMR and FT-IR) for metallodendrimer (**4.6**)[a].

Compound	**^{13}C NMR**		**FT-IR**	
	H**C**=N (ppm)	**Ar** (ppm)	ν(C=N)$_{imine}$ (cm^{-1})	ν(C=N)$_{pyridyl}$ (cm^{-1})
4.6	174.79 (163.09)	125.22-156.71	1625 (1649)	1604 (1596)

[a]Ligand values in parentheses.

There was a wavelength shift of the imine absorption band towards lower wavenumbers as represented in **Table 4.5**, while the pyridyl imine absorption band shifted towards a higher wavelength as has been previously reported for first and second generation polypropyleneimine palladium dendrimers. [4a,c]

*4.5.2 Synthesis and characterization of tris-2-(2-pyridylimine ethyl) amine rhodium dendrimers (**4.7-4.8**)*

Rhodium complexes of the tris-2-(2-pyridylimine ethyl)amine ligand (**4.2**) were obtained by treating ligand (**4.2**) with $[RhCl(CO)_2]_2$ and $[RhCl(COD)]_2$ in DCM and DCM:MeOH (4:1) as outlined in **Scheme 4.2**. Synthesis of metallodendrimer (**4.8**) proceeds *via* formation of an intermediate bearing the chloride counter-ions. Attempts to isolate this species were unsuccessful as this afforded an unstable sticky red product. However, addition of 3 equivalents of $NaPF_6$ 10 minutes into the reaction yielded compound (**4.8**) in a stable form. The rhodium dendrimers were isolated in stable forms as dark purple (**4.7**) and reddish brown powders (**4.8**) in good yields (78% and 65%) respectively.

The metallodendrimers (**4.7** and **4.8**) are soluble in chloroform (**4.7**) and dimethylsulfoxide (DMSO) (**4.7** and **4.8**) and are fairly thermally stable showing decomposition without melting at the onset temperatures of 280 °C and 315 °C respectively.

The structures of these new metallodendrimers (**4.7** and **4.8**) with rhodium-chlorocarbonyl and –COD moieties were established by ^{1}H NMR, ^{13}C NMR and FT-IR spectroscopy, elemental analysis as well as mass spectrometry (^{31}P NMR was also used in the case of (**4.8**)).

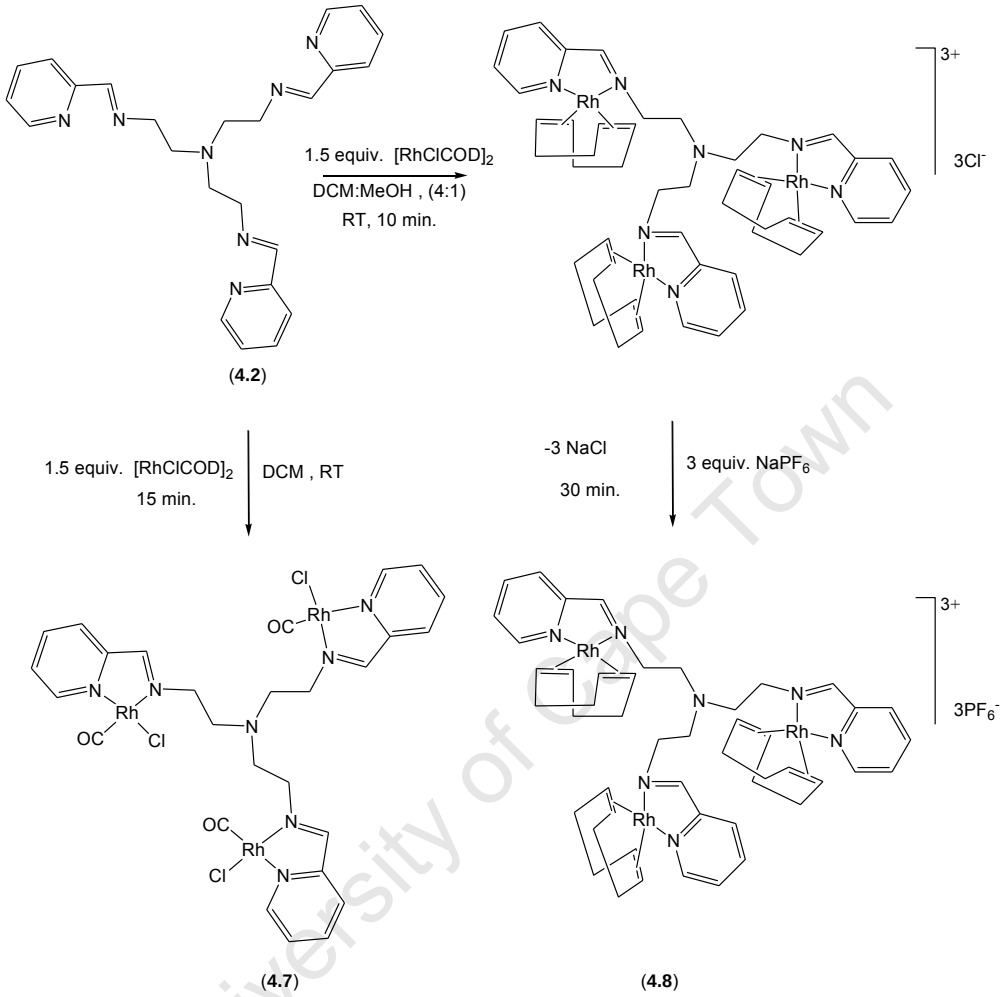

Scheme 4.2. Outline of the preparation of Rh dendrimers (**4.7** and **4.8**).

The ^{1}H NMR spectra of both metallodendrimers were similar to their palladium counterpart, displaying broad overlapping multiplets in the aromatic and aliphatic regions. Additionally, metallodendrimer (**4.8**) gave rise to a broad singlet and multiplet at δ 4.25 and 1.83 ppm (integrating for 12 protons each) for the =C**H** and C**H**$_2$ functionalities of the COD co-ligands. The remaining 12 protons due to the C**H**$_2$ in the COD co-ligands were incorporated in a broad overlapping multiplet ranging from δ 2.08-3.52 ppm.

The ^{13}C NMR spectra of metallodendrimers (**4.7** and **4.8**) displayed all expected signals. For compound (**4.7**), a doublet at *ca* δ 181 ppm for the carbonyl carbon along with a Rh-C coupling of 71.6 Hz was seen (**Fig. 4.2**). There was also a signal of very low intensity at *ca* δ 189 ppm, suggesting the presence of a less favoured isomer under solution NMR conditions. This isomer may be either where the carbonyl co-ligands are *cis* or *trans* to the imine nitrogen. There were downfield shifts of the imine carbon to *ca* δ 165 ppm (**4.7**) and *ca* δ 174 ppm (**4.8**) thus proving coordination of rhodium centres to the dendritic ligand. No noticeable shifts in the signals due to the aromatic and aliphatic carbons were evident, thus they remained in the region of *ca* δ 122-150 ppm and *ca* δ 60-46 ppm respectively.

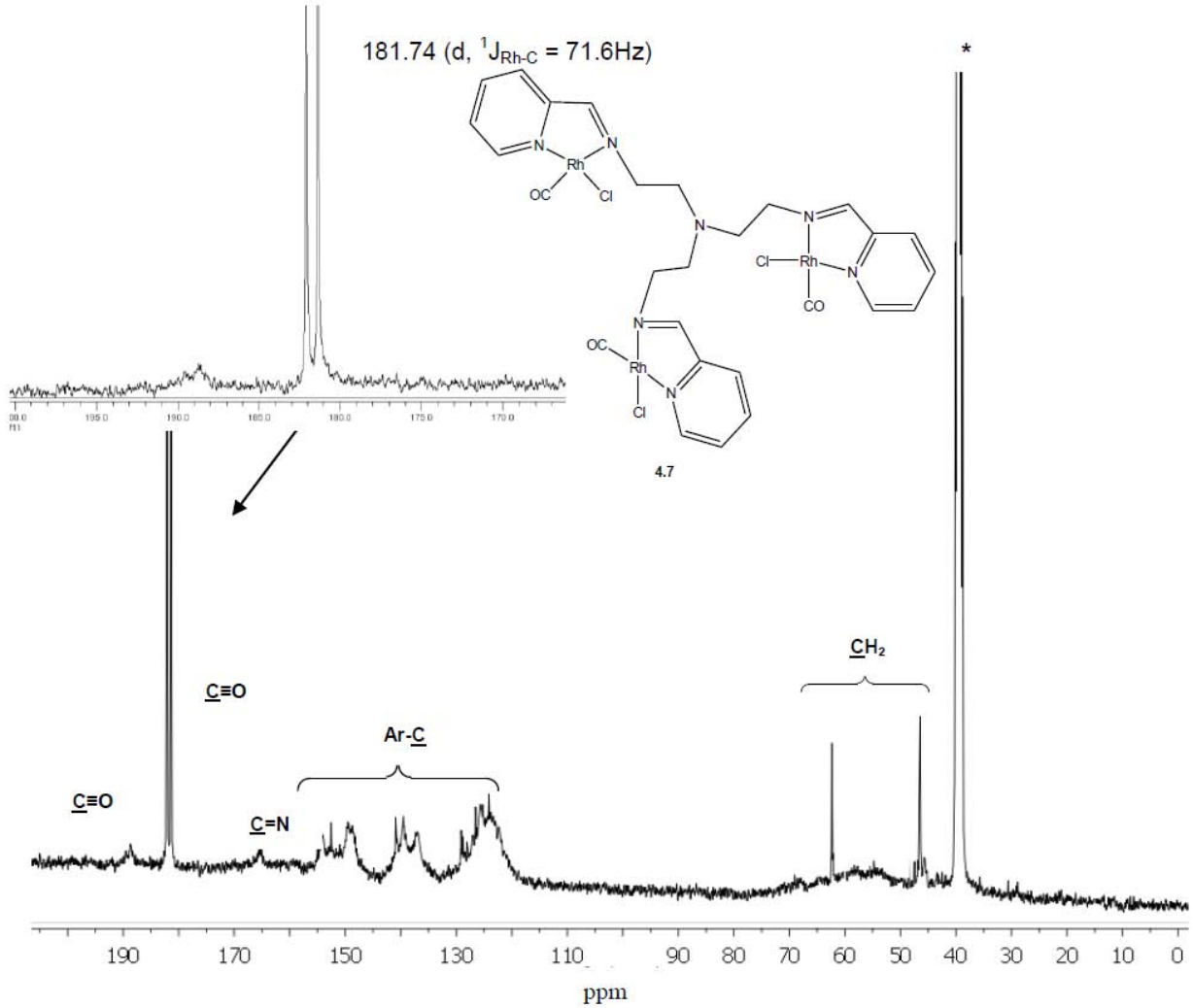

Fig. 4.2. ^{13}C NMR spectrum of rhodium chlorocarbonyl dendrimer (**4.7**) conducted at 25°C (* = DMSO-d_6).

Broad signals due to COD (*ca* δ 83, 30 and 27 ppm) were also observed in the ^{13}C NMR spectrum of metallodendrimer (**4.8**) and its ^{31}P NMR spectrum displayed a septet assigned to the three PF_6^- counter ions at *ca* δ -144 ppm along with P-F coupling of 712 Hz.

The FT-IR spectra of metallodendrimers (**4.7** and **4.8**) clearly displayed absorption peaks at ≈ 1630 cm^{-1} due to the coordinated imine moieties and no absorption at 1649 cm^{-1} for the uncomplexed ligand (**4.2**) (**Fig. 4.3**a-c). Notably, two carbonyl absorption bands were observed in the spectrum for metallodendrimer (**4.7**). This indicates that in the solid state, this compound exists as isomers, where the carbonyl co-ligands (2075 cm^{-1} and 1996 cm^{-1}, **Fig. 4.3**b) are *cis* or *trans* to the imine nitrogen as also seen in ^{13}C NMR experiments.

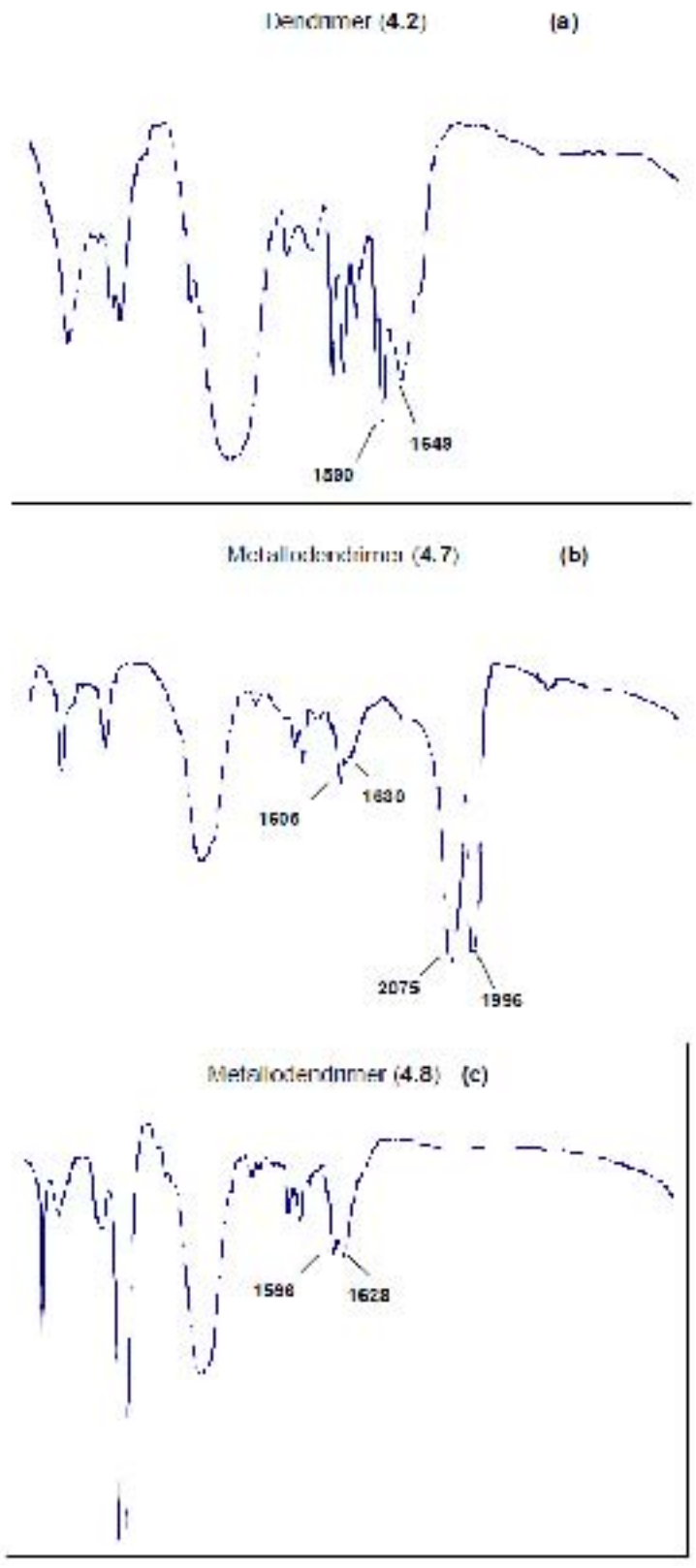

Fig. 4.3. FT-IR spectra of (a) dendrimer (**4.2**); (b) rhodium-chlorocarbonyl dendrimer (**4.7**) and (c) rhodium-COD dendrimer (**4.8**) (all obtained using KBr pellets).

Elemental analyses (C,H, and N) of (**4.7** and **4.8**) corresponded with the calculated values and their mass spectra confirmed the structures of these metallodendrimers through exhibiting $[M\text{-}CO]^+$ (m/z = 889.2) (**4.7**) and $[M\text{-}3PF_6^-]^+$ (m/z = 349.03) ion peaks for compound (**4.8**) (where M = the positively charged complex without the PF_6^- counter ion). The fragmentation pattern of metallodendrimer (**4.7**) followed sequential loss of the carbonyl ligands, this was observed in the mass spectrum of this compound which exhibited $[M\text{-}2CO]^+$ (m/z = 861.2) and $[M\text{-}3CO]^+$ (m/z = 833.2)

4.6 Summary and Conclusions

New Pd^{II} and Rh^{I} low generation pyridylimine metallodendrimers and their precursors have been successfully prepared and characterized using spectroscopic and analytical techniques including: elemental analysis, FT-IR, ^1H NMR, ^{31}P NMR and ^{13}C NMR spectroscopy as well as mass spectrometry. Mononuclear Pd^{II} and Rh^{I} pyridylimine complexes were also prepared and characterized using the above mentioned techniques as well as single X-ray crystallography for complex (**4.3**). These low generation metallodendrimers and the mononuclear complexes constitute the type of systems that can be applied in catalysis. Chapter 6 investigates the efficacy of the Rh^{I} systems in the hydroformylation reaction and comparison of their activity and selectivity against biopolymer-supported catalysts is discussed.

4.7 Experimental

4-Amino benzyl alcohol, 2-pyridinecarboxaldehyde, COD, sodium hexafluorophosphate ($NaPF_6$), sodium tetraphenylborate ($NaBPh_4$) and tris(2-aminoethyl) amine, were purchased from Sigma Aldrich and used as received. All solvents were obtained commercially. [$PdCl_2$] and [$RuCl_3.3H_2O$] were obtained either from Johnson Matthey or Anglo Platinum Coorporation. $[RhCl(CO)_2]_2$ [17a], $[RhCl(COD)]_2$[17b] and $[PdCl_2(COD)]$ [18] were prepared according to literature procedures.

IR spectra were recorded as KBr pellets using either a Bruker Tensor 27 or a Perkin Elmer 100 Spectrum spectrometer. Elemental analyses were conducted with a Fision EA 110 CHNS Analyzer. ^1H, ^{13}C and ^{31}P NMR spectra were recorded on either a Varian XR400 MHz , Varian Mercury XR300 or Bruker Ultrashield 400 Plus spectrometer using tetramethylsilane (TMS) as the internal standard (for ^1H and ^{13}C) and H_3PO_4 as the external standard (for ^{31}P) all at ambient temperature. Melting points were determined using a Kofler hot stage microscope (Riechter Thermo). Electrospray Ionization (ESI) mass spectrometry was carried out at the University of Stellenbosch on a Waters API Quattro Micro triple quadrupole mass spectrometer in the positive-ion mode. Electron Impact mass spectrometry was conducted on an Agilent 6890 N spectrometer. Single crystal X-ray intensity data were collected on a Nonius Kappa-CCD diffractometer using graphites monochromated MoKα radiation. The temperature was controlled by an Oxford Cryostream cooling system (Oxford Cryostat). The strategy for data collections was evaluated using the Bruker Nonius "Collect" program. Data were scaled and reduced using DENZO-SMN software. Absorption corrections were made empirically utilizing the SADABS program. The structure was solved by direct methods and refined using full matrix least-squares with the program SHELXL-97 refining F^2. Packing diagrams were produced using the program PovRay and graphic interface X-seed. All non-H atoms were refined anisotropically.

*4.7.1 Preparation of 4-(2-pyridylimine)benzyl alcohol ligand (**4.1**).*

4-Amino benzyl alcohol (1.000 g, 8.12 mmol) and 2-pyridine-carboxaldehyde (0.869 g, 8.12 mmol) were stirred in MeOH: CH_2Cl_2 (1:2 ratio) for 24 hours in the presence of anhydrous magnesium sulfate. After 24 hours, more anhydrous magnesium

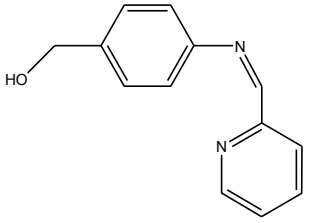

4.1

sulfate was transferred to the stirring solution and this was stirred for a further 15 minutes before filtering. The solvent was removed by rotary evaporation and a concentrated solution of the crude ligand product (in CH_2Cl_2, 5 ml) was loaded onto a silica packed column and eluted with ethyl acetate. After removal of solvent ligand (**4.1**) was dried under vacuum for 12 hours.

Ligand (**4.1**) was obtained as a light brown solid. Yield, (1.537 g, 89%). Mp.: 72-73 ˚C. **FT-IR** (KBr): 3364 (vs) ν(O-H), 1646 (s) $\nu(C{=}N)_{imine}$, 1599 (m) $\nu(C{=}N)_{pyridyl}$, 1506 (s) ν(C=C), 1201 cm^{-1} (s) ν(C-O). **^{1}H NMR** (400 MHz, DMSO-d_6, 25°C): δ (ppm) = 8.73 (m, 1H, **Ar**), 8.69 (s, 1H, C**H**$_{imine}$), 8.13 (m, 1H, **Ar**), 7.87-7.96 (m, 1H, **Ar**), 7.46-7.51 (m, 1H, **Ar**), 7.25-7.38 (m, 4H, **Ar**), 5.15 (m, 1H, O**H**), 4.50 (s, 2H, C**H$_2$**). **^{13}C{H} NMR** (75 MHz, DMSO-d_6, 25°C): δ (ppm) = 160.63 (**C**-$_{imine}$), 154.61, 150.13, 149.65, 141.72, 137.48, 127.87, 126.00, 121.86, 121.37 (**Ar**), 64.70 (**C**H_2). **Elemental Analysis (**calculated for $C_{13}H_{12}N_2O$) (%): C, 73.56; H, 5.70; N 13.20. Found: C, 73.42; H, 5.88, N, 13.64,. **EI-MS**: m/z 210.9 (100% $[M\text{-}H]^+$).

*4.7.2 Preparation of tris-2-(2-pyridylimine ethyl) amine ligand (**4.2**).*

Tris(2-aminoethyl)amine (1.00 g, 5.838 mmol) and 2-pyridinecarboxaldehyde (2.107 g, 20.514 mmol) were refluxed in MeOH (40 ml) in the presence of anhydrous magnesium sulfate for 16 hours, resulting in an orange to brown solution. The solution was filtered by gravity and the solvent was reduced to ≈ 15 ml. Et_2O (20 ml) was added to the concentrated solution and a light brown solid precipitated out. The precipitate was isolated by filtration (suction), washed with Et_2O (30 ml) and dried under vacuum for 4 hours. Ligand (**4.2**) was obtained as a light brown solid. Yield, (1.872, 66%). Mp.: decomp without melting onset occurs at 250 °C. **FT-IR** (KBr): 1649 (s) $\nu(C{=}N)_{imine}$, 1590 (s) $\nu(C{=}N)_{pyridyl}$, 1565 cm^{-1} (s) ν(C=C). **^{1}H NMR** (400 MHz, DMSO-d_6, 25°C): δ (ppm) = 8.57 (br s, 3H, **Ar**), 8.42 (br s, 3H, C**H**-$_{imine}$), 7.79 (br m, 3H, **Ar**), 7.40 (br s, 3H, **Ar**), 7.15 (br m, 3H, **Ar**), 3.42-2.09 (overlapping multipltes, 12H, C**H$_2$**),. **^{13}C{H} NMR** (75 MHz, DMSO-d_6, 25°C): δ (ppm) = 163.09 (**C**-$_{imine}$), 153.21, 149.67, 136.18, 125.85, 121.22 (**Ar**), 58.42, 54.17 (C**H**$_2$). **Elemental Analysis**

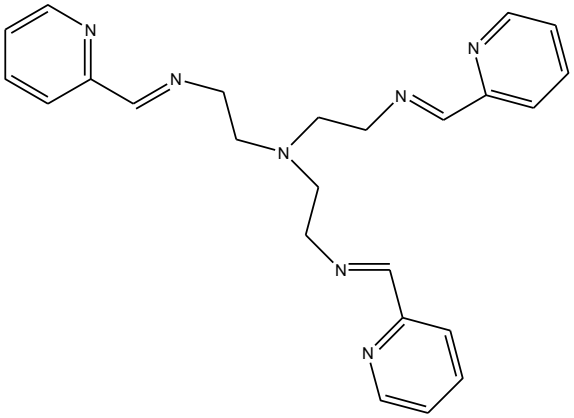

4.2

(calculated for $C_{24}H_{27}N_7$) (%): C, 69.71; H, 6.58; N, 23.71. Found: C, 69.07; H, 6.28; N, 23.35. **EI-MS**: m/z 412.78 (13 % $[M-H]^+$).

*4.7.3 Preparation of 4-(2-pyridylimine) benzyl alcohol palladium(II) complex (**4.3**).*

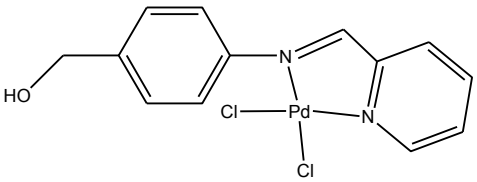

4.3

$[PdCl_2(COD)]$ (0.242 g, 0.848 mmol) in CH_2Cl_2 (15 ml) was added to a solution of 4-(2-pyridylimine)phenylmethanol ligand (**4.1**) (0.180 g, 0.848 mmol) in CH_2Cl_2 (15 ml) and this stirred at room temperature. After 12 hours, the product had precipitated out of solution and was obtained by filtration (suction) as a yellow solid of complex (**4.3**) which was dried under vacuum for 3 hours. Yield, (0.242 g, 73%). Mp : 229-230 ˚C. **FT-IR** (KBr): 3459 (vs) ν(O-H), 1635 (s) $\nu(C=N)_{imine}$, 1614 (m) $\nu(C=N)_{pyridyl}$, 1571 (s) ν(C=C), 1206 cm^{-1} (s) ν(C-O). **^{1}H NMR** (300 MHz, DMSO-d_6, 25°C): δ (ppm) = 9.05 (m, 1H, **Ar**), 8.67 (s, 1H, C**H**-*imine*), 8.28 (m, **Ar**), 8.13 (m, 1H, **Ar**), 7.86 (m, 1H, **Ar**), 7.30-7.38 (m, 4H, **Ar**), 5.25 (br s, 1H, O**H**), 4.56 (s, 2H, C**H_2**). **^{13}C{H} NMR** (75 MHz, DMSO-d_6, 25°C): δ (ppm) = 172.50 (**C**-*imine*), 156.91, 150.43, 146.55, 144.00, 141.68, 129.85, 129.41, 126.42, 124.18, (**Ar**), 62.87 (**C**H_2). **Elemental Analysis** (calculated for $C_{13}H_{12}Cl_2N_2OPd$) (%): C, 40.08; H, 3.10; N, 7.19. Found: C, 40.75; H, 3.41; N, 7.57. **ESI-MS**: m/z 353.03 ($[M-Cl]^+$).

*4.7.4 Preparation of 4-(2-pyridylmine) benzyl alcohol rhodium(I) complex (**4.4**).*

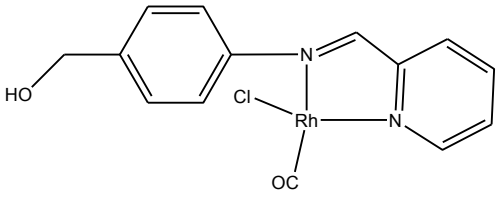

4.4

$[RhCl(CO)_2]_2$ (73 mg, 0.189 mmol) in MeOH (10 ml) was added to a solution of 4-(2-pyridyl imine)phenylmethanol ligand (**4.1**) (80 mg, 0.253 mmol) in CH_2Cl_2 (15 ml) and this stirred at room temperature. After 15 minutes, a dark orange solution had formed. The product was precipitated using cold EtOAc, filtered and washed thoroughly with EtOAc and finally dried under vacuum for 3 hours. Product (**4.4**) was isolated as a dark orange solid. Yield, (60 mg, 84%). Mp.: 178-180 ˚C. **FT-IR** (KBr): 3328 (vs) ν(O-H), 1993 (vs) ν(C≡O), 1626 (s), $\nu(C=N)_{imine}$, 1588 (s) $\nu(C=N)_{pyridyl}$, 1599 (s) ν(C=C), 1203 cm^{-1} (s) ν(C-O). **^{1}H NMR** (400 MHz, DMSO-d_6, 25°C): δ (ppm) = 8.86 (m, 1H, **Ar**),

8.51 (s, 1H, C**H**-*imine*), 8.26 (m, 1H, **Ar**), 8.08 (m, 1H, **Ar**), 7.28-7.71 (br m, 4H, **Ar**), 7.18 (m, 1H, **Ar**), 5.11 (m, 1H, O**H**), 4.22 (m, 2H, C**H$_2$**). **^{13}C{H} NMR** (75 MHz, DMSO-d$_6$, 25°C): δ (ppm) = 180.47 (d, $^1J_{RhC}$ = 70.28 Hz, **C**O), 173.08 (**C**H-*imine*), 166.82, 154.13, 138.22, 129.788, 128.53, 126.78, 123.10, 121.98, 121.64 (**Ar**), 62.20 (**C**H$_2$). **Elemental Analysis (**calculated for $C_{14}H_{13}N_2O_2ClRh$) (%): C, 44.29; H, 3.45; N, 7.38. Found: C, 44.10; H, 3.19; N; 7.60. **ESI$^+$-MS**: m/z 343.8 (51 % [M-Cl]$^+$).

*4.7.5 Preparation of 4-(2-(diphenylphosphino)imine)benzyl alcohol rhodium(I) complex (**4.5**)*

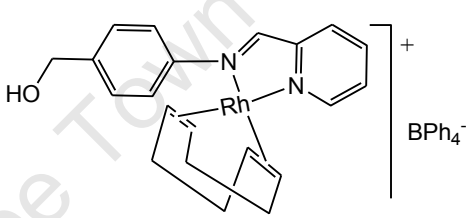

4.5

[RhCl(COD)]$_2$ (0.070 g, 0.141 mmol) was dissolved in CH_2Cl_2 (15 ml) at room temperature. A solution of tris-2-(2-pyridylimine ethyl) amine ligand (**4.2**) in MeOH (10 ml) (0.060 g, 0.253 mmol) was added to the solution dropwise. There was immediate formation of a deep dark red solution. The reaction was stirred for 10 minutes followed by addition of sodium tetraphenyborate ($NaBPh_4$) (0.048 g, 0.141 mmol) in MeOH (5 ml). After stirring for a further 10 minutes, the solution was placed in a freezer (0 °C) for 8 hours during which time the product precipitated out. The deep dark red product (**4.5**) was obtained by filtration (suction), washed with Et_2O (30 ml) and dried under vacuum for 5 hours. Yield, (0.051 g, 49%). Mp.: 110-113 ˚C. **FT-IR** (KBr): 3413 (vs) ν(O-H), 1617 (s) ν(C=N)$_{imine}$, 1591 (s) ν(C=N)$_{pyridyl}$, 1578 (m) ν(C=C), 1299 cm^{-1} (s) ν(C-O). **^{1}H NMR** (300 MHz, DMSO-d$_6$, 25°C): δ (ppm) = 8.70 (s, 1H, **Ar**), 8.31 (s, 1H, C**H**-*imine*), 8.18 (m, 1H, **Ar**), 7.91 (m, 1H, **Ar**), 7.44 (m, 1H, **Ar**), 7.30-6.81 (m, 4H, **Ar**), 7.18, 6.92 (m, 20H, B**Ph$_4$**) 5.26 (s, 1H, O**H**), 4.55 (s, 2H, C**H$_2$**), 4.29 (s, 4H, C**H**-*COD*), 2.43 (br s, 4H, C**H$_2$**-*COD*), 1.95 (m, 4H, C**H$_2$**-*COD*). **^{13}C{H} NMR** (75 MHz, DMSO-d$_6$, 25°C): δ (ppm) = 173.09 (**C**H-*imine*), 163.75-121.28 (**Ar**), 84.63 (**C**H-*COD*), 64.80 (**C**H$_2$-*ligand*) 29.83 (**C**H$_2$-*COD*). **Elemental Analysis (**calculated for $C_{45}H_{44}BN_2ORh$) (%): C, 72.79; H, 5.97; N, 3.77. Found: C, 72.10; H, 3.73; N, 6.13. **ESI-MS**: m/z 441.09 (68% [M-BPh$_4^-$]$^+$) (where M = the positively charged complex without the BPh_4^- counter ion).

4.7.6 Preparation of tris-2-(2-pyridylimine ethyl)amine palladium(II) complex ***(4.6)***

$[PdCl_2(COD)]$ (0.311 g, 1.038 mmol) in acetone (20 ml) was added to a solution of tris-2-(2-pyridylimine ethyl)amine ligand (**4.2**) (0.150 g, 0.363 mmol) in dichloromethane (10 ml). The solution was stirred at room temperature for 24 hours during which time a yellow precipitate formed. The precipitate was isolated by filtration (suction), washed with Et_2O (30 ml) and dried under vacuum for 4 hours. The product (**4.6**) was obtained as an off-yellow powder. Yield, (0.295 g, 86%). Mp.: decomp without melting onset occurs at 291 °C. **FT-IR** (KBr): 1625 (s) $\nu(C{=}N)_{imine}$, 1604 (s) $\nu(C{=}N)_{pyridyl}$, 1570 cm^{-1} (s) $\nu(C{=}C)$. **^{1}H NMR** (400 MHz, DMSO-d_6, 25°C): δ (ppm) = 8.96-7.85 (overlapping multiplets, 15H, **Ar**, C**H**-*imine*), 3.61-2.08 (overlapping multipltes, 12H, C**H$_2$**),. **^{13}C{H} NMR** (75 MHz, DMSO-d_6, 25°C): δ (ppm) = 174. 79 (**C**-*imine*), 156.71, 156.71, 142.12, 128.85, 125.22 (**Ar**), 60.42, 46.39 (**C**H_2). **Elemental Analysis (**calculated for $C_{24}H_{27}Cl_6N_7Pd_3$) (%): C, 30.49; H, 2.88; N,10.37. Found: C, 29.93; H, 2.62; N, 9.96. **ESI-MS**: m/z 905.8 (52% $[M\text{-}Cl]^+$).

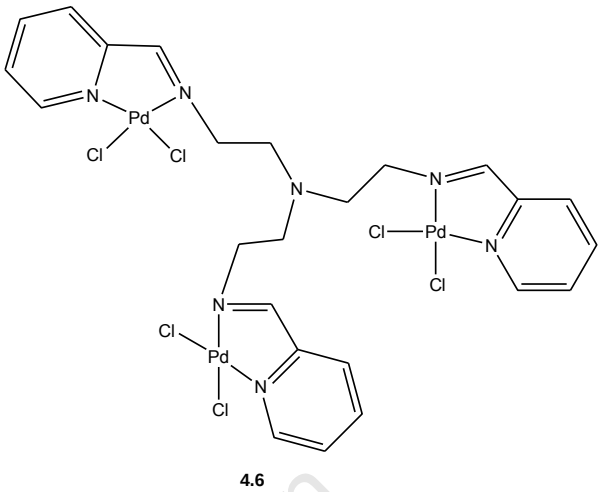

4.6

4.7.7 Preparation of tris-2-(2-pyridylimine ethyl)amine rhodium(I) complex ***(4.7)***

$[RhCl(COD)]_2$ (0.140 g, 0.363 mmol) in dichloromethane (15 ml) was added to a solution of tris-2-(2-pyridylimine ethyl)amine ligand (**4.2)** (0100 g, 0.242 mmol) in dichloromethane (10 ml). There was immediate formation of a dark purple precipitate. The reaction was stirred at room temperature for 15 minutes. The precipitate was isolated by filtration (suction), washed with Et_2O (20 ml) and dried under vacuum for 5 hours. The product (**4.7**) was obtained as a dark purple powder. Yield, (0.173 g, 78%). Mp.: decomp without melting onset occurs at 280 °C. **FT-IR** (KBr): 2075, 1996 (vs) $\nu(C{\equiv}O)$, 1630

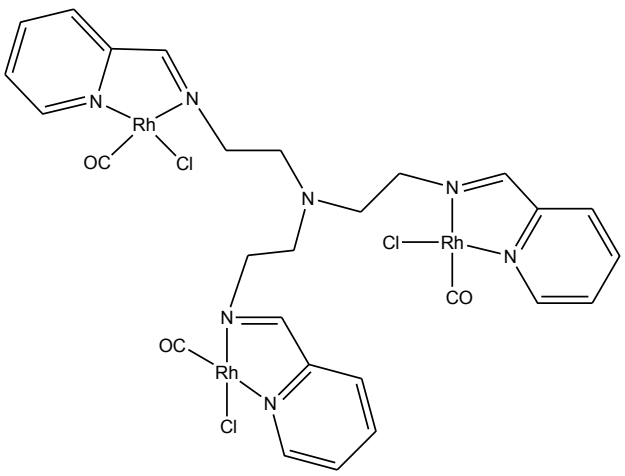

4.7

(s) ν(C=N)$_{imine}$, 1605 (s) ν(C=N)$_{pyridyl}$, 1570 cm^{-1} (m) ν(C=C). **^{1}H NMR** (400 MHz, DMSO-d$_{6,}$ 25°C): δ (ppm) = 8.66-7.06 (overlapping multiplets, 15H, **Ar**, C**H**-$_{imine}$), 3.48-2.06 (overlapping multiplets, 12H, C**H$_2$**),. **^{13}C{H} NMR** (75 MHz, DMSO-d$_{6,}$ 25°C): δ (ppm) = 181.74 (d, ^{1}J $_{Rh-C}$ = 71.6 Hz, **C**O), 165.65 (**C**-$_{imine}$), 154.61-122.02 (**Ar**), 62.33, 46.45 (**C**H$_2$). **Elemental Analysis (**calculated for $C_{27}H_{27}Cl_3N_7O_3Rh_3$) (%): C, 35.53; H, 2.98; N, 10.74. Found: C, 35.35; H, 2.85; N, 10.18. **ESI-MS**: m/z 889.2 (96% [M-CO]$^{+}$).

*4.7.8 Preparation of tris-2-(2-pyridylimine ethyl)amine rhodium(I) complex **(4.8)***

[RhCl(COD)]$_2$ (0.089 g, 0.182 mmol) in dichloromethane (10 ml) was added to a solution of tris-2-(2-pyridylimine ethyl)amine ligand (**4.2**) (0.050 g, 0.121 mmol) in dichloromethane (10 ml). There was an immediate formation of a dark red solution which was stirred at room temperature for 10 minutes. Sodium hexafluorophosphate ($NaPF_6$) (0.020 g, 0.121 mmol) in MeOH (5 ml) was added dropwise to the solution. A reddish brown precipitate formed immediately and the mixture was stirred for a further 30 minutes. The precipitate was isolated by filtration (suction), washed with Et_2O (30 ml) and dried under vacuum for 4 hours. The product (**4.8**) was obtained as a reddish brown powder. Yield, (0.116, 65%). Mp.: decomp without melting onset occurs at 315 °C. **FT-IR** (KBr): 1628 (s) ν(C=N)$_{imine}$, 1596 (s) ν(C=N)$_{pyridyl}$, 1572 cm^{-1} (s) ν(C=C). **^{1}H NMR** (300 MHz, DMSO-d$_{6,}$ 25°C): δ (ppm) = 8.91-7.16 (overlapping multiplets, 15H, **Ar**, C**H**-$_{imine}$), 4.25 (br s, 12H, C**H**$_{COD}$) 3.52-2.08 (overlapping multipltes, 24H, C**H$_{2}$**$_{amine\ core}$ C**H$_{2}$**$_{COD}$), 1.83 (m, 12H, C**H$_{2}$**$_{COD}$). **^{13}C{H} NMR** (75 MHz, DMSO-d$_{6,}$ 25°C): δ (ppm) = 174. 90 (**C**-$_{imine}$), 150.3-122.67 (**Ar**), 83.73 (**C**H$_{COD}$) 60.42, 46.39 (**C**H$_{2\ amine\ core}$) 30.24, 27.42 (**C**H$_{2COD}$). **^{31}P{H} NMR** (121 MHz, DMSO-d$_{6,}$ 25°C): δ (ppm) = -144.24 (sept, $^{1}J_{P-F}$ = 712 Hz). **Elemental Analysis (**calculated for $C_{48}H_{63}F_{18}N_7P_3Rh_3$) (%): C, 38.91; H, 4.29; N, 6.62. Found: C, 38.69; H, 4.22; N, 6.65. **ESI-MS**: m/z 349.03 (33% [M-3PF$_6^-$]$^{+}$) (where M = the positively charged complex without the PF_6^- counter ion).

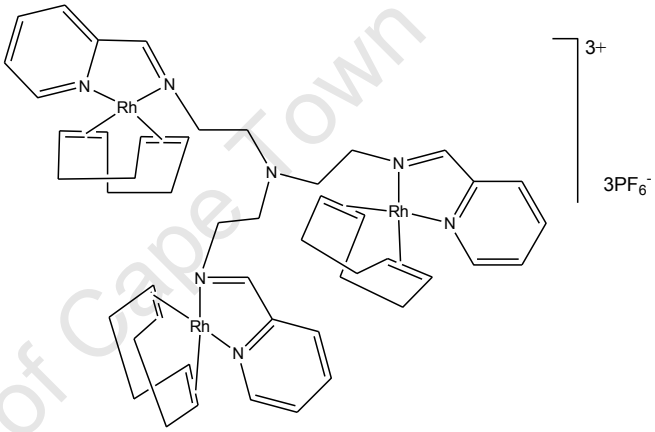

4.8

4.8 References

1. (a) Q. Han, Q-L. Li, J. He, B. Hu, H. Tan, Z. Abliz, C-H. Wang, Y. Yu, H-B. Yang, *J. Org. Chem., (***2011**), 76, 9660. (b) T. Yi-Hsuan, Y-T.H. Adela, C. Po-Yu, C. Hui-Ting, K. Chai-Lin, *Current Pharmaceutical Design,* (**2011**), 17, 2308. (c) W.A. Hoffert, A.K. Rappè, M.P. Shores*, J. Am. Chem. Soc.,* (**2011**), 133. 20823. (d) J-L. Wang, X. Li, C.D. Shreiner, X. Lu, C.N. Moorefield, S.R. Tummalapalli, D.A. Medvetz, M.J. Panzner, F.R. Fronczek, C. Wesdemoitis, G.R. Newkome, *New J. Chem.,* (**2012**), 36, 484. (e) F. Corana, M. Monge, E. Sánchez-Forcada, *Inorg. Chim. Acta,* (**2012**), 380, 31. (f) E.J. Juárez-Pèrez, C. Viñas, F. Teixidor, R. Santillan, N. Farfán, A. Abreu, R. Yèpez, R. Núñez, *Macromol.,* (**2010**), 43, 150. (g) S. Dietrich, S. Schulze, M. Hietschold, H. Lang, *J. Colloidal Interface Science,* (**2011**), 359, 454. (h) T. Ahamad, S.F. Mapolie, S.M. Alshehri, *Med Chem. Res.,* (**2010**), 138, 171. (i) P. Govender, A.K. Renfrew, C.M. Clavel, P.J. Dyson, B. Therrien, G.S. Smith, *Dalton Trans.,* (**2011**), 40, 1158. (j) C.G. Hartinger, P.J. Dyson, *Chem. Soc. Rev.*, (**2009**), 38, 391. (k) M.A. Mintzer, M.W. Grinstaff, *Chem. Soc. Rev.,* (**2011**), 40, 173. (l) D. Astruc, E. Boisselier, C. Ornelas, *Chem. Rev.,* (**2010**), 110, 1857.
2. (a) G.R. Whittell, I. Manners, *Adv, Mater*., (**2007**), 19, 3439. (b) J-C. Eloi, L. Chabanne, G.R. Whittell, I. Manners, *Materials Today*, (**2008**), 11, 28.
3. X. Wang, R. McHale *Macromol. Rapid Commun.,* (**2010**), 31, 331.
4. (a) G. Smith, R. Chen, S. Mapolie, *J. Organomet. Chem.,* **(2003**), 673, 111. (b) R. Malgas, S.F. Mapolie, S.O Ojwach, G.S. Smith, J. Darkw*a, Catal. Commun.,* **(2008**), 9, 1612. (c) G.S. Smith, S.F. Mapolie, *J. Mol. Cat. A: Chem.,* **(2004**), 213, 187. (d) T. Ahamad, S.M. Alshehri, *Catal. Lett.,* (**2010**), 138, 171. (e) P. Govender, N.C. Antonels, J Mattsson, A.K. Renfrew, P.J. Dyson, J.R Moss, B. Therrien, G.S. Smith, *J. Organomet. Chem.,* (**2009**), 694, 3470. (f) D.E. Bergbreiter, J. Tian, C. Hongfa, *Chem. Rev.,* (**2009**), 109, 530.
5. N.C. Antonels, B. Therrien, J.R. Moss, G.S. Smith*, Inorg. Chem. Commun.,* (**2009**), 12, 716.
6. (a) B. Blom, M.J. Overett, R. Meijboom, J.R. Moss, *Inorg. Chim. Acta,* (**2005**), 358, 3491. (b) M.A. Hearshaw, J.R. Moss, *Chem. Commun.,* (**1999**), 1.
7. D. De Groot, P.G. Emmerink, C. Coucke, J.N.H. Reek, P.C.J. Kamer, P.W.N.M. van Leeuwen, *Inorg. Chem. Commun.,* (**2000**), 3, 711.
8. S.C. Bourgu, H. Alper, L.E. Manzer, P. Arya, *J. Am. Chem. Soc.,* (**2000**), 122, 956.

9. T. Fujihara, Y. Obora, M. Tokunaga, H. Sato, Y. Tsuji, *Chem. Commun.*, (**2005**), 4526.
10. N.C. Antonels, J.R. Moss, G.S. Smith, *J. Organomet. Chem.,* (**2011**), 696, 2003.
11. (a) A. Bacchi, M. Carcelli, T. Chido, G. Cantoni, C. De Filippo, S. Pipolo, *Cryst. Eng. Comm.,* (**2009**), 11, 1433. (b) The mass spectrum of ligand (**4.1**) is given in the **Appendix: Section h (Fig. d)**.
12. K.R. Reddy, W-W. Tsai, K. Surekha, G-H. Lee, S-M. Peng, J-T. Chen, *J. Chem. Soc. Dalton Trans.,* (**2002**), 1776.
13. (a) J. Flapper, H. Kooijman, M. Lutz, A.L. Spek, P.W.N.M. Leeuwen, C.J. Elsevier, P.C.J. Kamer, *Organometallics*, (**2009**), 28, 1180. (b) P. Crochet, J. Gimeno, J. Borge, S. Garcia-Granda, *New J. Chem.,* (**2003**), 27, 414. (c) A.D. Zotto, W. Baratta, M. Ballico, E. Herdtweck, P. Rigo, *Organometallics,* (**2007**), 26, 5636. (d) P. Bhattacharyya, M.L. Loza, J. Parr, M.Z. Slawin, *J. Chem. Soc. Dalton Trans.,* (**1999**), 2917. (e) O. Daugulis, M. Brookhart, *Organometallics,* (**2003**), 21, 5926. (f) Summary of data collection and CIF file for the single crystal X-ray structure of complex **4.3** is given in the **Appendix: Section h (Tables b)**.
14. (a) W. Solodenko, C. Bronchwitz, R. Wartchow, Md. A. Hashem, K.M. Dawood, M. Vaultier, A. Kirschning, *Molecular Diversity*, (**2005**), 9, 333. (b) D.J. Tempel, L.K. Johnson, R.L. Huff, P.S. White, M. Brookhart, *J. Am. Chem. Soc.,* (**2000**), 122, 6686.
15. L. Gonsalvi, J.A. Gaunt, H. Adams, A. Castro, G.J. Sunley, A. Haynes, *Organometallics,* (**2003**), 22, 1047.
16. J. Best, J.M. Wilson, H. Adams, L. Gonsalvi, M. Peruzzini, A. Haynes, *Organometallics,* (**2007**), 26, 1960.
17. (a) A.J. Deeming, P.J. Sharratt, *J. Organomet. Chem*., (**1975**), 99, 447. (b) G. Giordano, R.H. Crabtree, *Inorg. Synth*., (**1979**), 19, 218.
18. C.T. Bailey, G.C. Linsesky, *J. Chem. Edu.,* (**1985**), 62, 896.

Chapter 5

Catalytic studies using metallodendrimers: *Hydroformylation reactions*

5.1 Introduction

Rhodium-catalysed hydroformylation is one of the most important industrial processes involving the use of a homogeneous catalyst. [1] As mentioned in Chapter 3 (**section 3.4**), catalysts containing rhodium are more stable than cobalt during hydroformylation reactions and operate under milder reaction conditions.

However, the use of homogeneous catalysts presents the challenge of separating the catalyst/product mixture after the reaction. Separation of catalyst/product mixture by distillation is known but is costly and not viable especially in an industrial context. [1-2] Some of the ways of overcoming the separation challenge include using aqueous biphasic conditions or anchoring the catalyst precursor on a support.

Dendrimers are suitable supports for homogeneous catalysts and can be recovered by ultra- or nanofiltration methods. [2-5] In addition, the dendrimers play a stabilising role for the catalyst precursor which can impact positively on its life-time. Dendrimers also provide a high local concentration of metal which in turn can enhance activity and reaction rates. [3,6-7]

The current chapter discusses the evaluation of trinuclear pyridylimine metallodendrimers and mononuclear pyridylimine complexes as catalyst precursors for 1-octene hydroformylation.

5.2 Hydroformylation reactions

The trinuclear pyridylimine metallodendrimers (**4.7** and **4.8**) and pyridylimine rhodium(I) complexes (**4.4** and **4.5**) (**Fig. 5.1**) were employed as catalyst precursors in the hydroformylation reaction of 1-octene at 55-95 °C and 5-30 bars of syngas pressure ($CO:H_2$ = 1:1) in toluene (10 ml). A minimal amount of 2.87 x 10^{-4} mol% (metal) of each catalyst precursor (**4.4**-**4.5**) and (**4.7**-**4.8**) was used (catalyst:substrate = 1:2500) (**Scheme 5.1**).

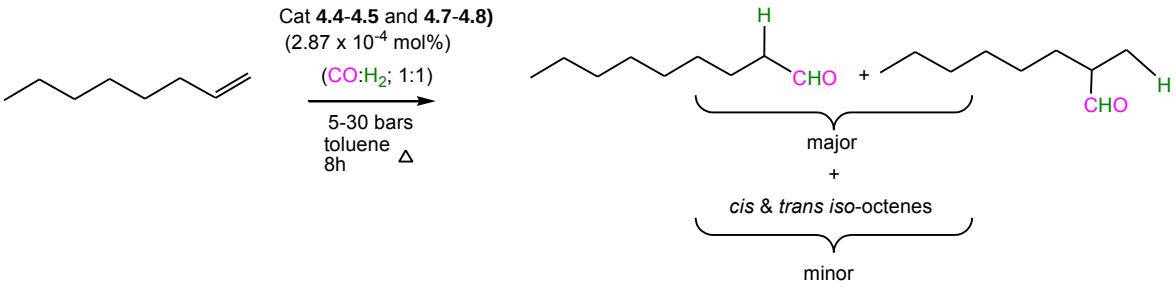

Scheme 5.1. Outline for the hydroformylation reactions carried out using catalysts (**4.4-4.5**) and (**4.7-4.8**).

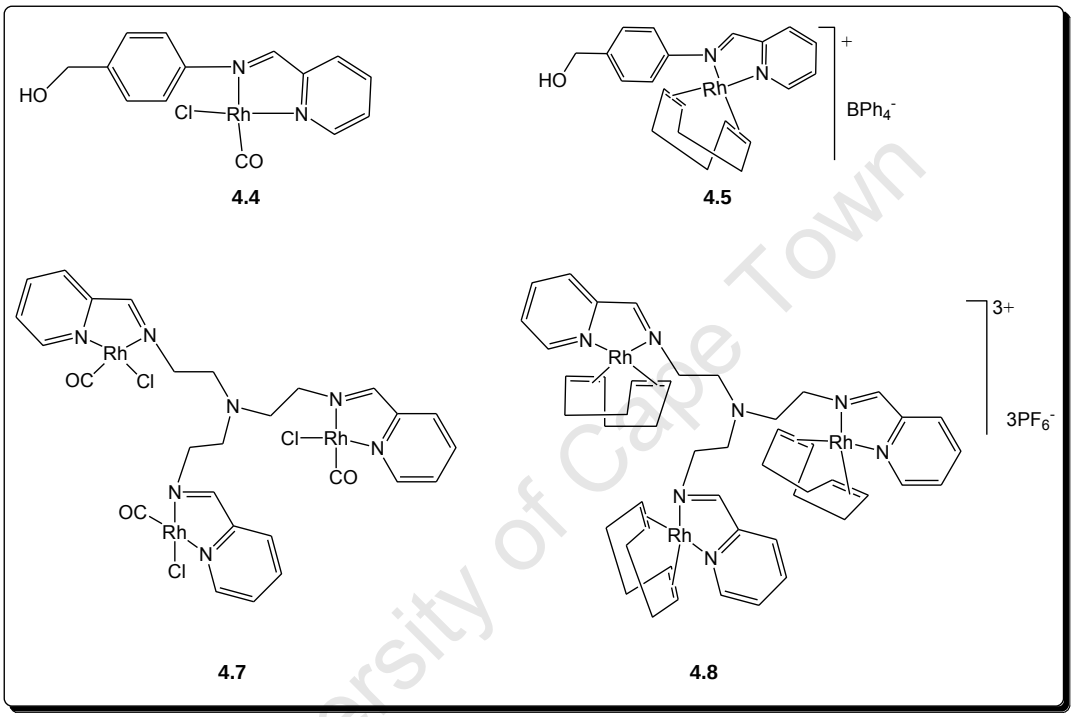

Fig. 5.1. Catalyst precursors employed in hydroformylation reactions (**4.4-4.5**) and (**4.7-4.8**).

In general, conversions of 1-octene were good (71-100%) and in some instances moderate (50-70%). Near quantitative conversion of 1-octene was observed after 8 hours with slight differences in catalytic rates seen in the first 4 hours (**Fig. 5.2**). In the first 4 hours, the COD-based systems (**4.5** and **4.8**) displayed slightly inferior conversions to their chlorocarbonyl counterparts (**4.4** and **4.7**). This suggests that the COD-based systems take a longer period to generate the active species as compared to the catalyst precursors (**4.4** and **4.7**) already bearing CO on the active site.

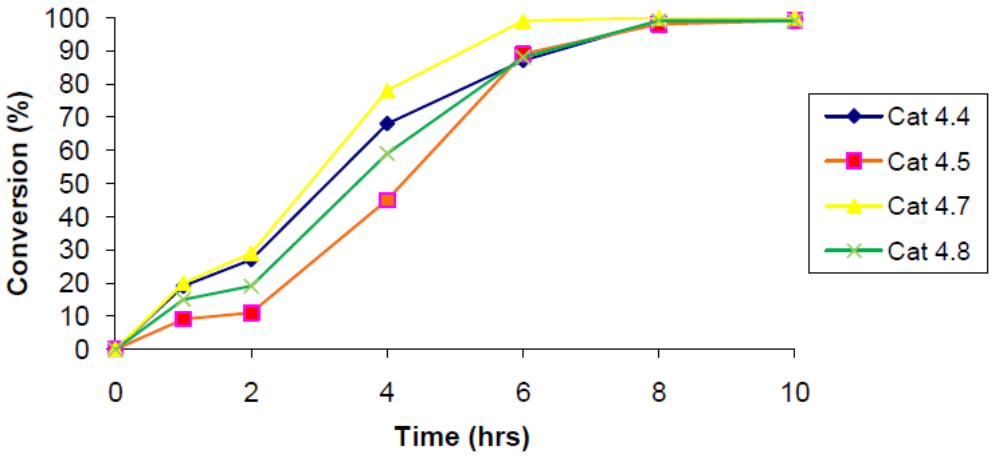

Fig. 5.2. Percentage conversion of 1-octene over 8 hours using catalysts (**4.4**-**4.5**) and (**4.7**-**4.8**), data collected at 75 °C and 30 bars. (Average error estimate: (**4.4**) = ± 0.11; (**4.5**) = ± 0.18; (**4.7**) = ± 0.11 and (**4.8**) = ± 0.10).

5.2.1 Effect of pressure

When the reactions were carried out at 5 bars (75 °C), good to moderate conversion of 1-octene was observed (51 to 98%). The products constituted mostly *iso*-octenes (*cis* and *trans* 2- and 3-octenes) (**Fig. 5.3 a**). At 10 bars (75 °C), conversion of 1-octene increased to 67-99% with the metallodendrimers (**4.7** and **4.8**) displaying the best conversion of 99% and 98% respectively. The chlorocarbonyl-based systems (**4.5** and **4.7**) exhibited better selectivity for aldehydes than the COD-based systems (**4.5** and **4.8**) (**Fig. 5.3 b**). Excellent conversion and chemoselectivity was seen at 30 bars syngas pressure as has previously been seen with Rh^{I} systems (**Fig. 5.3 c**). [3,8] At this pressure, the best regioselectivity for nonanal was observed (**Fig. 5.3 c**), thus all subsequent reactions were carried out at 30 bars syngas pressure.

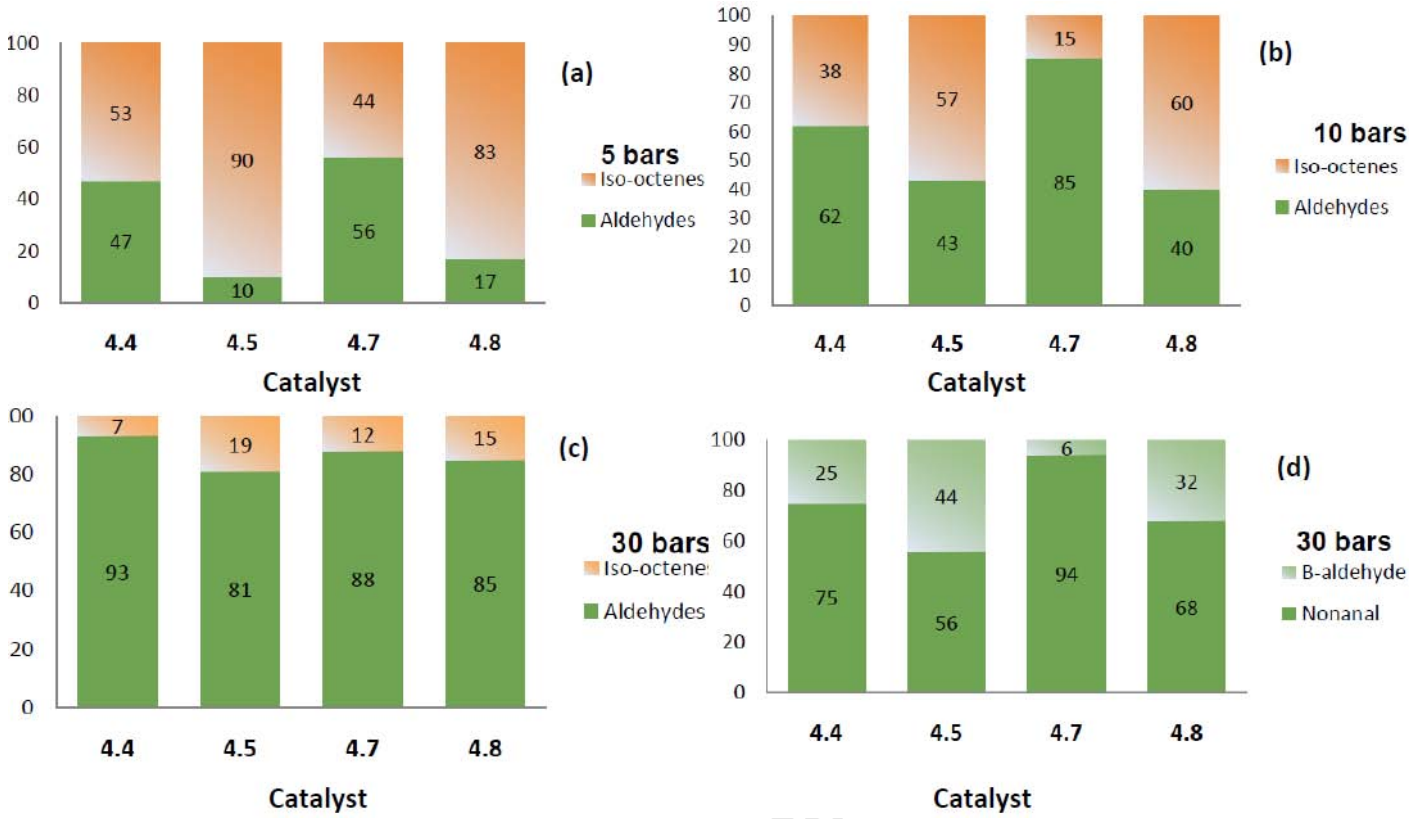

Fig. 5.3. Effect of pressure on chemo- and regioselectivity in hydroformylation of 1-octene using catalysts (**4.4**-**4.5**) and (**4.7**-**4.8**) at 75 °C and: (a) 5 bars, (b) 10 bars and (c-d) 30 bars. (Average error estimate: (**4.4**) = ± 0.11; (**4.5**) = ± 0.16; (**4.7**) = ± 0.10 and (**4.8**) = ± 0.11).

5.2.2 Effect of temperature

Temperature variation studies were conducted at 55, 75 and 95 °C. Lower temperature (55 °C, 30 bars) saw minimal conversion of 1-octene to largely *iso*-octenes and almost exclusively, so in the case of reactions carried out using catalyst precursors (**4.5** and **4.8**) (**Fig. 5.4 a**). There was a marked increase in conversion of 1-octene (94-99%) when operating at 95 °C and 30 bars syngas pressure. Moreover, 1-octene was converted almost quantitatively to aldehyde products (**Fig. 5.4 b**). Similarly, at 75 °C (30 bars) conversion to mostly the desired aldehyde was seen (*vide ante* **Fig. 5.3c**). Therefore, 75 °C and 95 °C were established as the optimum operating temperatures to operate at depending on the type of aldehyde (linear or branched) desired when using catalyst precursors (**4.4**-**4.5**) and (**4.7**-**4.8**). (*vide ante* **Fig. 5.3 d** and *vide infra* **Fig. 5.5**).

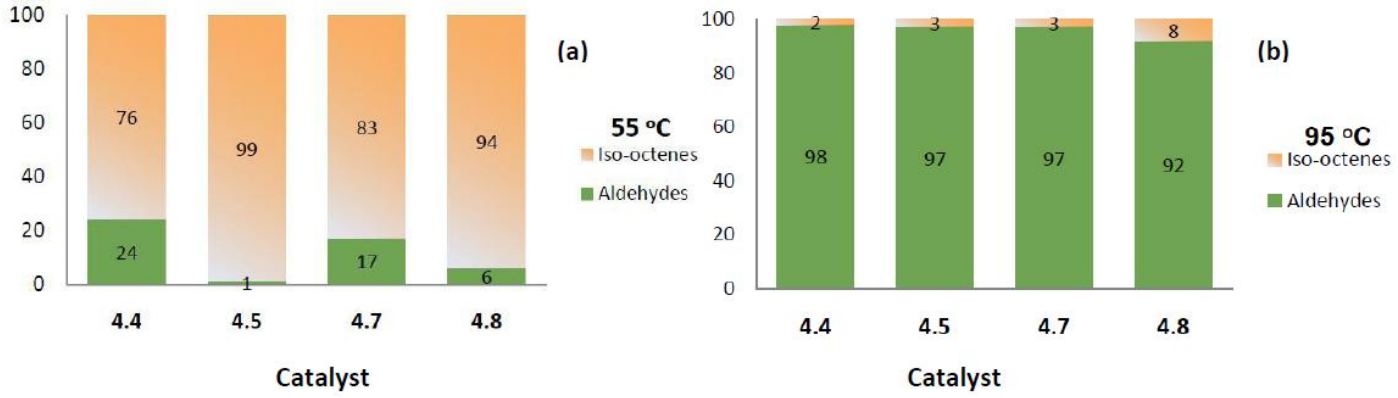

Fig. 5.4. Effect of temperature on chemoselectivity in hydroformylation of 1-octene using catalysts (**4.4**-**4.5**) and (**4.7**-**4.8**) at 30 bars and : (a) 55 °C and (b) 95 °C. (Average error estimate: (**4.4**) = ± 0.10; (**4.5**) = ± 0.14; (**4.7**) = ± 0.12 and (**4.8**) = ± 0.11).

5.2.3 Chemoselectivity, regioselectivity and turnover frequency (TOF.h^{-1}).

Overall, catalyst precursors (**4.4**-**4.5**) and (**4.7**-**4.8**) favoured the formation of *iso*-octenes at low temperature (55 °C) and pressures (5 and 10 bars) as has been previously seen with other Rh^{I} systems (Chapter 3, Section 3.4). At the optimal temperatures (75 and 95 °C) and pressure (30 bars), the catalyst precursors displayed the best chemoselectivities towards aldehydes (*vide ante* **Fig 5.3c**; **Fig. 5.4 b**) (55-98%). Careful investigations indicated that the linear aldehyde (nonanal) was favoured at 75°C with the chlorocarbonyl-based systems (**4.4** and **4.7**) displaying superior selectivity in this regard (75 and 94% respectively) (*vide ante* **Fig 5.3d**). Notably, regioselectivity for nonanal tends to improve on moving from mononuclear to dendritic catalyst precursor. This phenomenon suggests that the dendrimer may provide a favourable microenvironment for the catalytically active rhodium that drives selectivity towards nonanal. [9] Conversely, branched aldehydes were favoured at 95 °C (30 bars) (**Fig. 5.5**). It is known that isomerization is dominant at higher temperatures, therefore this implies that branched aldehydes are formed *via iso*-octenes. [8,10-11] The dendritic support appears to stabilize both COD- and chlorocarbonyl-based systems (**4.7** and **4.8**) since reactions carried out at 95°C (30 bars) using mononuclear catalyst precursors (**4.4** and **4.5**) afforded black solution due to catalyst decomposition after 8 hours. No such black solution was formed when the metallodendrimer catalyst precursors (**4.7** and **4.8**) were employed. This reaffirms the stabilizing role of the dendritic scaffold.

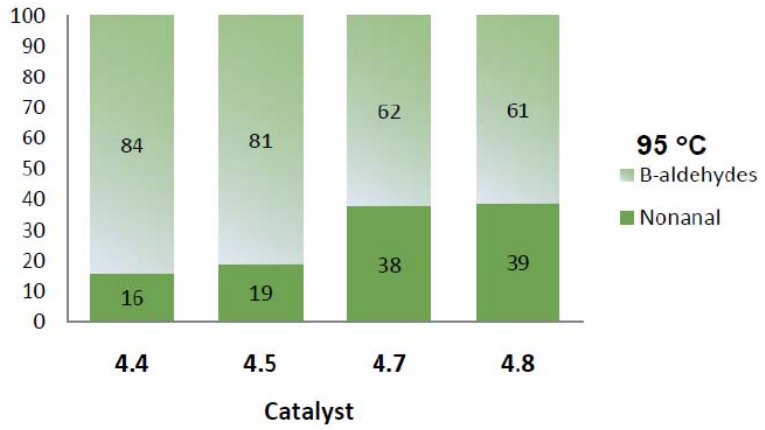

Fig. 5.5. Regioselectivity in hydroformylation of 1-octene using catalysts (**4.4**-**4.5**) and (**4.7**-**4.8**) all at 30 bars and 95 °C. (Average error estimate: (**4.4**) = ± 0.10; (**4.5**) = ± 0.14; (**4.7**) = ± 0.12 and (**4.8**) = ± 0.11).

The Rh^{I} catalyst precursors showed good TOF (where TOF = ($mol_{product}/mol_{catalyst}$ x h^{-1}) values with activities observed in the range of 200-338 h^{-1} (at 75 °C, 30 bars) and 334-356 h^{-1} (at 95°C, 30 bars) (**Fig. 5.6 a** and **b**). The key factors to consider in interpreting TOF are steric bulk of the catalyst precursor or active species stability. At 75 °C and 30 bars syngas pressure, the mononuclear catalyst precursors (**4.4** and **4.5**) exhibited better TOF values while the metallodendrimers (**4.7** and **4.8**) gave slightly lower TOFs. Although the dendritic scaffold may play a stabilizing role under hydroformylation conditions, these observations suggest that the pendant hydroxyl group on (**4.4** and **4.5**) stabilizes the active species to a slightly greater extent. This subsequently results in increased stability, a feature which assists in preventing catalyst deactivation. Furthermore, poor accessibility of the substrate to the active rhodium centres may be induced by the bulky dendritic scaffold thus slightly hampering hydroformylation. The current catalyst precursors (with the exception of (**4.8**)) outperform the common hydroformylation catalyst precursor [Rh(acac)$(CO)_2$] which gave a TOF of 209 h^{-1} under similar conditions. [3]

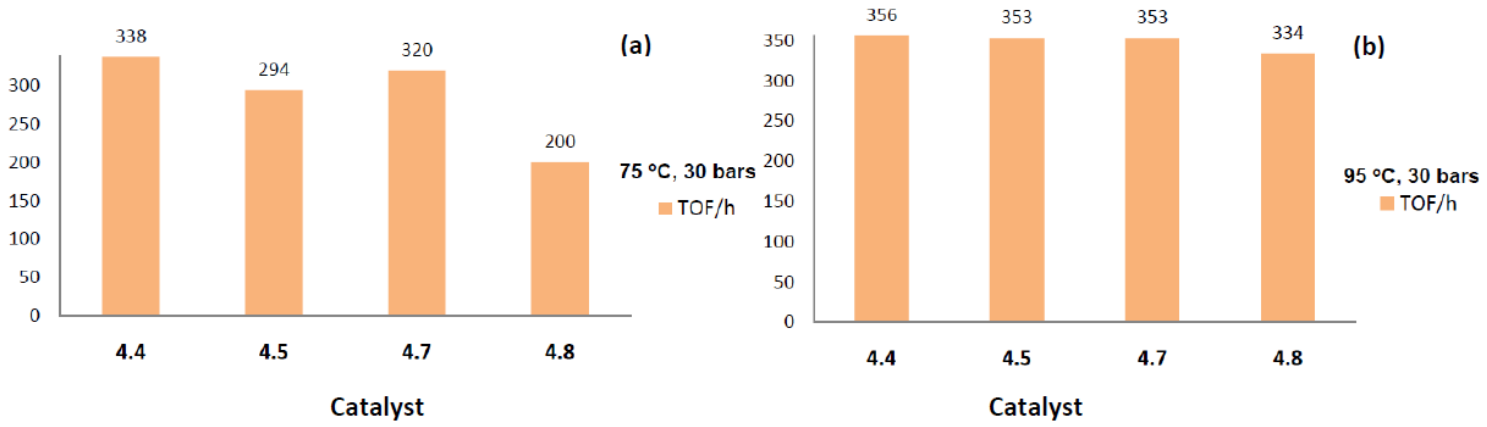

Fig. 5.6. TOF for the Rh^{I} catalyst precursors (**4.4**-**4.5**) and (**4.7**-**4.8**) all at 30 bars and : (a) 75 °C and (b) 95°C.) (TOFs are calculated based on total aldehyde products formed). (Average error estimate: (**4.4**) = ± 0.10; (**4.5**) = ± 0.14; (**4.7**) = ± 0.12 and (**4.8**) = ± 0.11).

5.3 Summary

The Rh^{I} catalyst precursors (**4.4**-**4.5**) and (**4.7**-**4.8**) are active in the hydroformylation of 1-octene under mild conditions (75 or 95 °C and 30 bars). The activities and selectivities of these catalyst precursors were affected by temperature and pressure, with lower temperature and pressures yielding more of the *iso*-octene fractions. Good selectivity for aldehydes was achieved at 75 or 95 °C and 30 bars syngas pressure. Based on these studies, the temperature can be varied to either 75 °C in order to obtain more nonanal or to 95 °C to obtain more branched aldehydes. The chlorocarbonyl-based systems (**4.4** and **4.7**) exhibited the best activity (TOFs), chemoselectivity and regioselectivity in comparison to COD-based systems (**4.5** and **4.8**).

5.4 Experimental

Catalysis products were analyzed using a Varian 3800 GC.

5.4.1 General procedure for the hydroformylation reactions

Hydroformylation reactions were conducted in a 90 ml stainless steel autoclave. The autoclave was charged with toluene (10 ml), 1-octene (715 mg, 6.37 mmol), *n*-decane internal standard (180 mg, 1.26 mmol) and either of the Rh catalyst precursors (**4.4**, **4.5**, **4.7** or **4.8**) (2.87 x 10^{-3} mmol, substrate: Rh ratio = 2500:1). The autoclave was flushed three times with syngas ($CO:H_2$, 1:1 ratio) followed by pressurizing and heating to the desired syngas pressure and temperature respectively. Samples were taken every 2 hours and analyzed using gas chromatography (GC). The products were confirmed in relation to authentic *iso*-octenes and aldehydes.

5.5 References

1. (a) C.W Kohlpaintner, R.W. Fischer, B. Cornils, *Appl. Catal. A: General,* (**2001**), 221, 212. (b) B. Cornils, W.A. Herrmann, *Aqueous-Phase Organometallic Catalysis, 2nd Ed.* Chapter 4, Wiley-VCH, Verlag GmbH and Co., Weinheim, 2004, pp 244.
2. N.J. Ronde, D. Vogt, *Catalyst Separation, Recovery and Recycling, Chemistry and Process Design*, Springer Ed., Dordrecht, Netherlands, 2006, pp 1-37.
3. N.C. Antonels, J.R. Moss, G.S. Smith, *J. Organomet. Chem*., (**2011**), 696, 2003.
4. A.V. Gaikwad, V.Boffa, J.E. ten Elshof, G. Rothenberg, *Angew. Chem. Int. Ed.,* (**2008**), 47, 5407.
5. (a) D. De Groot, B.F.M. de Waal, J.N.H. Reek, A.P.H.J. Schenning, P.C.J. Kamer, E.W. Meijer, P.W.N.M. van Leeuwen, *J. Am. Chem. Soc.,* (**2001**), 123, 8453. (b) R. Van Heerbeek, P.C.J. Kamer, P.W.N.M. van Leeuwen, J.N.H. Reek, *Chem. Rev.,* (**2002**), 102, 3717.
6. (a) G.S. Smith, R. Chen, S. Mapolie*, J. Organomet. Chem.,* (**2003**), 673, 111. (b) G.S. Smith, S.F. Mapolie*, J. Mol. Catal. A: Chem.,* (**2004**), 213, 187.
7. R. Malgas, S.F. Mapolie, S.O. Ojwach, G.S. Smith, J. Darkwa*, Catal. Commun.,* (**2008**), 9, 1612.
8. B.C.E. Makhubela, G.S. Smith, A. Jardine, *Green Chem.,* (**2012**), 14, 338.
9. (a) M.T. Zarka, M. Bortenschlager, K. Wurst, O. Nuyken, R. Weberskirch, *Organometallics,* (**2004**), 23, 4817. (b) D. Cauzzi, M. Costa, L. Gonsalvi, M.A. Pellinghelli, G. Predieri, A. Tiripicchio, R. Zanoni, *J. Organomet. Chem.,* (**1997**), 547, 377.
10. A.A. Dabbawala, H.C. Bajaj, H. Bricout, E. Monflier, *Applied Catal. A: General,* (**2012**), 414, 273.
11. S-Y. Yun, M.J. Seong, J-H. Yim, Y.S. Ko, Y.K. Park, J-K. Jeon, *Rev. Adv. Mater. Sci.,* (**2011**), 28, 154.

Chapter 6

Overall Summary and Conclusions

The main objective was to prepare new biopolymer- and dendrimer-supported transition metal complexes. These would contribute to the development the field of organometallics and material science. Furthermore, these materials constitute the type of systems which can be applied in catalysis.

A number of new chitosan-supported iminopyridyl and iminophosphine ligands were prepared. These supported-Schiff base ligands were synthesized by functionalizing commercially available chitosan and modified 6-deoxy-6-amino chitosan *via* the Schiff base condensation reaction of either 2-pyridinecarboxaldehyde or 2-(diphenylphosphino)benzaldehyde with the surface accessible amino groups on the chitosan. This afforded chitosan and 6-deoxy-6-amino chitosan functionalized with iminopyridyl and iminophosphine moieties on the surface with ≈ 0.1 mmol/g loading.

Complexation reactions using either $[PdCl_2(COD)]$ or $[RhCl(CO)_2]_2$ produced the corresponding chitosan-supported complexes with ≈ 0.05 mmol/g and 0.1 mmol/g loading (Pd) as well as 0.1 mmol/g (Rh) loading. These metal-containing materials and their precursors were isolated as stable solids which are insoluble in common organic solvents such as THF, EtOH and DCM, but displayed slight swelling in DMSO. The materials have all been characterized using various analytical and spectroscopic techniques including UV-vis, FT-IR, solid state ^{13}C NMR and solid state ^{31}P NMR spectroscopy, elemental analysis, TGA, TEM, P-XRD and ICP-MS.

Mononuclear Pd^{II} and Rh^{I} complexes were also prepared by initially forming Schiff base ligands from the reaction of 1,3,4,6-tetra-*O*-acetyl-β-D-glucosamine hydrochloride and cyclohexylamine with either 2-pyridinecarboxaldehyde or 2-(diphenylphosphino)benzaldehyde. The resulting iminopyridyl and iminophosphine ligands were subsequently reacted with either $[PdCl_2(COD)]$ or $[RhCl(CO)_2]_2$ to obtain the respective model complexes. These new complexes have been characterized using ^{1}H NMR, ^{31}P NMR, UV-vis and FT-IR spectroscopy, elemental analysis and mass spectrometry. The molecular

structure of rhodium chlorocarbonyl iminophosphine complex (**2.17**) was determined by single crystal X-ray diffraction.

Suzuki-Miyaura and Heck cross-coupling reactions were carried out using the chitosan-supported Pd complexes and their mononuclear analogues. These catalyst precursors were active and selective (TON up to 1167 for the Suzuki-Miyaura and 1209 for the Heck reaction) for the cross-coupled products with the iminophosphine based systems exhibiting superior activity over the iminopyridyl systems. No homo coupling was observed in all the reactions and the Heck reactions produced *trans* coupled products exclusively. The chitosan-supported catalyst precursors were stable and could be recycled up to five times while the mononuclear catalyst precursors decomposed to black species during the reactions.

The chitosan-supported Rh complexes and their mononuclear analogues were active hydroformylation of 1-octene in xylene solvent. It was found that, the chiral backbone of the chitosan support did not influence selectivity during these reactions. Selectivity was affected by temperature and pressure with optimal conditions realized at 75°C and 30 bars where selectivity for the desired nonanal was favoured for catalyst precursors. The iminophosphine-based chitosan-supported catalyst precursor remained stable during the reaction period and was reused four times without loss in activity and selectivity. Leaching of Rh into the reaction mixture was minimal (≈ 0.02% and 0.05%).

Low generation tris-2-(2-pyridylimine ethyl)amine metallodendrimers were prepared and characterized successfully. Upon reacting tris-2-(aminoethyl)amine with 2-pyridine-carboxaldehyde, the low generation iminopyridyl dendrimer (**4.2**) was isolated as a light brown solid in a good yield.

Subsequent complexation of this dendrimer with either $[PdCl_2(COD)]$, $[RhCl(CO)_2]_2$ or $RhCl(COD)]_2$ afforded the corresponding new trinuclear metallodendrimers (**4.6**-**4.8**) bearing $–PdCl_2$, -RhCl(CO) and -Rh(COD) units on the periphery. The metallodendrimers and their precursor were poorly soluble in most solvents and highly thermally stable and have been characterized by ^{1}H NMR, ^{13}C NMR, ^{31}P NMR and FT-IR spectroscopy, elemental analysis as well as mass spectrometry.

Mononuclear pyridylimine complexes have been prepared and fully characterized. Firstly, the 4-(2-pyridylimine) benzyl alcohol ligand (**4.1**) was obtained *via* Schiff base condensation of 4-amino benzyl alcohol with 2-pyridine carboxaldehyde. This ligand was then treated with

either $[PdCl_2(COD)]$, $[RhCl(CO)_2]_2$ or $RhCl(COD)]_2$ to give the corresponding new complexes. ^1H NMR, ^{13}C NMR and FT-IR spectroscopy, elemental analysis as well as mass spectrometry provided evidence for the formation of these complexes. The single crystal X-ray structure of Pd complex (**4.3**) has been determined.

The final section of this work describes the catalytic hydroformylation of 1-octene using the Rh-containing pyridylimine metallodendrimers (**4.7** and **4.8**) and pyridylimine mononuclear complexes (**4.4** and **4.5**). Hydroformylation of 1-octene was carried out in toluene at various temperatures (55, 75 and 95°C) and pressures (5, 10 and 30 bars). These catalyst precursors were active in hydroformylation of 1-octene giving conversions in the range of (50-100%), Of the converted species *iso*-octenes were dominant when reaction were carried out at 55 °C, 5 and 10 bars, while the sought after aldehydes were favoured at 75 °C, 95 °C and 30 bars. Similar, to the chitosan-supported Rh^I catalyst precursors, high amounts of nonanal were formed at 75 °C while branched aldehydes took precedence at 95 °C.

Across the chlorocarbonyl-based systems, the metallodendrimers proved to be comparably more active and selective than the chitosan-supported catalyst precursors under optimal conditions. This suggests that the diffusion factors are reduced when metallodendrimers are applied in 1-octene hydroformylation thereby exploiting the homogeneous nature of the system.

The catalyst precursors presented in this thesis have proven their relative ease of preparation and applicability with vital properties such as versatility, efficiency, robustness, selectivity and reusability.An area of future investigation would be to explore expanding the scope of catalytic reactions that such catalyst precursors can be applied in.

Appendix

Supporting Information: X-ray diffraction data for complexes (**4.3**) and (**2.17**) including tables of all b**o**nd lengths and angles (CIF files) are contained in the attached disc.

Appendix

Section a

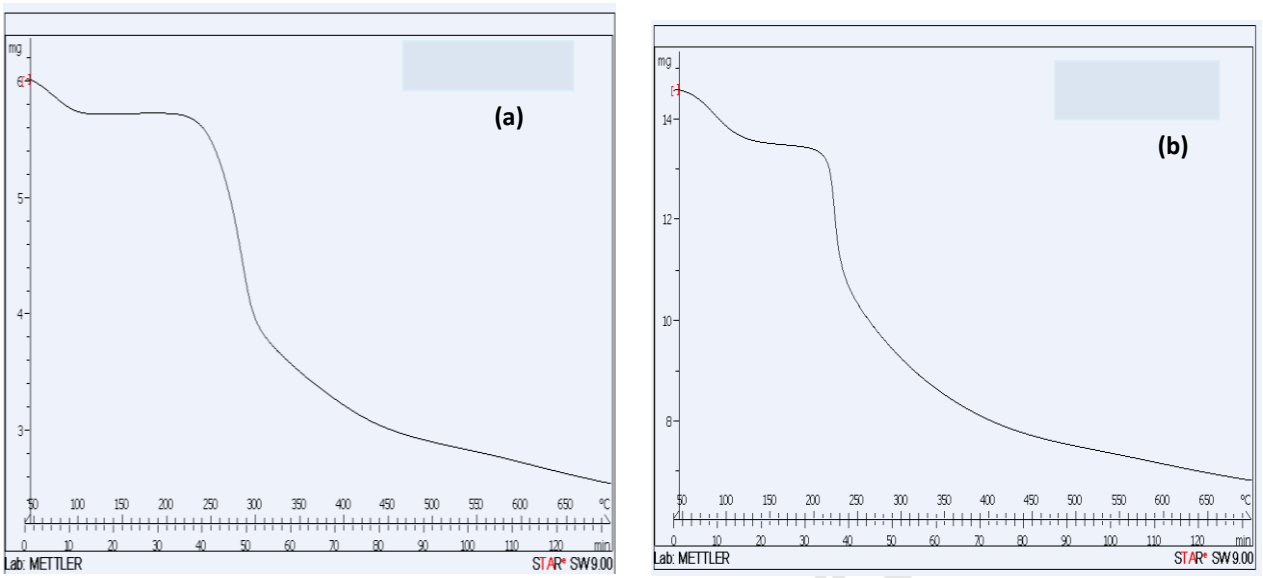

Fig. a TGA plots of chitosan-supported complexes (a) **2.7**, (b) **2.8**.

Section b

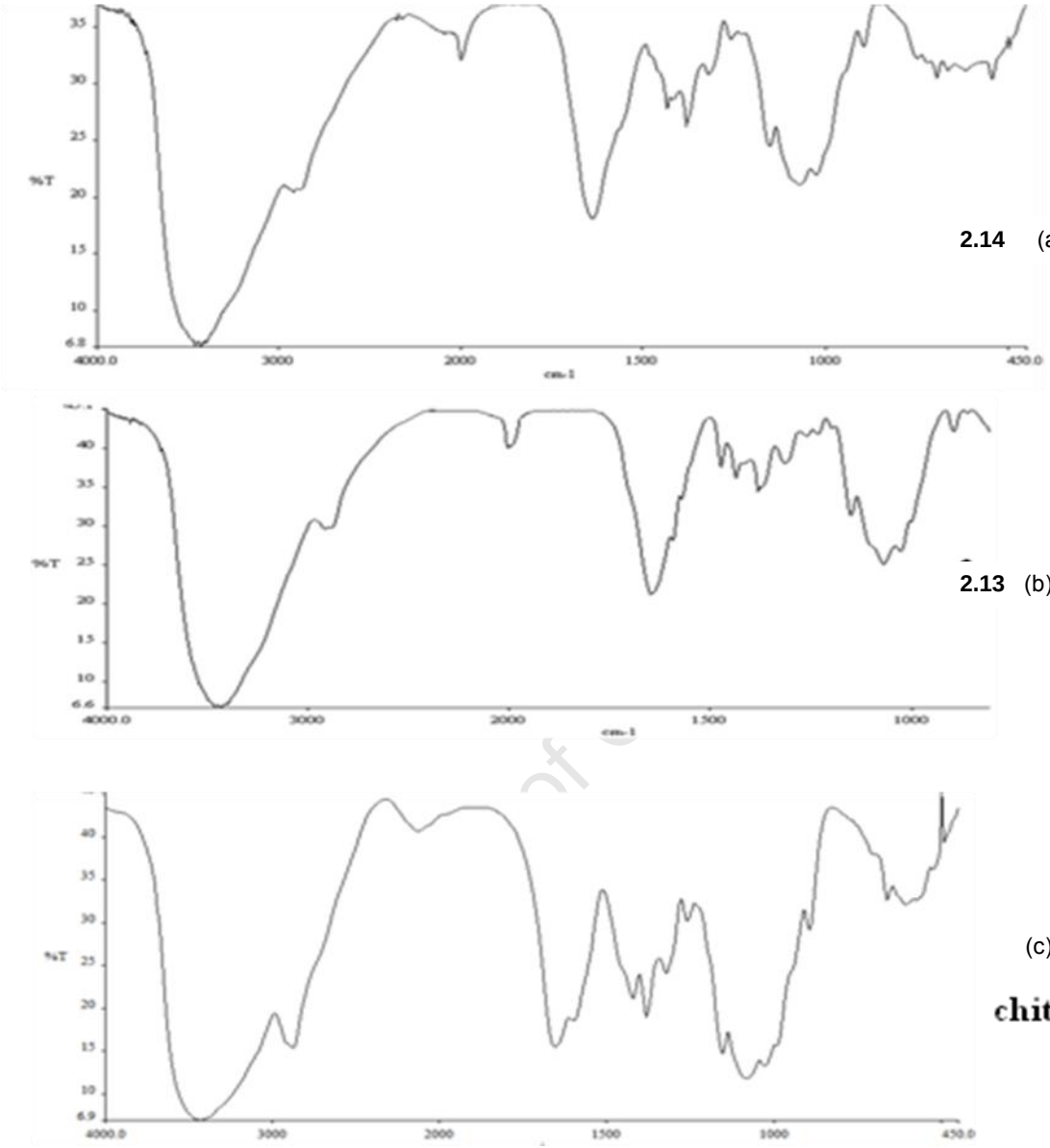

Fig. b FT-IR spectra of chitosan-supported Rh^{I} complexes (a) **2.14**, (b) **2.13** and chitosan (c).

Section c

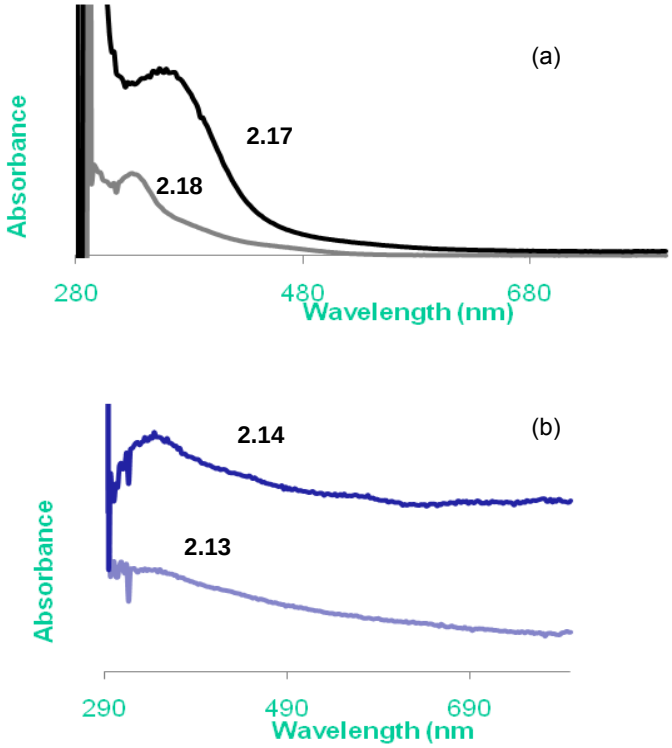

Fig. c UV-vis spectra showing absorbance peaks of complexes (a) **2.18** and **2.17** and supported catalysts (b) **2.13** and **2.14**.

Section d.

1. Orange crystals of complex (**2.17**) (0.10 x 0.08 x 0.05 mm) suitable for X-ray diffraction analysis were grown by slow evaporation from dichloromethane : *n*-hexane (1:1, ratio) Crystal data for complex (**2.17**):

Empirical formula	$C_{26}.50\ H_{27}\ Cl_2\ N\ O\ P\ Rh$
Formula weight	580.27
Temperature	100(2) K
Wavelength	0.71073 A
Crystal system, space group	Triclinic, P^{-1}
Unit cell dimensions	a = 9.7477(5) A alpha = 72.9480(10)°.
	b = 11.3212(6) A beta = 88.6650(10)°.
	c = 12.8467(7) A gamma = 65.9030(10)°.
Volume	1229.69(11) A^3
Z, Calculated density	2, 1.567 mg/m^3
Absorption coefficient	0.997 mm^-1
F(000)	590
Crystal size	0.10 x 0.08 x 0.05 mm
θ range for data collection	2.07 to 30.49°.
Limiting indices	-13<=h<=13, -16<=k<=15, -18<=l<=18
Reflections collected / unique	30276 / 7401 [R(int) = 0.0308]
Completeness to	θ = 30.49 98.9 %
Max. and min. transmission	0.9518 and 0.9069
Refinement method	Full-matrix least-squares on F^2
Data / restraints / parameters	7401 / 2 / 304
Goodness-of-fit on F^2	1.041
Final R indices [I>2σ(I)]	R1 = 0.0243, wR2 = 0.0590
R indices (all data)	R1 = 0.0288, wR2 = 0.0612
Largest diff. peak and hole	0.909 and -0.738 A^{-3}

CIF File data for complex (**2.17**)

BM50B_final.CIF.txt

BM50B.FCF.txt

Section e

Table a Hydroformylation of 1-octene over 8hrs-Rh leaching studies. [a]

Entry	Cat.	Time (hrs)	% Conversion	% Aldehyde	% *iso*-octenes	n:iso	TOF[f]
1	**3**	2	24	52	48	73:27[b]	133
2	**3**	4	35	25	75	20:70[c]	64
3	**3**	6	40	18	82	20:70[d]	16
4	**3**	8	45	11	89	22:78[e]	10
5	**4**	2	20	20	80	69:31[b]	18
6	**4**	4	30	14	86	54:46[c]	13
7	**4**	6	38	11	89	41:59[d]	10
8	**4**	8	39	9	91	33:66[e]	8

Reactions carried out at 30 bars ($CO:H_2$) (1:1) and 75°C in xylene (10ml) with 6.37 mmol of 1-octene and $2.87x10^{-3}$ mmol Rh catalyst (loading = 0.145 (**3**); 0.092 (**4**) $mmolg^{-1}$). GC conversions obtained using *n*-decane as an internal standard in relation to authentic standard *iso*-octenes and aldehydes. [b] Regioselectivity calculated at 2hrs. [c] Regioselectivity calculated at 4hrs. [d] Regioselectivity calculated at 6hrs.[e] Regioselectivity calculated at 8hrs. .). [f]TOF = (mol product/mol cat.) x h^{-1}.

Section f

Table b Hydroformylation of 1-octene over 8hrs- catalyst reuse studies. [a]

Run	Cat.	% Conversion	% Aldehyde	% *iso*-octenes	n:iso	TON[c]	TOF[d]
1	**3**	75	95	5	70:30[b]	2088	261
2	**3**	77	86	14	74:26[b]	1712	252
3	**3**	79	70	30	74:26[b]	2013	214
4	**3**	72	71	29	72:28[b]	2011	223
5	**3**	52	63	37	71:30[b]	1064	132
1	**4**	73	51	49	57:43[b]	1097	137
2	**4**	4	39	61	67:33[b]	838	104
3	**4**	3	29	71	62:38[b]	623	77

[a] Reactions carried out with ($CO:H_2$) (1:1) at 75°C in xylene (10ml) with 6.37 mmol of 1-octene and 2.87×10^{-3} mmol Rh catalyst (loading = 0.145 (**3**); 0.092 (**4**) $mmol g^{-1}$). GC conversions obtained using *n*-decane as an internal standard in relation to authentic standard *iso*-octenes and aldehydes.[b] Regioselectivity calculated at 4hrs. [c]TON = (mol product/mol cat.). [d]TOF = (mol product/mol cat.) x h^{-1}.

Section g

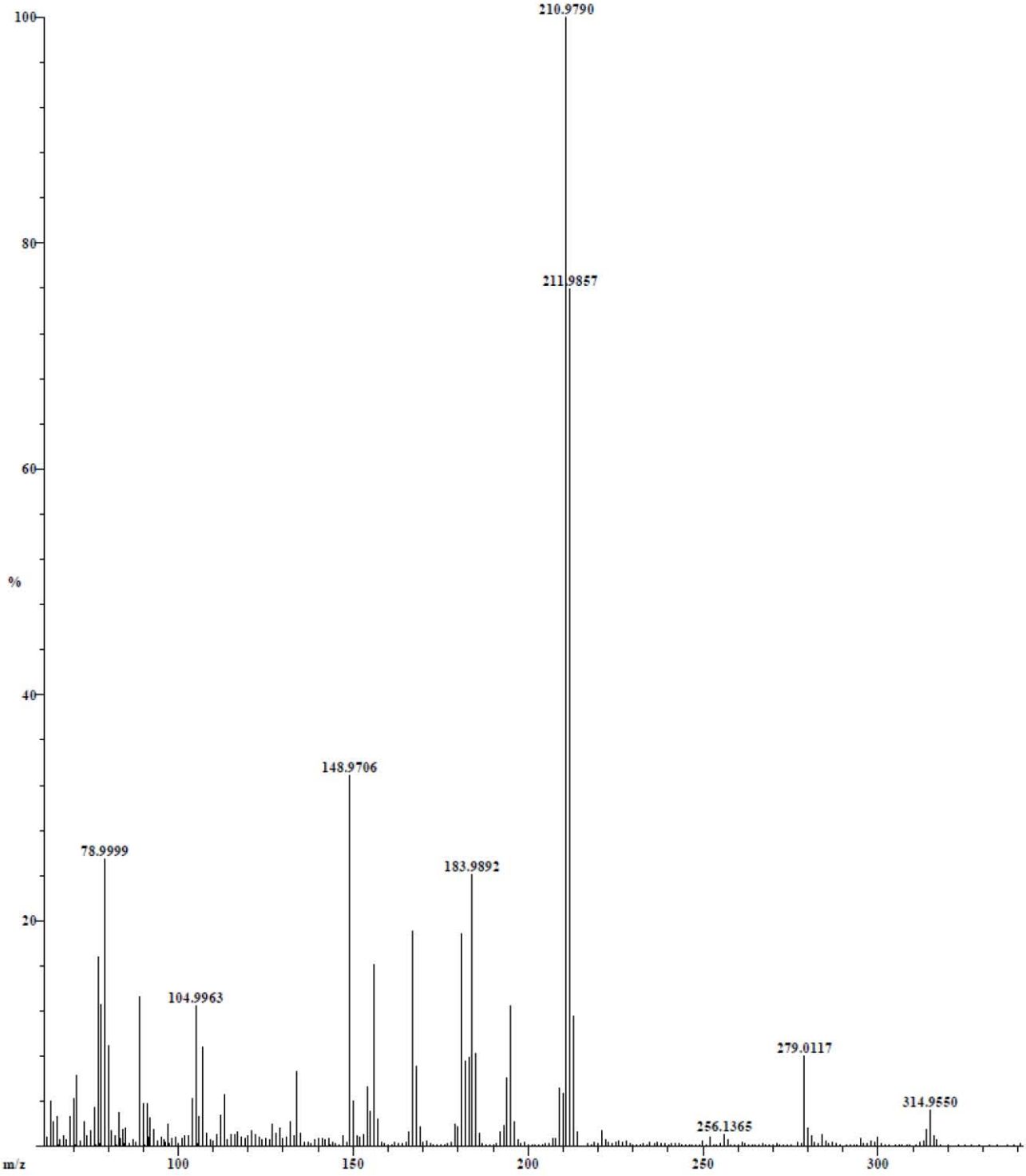

Fig. d Electron impact (EI) mass spectrum of ligand **4.1**.

Section h

Summary of data and collection for the single crystal X-ray structure of complex **4.3** is given in **Tables b**.

Table b X-ray crystallographic data collection parameters for complexes **4.3**.

	4.3
Empirical formula	C_{13} H_{12} Cl_2 N_2 O Pd
Formula weight	389.55
T/K	173(2)
λ/Å	0.71073
space group	Orthorhombic, Pbca
a	14.3558(12)
b	10.0809(8)
c	18.3266(15)
α(deg)	90
β(deg)	90
γ(deg)	90
V(Å^3)	2652.2(4)
Z	8
Densitycalc (mg/mL)	1.951
Absorption coefficient (mm^{-1})	1.793
F(000)	1536
Crystal Size (mm)	0.11 x 0.10 x 0.05
Theta Range for Data Collection (deg)	2.22 to 28.46

Limiting Indices	-19<=h<=19
	-13<=k<=13
	-24<=l<=24
Reflections Collected / Unique	39282 / 3334 [R(int) = 0.0807
Completeness to theta	28.46 (99.6 %)
max. and min. transmission	0.9157 and 0.8272
Refinement Method	Full-matrix least-squares on F^2
Data / Restraints / Parameters	3334 / 0 / 172
Goodness-of-fit on F2	1.012

CIF file data for complex (**4.3**).

BM54.txt

BM54 (2).txt